University of Kentucky
UKnowledge

Theses and Dissertations--Microbiology, Immunology, and Molecular Genetics

Microbiology, Immunology, and Molecular Genetics

2019

FUNCTIONAL ANALYSES OF THE DNA- AND RNA-BINDING PROTEIN SPOVG IN *BORRELIA BURGDORFERI*

Christina R. Savage
University of Kentucky, christina.savage@uky.edu
Digital Object Identifier: https://doi.org/10.13023/etd.2019.372

Right click to open a feedback form in a new tab to let us know how this document benefits you.

Recommended Citation

Savage, Christina R., "FUNCTIONAL ANALYSES OF THE DNA- AND RNA-BINDING PROTEIN SPOVG IN *BORRELIA BURGDORFERI*" (2019). *Theses and Dissertations--Microbiology, Immunology, and Molecular Genetics*. 21.
https://uknowledge.uky.edu/microbio_etds/21

This Doctoral Dissertation is brought to you for free and open access by the Microbiology, Immunology, and Molecular Genetics at UKnowledge. It has been accepted for inclusion in Theses and Dissertations--Microbiology, Immunology, and Molecular Genetics by an authorized administrator of UKnowledge. For more information, please contact UKnowledge@lsv.uky.edu.

STUDENT AGREEMENT:

I represent that my thesis or dissertation and abstract are my original work. Proper attribution has been given to all outside sources. I understand that I am solely responsible for obtaining any needed copyright permissions. I have obtained needed written permission statement(s) from the owner(s) of each third-party copyrighted matter to be included in my work, allowing electronic distribution (if such use is not permitted by the fair use doctrine) which will be submitted to UKnowledge as Additional File.

I hereby grant to The University of Kentucky and its agents the irrevocable, non-exclusive, and royalty-free license to archive and make accessible my work in whole or in part in all forms of media, now or hereafter known. I agree that the document mentioned above may be made available immediately for worldwide access unless an embargo applies.

I retain all other ownership rights to the copyright of my work. I also retain the right to use in future works (such as articles or books) all or part of my work. I understand that I am free to register the copyright to my work.

REVIEW, APPROVAL AND ACCEPTANCE

The document mentioned above has been reviewed and accepted by the student's advisor, on behalf of the advisory committee, and by the Director of Graduate Studies (DGS), on behalf of the program; we verify that this is the final, approved version of the student's thesis including all changes required by the advisory committee. The undersigned agree to abide by the statements above.

Christina R. Savage, Student

Dr. Brian Stevenson, Major Professor

Dr. Carol Pickett, Director of Graduate Studies

FUNCTIONAL ANALYSES OF THE DNA- AND RNA-BINDING PROTEIN SPOVG IN *BORRELIA BURGDORFERI*

DISSERTATION

A dissertation submitted in partial fulfillment of the requirements for the degree of Doctor of Philosophy in the College of Medicine at the University of Kentucky

By
Christina Renee Savage
Lexington, Kentucky
Director: Dr. Brian Stevenson, Professor of Microbiology
Lexington, Kentucky
2019

Copyright © Christina Renee Savage 2019

ABSTRACT OF DISSERTATION

FUNCTIONAL ANALYSES OF THE DNA- AND RNA-BINDING PROTEIN SPOVG IN *BORRELIA BURGDORFERI*

Borrelia burgdorferi, the causative agent of Lyme disease, exists in a defined enzootic cycle involving *Ixodes scapularis* ticks and various vertebrates. Humans can serve as an accidental host, if a tick colonized with *B. burgdorferi* happens to feed on a human. *B. burgdorferi* are also accidental pathogens: they do not make toxins, or destroy host tissue by other mechanisms. They merely transmit between vector and host to survive. In order to do this, they must effectively sense their current environment, and appropriately alter cellular processes. Understanding the regulatory mechanisms of how *B. burgdorferi* manages to do this has been a focus of the Stevenson lab for many years.

Previous work identified SpoVG as a DNA-binding protein. Although a homologue of this protein had been implicated to serve a regulatory role in other bacteria, the Stevenson lab was the first to demonstrate a function for the protein, both for *B. burgdorferi* and two other bacteria. Studies contained in this body of work aim to provide insight into regulation of SpoVG by *B. burgdorferi* as well the impact that it has on gene regulation.

By using genetic mutants, we determined that SpoVG is regulated at the levels of transcription and translation in culture by growth rate, temperature, and other regulatory factors. Additionally, we provide evidence that SpoVG regulates its own expression. Numerous genes are under control of SpoVG. Biochemical analyses revealed that SpoVG specifically interacts with DNAs and RNAs associated with genes found to be under its regulatory control. Finally, we provide evidence for SpoVG acting in concert with other known regulatory factors such as other DNA-binding proteins and the cyclic di-nucleotide second messengers cyclic-di-GMP and cyclic-di-AMP.

All together, these studies provide insight into how *B. burgdorferi* broadly regulates cellular processes during different stages of the enzootic cycle. We hypothesize that SpoVG does this through globally manipulating the three-dimensional structure of the bacterial chromosome, and that exactly how SpoVG acts at any given point will be dependent on the other regulatory factors that are also present in the cell.

KEYWORDS: *Borrelia burgdorferi,* gene regulation, SpoVG, DNA-binding proteins, RNA-binding proteins

Christina Renee Savage

(Name of Student)

07/23/2019

Date

FUNCTIONAL ANALYSES OF THE DNA- AND RNA-BINDING PROTEIN SPOVG IN *BORRELIA BURGDORFERI*

By
Christina Renee Savage

Dr. Brian Stevenson
Director of Dissertation

Dr. Carol Pickett
Director of Graduate Studies

07/23/2019

DEDICATION

This work is dedicated to my sisters Camille Savage-Kroll and Carissa Savage

ACKNOWLEDGMENTS

I would like to thank the following people for their contributions to the studies described in this work:

Alex Nail for making plasmid pAG1 and *B. burgdorferi* strain AG1

Gabby Keb for making strain GK1

Dr. Tomasz Bykowski for making strains TB3, TB11, TB13

Dr. Md Motaleb for making strain Δ*spoVG* and for sharing his unpublished data on the interaction between SpoVG and PlzA

Dr. Eric Garcia for RNA-sequencing analysis

Timothy Saylor for assistance with making reagents, ordering supplies, and generally helping the lab to run smoothly

I am grateful to Dr. David Orren for taking the time to serve as my outside examiner.

To my committee members Dr. Sarah D'Orazio, Dr. Anthony Sinai, and Dr. Hunter Moseley: for your criticisms when I was losing focus, and patience when I didn't want to listen.

And finally: Brian. For welcoming me into your lab, for flinging wide the doors of Science, and introducing me to the community of microbiology. For endless encouragement and freedom to pursue my own questions. Thank you.

This work was carried out on occupied Shawnee lands.

TABLE OF CONTENTS

ACKNOWLEDGMENTS iii

LIST OF TABLES vii

LIST OF FIGURES viii

CHAPTER 1. Introduction 1

1.1 Bacteria sense and respond to their environments 1

1.2 Borrelia burgdorferi as the causative agent of Lyme disease 2

1.3 Enzootic transmission cycle of B. burgdorferi 4

1.4 Distribution of Ixodes scapularis ticks and Lyme Disease 5

1.5 Borrelia burgdorferi physiology 6

1.6 Motility and Chemotaxis 8

1.7 Tick and vertebrate interfaces 8

1.8 B. burgdorferi regulatory factors 9

1.9 Initial studies on SpoVG 10

CHAPTER 2. Materials and Methods 13

2.1 Media and Stock Solutions 13

2.2 Bacterial Cultivation 18

2.3 Isolation of individual Borrelia burgdorferi colonies 19

2.4 Growth Curves 20

2.5 Plasmid Construction 21

2.6 Transformation of Bacteria with Foreign DNA 22

2.7 Colony PCR 24

2.8 Recombinant Protein Purification 25

2.9 RNA Extraction 28

2.10 Quantitative Reverse Transcriptase Polymerase Chain Reaction (qRT-PCR) 31

2.11 Western Blotting 33

2.12 Creating Images 38

2.13 Electrophoretic Shift Assays (EMSAs) 38

2.14 In Silico Proteomic Analyses 42

2.15 Nucleotide Extraction and cyclic-di-AMP analysis in E. coli and B. burgdorferi 43

2.16 RNA Sequencing and Analysis 43

2.17 MS/MS on SpoVG in cultured B. burgdorferi and recombinant protein *44*

2.18 In Silico Modeling of SpoVG Structure *45*

2.19 Mouse Infection Studies *45*

2.20 Green Fluorescent Protein (GFP)-transcriptional fusions analyzed by Flow Cytometry *47*

2.21 Antibody production *48*

2.22 2-dimensional gel electrophoresis *48*

CHAPTER 3. Regulation of SpoVG as a Global regulator in *B. burgdorferi* 55

3.1 Introduction *55*

3.2 Creation of Mutants *56*

3.3 Infection Studies *57*

3.4 RNA-Sequencing on wild-type, spoVG-ON, and ΔspoVG B. burgdorferi *59*

3.5 ParA transcript abundance and Plasmid Quantification *61*

3.6 Growth Rates of Wild-type, spoVG-ON, and ΔspoVG *62*

3.7 spoVG Expression in wild-type and spoVG-ON grown at 34°C and 23°C *63*

3.8 SpoVG Binds Its Own DNA and RNA in Vitro *64*

3.9 SpoVG expression in B. burgdorferi deficient for PlzA, or c-di-GMP *66*

3.10 Discussion *67*

CHAPTER 4. SpoVG Regulates Expression of Numerous genes 100

4.1 Introduction *100*

4.2 SpoVG Regulates Expression of the glpFKD Operon *102*

4.3 SpoVG binds to glpFKD DNA and RNA *103*

4.4 PlzA binds to glpF DNA *104*

4.5 Impact of Glycerol on Growth Rate *105*

4.6 SpoVG and PlzA impact VlsE protein expression *107*

4.7 SpoVG Does Not Impact vlsE Transcription *108*

4.8 SpoVG and PlzA bind DNA just up-stream of the vlsE gene *109*

4.9 Potential role for SpoVG in vlsE recombination *110*

4.10 SpoVG and acetylation *111*

4.11 Discussion *113*

CHAPTER 5. SpoVG and Cyclic-di-AMP regulate OspC translation independently of transcription 133

5.1 Introduction *133*

5.2 Bb0008 Encodes a Cyclic-di-AMP synthase *135*

5.3 Overexpression of CdaA does not alter intracellular levels of c-di-AMP *136*

5.4 CdaA affects expression levels of OspC protein 137

5.5 SpoVG regulates OspC protein but not transcript 138

5.6 SpoVG binds to RNA associated with ospC gene 139

5.7 Discussion 141

CHAPTER 6. Discussion 153

6.1 SpoVG in B. burgdorferi 153

6.2 Transcriptomics on spoVG-ON, ΔspoVG and wild-type 153

6.3 Regulation of ospC gene by SpoVG and c-di-AMP 155

6.4 Structural insights into SpoVG 156

6.5 SpoVG as a potential nucleoid-associated protein 157

6.6 Presence of Poly-T sites 159

6.7 Post-translational modification of SpoVG 160

6.8 Model of SpoVG network in B. burgdorferi 160

6.9 SpoVG as potentially analogous to a eukaryotic cell-cycle checkpoint protein 161

APPENDICES 165

APPENDIX 1. *cheA* mutants respond to glycerol differently than wild-type *B. burgdorferi* 165

APPENDIX 2 . Intracellular c-di-GMP analysis by FRET 170

APPENDIX 3: Additional binding interactions 174

APPENDIX 4: Proteomics 179

APPENDIX 5: Full transcriptomic tables 183

REFERENCES 221

VITA 226

LIST OF TABLES

Table 2.1 Plasmids used in this study 52
Table 2.2 Bacterial Strains used in this study 53
Table 2.3 Antibodies used in this study 54
Table 3.1 Small RNAs differentially expressed between wild-type and *spoVG*-ON 84
Table 3.2 Small RNAs differentially expressed between wild-type and Δ*spoVG* 87
Table 3.3 mRNAs differentially expressed between wild-type and *spoVG*-ON..... 89
Table 3.4 mRNAs differentially expressed between wild-type and Δ*spoVG* 95

LIST OF FIGURES

Figure 1.1 Enzootic cycle of *Borrelia burgdorferi* 12
Figure 3.1 pCRS5 (*spoVG*-ON) plasmid and Δ*spoVG* constructions 71
Figure 3.2 Infection Study 72
Figure 3.3 RNA-seq transcripts 73
Figure 3.4 *parA* transcript abundance and plasmid quantification 74
Figure 3.5 Effect of *spoVG* on growth rate of *B. burgdorferi* 76
Figure 3.6 SpoVG transcript and protein expression in culture 77
Figure 3.7 SpoVG binds its own DNA and RNA 78
Figure 3.8 Multiple SpoVG complexes bind to a single DNA 80
Figure 3.9 PlzA and c-di-GMP are necessary for expression of SpoVG 81
Figure 3.10 Distribution of differentially expressed RNAs 82
Figure 3.11 Functional clustering of differentially expressed transcripts 83
Figure 4.1 Glycerol metabolism 118
Figure 4.2 SpoVG regulates expression of *glpFKD* operon 119
Figure 4.3 SpoVG binds to *glpFKD* DNA and RNA 120
Figure 4.4 PlzA binds to *glpF* DNA 123
Figure 4.5 Complete BSK + glycerol 124
Figure 4.6 BSK-Lite + glycerol 125
Figure 4.7 VlsE expression 126
Figure 4.8 Transcriptional GFP fusions 127
Figure 4.9 SpoVG and PlzA bind to *vlsE* DNA 128
Figure 4.10 Potential role for SpoVG in *vlsE* recombination 129
Figure 4.11 Acetylation and *ackA* expression 130
Figure 4.12 Effect of Acetylation on SpoVG activity 131
Figure 4.13 SpoVG alignments 132
Figure 5.1 *cdaA* alignments 144
Figure 5.2 *B. burgdorferi* synthesizes c-di-AMP 145
Figure 5.3 Effects of overexpression *cdaA* in *B. burgdorferi* 146
Figure 5.4 Impact of cdaA on OspC and SpoVG expression 148
Figure 5.5 Impact of SpoVG on *cdaA* and OspC expression 149
Figure 5.6 SpoVG binds to *ospC* RNA 150
Figure 5.7 Mutated *ospC* RNAs to test SpoVG-RNA binding 151
Figure 5.8 SpoVG binding to mutated RNAs 152
Figure 6.1 Modeled SpoVG structure 163
Figure 6.2 Model of SpoVG activities 164

CHAPTER 1. INTRODUCTION

"Happy families are all alike; every unhappy family is unhappy in its own way"

1.1 Bacteria sense and respond to their environments

Thus begins Tolstoy's Anna Karenina. But what can be said of the Domain Bacteria? There is enormous diversity in where individuals live, the nutrients they need to survive, and environments within which they flourish. *Thermus aquaticus* was isolated from deep-sea hot-water vents (1). Many bacteria can metabolize sulfur, and some are magnetotactic, by storing iron in specialized organelles (2, 3). Different bacteria can live in volcanos, soil, water, within various hosts, and even within other cells (4-8). Happy bacteria are certainly not all alike.

And what of unhappy bacteria? Bacteria have evolved a number of strategies to deal with harsh environments and toxic components in their environments. Not every bacterium employs every strategy, however there is remarkable conservation in the ways in which bacteria cope with "unhappiness". At the core of evolutionary survival is the ability of bacteria to recognize when stressful factors are present, and drastically slow-down cellular processes that require energy, such as growth and division, transcription and translation (9-11).

This simple strategy essentially gives bacteria time to employ other strategies they may have evolved to cope with stress without dying. This has particularly relevant implications for how bacteria are so adept at developing resistance to antimicrobial drugs. Bacteria only need to survive while the drug is present, then can go on happily growing

afterwards (12). There are two main classes of antibacterial drugs, based on the effect that they have on bacteria. Bacteriostatic drugs prevent bacterial growth, and work by allowing human immune systems to kill the bacteria, and bactericidal drugs work by directly killing bacteria. The majority of antibiotics approved for human use are bacteriostatic, and these are far easier for bacteria to develop resistance to (12, 13) .

Although strategies that bacteria employ to survive harsh environments evolve, and development of resistance to antibiotics is well documented and studied, very little is known about the mechanism by which bacteria distinguish a "harsh environment" or "toxic compounds", and exactly how they go about reprogramming their cellular processes (14). *Borrelia burgdorferi* provides a unique model for studying how bacteria sense and respond to changing environments. The bacterium exists by transmitting within a rigid enzootic cycle that includes surviving within a tick midgut for months at a time with very few available nutrients.

1.2 *Borrelia burgdorferi* as the causative agent of Lyme disease

Lyme disease was first described in 1976, when a cluster of children living in Lyme Connecticut presented with symptoms that appeared to be consistent with rheumatoid arthritis (15-17). A few years later, at the NIH Rocky Mountain Laboratories, the link between Lyme disease and the tick-borne spirochete *Borrelia burgdorferi* was established (18-20). Although the disease has only relatively recently been named, *B. burgdorferi* has been endemic to North America for approximately 60,000 years (21).

Lyme disease (LD) presents in patients as immunologically driven symptoms. The bacteria do not make any toxins, or attack host cells (22, 23). The disease is driven entirely

by immune responses that do not efficiently target *B. burgdorferi,* and instead damage host tissue. The most visibly obvious symptom is the "bulls-eye" rash. Approximately 70% of people infected with *B. burgdorferi* present with a round rash expanding from the tick bite site (24-26). Other common symptoms include facial palsy and arthritis (27). It is estimated that approximately 60% of LD patients who are not treated in the early stages of infection with antibiotics develop arthritis in one or more large joints after several months (17).

There have been no reported cases of antibiotic resistant *B. burgdorferi* in an infected human (16, 28-31). The majority of Lyme disease patients who receive antibiotic therapy in a timely manner recover with no long-term side effects. A small sub-set of treated patients (less than 10%) suffer from refractory Lyme arthritis, a condition that is caused by continued immunological responses in the previously infected tissues (32-35).

There is no evidence to support claims that *B. burgdorferi* forms persister cells, or that patient's symptoms are dependent on the presence of live, uncleared bacteria (36, 37). The details of the mechanism of what causes persistent symptoms in this sub-population of patients remain to be fully examined. A recent study, however, demonstrated that *B. burgdorferi* peptidoglycan can be detected in human synovial tissue long after bacteria are cleared (38). *B. burgdorferi* peptidoglycan is constructed in a unique manner, and is highly immunogenic on its own (38, 39). Additionally, *B. burgdorferi* lacks any pathway to recycle peptidoglycan (23). During the process of cell growth and cell wall remodeling, *B. burgdorferi* peptidoglycan accumulates in its environment (38, 39).

1.3 Enzootic transmission cycle of *B. burgdorferi*

Borrelia burgdorferi exists in nature by transmitting between *Ixodes* spp. ticks and vertebrates (Figure 1.1). The bacterium cannot survive outside of a host, and does not live intracellularly within eukaryotic cells. *B. burgdorferi* is not transmitted transovarially within the tick, meaning the bacteria cannot infect the eggs. After hatching, the larvae take a blood meal. If a larva feeds on an animal that has been infected with *B. burgdorferi,* some of those bacteria can be transmitted to the tick. While the blood meal is digested, *B. burgdorferi* reduces its growth and replication rate, and attaches to the cells of the tick mid-gut (40-43). The larva will then over-winter, molt into a nymph, and take a blood meal. Once the blood begins to come in, *B. burgdorferi* detaches from the mid-gut, traverses through the hemolymph, and into the salivary glands where they can transmit into the host that the tick is feeding on (44, 45). The nymph is the stage most likely to transmit *B. burgdorferi* to humans. They are very tiny--about the size of a sesame seed--which makes them exceptionally difficult to detect (46-50).

There is an important distinction to be made for *Ixodes,* the genus of ticks that carry *B. burgdorferi.* There are two main classifications of ticks: soft-bodied and hard-bodied (51). The group which *Ixodes* belongs to are hard-bodied. One of the most important distinctions between these two groups, and essential for understanding *B. burgdorferi* survival and transmission, is how these two groups of ticks feed. Soft-bodied ticks feed often and very quickly. They can take blood-meals as often as once every few weeks, but they only feed for about 15 minutes at a time. Hard-bodied ticks, however, take only one blood meal per life cycle stage, and can take up to seven days to complete a feeding (51-53). A larva takes one blood meal then molts into a nymph. The nymph takes one blood

meal, then molts into either a female or male adult. Only the female adult will take a blood meal, although males at this stage will attach to vertebrates as well, in order to mate with the females. After the female has taken her blood meal, she uses all of her resources to develop a clutch of eggs, and dies in the process (51-55).

The range of vertebrate hosts that can be infected with, and transmit *B. burgdorferi* is quite wide, ranging from birds to rodents such as mice and squirrels to reptiles such as lizards (40, 56-59). Ticks do not fly or jump, but rather lie in-wait for their victim to brush past. The vertebrate animal most likely to serve as host in this cycle is largely dependent on geographic location, and the preferred "blood buffet" for the tick species in that region. For example, in the southern United States, *Ixodes scapularis* ticks exhibit a very different questing behavior than ticks in the North Eastern states, and tend to feed on reptiles rather than small mammals. Rather than climbing as high as possible on blades of grass, for instance, the southern *Ixodes* prefer to remain low in the leaf litter (57, 60, 61). On the western coast, *Ixodes pacificus* can feed on humans, but the percentage of *I. pacificus* infected by *B. burgdorferi* is much lower than the percentage of *I. scapularis* that is infected in endemic areas. Whereas up to 30% of *I. scapularis* nymphs are infected with *B. burgdorferi*, only about 3% of *I. pacificus* ticks are. (62-66).

1.4 Distribution of *Ixodes scapularis* ticks and Lyme Disease

Although there is a smattering of Lyme disease cases throughout the U.S., particularly in California, the majority of cases reported are concentrated on the East coast and in the Midwest in Minnesota, Wisconsin and Illinois. The CDC began recording reported cases in 1997. That year, there were 12,801 confirmed cases. For 2017, the most

recent year with available data, there were 29,513 confirmed cases, and an additional 13,320 probable cases were reported. The CDC estimates that up to 300,000 people contract Lyme disease each year, but that the majority of cases go undiagnosed and unreported. The increase in reported cases is due to a number of factors, including an increasing awareness, diagnosis, and reporting of Lyme disease cases (67, 68).

The most significant impact on the increase in Lyme disease is due to expanding tick populations (57, 69). There could be two contributing factors to this: 1) the percentage of ticks within a population that harbors *B. burgdorferi* could increase, and 2) the tick population itself could increase, and its geographical footprint could expand. Even in areas where *I. scapularis* ticks and Lyme disease are endemic, about 30% of the total tick population carries *B. burgdorferi*, and this percentage has been fairly consistent since these ecological studies were first conducted (61, 70-73). The *Ixodes scapularis* population has been expanding, in part due to climate change (44, 61, 74).

1.5 *Borrelia burgdorferi* physiology

Borrelia burgdorferi is a spirochete, a group of bacteria easily identified by their distinctive corkscrew-like shape. These bacteria are very thin (approximately 200 nm) and very long (approximately 20 μm). *B. burgdorferi* is classified as a gram-negative bacterium due to the fact that it has an outer membrane, however, many of its proteins are more closely related to those found in gram-positive bacteria, and it has no lipopolysaccharide (LPS) as other gram-negative bacteria do (23, 75, 76). The corkscrew shape of *Borrelia* spp. comes from the periplasmic flagella that are present at each end of the cell. The motors are anchored in the inner membrane of the cell, and the flagella wrap around the body of

the cell, within the periplasmic space between the outer and inner membranes. The rotation of flagella are the source of the corkscrew shape (77-81).

B. burgdorferi also posseses an unusual genome that is both reduced and highly segmented. The entire genome is about 1.5 million base pairs in total. Approximately 900 KB is located on the main, linear chromosome, while the remaining 6 KB is distributed across as many as two dozen circular and linear plasmids of varying sizes (76, 82-89). Cultured *B. burgdorferi* loses plasmids over the course of laboratory passages, however *B. burgdorferi* in the wild maintain approximately two dozen (85, 90-92). Some plasmids contain genes that are necessary for survival within the tick, such as lp45. This plasmid encodes two genes *ospA* and *ospB*, which encode outersurface lipoproteins that interact with TROSPA/B receptors on the cells lining the tick mid-gut (93). This enables *B. burgdorferi* to attach to the mid-gut of the tick during digestion and molting. Some plasmids contain genes necessary for survival within vertebrates, such as the group of cp32 plasmids, which are prophages and contain the *erp* genes which code for outersurface lipoproteins that bind to complement inhibitor protein factor H (94). Finally, some plasmids are always faithfully maintained, because they harbor genes that code for essential proteins. For example, cp26 contains the gene *resT*, which codes for the telomere resolvase protein, which is necessary for replication of all linear DNA elements in *B. burgdorferi*, including the main chromosome (93, 95-98). *B. burgdorferi* that is serially passaged in culture lose plasmids over time, therefore individual strains are noted as either high-passage non-infectious (such as B31-e2) or low-passage, infectious (such as B31-A3). B31-e2 is non-infectious, grows more quickly, and is more easily transformable because it has lost most plasmids not necessary for survival in culture. These include lp28-1 which carries

the *vlsE* locus, and lp25 which carries the locus for one of the two restriction modification systems.

1.6 Motility and Chemotaxis

B. burgodrferi is highly motile. Seven to eleven falgellar motors are positioned in the inner membrane on both ends of the cell (99). The flagellelar filaments extend from the motors into the periplasmic space between the peptidoglycan and the outer membrane, and wrap back around the body of the cell. The motion of the flagella turning give the charactaristic corkscrew shape to the bacterium (77, 79, 100, 101).

B. burgdorferi maintains chemotactic systems that allow the bacteria to very quickly and efficiently detect incoming signals (77, 79, 102-105). The process of transmitting from a tick to a vertebrate or from a vertebrate to a tick is an active one. When the blood meal comes into a tick, *B. burgdorferi* must detach from the midgut, enter the hemolymph, travel to the salivary glands, and out into the vertebrate. Likewise, when a tick feeds on a vertebrate, *B. burgdorferi* actively migrates to the tick bite site to be taken up with the blood meal. Although it is unknown exactly what molecules *B. burgdorferi* migrates towards, bacteria deficient in the chemotactic proteins CheX, CheY3 and CheA2 are unable to transmit between tick and vertebrate in either direction (106-109).

1.7 Tick and vertebrate interfaces

Numerous studies have demonstrated that *B. burgdorferi* drastically alters its transcriptome and proteome, depending on whether it is transmitting from a tick to a vertebrate, establishing an infection within a vertebrate, transmitting to a tick, or colonizing

the tick after the blood meal has been digested by the tick (110-116). *B. burgdorferi* expresses different outer surface proteins at different points. OspA and OspB interact with TROSPA/B receptors on cells in the tick mid-gut, allowing *B. burgdorferi* to effectly adhere onto the lining of the midgut (117) (118-122).

Other outer surface proteins are expressed when *B. burgdorferi* is in the vertebrate which binds to extracellular matrix material such as fibronectin and laminin. This has the effect of "coating" the bacteria and appearing as "self" to the host immune cells (123-129). "Erp" and CRASP outer surface proteins encoded on the cp32 prophages bind Factor H, and thus prevent killing by the complement pathway (94, 130-137). VlsE is only expressed in vertebrates, and although it is highly immunogenic, it undergoes antigenic variation by a mechanism that remains to be defined (138-141).

1.8 *B. burgdorferi* regulatory factors

Although some bacteria have evolved hundreds of regulatory factors, *B. burgdorferi* encodes surprisingly few. This may be in part due to the fact that *B. burgdorferi* has evolved to exist in a very defined enzootic cycle. Where *B. burgdorferi* has been informs the bacteria of its current environment, the current environment informs the bacteria of what is coming next. In contrast to bacteria that have evolved to survive in a wide variety of environments (think *Pseudomonas* spp), *B. burgdorferi* has evolved to be prepared for a defined set of niches.

B. burgdorferi has two two-componant systems (not including those in the chemotaxis pathway), termed Hk1-Rrp1 and Hk2-Rrp2 (23). When phosphorylated, Rrp1 synthesizes the small molecule c-di-GMP (142). C-di-GMP, is essential for survival in the

tick, although it is dispensible for survival in mice (143), and controls gene expression likely through its interaction with PlzA (144-148). Rrp2 is the alternative sigma factor RpoN, which together with the DNA-binding protein BosR, stimulates expression of the only other alternative sigma factor, RpoS (149-151). Together, Rrp2 and RpoS govern gene expression of proteins necessary for transmission from a tick to a vertebrate, and for establishing vertebrate infection (110, 152-154).

The Stevenson lab has long been interested in identifying and characterizing novel factors that regulate these processes. Previous work from the lab has identified BpuR, a DNA/RNA-binding protein unique to Spirochetes and eukaryotes, and EbfC, a DNA-binding protein found in all bacteria, as well as ascribed a role for plasmid BpaB proteins in gene regulation (38, 155-163). Most recently, SpoVG, which is conserved across many gram-positive bacteria, was identified as a DNA binding protein in *B. burgodorferi, Listeria monocytogenes* and *Staphyloccocus aureus* (164).

1.9 Initial studies on SpoVG

SpoVG was initially identified in 1981 (165, 166) in *Bacillus subtilis*, and was so named because it was determined to have some role in stage five of sporulation. Cells that lacked SpoVG were far less likely to complete sporulation(165, 167, 168). It was noted, however, that the few spores that did form were fully functional--they were resistant to sodium dodecyl sulfate (SDS) and could regenerate into active cells. The early studies noted that *spoVG* was transcribed during stage one of sporulation, and there appeared to be some evidence for self-regulation (165, 166, 168). Later in the 1990s, SpoVG was identified in a suppressor screen. The transcriptional regulator SpoIIB inhibits sporulation

at stage two. Sporulation was restored in a Δ*spoIIB B. subtilis* strain in which a non-sense mutation arose in *spoVG* (167, 169).

In the 2000s, SpoVG was identified as having some role in the regulation of capsule gene *esxA* in *Staphylococcus aureus*, although the mechanism of action remained unclear (170-173). While this work was in progress, two studies provided further insight into the mechanism of how SpoVG regulates gene expression. One study demonstrated that *S. aureus* SpoVG bound to DNA with a higher affinity when phosphorylated (174). Another study demonstrated that *L. monocytogenes* SpoVG bound to RNA with a higher affinity than either double-stranded or single-stranded RNA (175).

Studies from the Stevenson lab on the regulation of the outer surface protein VlsE identified SpoVG as binding to DNA. This was the first time a function had been ascribed to any SpoVG homologue. The same study demonstrated that SpoVG from *Listeria monocytogenes* and *S. aureus* also bind DNA (164). We hypothesized that SpoVG acts as a regulator in *B. burgdorferi,* and that SpoVG itself is regulated. The studies in this work aim to understand regulation of SpoVG by *B. burgdorferi* as well as what impact SpoVG has on the cell.

Figure 1.1 Enzootic cycle of *Borrelia burgdorferi*

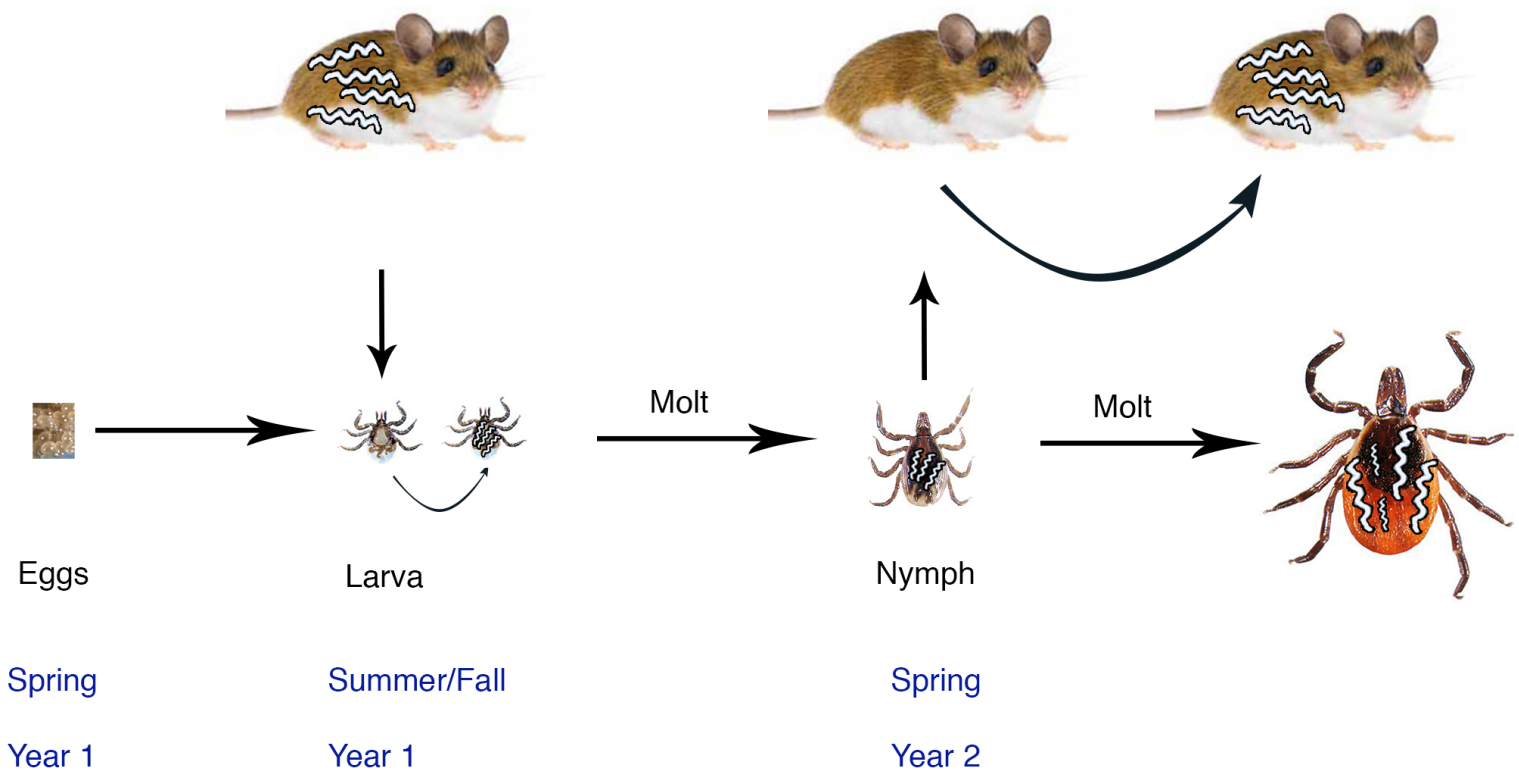

Ixodes scapularis eggs hatch free from *B. burgdorferi*. If a larvae feeds on a vertebrate infected with *B. burgdorferi*, spirochetes will pass along with the blood meal, and colonize the larvae. After molting, as the nymph feeds on a vertebrate, *B. burgdorferi* will transmit along with the blood meal, thus completing the enzootic cycle. Adult female ticks tend to feed on larger animals, such as deer, and do not contribute to spirochetal survival in the enzootic cycle.

CHAPTER 2. MATERIALS AND METHODS

2.1 Media and Stock Solutions

BSK-II	**1L**
ddH_2O	750 ml
CMRL (w/o glutamine) ThermoFisher	9.7 g
Neopeptone	4.18 g
Probumin	41.7 g

*Let stir to dissolve Probumin/Neopeptone (~20 min)

HEPES	5.0 g
Sodium Citrate	0.575 g
Glucose	4.175 g
Tc yeastolate (BD Biosciences)	1.68 g
Pyruvic acid	0.668 g
N-acetyl-D-glucosamine	0.333 g
Sodium bicarbonate	1.833 g

Add to media, let stir 20 min. pH to 7.6, QS to 1 L with ddH_2O. Filter through 0.45 µm, fitted with extra filter. Filter through 0.2 µm filter. Move into hood, aliquot 94 ml into 100 ml sterile glass bottles. Store at -20° C until needed. When ready to use, thaw one 94 ml bottle of BSK, and add 6 ml rabbit serum (Gibco) (final concentration 6% vol/vol). This is complete BSK.

BSK-II 1.5x for plates	**1 L**
Probumin	83.25 g
CMRL	14.6 g
Neopeptone	8.33 g
HEPES	9.99 g
Citrate, Sodium	1.22 g
Glucose	8.33 g
Pyruvic acid	1.33 g
N-acetyl-glucosamine (NAG)	0.67 g
Sodium Bicarbonate	3.66 g
TC yeastolate	4.23 g

Adjust pH to 7.5 with NaOH (takes a lot) stir slowly for minimum 3 hours
Filter sterilize through 0.45 µm then 0.2 µm filter. Aliquot 100 ml into a 400 ml bottle. Store at -20° C.

LB Broth	**500 ml**
Tryptone	5.0 g
Yeast extract	2.5 g
NaCl	5.0 g

** QS to 500 ml with ddH_2O, autoclave

LB Agar	**500 ml**
Tryptone	5 g
Yeast extract	2.5 g
NaCl	5 g
Agar (1.5% w/vol)	7.5 g

**QS to 500 ml with ddH_2O, autoclave, cool to 55° C in water bath, add antibiotic, mix by swirling. Pour plates, allow to dry for 24 hours upright, in a single layer, store at 4° C.

Super Broth (SB)	**1 L**
Tryptone	32 g
Yeast	20 g
NaCl	5 g

** QS to 1 L with ddH_2O, autoclave

SOC	**200 ml**
Bacto-Tryptone	4 g
Bacto-Yeast	1 g
NaCl	0.117 g
KCl	0.037 g

** QS to 200 ml with ddH_2O, autoclave

Antibiotics	**Stock conc.**	**Working/c. *E. coli***	**W/c *B.b***
Ampicillin	10 mg/ml	50 µg/ml	
Carbenicillin	10 mg/ml	50 µg/ml	
Chloramphenicol	34 mg/ml	34 µg/ml	
Gentamicin	3 mg/ml	15 µg/ml	150 µg/ml
Kanamycin	10 mg/ml	50 µg/ml	20 µg/ml
Streptomycin	10 mg/ml	50 µg/ml	100 µg/ml

PBS (Phosphate Buffered Saline)	**500 ml**
NaCl	4 g
KCl	0.1008 g
NaH_2PO_4	0.557 g
KH_2PO_4	0.10 g

**pH to 7.4, QS to 500 ml with ddH_2O. Autoclave.

EPS (Electroporation Solution)	**500 ml**
Sucrose	46.5 g
50% glycerol	150 ml

**QS to 500 ml, with ddH_2O Filter sterilize with 0.2 µM filter, store at 4° C.

Magne-His Washing/Binding buffer	**1 L**
HEPES 100mM	23.883 g
Imidazole 100mM	6.8 g
NaCl 100 mM	5.85 g

Magne-His Elution buffer	**100 ml**
HEPES 100mM	2.383 g
Imidazole 1M	6.8 g

EMSA Buffer	**1 L**
50% Glycerol	200 ml
0.5M EDTA	2 ml
PMSF (phenylmethylsulfonyl fluoride)	1 ml
1M Tris pH 7.5	50 ml
Tween-20	100 µl
KCl	3.72 g
DTT (dithiothreitol)	0.154 g

**QS to 1 Liter with ddH_2O, cool to 4° C for dialysis. Freeze 2 ml aliquots at -20° C for EMSA protocol.

EMSA 3xEO Buffer	**10 ml**
Tris-HCl 1M pH 8.0	1.5 ml
0.5M EDTA	60 µl
DTT 100mM	200 µl
Protease inhibitor (ThermoFisher)	240 µl
Phosphatase inhibitor (ThermoFisher)	60 µl
50% glycerol	6.0 ml
ddH_2O	1.84 ml

TBS-Tween	**16 L**
1 M Tris pH 7.5	320 ml
5 M NaCl	480 ml
Tween-20	8 ml
Sodium Azide	3 g

**QS to 16 L with ddH_2O, and store at room temperature.

20x Transfer buffer	**3 L**
Na_2PO_4 dibasic	181 g
$NaPO_4$ monobasic	31 g

**QS to 3 L with ddH_2O, store at room temperature.

SDS loading buffer	**1 L**
0.5 M Tris pH 7.5	1.0 ml
ddH_2O	1.0 ml
glycerol	1.5 ml
2-mercaptoethanol	0.8 ml
10% SDS	3.2 ml
0.1% (w/v) Bromophenol Blue	0.4 ml

**Combine in 15 ml Conical tube, store 4° C.

4x Resolving buffer for SDS-PAGE	**150 ml**
Tris Base	27.2 g
ddH_2O	100 ml

**pH to 8.8, QS to 150 ml with ddH_2O. Filter sterilize, store at 4° C.

4x Stacking buffer for SDS-PAGE	**150 ml**
Tris Base	9.1 g
ddH_2O	100 ml

** pH to 6.8, QS to 150 ml with ddH_2O. Filter sterilize, store 4° C.

EMSA Blocking buffer	**1 L**
NaCl	7.3 g
Na_2HPO_4	2.4 g
NaH_2PO_4	1 g
Sodium dodecyl sulfate (SDS)	50 g

**QS to 1 L with ddH_2O. Store in fridge. Warm to 55°C in water bath before use.

5x TBE	**1 L**
Tris Base	54 g
Boric acid	27.5 g
0.5 M EDTA pH 8.0	20 ml

**QS to 1 L with ddH_2O.

5x SDS Buffer for Protein gels	**1 L**
Tris base	15 g
Glycine	72 g
SDS	5 g

**QS to 1 L with ddH_2O.

Coomassie Blue stain	**500 ml**
MeOH	200 ml
ddH_2O	200 ml
glacial acetic acid	30 ml
Coomassie brilliant blue G250	0.8 g

Coomassie de-stain solution	**1 L**
ddH_2O	400 ml
MeOH	500 ml
Glacial Acetic acid	100 ml

EMSA loading dye	
Ficoll	15% (w/v)
Orange G	0.4% (w/v)

Nucleotide extraction buffer	**1 ml**
MeOH	400 µl
Acetonitrile (MS grade)	400 µl
ddH_2O	200 µl
Formic Acid	0.1 M

Pro-Q De-stain	**1 L**
1M Sodium acetate pH 4.0	50 ml
ddH_2O	750 ml
Acetonitrile (molecular grade)	200 ml

2.2 Bacterial Cultivation

Borrelia burgdorferi was grown in complete BSK-II medium, unless otherwise stated. *B. burgdorferi* grows much more slowly at 23°C than at 34°C, and as a result alters expression of numerous genes when grown at this temperature. For this reason, *B. burgdorferi* is occasionally cultured at 23°C in order to serve as a mechanism to perturb its growth.

In order to alter growth rate without altering temperature, two different deficient media were used, while culturing the bacteria at 34°C. One deficient medium consists of BSK-II that contains only 1.2% rabbit serum (instead of the usual 6%). The second deficient medium consists of 25% BSK-II diluted with PBS, but with the usual 6% rabbit serum.

In order to assess the effect of glycerol on growth rate, two different medias were used. In the first, glycerol was added to complete BSK-II medium to a final concentration of 4% (v/v). A simplified culture medium, BSK-Lite, contains all components of complete BSK-II except for glucose. Bacteria grow in BSK-Lite to a final density that is approximately 1 $\log_{10}$ lower than that achieved in complete BSK-II. This media was also complemented with either 0.4% glucose (w/v) or 0.4% glycerol (v/v).

Bacteria were aliquoted in individual stocks supplemented with 10% dimethyl sulfoxide (DMSO), and stored at -80°C until needed. To recover from frozen stocks, 500 μl of thawed bacterial stock was passaged into 5 ml fresh BSK-II at 34°C, and allowed to grow for a minimum of three days. Bacteria were visualized by dark field microscopy for density and movement, passaged 1:100 into fresh media, allowed to grow to mid-

exponential phase (approximately 10^7 bacteria/ml, which takes approximately 3 days), and then diluted 1:100 into fresh media for experiments.

E. coli was grown using either LB broth or on LB agar plates unless otherwise noted, with appropriate antibiotic as needed. Following transformation of *E. coli* with plasmids, bacteria were recovered in SOC broth. For plasmid purification, bacteria were grown overnight in Super Broth. For protein expression, bacteria were grown in Super Broth (SB). *E. coli* stocks were made by diluting mid-exponential phase culture 1:2 with 50% glycerol and maintained at -80°C. To recover from frozen stocks, a small scraping from the frozen stock was used to inoculate 50 ml LB with the appropriate antibiotic, and incubated at 37° C with shaking overnight.

2.3 Isolation of individual *Borrelia burgdorferi* colonies

Individual colonies of *B. burgdorferi* were isolated using BSK-II agarose plates. Agarose for the plates was prepared in the following manner. The percentage of agarose used is fairly high, since *B. burgdorferi* is highly motile. This ensures small, tight colonies that are easily distinguishable from one another. A 2.25 g molecular grade agarose (DO NOT USE LOW-MELT AGAROSE) was added to 80 ml ddH_2O, and autoclaved for 30 minutes. Next, 8 ml 5% (w/v) sodium bicarbonate was filter sterilized. While the agarose was autoclaving, one 100ml bottle of BSK-II 1.5x and 12 ml rabbit serum was thawed in a 55° C water bath. Thawed BSK, rabbit serum, and sodium bicarbonate were mixed together using aseptic technique and returned to the water bath. After autoclaving, the agarose was gently mixed by swirling, and allowed to equilibrate in the 55° C water bath for 30 minutes.

All of the agarose was added to the BSK under the hood, then returned to the water bath for 20 minutes. Under the culture hood, 15 ml of BSK-agarose mixture was added to each plate, and the BSK returned to the water bath. Plates were allowed to solidify for 1 hour. When ready to pour the second layer, 15 ml BSK-agarose was added to a sterile conical tube using a sterile pipette. 5 µl *B. burgdorferi* culture was added to the tube, gently mixed, then poured on top of a plate with a solidified layer of BSK-agarose. Plates were allowed to set for 1 hour at room temperature. Plates were incubated agar-side-up at 34° C with 3% CO_2. A pan with ddH_2O was placed in the bottom of the incubator to prevent the plates from drying out. Plates were incubated for approximately 2 weeks. Individual colonies were picked out with a sterile pipette tip, under the hood, and cultured in fresh BSK-II media.

2.4 Growth Curves

Borrelia burgdorferi cell density was assessed by enumerating cells/ml using a Petroff-Hauser counter under darkfield microscopy. A 5 µl culture, either undiluted, or diluted with PBS to an appropriate amount was added to the counter, and a cover slip carefully placed, resting on both edges of the counting frame. Four counting fields (each contain 16 large squares) were counted. To calculate the cell/ml density, the number from all four fields was averaged, multiplied by the dilution factor, and then multiplied by 50,000 as indicated by the manufacturer. Cells were counted once every 24 hours for cultures grown at 34° C, or once every 72 hours for cultures grown at 23° C, or cultures grown at 34° C in BSK + 1.2% rabbit serum and 25% BSK + 6% rabbit serum.

For the study using the *chA1* and *cheA2* mutants, the change in media color (acidification) was used as a proxy for growth rate. Cultures were set up in 5 ml screw-cap tubes as previously described, and analyzed in triplicate once every 24 hours. 150 µl culture was placed in the well of a 96-well culture plate. Three samples from each culture were taken for analysis. The plate was covered with an optically clear film, and read in a spectrophotometer set to read absorbance at 562 nm and 630 nm. The ratio of nm 562/630 was calculated for each well, and plotted for all cultures across 4 days.

2.5 Plasmid Construction

All plasmids were first cloned and transformed into *E. coli* DH5α. Plasmids were purified and sequenced for accuracy, then electroporated to *B. burgdorferi.* Plasmids were constructed either by Gibson assembly or restriction digest.

For Gibson cloning, oligonucleotide primers were designed to amplify both the plasmid backbone and the insert to be cloned. Each primer contained ~ 20 nucleotides that overlapped with its complementary primer. Each fragment was amplified using Expand High Fidelity polymerase (Sigma Aldrich). PCR products were run on a gel and purified using the WIZARD DNA clean-up kit (Promega). DNA fragments were mixed with isothermal assembly mix (NEB) and incubated for 60 minutes at 50° C. The mixture was then transformed into DH5α cells.

For cloning by restriction digest, the plasmid was digested with appropriate enzymes overnight at 37° C. DNA was extracted with phenol and chloroform, then briefly precipitated with ethanol. DNA pellets were briefly washed with 70% ice-cold ethanol. Pellets were allowed to dry before resuspending in ddH_2O. Plasmid and insert DNAs were

ligated together in 20 µl reactions with 4 µl 5x buffer, and 1 µl ligase. Mixtures were incubated for 1 hour at 37° C, then transformed into chemically competent *E. coli*.

2.6 Transformation of Bacteria with Foreign DNA

E. coli transformations were performed as follows: chemically competent cells (NEB) were thawed on ice and incubated with cloned products for 30 minutes, on ice. The cells were heat shocked at 45° C for 30 seconds, returned to ice, and 1 ml SOC media was gently added. The cells were allowed to recover for 1 hour at 37° C, then aseptically plated on LB Agar with appropriate antibiotic, and incubated agar-down overnight at 37° C.

E. coli electroporations were carried out in the following manner. A tube containing 10 ml LB with appropriate antibiotic was inoculated with a scraping of *E. coli* glycerol stock, and incubated overnight at 37° C with shaking. The following morning, a fresh 10 ml LB culture was inoculated 1:100 with the overnight culture, and incubated at 37° C with shaking until the OD reached between 0.3 and 0.5. Cells were harvested by transferring 2 ml culture into a 2 ml microfuge tube, and centrifuging at 14,000 RPM (24 x 1.5/2.0 ml rotor-ThermoFisher) for 15 minutes. The supernatant was removed, and cells gently washed with 500 µl ice cold autoclaved ddH_2O. Cells were centrifuged for 10 minutes at 10,000 RPM (24 x 1.5/2.0 ml rotor-ThermoFisher), washed with 500 µl ice cold ddH_2O, and centrifuged for 10 minutes at 10,000 RPM (24 x 1.5/2.0 ml rotor-ThermoFisher). Cells were gently resuspended in 50 µl ice cold ddH_2O, and 5 µl plasmid DNA was added. The mixture was transferred to a 1 mm electroporation cuvette, and placed into the cuvette bridge attached to a BioRad MicroPulser Electroporater with the following settings: charge

1.8kV, resistance 200 ohms, 25 μF. Both buttons of the electroporator were pushed simultaneously until the buzz could be heard. The contents of the cuvette were transferred to 250 μl SOC broth without antibiotic, and incubated in a heat block at 37° C for 30-45 minutes. Cells were then plated on an LB agar plate with antibiotic and incubated at 37° C overnight.

B. burgdorferi electrocompetent cells were prepared as follows: A 100 ml *B. burgdorferi* culture was grown to mid-log phase (about 5.0 x 10^7 cells/ml). Cells were harvested in a sterile centrifuge tube 6,000 rpm in a JA-17 fixed angle rotor for 10 minutes. The culture medium was decanted, and cells very gently resuspended in 10 ml ice-cold, filter-sterilized PBS, then transferred to a sterile 50 ml "oakridge" centrifuge tube. Cells were spun at 10,000 rpm for 10 minutes in a JA-10 fixed angle rotor, the supernatant removed, and bacteria resuspended in 10 ml ice-cold, filter-sterilized EPS. Cells were gently resuspended by swirling the oakridge tube (not shaken or vortexed). Cells were spun at 10,000 rpm in a JA-10 fixed angle rotor for 10 minutes, EPS removed, and 10 ml EPS added. Cells were gently resuspended as before. Cells were spun 10,000 rpm in a JA-10 fixed angle rotor for 10 min, EPS removed, and cells resuspended in 500 μl EPS. Aliquots were made with 50 μl of cells, then either electroporated right away, or stored at -80° C for later use.

10 μl DNA (as concentrated as possible (at least 200 ng/μl, ideally greater than 1 μg/μl) was added to a 50 μl aliquot of electrocompetent cells, and allowed to incubate on ice for 10 min. Cells were added to an electroporation cuvette with a 2mm gap, and placed into the cuvette bridge attached to a BioRad MicroPulser Electroporater set to charge 2.5kV, resistance 200 ohms, 25 μF. Both pulse buttons were pushed simultaneously until

a continuous beep was heard. Under the hood, about 200 µl BSK-II without antibiotic was added to the cuvette with a Pasteur pipette. Media was gently mixed up and down over the sides of the cuvette to ensure all the cells were taken up, then inoculated into 5 ml BSK-II. Cells were allowed to recover overnight before the appropriate antibiotic was added. Cells were allowed to grow for up to 4 weeks, and checked for the presence of living cells. If live cells were found, they were passaged 1:100 into fresh BSK-II plus antibiotic, allowed to grow to log-phase, then passaged 1:100 again.

To confirm the cells had taken up the DNA of interest, and had not spontaneously developed resistance to the antibiotic used, a 1 ml aliquot of cells from the second passage was harvested by centrifugation for 10 minutes at 10,000 RPM (24 x 1.5/2.0 ml rotor-ThermoFisher). Cells were washed 2x with PBS, then lysed in 100 µl water, and boiled 10 minutes. Cell debris was removed by centrifuging at 15,000 RPM (24 x 1.5/2.0 ml rotor-ThermoFisher) for 1 minute. 1µl of the supernatant was used as the DNA template for confirmatory PCR.

2.7 Colony PCR

Colonies from *E. coli* transformations were screened for the presence of the correct plasmid with the correct insert in the following manner. First, 0.6 ml microfuge tubes were labeled with a number 1- X, where X stands for the number of colonies to be screened. 50 µl ddH_2O was added to each one. An LB plate made with the appropriate antibiotic was prepared by drawing a grid on the bottom of the plate with a sharpie. Each box on the grid was labeled with a number 1- X. Using an autoclaved toothpick, a single bacterial colony was picked up, being careful not to gauge the agar, swirled in the 50 µl ddH_2O, then spread

on the corresponding box on the LB reference plate. Once all of the colonies were prepared, the plate was placed in the 37° C incubator, and the tubes with water and bacteria were boiled for 10 minutes in a heat block. After boiling, the tubes were centrifuged for 1 minute at max speed. 10 µl PCR reactions were set up. A master mix was prepared that included Water, Taq buffer, dNTPs, forward and reverse primers, and Taq polymerase. 9 µl of the master mix was pipetted into each PCR tube, then 1 µl DNA (from the picked colonies) was added to the corresponding tube. After amplification in the thermocycler, 2 µl loading dye was added to each PCR mix, then run on an agarose gel, stained with Ethidium bromide, and imaged on a UV transilluminator.

2.8 Recombinant Protein Purification

Day 1: Prepare overnight culture

A culture of *E. coli* Rosetta II transformed with plasmid pCRS2 was inoculated into SB media with appropriate concentrations of carbenicillin and chloramphenicol, and grown overnight at 37° C with shaking.

Day 2: Protein induction

The following morning, two 1 L cultures of SB were each inoculated with 10 ml of the overnight culture and appropriate antibiotics. Cultures were grown for 4 hours at 37° C with shaking, then induced with 1 mM isopropyl-beta-D-thiogalactoside (IPTG) (final concentration) for 2 hours. Cells were harvested by centrifugation for 20 minutes at 6,000 RPM in a JA-17 fixed angle rotor. Supernatant was removed, cell pellets scraped into a single centrifuge tube, and stored at -80° C overnight.

Day 3: Protein purification

The following day, the cell pellet was thawed and resuspended in 50 ml ice-cold washing/binding buffer. The mixture was transferred to a 100 ml flask, with 2 ml Bper lysis (Thermo Fisher) buffer added. Cells were lysed by sonication at amplitude 20% 15 seconds on, 30 seconds off until solution turned a milky color (approximately 10-15 cycles). Solution was stirred in between each sonication. Lysed cells were then centrifuged at 15,000 RPM in a JA-10 fixed angle rotor for 30 minutes to separate the soluble proteins from the insoluble fraction.

Following centrifugation, lysate was poured over 1 ml Magne-His beads (Promega) in a 50 ml conical tube and incubated at 4° C for 1 hour while rocking. The conical tube was placed in a magnetic holder and rocked at 4° C for 15 minutes to allow the beads to adhere to the side of the tube. While the conical tube was still in the magnetic holder, the lysate was poured off, and 40 ml washing/binding buffer added. The conical tube was taken out of the magnetic holder, gently shaken to mix the beads, then incubated for 15 minutes at 4° C, while shaking. The conical tube was placed back in the magnetic holder for 5 minutes at 4° C, while shaking. The washing steps were repeated 3 more times.

Finally, after the fourth washing/binding buffer had been removed, the conical tube was taken out of the magnetic holder, placed in ice, and 1 ml of washing/binding buffer was used to wash the beads down the side of the tube. The beads were transferred to a 2 ml microfuge tube, placed in a magnetic holder, and rocked to allow the beads to adhere to the side of the tube. The Washing/binding buffer was removed. 1 ml Magne-His elution buffer was used to wash any remaining beads from the 50 ml conical tube, added to the 2 ml microfuge tube with the remaining beads, gently shaken to mix the beads, then incubated

at 4° C, while shaking for 5 minutes. The microfuge tube was placed in the magnetic holder, and the elution buffer was carefully removed, and placed in a clean 2 ml microfuge tube, on ice. The elution steps were repeated 3 more times. 1 small section of dialysis Snakeskin membrane (Thermo-Fisher) was cut, and sealed closed on both ends with plastic green clips, and allowed to rehydrate in 1 L EMSA buffer at 4° C. One clip was removed, all 4 mls of elution were added to the snakeskin, the clip returned to seal the dialysis bag, and placed in the EMSA buffer at 4° C overnight to dialyze.

Day 4: Concentrate protein, and measure concentration by BCA assay

Dialysis membrane was carefully opened by removing one of the clips, and contents transferred to 2 ml microfuge tubes pre-chilled on ice. Microfuge tubes were centrifuged at 15,000 RPM (24 x 1.5/2.0 ml rotor-ThermoFisher) at 4° C for 1 minute to remove any residual beads or aggregated protein. Supernatant was transferred to fresh 2 ml microfuge tubes, chilled on ice. Contents were then transferred to a centrifuge concentrator, size 10,000 Kda for rSpoVG. Protein was concentrated to a total of 200-500 µl, aiming for a NaonoDrop reading of greater than 1mg/ml concentration. Protein was aliquoted by 15 µl into either PCR tubes or 600 µl Microfuge tubes and flash frozen in liquid nitrogen. Protein aliquots were store at -80° C until needed.

Protein concentration was measured using a Micro BCA kit (Thermo Scientific). Purified rSpoVG was diluted 1:10 and 1:100 in ddH_2O, and all of the standards were diluted in ddH_2O as well. The working range of the kit is 2-40 µg/ml. Use of the two different dilutions was to ensure that one of them fell within the range that can be accurately measured.

Standards were prepared as follows:

Vial	ddH_2O	Volume of bovine serum albumin (BSA)	Final concentration
A	900 µl	100 µl (2 mg/ml stock)	200 µg/ml
B	1200 µl	300 µl of vial A	40 µg/ml
C	800 µl	800 µl of vial B	20 µg/ml
D	800 µl	800 µl of vial C	10 µg/ml
E	800 µl	800 µl of vial D	5 µg/ml
F	800 µl	800 µl of vial E	2.5 µg/ml
G	960 µl	640 µl of vial F	1 µg/ml
H	800 µl	800 µl of vial G	0.5 µg/ml
I	500 µl	0	0 ug/ml

Prepared the working solution by mixing 5 ml Reagent A with 4.8 ml Reagent B and 200 µl Reagent C in a reservoir for multi-channel pipettes. 150 µl of each standard and purified protein was pipetted into a microplate well. Technical triplicates were set up for all standards and purified proteins. Using a multichannel pipette, 150 µl of the working solution was added to each well and mixed by carefully pipetting up and down without introducing bubbles. The plate was covered and incubated at 37° C for 2 hours. The plate was read on a spectrophotometer by measuring the absorbance at 562 nm. A standard curve was generated in Prism 6 using a best-fit polynomial equation (nonlinear equation). From this, the concentration of the purified proteins was derived.

2.9 RNA Extraction

RNA was purified from *B. burgdorferi* cells in the following manner:

B. burgdorferi was inoculated 1:100 into fresh media (typically 5 ml) and grown to mid-log phase unless otherwise noted. Cells were harvested by centrifugation for 10 minutes, 4° C, 15,000 RPM in a JA-17 fixed angle rotor. The culture media was decanted, and cell pellets gently resuspended in 1ml PBS by carefully flicking the centrifuge tube. Cells were transferred to 1.6 ml Microfuge tube and centrifuged for 10 minutes at 4° C, 10,000 RPM (24 x 1.5/2.0 ml rotor-ThermoFisher). The supernatant was removed, 1ml Trizol added to the cell pellet, and incubated at 70° C for 10 minutes. Trizol-lysates were stored at -80° C until further use.

Trizol-lysed cells were thawed on ice, then 200 µl 1-Bromo 3-Chloropropanol was added, tube shaken (not vortexed) and incubated 3 minutes at room temperature. Tubes were centrifuged for 15 minutes at 4° C, 12,000 RPM (24 x 1.5/2.0 ml rotor-ThermoFisher). Taking care not to disturb the separated phases, the aqueous phase was transferred to a fresh RNAse-free microfuge tube. 500 µl Isopropanol was added, tubes shaken, then incubated for 10 minutes at room temperature. Tubes were centrifuged for 10 minutes at 4° C, 12,000 RPM (24 x 1.5/2.0 ml rotor-ThermoFisher). Liquid was removed, taking care not to disturb the small white pellet. The pellet was washed by pipetting 1 ml of 75% EtOH, without dislodging the pellet. Tubes were centrifuged for 10 minutes at 4° C, 12,000 RPM (24 x 1.5/2.0 ml rotor-ThermoFisher). Liquid was carefully removed, and pellets allowed to dry by propping the tubes upside-down (with the lids open) on kimwipes.

RNAsecure (Roche) was preheated for 10 minutes at 60° C. RNA pellets were suspended in 20 µl RNA secure, and incubated for 10 minutes at 60° C.

DNAse treatment

10x DNase buffer and the inactivation reagent were thawed on ice. 2.5 µl DNase buffer was added to each tube, then 3 µl DNaseI (Roche) was added. Tubes were incubated for 30 minutes at 37° C. Tubes were then placed on ice, and DNase inactivation reagent was vortexed. 10 µl DNase inactivation reagent was added to each tube, and briefly vortexed. Tubes were incubated for 2 minutes at room temperature. Tubes were then centrifuged for 5 minutes at 4° C, 5,000 RPM (24 x 1.5/2.0 ml rotor-ThermoFisher). The top phase containing the RNA (clear, not opaque), was transferred to fresh RNAse-free microfuge tubes.

Assessing RNA purity

RNA integrity was analyzed using an Agilent 2100 Bioanalyzer following the RNA 6000 Nano Kit protocol (Agilent technologies).

Preparing cDNA libraries

20 µl reactions were set up to make cDNA using the iScript cDNA synthesis kit from BioRad. Each reaction contained 4 µl of 5x iScript cDNA buffer, ~500 ng RNA, 1 µl Reverse transcriptase and RNase-free H_2O. No Reverse Transcriptase controls (no-RT) were set up to set for DNA contamination. These reactions contained 2 µl RNA and 18 µl RNAse-free H_2O. Reactions took place in a thermocycler, programed for 5 min at 25° C, 20 min at 46° C, 1 minute at 95° C.

cDNAs were then diluted 1:100 in nuclease-free water for analysis by qRT-PCR.

2.10 Quantitative Reverse Transcriptase Polymerase Chain Reaction (qRT-PCR)

qRT-PCR reactions were set up in 96 well plates for thermocycle analysis (BioRad). The first reaction used primers for *flaB*, and analyzed all samples, including the no-RT controls. If *flaB* did not amplify in the no-RT controls, they were not included in subsequent analyses. Each reaction contained the following:

5.0 µl	Sybr Green Master Mix (BioRad) (Sybr Green, polymerase, buffer)
0.125 µl	Primer 1
0.125 µl	Primer 2
2.75 µl	Nuclease-free water
2.0 µl	cDNA

The Sybr Green master mix was covered in aluminum foil and thawed on ice. A master mix was made containing the Sybr Green Master Mix, both primers and water. Enough was made for each cDNA to be analyzed in triplicate. Working quickly, but carefully, 8 µl was pipetted into each well. Then 2 µl cDNA was added to each well. The plate covered in a clear plate cover (BioRad), and centrifuged for 5 minutes at 4° C, 2,000 RPM (24 x 1.5/2.0 ml rotor-ThermoFisher) to ensure the mixture was situated in the bottom of the well. The plate was then placed in the BioRad light cycler, and set for the following parameters:

95° C	2:00 minutes	
95° C	0:05 minutes	X 40 cycles
60° C	0:30 minutes	

Next, the plate was set up in the software, with all variables input into the correct well. The sample, the gene targeted, and whether the sample was unknown or a no-RT control. The technical replicates were grouped together so that the standard deviation for them could be calculated.

qRT-PCR Analysis

Data from the Thermocycler run was checked for quality control in the following manner. First, the Relative fluorescent units (RFUs) should be in the10,000-99,000 range. If the maximum RFUs of a run are in the hundreds or low thousands, that suggests that either the Sybr Green or polymerase is no longer active. The entire assay should be re-run using a fresh vial of the Sybr Green Master Mix. Next, the standard deviation for each technical replicate was checked, to ensure that all were less than 0.3. High standard deviations are an indication of poor pipetting, which will introduce a high amount of error into the calculations. Finally, the quantification cycle (Cq) of all *flaB* amplifications were analyzed to ensure that all samples were within just a few Cqs of each other, and that they fell between a range of 17-22 Cqs. If too much or too little cDNA is loaded, this can also introduce a high amount of error.

Once the data were checked for quality control, and *flaB* from the no-RT samples did not amplify, all other genes of interest were run. After all data were collected, the *flaB* Cq was subtracted from each gene of interest for all samples. This is termed as ΔCq. In order to ascertain whether a particular gene was differentially expressed in one strain of *B. burgdorferi* versus another, t-tests were performed on the difference in ΔCq between one strain (or condition) and another. The difference in ΔCq between one strain (or condition) and another is also termed the ΔΔCq. The measurement can also be used to ascertain

whether the difference in expression of a particular gene is different between different strains or conditions. The data were plotted using the GraphPad Prism software.

2.11 Western Blotting

Lysates for Western Blots were prepared in the following way. *B. burgdorferi* were grown to mid-log phase, unless otherwise stated, and cells harvested by centrifugation for 10 minutes at 4° C, 15,000 RPM in a JA-10 fixed angle rotor. Supernatant was poured off, and pellet allowed to dry briefly by propping the centrifuge tube upside down for about 5 minutes. PBS (1 ml) was added, and cells gently resuspended by flicking the bottom of the tube until the cell pellet was dislodged and broken up. The cells were then transferred to a 1.6 ml microfuge tube, and centrifuged for 10 minutes at 4° C, 10,000 RPM (24 x 1.5/2.0 ml rotor-ThermoFisher). Supernatant was removed and cell pellet dried using a Pasteur pipette fitted with a fresh sterile pipette tip attached to a vacuum hose. Cell pellets were stored at -80° C at least overnight, until ready to be used. Cell pellets were taken out of the -80° C freezer, and an aliquot of SDS loading buffer was added, and mixed by pipetting up and down. The amount of buffer used depended on the size and density of the initial culture. For 5 ml mid-log *B. burgdorferi* culture, 200 µl of SDS loading buffer was added. Whole cell lysates were boiled for 10 minutes, and stored at 4° C until further use.

<u>Making SDS-PAGE gels</u>

12.5% SDS polyacrylamide gels were prepared for protein separation, unless otherwise noted. To make 4 gels, the following was used:

Resolving Gel

ddH_2O	12.63 ml

Bisacrylamide	16.68 ml
4x Resolving buffer	10 ml
10% SDS	0.40 ml
10% Ammonium persulfate	0.30 ml
TEMED	0.10 ml

Stacking Gel

ddH_2O	6.0 ml
Bisacrylamide	1.34 ml
4x Resolving buffer	2.5 ml
10% SDS	0.10 ml
10% Ammonium persulfate (APS)	0.05 ml
TEMED	0.05 ml

All components of the resolving gel except the APS and TEMED were combined in a 50 ml conical tube. Four empty 1.5 ml cassettes were set up in a rack, with appropriate combs sitting to the side. The pipetman was fitted with a 25 ml glass pipette, and set to the side ready to pick up. Working carefully but quickly, the APS and TEMED were added. Without pipetting up and down, the solution was gently mixed by swirling the glass pipette around in the solution for 1-2 seconds. As much of the solution as will fit in the pipette was taken up, then each cassette filled up to the 3rd line. The cassette was sealed by placing the comb in the top, and solution allowed to polymerize at least 15 minutes. If any bubbles formed at the interface between the gel and air, they were popped by sliding the corner of a piece of paper down into the cassette, before the comb was placed.

Same steps were repeated for the stacking gel, although a 10 ml glass pipette was used, and the solution pipetted until the cassette just overflowed. When placing the combs, it was imperative not to introduced bubbles. Therefore, the comb was introduced at an angle, starting at one end of the cassette, and letting the comb fall/pushing it into the cassette from there.

Running the gels

Page Ruler-Plus (5 µl) was loaded into the first lane. Equal amounts of lysate were loaded into the subsequent lanes (measured by FlaB quantity). Generally, if the blot was to be probed for FlaB, 5 µl of lysate was used, since it is abundantly expressed. For probing of most other proteins, 10 µl was used. Gels were run at 200 volts for 50-60 minutes.

Transferring proteins from gel to nitrocellulose membrane

Gel cassettes were cracked open using a metal spatula, then the bottom ridge of the gel, and the stacking portion of the gel cut off. A plastic cassette was placed in a glass tray filled with 1x phospho-transfer buffer. One black sponge was placed on top of the black side of the cassette, then a piece of filter paper placed on top. Being careful not to touch the gel, it was transferred onto the filter paper, and the metal spatula was used to gently smooth out any bubbles. Using tweezers, 1 piece of nitrocellulose paper was placed on the gel, and bubbles smoothed out with the spatula. One piece of filter paper was placed on top of the nitrocellulose, then the other black sponge placed on top. Once again, the spatula was used to ensure there were no bubbles present. The plastic sandwich cassette was closed, and placed in the transfer rig (BioRad). The cassette was placed in the red/black holder arranged so the black side of the cassette faced the black side of the holder. An ice

pack was placed in the empty space, touching the black side of the holder. Proteins were transferred at 35 volts for 60 minutes.

Blocking and Probing

After the transfer was set up, 50 ml TBS-T was poured into a plastic holder, 2.5 grams of non-fat milk added, and placed on a rocker so the milk could mix thoroughly during the transfer. Once the transfer was completed, the cassette was opened clear side up, as it is easier to peel the nitrocellulose membrane off the gel, than to peel the gel off the membrane. Using tweezers, the membrane was placed face-up (note the side that has the colored ladder) in the milk, and allowed to block at room temperature for 1 hour, while rocking.

The milk was then poured off, about 10 ml of TBS-T was added, shaken vigorously, then poured off to remove most of the remaining milk. About 20 ml TBS-T was added, then allowed to wash for 5 minutes at room temperature, while shaking. TBS-T was poured off, fresh TBS-T was added, allowed to wash for 5 minutes at room temperature, while shaking. TBS-T was poured off, and primary antibody added. Primary antibodies were incubated for 1 hour, at room temperature, while shaking, unless otherwise noted. Primary antibodies were returned to their conical tube and stored at 4° C for future uses.

Note: antibodies were diluted in TBS-T, which has a small amount of sodium azide to help prevent mold from growing. If some mold does grow in the antibody, it will be evident by a western blot that has many bands that are recognized that shouldn't have been, and splotches all over the blot. If this occurs, the antibody can be filtered using a 0.22 μm filter into a sterile conical tube.

After the primary antibody was removed, 10 ml TBS-T was added, and vigorously shaken for 5 seconds to remove the majority of the antibody. That TBS-T was poured off, 20 ml TBS-T added, and allowed to wash for 10 minutes at room temperature while shaking. The TBS-T was poured off, 20 ml TBS-T added, and allowed to incubate for 10 minutes at room temperature with shaking.

Finally, the secondary reagent was added. Protein A-conjugated to HRP (horse radish peroxidase) was diluted 1:5,000 in TBS-T. The blot was transferred to a small plastic holder, 10 ml of secondary solution was added, and incubated for 1 hour at room temperature, while shaking.

For use with the fluorescently tagged antibodies, the blot was transferred to a red box with lid. All antibodies were diluted in TBS-T, and 50 ml was used. IRD800/α-Mouse and IRD800/α-Rat were diluted 1:25,000, and IRD700/α-Rabbit was diluted 2:25,000. All were incubated for 1 hour at room temperature with shaking.

All secondaries were washed in the same manner before imaging. The antibody was poured off (secondaries were not re-used), and a small amount of TBS-T was added, briefly shaken to remove excess antibody. 20 ml TBS-T was added, and allowed to wash for 10 minutes at room temperature with shaking. This was poured off, fresh 20 ml TBS-T was added, and allowed to wash for 10 minutes at room temperature with shaking.

Protein A was imaged in the following manner: 5 ml of Luminol and 5 ml of peroxide solution were added to the blot, and covered with tin foil. The blot was imaged by multiple exposures to x-ray film, which then developed.

The IRD-conjugated antibodies were imaged directly after the last wash using the Li-Cor Odyssey. There is no password to login in to the computer. Once the Odyssey

software is opened, select new, then find your folder (Mine is named 'Savage' and saved to the desktop. All my files are named for the date on which they were imaged). Create a new file with the date. Select the blue arrow at the top of the screen. The user name is 'user' and the password is 'user'. At this point, select the area of the blot on the grid, then check the appropriate channel, and 'Preview' to find the appropriate intensity. After the appropriate intensity is found, select 'medium' quality and '89' resolution. Now click 'scan' to generate a useable file. After the scan is complete, click 'save' after the file is saved, click 'File' -> 'Export' -> 'Colorized TIF' to generate a file that can be saved and read by imageJ and Photoshop.

2.12 Creating Images

All Files, whether scanned images of x-ray film, or digital files from BioRad or Odyssey were converted to black and white in ImageJ, and appropriately cropped. The file was saved as a TIF, then opened in Photoshop to add appropriate headings, etc. Final images for journals were assembled in photoshop, and always saved as TIF files.

2.13 Electrophoretic Shift Assays (EMSAs)

Electrophoretic mobility shift assays (EMSAs) were performed using nucleotides in one of the following manner. Unlabeled DNA imaged by staining with Gel Star (Lonza), labeled with biotin, and imaged with streptavidin conjugated to HRP, or labeled with a fluorophore, and imaged on either an Li-Cor Odyssey or BioRad Chemidoc. All methods will be described in detail below, but using nucleotide probes conjugated to a fluorophore (either Alexa488 or IRD800 work well) is the preferred method. No downstream transfer,

block, incubation with streptavidin, washing, etc steps are needed as with the biotin labeled probes: simply run the gel and image on either a Li-Cor Odyssey or BioRad Chemidoc right away. And these probes are far more sensitive when imaged than staining with Gel Star, meaning far less probe is needed, and binding kinetics can be measured far more accurately.

Preparing the probes

Both DNA and RNA probes were used in EMSAs. Initially, a large sequence was hypothesized to be bound by DNA. In this instance, primers were designed to amplify the whole region by PCR. At the stage of designing primers (ordered from Integrated DNA Technologies), molecules can be added to the 5' ends. Only one primer was ordered with a modification. Long probes were generated by amplifying the region of interest using Q5 high fidelity polymerase (NEB). The entire PCR product was run on an agarose gel and stained with ethidium bromide to ensure the correct size had been generated. The correct band was cut out and purified using a PCR clean-up Wizard kit (Promega).

Once the binding region had been narrowed to less than 60 base pairs, complimentary oligos (one with a modification) were ordered of the exact size needed. 60 base pairs was used as the cut off, as primers that are longer than 60 base pairs are far more expensive. These oligos were annealed together by combining in equal parts (30 μM final concentration) in a PCR tube, heated to 95° C for 5 minutes in a thermocycler, then allowed to slowly cool to room temperature (on the bench) for a minimum of 1 hour before using. Annealed probes were diluted to a concentration of 1-5 ng/μl for use in EMSAs.

RNAs less than 60 base pairs, that contained the same nucleotide sequence as the DNA probes (albeit with uracil instead of thymidine) were also ordered, with a

modification on the 5' end. RNAs were diluted to 100 μM using nuclease-free water. RNAs were further diluted (down to 25 nM – 5 μM), aliquoted in nuclease-free microfuge tubes and stored at -80° C.

Setting up the reactions

Protein aliquots and RNA aliquots (when applicable) were thawed on ice. For the probes modified with a biotin, 25 μl reactions were set up in the following manner.

All reactions were set up in 0.6 ml microfuge tubes. Competitors were unlabeled, and diluted to 100x the concentration of the labeled probe. These either contained the same sequence as the probe (specific competitor) or a different sequence (non-specific competitor).

The Master Mix contained 65.3 μl 3xEO buffer, 14 μl Poly-dI-dC (ThermoFisher), 88.7 μl ddH_2O.

Master Mix	EMSA buffer	Protein	Probe	competitor
11.5 μl	to final 25 μl	0-4 μl	1 μl	0-1 μl

All reactions contained 11.5 μl Master mix and 1 μl Probe (either DNA or RNA, diluted to the appropriate amount). One reaction contained only master mix, EMSA buffer and probe. The next few also included protein, in increasing amounts. The next included protein as well as non-specific competitor. The next included protein as well as specific competitor. All reactions contained enough EMSA buffer to make the final total volume 25 μl. All reactions were incubated at room temperature for 15 minutes.

2.5 μl EMSA loading dye was carefully added to each reaction, which were then loaded into a 6% TBE precast gel (ThermoFisher) that had been pre-run for 30 minutes. Gels were run at 100 volts for 45-100 minutes, depending on the length of the probe. Gels

were set up in rigs designated and marked “For EMSA Only” to avoid contamination with SDS. 0.5x TBE was used as the running buffer.

DNA was transferred to positively charged Nylon membrane (GE) in the following manner. Plastic cassettes were set up in a glass dish filled with 0.5x TBE. One black sponge was placed on the black side of the cassette, then a piece of filter paper placed on top. The gel was carefully transferred to the filter paper, and any bubbles gently removed using a metal spatula. The nylon membrane was placed on top of the gel, and the corner just above the top of the first loaded lane was cut, to help orient the membrane when imaging. Once again, bubbles were pushed out with the spatula. A piece of filter paper was placed on top of the membrane, with the other black sponge on top of that. Any bubbles were firmly pressed out with the spatula, then the cassette closed, and placed inside the cassette holder oriented so the black side of the cassette faced the black side of the holder. The holder was placed in the transfer apparatus oriented so the ice block is against the black side of the holder. Once both the cassette holder and the ice block were placed in the transfer apparatus, it was filled with the 0.5x TBE in the glass tray. A small layer of ice was placed in a large ice bucket, then the transfer apparatus placed in the ice bucket, and the ice bucket was packed full of ice. The transfer took place at 45 volts for 45 minutes.

While the transfer took place, the blocking buffer and 4x Wash Buffer (stored at 4° C) was pre-warmed to 50° C in a water bath. After the transfer was complete, the membrane was transferred face up into a plastic box with 20 ml Blocking buffer, and incubated at room temperature for 15 minutes with gentle shaking. The blocking buffer was poured off, fresh 20 ml blocking buffer plus 70 µl streptavidin-HRP was added, and incubated at room temperature for 15 minutes with gentle shaking.

1x Wash buffer was prepared by mixing 40 ml 4x Wash buffer with 120 ml ddH_2O. The streptavidin mixture was poured off, and about 40 ml of 1x Wash buffer was added, quickly shaken, then poured off to remove excess streptavidin. Approximately half of the remaining wash buffer was added, and incubated at room temperature for 10 minutes with gentle shaking. After the wash buffer was removed, the remaining wash buffer was added to the membrane, and incubated at room temperature for 15 minutes with gentle shaking.

After the last wash buffer was removed, 30 ml of Equilibrium buffer was added, and quickly shaken. The equilibrium buffer was removed, and 6 ml of Luminol solution, and 6 ml Peroxide solution (ThermoFisher) were added to the membrane, and the box covered in aluminum foil to protect from light. The membrane, x-ray film and cassette were immediately developed.

2.14 In *Silico* Proteomic Analyses

The *B. burgdorferi* cyclic di-AMP synthase gene (termed *cdaA),* was identified and analyzed in the following manner. Using Blast-P, the *B. burgdorferi* B31 genome was searched against the c-di-AMP synthase from *Chlamydia trachomatis* (GenBank locus number YP_007715533). *B. burgdorferi* gene Bb_0008 was identified as a homologue. The predicted sequence of *B. burgdorferi* CdaA was aligned with sequences of other previously-defined c-di-AMP synthases: *Bacillus subtilis* CdaA (formerly YbbP, GenBank locus BAA19509), *Listeria monocytogenes* DacA (GenBank locus BN389_21520), *Staphylococcus aureus* (GenBank locus SAV2163), and *C. trachomatis* DacA (GenBank locus YP_007715533) using Clustal X.

2.15 Nucleotide Extraction and cyclic-di-AMP analysis in *E. coli* and *B. burgdorferi*

For nucleotides extracted from *E. coli*, an overnight culture was grown in LB media. The next morning, cultures were diluted 1:1000 (2 µl into 2 ml) in fresh LB with 1 mM IPTG. Cultures were grown for 3 hours, then cells were harvested by centrifuging at 15,000 RPM (24 x 1.5/2.0 ml rotor-ThermoFisher) for 1 minute.

For nucleotides extracted from *B. burgdorferi*, two 5 ml AG1 cultures were set up by diluting mid-log cultures 1:100. One culture contained 0.5 µg/ml ATc. Cultures were grown for 3 days, and harvested by centrifugation at 15,000 RPM (24 x 1.5/2.0 ml rotor-ThermoFisher) for 15 minutes.

Once the cells were harvested, the supernatant was removed, cell pellets resuspended in 1 ml ice cold extraction buffer (made the day before using) and transferred to a fresh 1.6 ml microfuge tube. Tubes were incubated at -20° C for 30 minutes, then centrifuged at 15,000 RPM (24 x 1.5/2.0 ml rotor-ThermoFisher) for 5 minutes to pellet cellular debris. The supernatant was transferred to a fresh 1.6 ml microfuge tube, and stored at -80° C until ready to ship. Samples were shipped on dry ice to Chris Waters at Michigan State University. c-di-AMP was quantified by ultra-performance liquid chromatography—tandem mass spectrometry (UPLC-MS/MS) of equal volumes of each bacterial extract, and analyzed as previously described.

2.16 RNA Sequencing and Analysis

Wild-type, *spoVG*-ON, and Δ*spoVG* cultures were grown in triplicate to mid-log phase. Cells were harvested by centrifugation, the supernatant was removed, and cells were

gently resuspended in PBS. The supernatant was removed, and cells stored at -80° C until further use. Frozen cell pellets were shipped on dry ice to igenbio (Chicago IL) for RNA extraction, library preparation, and sequencing.

RNA was extracted with Maxwell RSC simplyRNA Cells kit based on manufacturer's instructions. RNAseq libraries were prepared from total RNA utilizing the ScripSeq kit from Illumina, according to manufacturers instructions. 100ng of total RNA was used as input to the ribo-zero depletion reaction. Following fragmentation and terminal tagging, the cDNA was subjected to 15 cycles of amplification. Resulting amplified libraries were bead cleaned and pooled for sequencing on Illumina NextSeq at 2x75 bp sequencing.

2.17 MS/MS on SpoVG in cultured *B. burgdorferi* and recombinant protein

Lysates were prepared from wild-type and *spoVG*-ON cultures grown at 34° C and 23° C as described for western blots, and separated on a 12.5% SDS-PAGE gel. The gel was briefly stained with Coomassie, then thoroughly de-stained. Bands in each lane that ran just above the 10 kDa ladder were excised and given to the UK mass spectrometry Core Facility for analysis. Similarly, rSpoVG was incubated with either 1 µl EMSA buffer or 1 µl of 1mM acetyl-phosphate at 37° C for 1 hour, and run on a 12.5% SDS-PAGE gel. Purified recombinant SpoVG that had been incubated at 37° C for 1 hour either with or without acetyl-phosphate was run on a 12.5% SDS-PAGE gel, and stained with Coomassie. The bands were excised and submitted to the mass-spectrometry core for analysis.

Gel samples were treated with DTT, iodoacetamide (IAA), and digested with trypsin. The tryptic samples were filtered through a 0.22um PVDF filter and subjected to

LC-MS/MS analysis. Data dependent decision tree with ETD (DDDT) was applied. MS data sets were searched in MASCOT against a custom database containing only rSpoVG protein sequence. Dynamic Modifications including acetylation on lysine and phosphorylation on serine, threonine and tyrosine were used.

2.18 In *Silico* Modeling of SpoVG Structure

spoVG gene sequence was converted to protein sequence by Expasy Translate (https://web.expasy.org/translate/). The protein sequence was then fed into PHYRE2 protein fold recognition server (http://www.sbg.bio.ic.ac.uk/phyre2/html/page.cgi?id=index). $SpoVG_{Bb}$ was modeled with greater than 90% onto the crystal structure 2IA9, which is the *Bacillus subtilis* subspecies subtillis strain 168 SpoVG (DOI: 10.2210/pdb2IA9/pdb). Both the Phyre2 generated structure and structure 2IA9 were downloaded and opened using the PyMOL software (https://pymol.org/2/). Structures were over-layed on one another, and visualized using the ribbon structure.

2.19 Mouse Infection Studies

All animal procedures were approved by UK IACUUC. B31-A3, CS8, CS9, B31-S9, and GK1 *B. burgdorferi* strains were grown to mid-log phase, and cells harvested by centrifugation at 10,000 x RPM (24 x 1.5/2.0 ml rotor-ThermoFisher) for 10 minutes. Cells were resuspended in PBS to a final concentration of 1 x 10^6 cells per 100 µl (verified by counting). Six female Balbc-J mice (JAX) were infected with each strain. Syringes (1 ml) were fitted with size 28 hollow needle, and filled with appropriately concentrated bacteria.

Mice were briefly anesthetized by placing them in a glass drop Jar filled with a bed of tissues. Heavy mineral oil (5 ml) and 5 ml Isoflurane were added just prior to addition of mice. Two mice were anesthetized at a time, just until they lost consciousness. Mice were infected by injecting 100 µl containing 1 x 10^6 bacterial cells into the peritoneum. Mice were then transferred to a fresh cage (3 mice per cage) and monitored to ensure they recovered completely, then returned to animal facilities. Mice were observed the following day to ensure they were all alive, and showing no signs of distress. After three weeks, mice were euthanized in the following manner. Mice were placed two at a time in a CO_2 chamber. 100% CO_2 from a compressed chamber was introduced at a rate of approximately 50% of container volume per minute. Mice were left in the chamber past the point that respiratory arrest had been noted. Mice were then removed from the chamber and decapitated.

Blood was collected by removing the head, and draining the body over a centrifuge tube, and immediately spun max speed for 10 minutes to prevent clotting. The serum was then transferred to a fresh centrifuge tube. Bladders were removed using sterile surgical scissors, and placed into 5 ml complete BSK-II. Bladders were incubated at 34° C to allow for outgrowth of any spirochetes. Cultures were monitored periodically for five weeks for the presence of *B. burgdorferi*. A few of the bladders were contaminated in the process, which was obvious within the first week by turbidity of the culture medium. These cultures were not included in the infectivity count.

Hearts were collected from each mouse, flash frozen in liquid nitrogen and stored at -80° C. DNA was extracted from the hearts using the NucleoSpin Tissue genomic DNA purification kit from TaKaRa in the following manner. Hearts were wrapped in aluminum

foil, dunked into liquid nitrogen, then quickly pounded with a mortar and pestle to break up into small pieces. Each heart was then placed in a 2 ml tube containing 180 µl Buffer T1 and 25 µl Proteinase K. Samples were briefly homogenized with an Omni Tissue Homogenizer. Samples were incubated at 56° C for 3 hours, while occasionally vortexed. Samples were lysed by adding 200 µl Buffer B3, vigorously vortexed, then incubated at 70° C for 10 minutes. 210 µl ethanol was added and tubes vigorously vortexed.

Samples were added to NucleoSpin Tissue columns, then centrifuged for 1 min at 11,000 x g. Flow-through was discarded, and 500 µl Buffer BW was added. Tubes were centrifuged for 1 min at 11,000 x g. Flow-through was discarded and 600 µl Buffer B5 was added to each column. Tubes were centrifuged for 1 minute at 11,000 x g. The flow-through was discarded, and membrane dried by centrifuging for 1 min at 1,000 x g. DNA was eluted with ddH_2O.

Eluted DNA from each heart was diluted 1:10, then subjected to qPCR, using primers that amplify the *nido* gene from mice and *flaB* gene from *B. burgdorferi.* Cq values from *nido* were subtracted from Cq values for *flaB* for each heart, and plotted using GraphPad Prism version 6. Tukey's Multiple comparisons statistical test was used to determine if the infectious burden of *B. burgdorferi* was significantly different between any of the strains.

2.20 Green Fluorescent Protein (GFP)-transcriptional fusions analyzed by Flow Cytometry

B. burgdorferi strains TB3, TB3 + pCRS5, TB11, TB11 + pCRS5, TB14 and TB14 + pCRS5 and B31-A3 (GFP negative control) were grown to mid-log phase at 34° C. Cells were harvested by centrifugation at 15,000 RPM in a JA-10 fixed angle rotor for 10

minutes, 4° C. Cells were gently resuspended in 1 ml PBS, transferred to a 1.6 ml microfuge tube, then centrifuged for 10 minutes at 10,000 RPM (24 x 1.5/2.0 ml rotor-ThermoFisher), 4° C. Supernatant was removed, and cells gently resuspended in 1 ml PBS, then transferred to a 5 ml round-bottom polystyrene tube for analysis by flow cytometry. Cells were analyzed on an LSR II Flow cytometer, set with the 488nm Laser, and read with both forward and side scatter. B31-A3 cells were used as the GFP negative control. At least 5,000 gated events were measured for each culture. Graphs were generated by plotting cell counts against GFP fluorescence intensity, then overlaying each strain with and without the plasmid pCRS5.

This research was supported by the Flow Cytometry and Cell Sorting Shared Resource Facility of the University of Kentucky Markey Cancer Center (P30CA177558).

2.21 Antibody production

PlzA protein was expressed and purified from *E. coli* as described above. 5 mg was sent to AbClonal (Woburn, MA) for antibody production in 2 New Zealand white rabbits. Rabbits were serially inoculated with whole protein three times, and the serum collected. Bb0648 was analyzed for a specific, highly antigenic peptide by AbClonal. This peptide (VQKIDSPKSNVETLIYFY) was synthesized, and used to serially inoculate 2 New Zealand white rabbits. Antibodies against Bb0648 were affinity purified from rabbit serum.

2.22 2-dimensional gel electrophoresis

B. burgdorferi wild-type, *spoVG*-ON and Δ*spoVG* strains were cultured at 34° C to mid-log phase in 10 ml. Cells were harvested by centrifugation, at 15,000 RPM for 10

minutes at 4° C using a JA-17 fixed angle rotor. Cell pellets were gently resuspended in 1 ml PBS, moved to Microfuge tubes, and centrifuged for 10 minutes at 10,000 RPM (24 x 1.5/2.0 ml rotor-ThermoFisher), 4° C. Supernatant was removed, cells washed in 1 ml PBS, and centrifuged for 10 minutes at 10,000 RPM (24 x 1.5/2.0 ml rotor-ThermoFisher), 4° C. Supernatants were removed, and cell pellets stored at -80° C until further use.

Cell pellets were gently thawed on ice, then resuspended in 150 µl cell lysis buffer (Qiagen) containing protease and phosphatase inhibitors (ThermoFisher). Cells were incubated for 30 minutes at 4° C, and vortexed for 30 seconds every 10 minutes. Lysed cells were centrifuged for 30 minutes at 10,000 RPM (24 x 1.5/2.0 ml rotor-ThermoFisher), 4° C to separate cellular debris from proteins. 100 µl of the soluble fraction was transferred to a clean Microfuge tube for protein precipitation.

Proteins were precipitated using the BioRad ReadyPrep 2-D protein precipitation kit as follows. To the 100µl protein, 300 µl Precipitation agent 1 was added, mixed well by vortexing, and incubated on ice for 15 minutes. 300 µl Precipitation agent 2 was added, and mixed well by vortexing. Tubes were centrifuged max speed for 5 minutes. The supernatant was removed, being sure not to disturb the pellet. Tubes were centrifuged for 30 seconds to collect any remaining liquid, which was promptly removed. 40 µl Wash reagent 1 was added, the tubes centrifuged at max speed for 5 minutes, and supernatant removed. 25 µl Proteomic grade water was added to the pellet and vortexed for 30 seconds.

1 ml wash reagent 2 (stored at -20° C) was added along with 5 µl wash reagent 2 additive. Tubes were vortexed for 1 minute, then incubated at -20° C for 30 minutes. Tubes were vortexed every 10 minutes for 30 seconds during this incubation period. Tubes were centrifuged for 5 minutes at max speed, and supernatant removed. Tubes were centrifuged

again for 30 seconds, and residual supernatant removed. Protein pellets were allowed to dry for 5 minutes at room temperature with the cap open. Proteins were resuspended in 185 µl 2-D sample rehydration buffer (BioRad).

The 185 µl protein sample was carefully added to a sample rehydration tray, then 1 11cm IPG strip pH 3-10 (BioRad) was carefully overlaid on the sample, gel side down. IPG strips were allowed to re-hydrate in the protein sample overnight at room-temperature.

The following day, rehydrated IPG strips were carefully placed in the Isoelectric focusing tray, and covered with mineral oil. The voltage was incrementally increased from 250 V to 3500 V over the course of 1.5 hours to avoid setting the strips on fire. Once the voltage reached 3500 V, strips were allowed to focus for an additional 11 hours. Strips were placed into individual conical tubes and stored at -80° C overnight.

The following day, IPG strips were thawed at room temperature for no longer than 20 minutes. Equilibration Buffers I and II were brought to room temperature on a stir plate. IPG strips were placed gel side up in individual lanes of the equilibration tray. 2 ml of Equilibration Buffer 1 was overlaid on top of each strip, and allowed to incubate at 10 minutes on an orbital shaker at room temperature. The buffer was carefully poured off, being sure not to dump out the IPG strips. 2 ml of Equilibration Buffer II was added to each strip, and allowed to incubate for 10 minutes on an orbital shaker at room temperature.

The IPG strip was then carefully removed using tweezers, and rinsed by dipping into a 100 ml graduated cylinder of SDS running buffer. The strip was then carefully loaded into the large well of the 20 % polyacrylamide gel, oriented such that the plastic backing of the IPG strip was against the plastic cassette, and the end marked "-" was closest to the small well for the ladder. 1 ml of melted agarose (from the 2-D ReadyPrep kit) was overlain

over both wells. Before the agarose set, 10 µl PageRuler Plus ladder (ThermoFisher) was loaded into the ladder well, by inserting the loading tip underneath the agarose.

Gels were run for 50 minutes at 200 V, then immediately removed from their cassettes and incubated in 200 ml fixing solution (same as SDS de-stain solution) overnight at room temperature on an orbital rocker. All fixing, staining and de-staining steps were carried out in the red boxes with lids to protect from light.

The following morning, the gels were washed 2x in 100 ml ddH_2O, for 10 minutes with shaking. Gels were stained with 100 ml Pro-Q Diamond stain for 90 minutes with gentle shaking. Gels were de-stained with 100 ml Pro-Q de-stain solution and incubated for 30 minutes at room temperature with shaking. This was repeated 2 more times. Gels were washed 3x in 200 ml ddH_2O for 10 minutes. The wash step was repeated 2 more times. Gels were imaged on a Typhoon imager (GE) using the preset settings for imaging Pro-Q Diamond stain.

Gels were then stained with 100 ml Coomassie by microwaving for 2 minutes, then incubating at room temperature for 1 hour on an orbital shaker. Gels were rinsed several times with ddH_2O to remove excess stain, then de-stained overnight in 200 ml Coomassie de-stain solution. The following morning, gels were washed with ddH_2O to remove de-stain solution. Gels were imaged with the Odessey imager on the 700 channel.

Table 2.1 Plasmids used in this study

Name	Background	Insertion	Resistance	Source
pCRS0	pCR2.1	*cdaA*	Kanamycin	This study
pCRS1	pSZW53-4	Bb_0471	Kanamycin	This study
pCRS2	pET102	*spoVG*	Carbenicilin	This study
pCRS5	pBLS715	*spoVG*	Gentamycin	This study
_0648	pET28a	Bb_0648	Carbenicilin	This study
Spy-FRET	pBLS715	*Spy-FRET*	Gentamycin	This study
pAG1	pSZW53-4	*cdaA*	Kanamycin	This study
pTB3	pBLS590	*PvlsE*-full	Kanamycin	Bykowski, 2006
pTB11	pBLS590	P*vlsE*-shorter	Kanamycin	Bykowski, 2006
pTB13	pBLS590	P*vlsE*-shortest	Kanamycin	Bykowski, 2006

Table 2.2 Bacterial Strains used in this study

Name	Background	Plasmid	Source	Passage
CS1	B31-e2	pCRS1	This study	high
CS2	5A4-NP1	pCRS1	This study	low
CS8	B31-A3	pCRS5	This study	low
CS9	B31-A3	pCRS5	This study	low
GK1	B31-S9	pCRS5	This study	low
GK2	Δ*plzA*	pCRS5	This study	low
Δ*rrp1*+*spoVG*-ON	Δ*rrp1*	pCRS5	This study	low
Δ*rpos*+*spoVG*-ON	Δ*rpos*	pCRS5	This study	low
TB3	B31-e2	pTB3	Bykowski, 2006	high
TB3+spoVG-ON	B31-e2	pTB3+pCRS5	This study	high
TB11	B31-e2	pTB11	Bykowski, 2006	high
TB11+spoVG-ON	B31-e2	pTB11+pCRS5	This study	high
TB13	B31-e2	pTB13	Bykowski, 2006	high
TB13+spoVG-ON	B31-e2	pTB13+pCRS5	This study	high
cdaA-ON	B31-A3	pAG1	This study	low
Δ*spoVG*+*spoVG*	Δ*spoVG*(A3)	pCRS5	This study	low
Spy-FRET	B31-A3	Spy-FRET	This study	low
Δ*cheA1*	B31-A	none	Li, 2002	high
Δ*cheA2*	B31-A	none	Li, 2002	high
B31-A				high
B31-e2				high
B31-S9				low
B31-A3				low
5A4-NPI				low

Table 2.3 Antibodies used in this study

Target	Origin	clone/purification
FlaB	Mouse, monoclonal	H9724
SpoVG	Rabbit, polyclonal	Anti-sera
GlpD	Rat, polyclonal	Anti-sera
AckA	Rabbit, polyclonal	Anti-sera
VlsE	Rabbit, polyclonal	Anti-sera
OspC	Mouse, monoclonal	B5
OspA	Mouse, monoclonal	C3.78
PlzA	Rabbit, polyclonal	Anti-sera
Bb0648	Rabbit, polyclonal	purified Ab
Ac-Lysine	Rabbit, polyclonal	purified Ab

Secondaries	Isotype	Origin	Modification	Source
Protein A	none		biotin	Thermo Fisher
α-Mouse	IgG	Goat	IRD800	Li-Cor
α-Rabbit	IgG	Goat	IRD700	Li-Cor
α-Rat	IgG	Goat	IRD800	Li-Cor

CHAPTER 3. REGULATION OF SPOVG AS A GLOBAL REGULATOR IN *B. BURGDORFERI*

3.1 Introduction

Having previously identified SpoVG as a DNA-binding protein in multiple bacteria, including *B. burgdorferi*, we sought to study how this protein acts in *B. burgdorferi* (164). We did this by generating mutant strains that over-express *spoVG*, or in which *spoVG* gene has been deleted. We performed global RNA-sequencing experiments to identify all of the transcripts that were differentially expressed. We also identified culture conditions and other regulatory factors that were involved in regulating SpoVG in *B. burgdorferi.*

Mouse infection models have been well-established for *B. burgdorferi* (176, 177). Previous work has determined that six infected mice are sufficient to determine infectivity (178). Since *B. burgdorferi* is so motile, bacteria can be cultured and detected in distal tissues approximately three weeks after infection. Common tissues assayed include bladders and hearts. Culturing tissues in complete BSK, and extracting DNA from tissues for quantitative analysis are commonly employed methods for determining whether a certain tissue has been infected (176, 179-183).

Bacteria that harbor extra-chromosomal plasmids must be able to faithfully replicate and partition those plasmids into each daughter cell during cell division (184, 185). This process is not well understood in *B. burgdorferi*, which must be able to replicate and segregate approximately 20 plasmids (85, 92). As discussed above, *B. burgdorferi* manages to carry out this process with extreme fidelity in the enzootic cycle (76). Although plasmids that do not carry genes essential for survival in culture may eventually be lost over the course of numerous passages, all plasmids appear to be necessary for completion of the

enzootic cycle (186). From an evolutionary perspective, only those bacteria that harbor all plasmids will be able to survive.

PlzA is the only known protein in *B. burgdorferi* that binds cyclic-di-Guanosine-Mono-Phosphate (c-di-GMP) (187). PlzA has previously been demonstrated to be essential for *B. burgdorferi* to infect mice and to colonize ticks, while c-di-GMP is only necessary for tick colonization (148, 188). This indicates that PlzA performs an important function both when c-di-GMP is present, and when it is absent. Until this point, no function had been ascribed to PlzA, either with or without c-di-GMP bound to it. Our collaborators found that the protein PlzA interacts with SpoVG in the cell, and confirmed this interaction in *vitro* (personal correspondence with Dr. Md. Motaleb, East Carolina University, unpublished data).

3.2 Creation of Mutants

In order to study the effect of SpoVG on *B. burgdorferi*, several mutants were generated. The *spoVG* gene was cloned under control of the constitutive *flgB* promoter, on plasmid pBLS715 (Figure 3.1A) (189). This construct was named pCRS5, and was introduced into wild-type *B. burgdorferi* on multiple occasions. pCRS5 was transformed into infectious strain B31-A3 to generate strains CS8 and CS9. pCRS5 was also transformed into infectious strain B31-S9 by Gabby Keb during her rotation to generate strain GK1. These strains demonstrated phenotypic homogeneity, and are collectively referred to as *spoVG*-ON.

Our collaborator, Dr. Md. Motaleb, generated a chromosomal deletion strain by replacing the *spoVG* gene with a kan^r cassette, and is termed Δ*spoVG* (Figure 3.1B). An

important consideration when generating mutants in infectious backgrounds of *B. burgdorferi* is ensuring that none of the plasmids are lost during the process of transformation. Certain plasmids, such as lp28-1, are necessary for vertebrate infectivity, and some such as lp25 are necessary for tick colonization (76, 85, 93, 190) (98, 186). Plasmid profiles were assayed for all strains by endpoint PCR, using primers specific for each plasmid (91). None of the strains generated lost any of plasmids necessary for transmission through the entire enzootic cycle, as assayed by endpoint PCR.

3.3 Infection Studies

Multiple studies have demonstrated that *spoVG* mRNA is more highly expressed when *B. burgdorferi* has colonized ticks than when it has infected mice (191, 192). Given this information, we hypothesized that *spoVG* is dispensable for vertebrate infection, and that *B. burgdorferi* that overexpresses *spoVG* will not be able to infect mice as efficiently as wild-type mice. To test this, we infected cohorts of mice with wild-type and *spoVG*-ON strains of *B. burgdorferi.* Six female mice were infected with each strain. Two wild-type strains (B31-A3 and B31-S9) and three *spoVG*-ON strains (CS8, CS9 {B31-A3 background}, and GK1 {B31-S9 background}) were used. Each mouse was infected with $1x10^6$ bacteria suspended in 100 µl, injected into the peritoneum (176).

After three weeks mice were euthanized, bladders aseptically removed and cultured in complete BSK-II media (193). Cultures were periodically examined by darkfield microscopy for the presence of *B. burgdorferi*. A few of the bladders were contaminated in the process of harvest, therefore those cultures were not included in the counts of how many bladders were infected. B31-A3 infected 6 out 6 mice, CS8 infected 5 out of 6 mouse

bladders, and CS9 also infected 5 out 6 mouse bladders. B31-S9 infected 4 out 4 mouse bladders, and GK1 infected 4 out 5 mouse bladders. In total, wild-type strains infected 10 out of 10 mice, while the *spoVG*-ON strains infected 14 out of 17 mouse bladders (Figure 3.2 A).

The heart from each mouse was also harvested, immediately flash frozen in liquid nitrogen, and stored at -80° C (177). DNA from each mouse was extracted using TaKaRa genomic DNA from tissue kit, then subjected to qPCR. Primers that amplified the *nido* mouse gene and the *flaB B. burgdorferi* gene were used. The mouse *nido* gene was also amplified as a control for tissue abundance. Whole mouse hearts were processed without weighing a specific amount. This allowed us to quantify bacterial load in a certain amount of mouse tissue. *flaB* was detectable in every sample, indicating that every animal was infected (Figure 3.2 B). Cq values for *nido* were subtracted from *flaB* Cq values, and plotted using GraphPad Prism version 6. Tukey's multiple comparisons statistical test was used to determine if the infectious burden was significantly different between the different strains. The infectious burden was not different between the strains. Lower Cq values correlate with higher abundance in the sample, since the fluorescence is detectable at an earlier cycle number. Therefore, lower plotted values correspond to higher *B. burgdorferi* genome abundance. This infection study, which was conducted once, disproved our hypothesis that *spoVG*-ON *B. burgdorferi* would be less infectious in mice than wild-type *B. burgdorferi.* We concluded that *B. burgdorferi* that constitutively express *spoVG* mRNA are not impaired for murine infection. This experiment was performed once, and we decided not to further pursue whether there is a fitness advantage for wild-type over *spoVG*-ON bacteria in competition infection experiments.

3.4 RNA-Sequencing on wild-type, *spoVG*-ON, and Δ*spoVG B. burgdorferi*

The Stevenson lab had previously demonstrated that SpoVG binds to DNA near the recombination site of the antigenically variable *vlsE* gene (164). We hypothesized that SpoVG likely binds numerous DNAs throughout the genome, and thereby influences expression of numerous transcripts. To test this, we performed RNA-sequencing on wild-type, *spoVG*-ON and Δ*spoVG* strains. All three strains were cultured in triplicate and grown to mid-log phase at 34° C. Harvested cells were sent out for RNA purification with strand-specific sequencing. Sorted Bam files were analyzed by a HISAT2 -> StringTie -> DESeq2 pipeline (194). Wild-type transcripts were compared to *spoVG*-ON transcripts, and wild-type transcripts were compared to Δ*spoVG* transcripts. Output files were then sorted by transcript ID, and separate files were created for mRNA and non-coding RNA transcripts (195). Files were filtered by adjusted p-value internally generated by DESeq2, keeping only those smaller than 0.05. Files were further filtered by $\log_2$ fold change between wild-type and mutant transcripts. Only values above 1.0 and below -1.0 were accepted.

188 mRNA transcripts were differentially expressed between wild-type and Δ*spoVG* bacteria (Table 3.3). 119 of those transcripts were on various plasmids, 66 were on the chromosome, and 3 were tRNAs (Figure 3.10 B). Similarly, 230 mRNA transcripts were differentially expressed between wild-type and *spoVG*-ON bacteria (Table 3.4). 107 of those transcripts were on various plasmids, 117 were on the main chromosome, and 6 were tRNAs (Figure 3.10 A). 75 sRNA transcripts were differentially expressed between wild-type and Δ*spoVG* bacteria (Table 3.2). 29 of those transcripts were on various plasmids, and 46 were on the chromosome (Figure 3.10 D). 110 sRNA transcripts were differentially expressed between wild-type and *spoVG*-ON bacteria (Table 3.1). 40 of those

transcripts were on plasmids, and 70 were on the main chromosome (Figure 3.10 C). mRNA and sRNA differentially expressed transcripts were found on the chromosome as well as numerous plasmids. Unsurprisingly, *spoVG* mRNA was significantly changed in both mutants as compared to wild-type. *spoVG* transcript was 2.6 $\log_2$ higher in the *spoVG*-ON strain compared to wild-type, with an adjusted p-value of 3.67E-27. *spoVG* transcript was 6.58 $\log_2$ fold lower in the Δ*spoVG* strain compared to wild-type with an adjusted p-value of 3.38E-167 (Figure 3.3).

The differentially expressed mRNA transcripts were analyzed for functional clustering by DAVID bioinformatics resource (https://david.ncifcrf.gov/). As the majority of genes in the *B. burgdorferi* genome remain annotated as "unknown function", many transcripts could not be grouped based on their function (23). The largest functional category for both *spoVG*-ON vs. wild-type and Δ*spoVG* vs. wild-type was membrane proteins (Figure 3.11 A-B). Each group also contained a number of DNA-binding proteins. Apart from that, there was not much similarity in how the differentially expressed transcripts were classified. For example, a number of coiled-coil domain-containing genes were differentially expressed in the Δ*spoVG* vs. wild-type, but not the *spoVG*-ON vs. wild-type.

There are numerous examples where a particular transcript is differentially expressed in one mutant as compared to wild-type, but not the other (Figure 3.3). One example of this is *rpoN*. *rpoN* was expressed 2.2 $\log_2$ times less in the *spoVG*-ON mutant as compared to wild-type, however expression was unchanged in the Δ*spoVG* mutant as compared to wild-type. Some transcripts were more or less abundant in both the *spoVG*-ON and Δ*spoVG* mutants compared to wild-type. For example, transcript BB_0746, which

codes for an ABC oligopeptide transporter, was expressed nearly 7 $\log_2$ times less in both *spoVG*-ON and Δ*spoVG* strains than in wild-type.

3.5 ParA transcript abundance and Plasmid Quantification

Although the process of DNA segregation in *B. burgdorferi* is not well understood, each plasmid does carry *parA/parB* genes, which have been studied extensively in other bacteria, and are known to be essential for plasmid replication and segregation (85, 196). ParB binds DNA and nucleates along sites near the origin of replication *oriC.* ParA is an ATPase that oscillates across the cell in much the same manner as MinD, and associates with the cytoplasmic membrane as well as ParB. In this way, ParA can anchor the plasmids to each of the soon-to-be newly formed daughter cells (197-199).

We observed that the *parA* transcripts on many of the different plasmids were differentially expressed in the *spoVG*-ON and Δ*spoVG* strains compared to wild-type (Figure 3.4 A). To test whether the differences in *parA* transcript abundance is due to differential expression of the gene between strains of *B. burgdorferi*, or due to differences in copy number of plasmid (either within a single cell, or within a population in which some cells maintain the plasmid and others do not), DNA was extracted from wild-type, *spoVG*-ON and Δ*spoVG* strains. Plasmid abundance was assayed by qPCR using primers specific for each plasmid. Plasmid Cq values were normalized *flaB* Cq values, essentially measuring plasmid copy per chromosome copy (Figure 3.4 B). Wild-type values were arbitrarily set to 1, and the difference in Cq measured for the mutant strains plotted against that. We found that there is a lower abundance of several plasmids compared to wild-type, but this was not sufficient to explain the differences in *parA* transcript abundance. For

example, lp28-1 *parA* transcript is more abundant in *spoVG*-ON than in wild-type, however there was no difference in copy number of lp28-1 between *spoVG*-ON and wild-type cells.

3.6 Growth Rates of Wild-type, *spoVG*-ON, and Δ*spoVG*

Given the fact that SpoVG binds DNA, we hypothesized that dysregulation of this protein could have an impact on growth rate in culture. At 34° C, there was no difference in growth rate between the wild-type, *spoVG*-ON or Δ*spoVG* strains (Figure 3.5 A). Wild-type *B. burgdorferi* grow significantly more slowly at 23°C than at 34°C. Although there was no difference in growth rate between wild-type and Δ*spoVG* cells at 23°C, *spoVG*-ON cells grew significantly more slowly than wild-type or Δ*spoVG* cells (Figure 3.5 B). This suggests that another factor(s) is either present or absent in *B. burgdorferi* at 23°C and not 34°C that somehow interacts with, or is influenced by, SpoVG, resulting in the further reduced growth rate. This demonstrated that our hypothesis was partially correct: at 34° C, there was no difference in growth rate, while at 23° C, there was a difference in growth rate.

Previous work from the Stevenson lab demonstrated that *B. burgdorferi* senses and responds to its own replication rate. By separating growth rate from absolute temperature, we demonstrated that differential expression of several proteins is actually growth-rate dependent, and not temperature dependent as previously thought (200). We hypothesized that the reason for reduced growth-rate of the *spoVG*-ON cells was due to the already reduced growth-rate of *B. burgdorferi* at 23°C, and not due inherently to temperature. To test this, we measured growth rate in WT and *spoVG*-ON cells in two different media that

result in reduced growth, even at 34°C. *B. burgdorferi* is normally grown in BSK supplemented with 6% rabbit serum. For the reduced growth rate media, one contains 1.2% rabbit serum added to full strength BSK, while the other has the standard 6% rabbit serum added to BSK that was diluted to 25% strength. Although we predicted that *spoVG*-ON cells would grow more slowly than WT, both cells grew at the same rate in both media at 34°C (Figure 3.5 C and D). This indicates that the disparity in growth rate between the WT and *spoVG*-ON strains at 23° is not specifically due to reduced growth rate, but to some as yet-unidentified factor, which may be temperature itself. These studies disproved our hypothesis that differences in growth rate between wild-type and *spoVG*-ON *B. burgdorferi* were due to growth rate and not temperature.

3.7 *spoVG* Expression in wild-type and *spoVG*-ON grown at 34° C and 23° C

We hypothesized that expression of SpoVG could be regulated in culture, since we had demonstrated that its expression was differentially regulated when *B. burgdorferi* colonized ticks or infected mice (191). In order to test this, WT *B. burgdorferi* cells were harvested for both RNA extraction and protein analysis from different time points, representing mid-log, stationary, and late stationary. *spoVG* transcript abundance normalized to *flaB* transcript abundance did not change during different stages of growth (Figure 3.6A). We had previously demonstrated by RNA-seq that *flaB* transcript abundance does not appreciably change across different growth stages (201). In contrast to transcript abundance, the amount of SpoVG protein made during different growth stages did significantly change. SpoVG protein is abundantly produced by mid-log growing cells, and is nearly undetectable in late stationary cells (Figure 3.6 C).

Expression of SpoVG transcript and protein was also measured in WT and SpoVG-ON cells grown both at 34°C and 23°C and harvested during mid-log growth. *spoVG* transcripts were significantly more abundant in the SpoVG-ON cells than WT cells grown at 34°C (Figure 3.6 B). The graph is plotted on a $\log_2$ scale on the y-axis to demonstrate the differences in Cq values that were measured. The difference in Cq value between WT cells grown at 34°C and 23°C is 3.63, which equates to 13.2 times more *spoVG* transcript made by WT cells growing at 34°C than at 23°C. SpoVG-ON cells grown at 23°C did not produce more *spoVG* transcript than SpoVG-ON cells grown at 34°C. At 23°C, there was an even greater difference in the amount of *spoVG* mRNA produced between WT and spoVG-ON cells. The difference in Cq values was measured to be 5.54, which equates to nearly 31 times more *spoVG* transcript in the *spoVG*-ON cells than the WT cells, both grown at 23°C.

SpoVG protein abundance was not significantly different between strains, or between cells grown at different temperatures (figure 3.6 D). This experiment was repeated on three different cultures with similar results. Taken together, these data indicate that *B. burgdorferi* regulates levels of SpoVG at both the level of transcription and translation, and that SpoVG plays a role in regulation of itself. This finding is not altogether surprising, given the evidence that *B. subtilis* also strongly regulates expression of SpoVG at multiple levels (165).

3.8 SpoVG Binds Its Own DNA and RNA in *Vitro*

Because SpoVG-ON cells did not produce more SpoVG protein than WT cells, we hypothesized that SpoVG could regulate its own expression by binding to nucleic acid

associated with its own gene. To test this, we performed electrophoretic mobility shift assays (EMSAs) between SpoVG and DNA or RNA. Corresponding to the *spoVG* upstream region, DNAs and RNAs were labeled with a biotin molecule to allow for visualization by streptavidin. Recombinant SpoVG was incubated with a labeled 38bp segment of double stranded DNA that consisted of the sequence just upstream of the translational start codon of *spoVG* (Figure 3.7 A). The presence of a shifted band of DNA when incubated with SpoVG indicated that SpoVG bound to that piece of DNA. Addition of 100x unlabeled non-specific DNA was insufficient to eliminate the shifted band, indicating that SpoVG preferentially binds to the DNA sequence upstream of its own gene. 100x unlabeled DNA that contained the exact DNA sequence as the labeled probe did result in reduction of the shifted band.

The lane containing 100x unlabeled DNA contains a band not present in any other lane, which is consistent with SpoVG "spreading". Once one SpoVG protein has bound to a single piece of DNA, it is possible that it acts as a nucleating factor, and more SpoVG proteins bind to the same DNA. A sufficient amount of SpoVG protein was added in the second lane such that all of the DNAs have multiple proteins bound to them, likely with free SpoVG as well. This is why there is only a single shift visible. The unlabeled competitor is able to shift away only some of the protein from the labeled piece of DNA because there is an excess of protein (i.e. enough to bind to all DNAs present in the mixture). In this case, the labeled DNAs contain fewer SpoVG protein complexes, which explains why there is still a shifted band, but that has migrated faster through the gel than the labeled DNAs in lane two. Figure 3.8 also demonstrates this. Adding more SpoVG protein to DNA resulted in additional higher protein-DNA complexes. It was not

investigated whether the DNA-bound SpoVG proteins can then attract an additional piece of DNA, which would provide evidence for DNA-bending and packing.

Measuring SpoVG transcript and protein abundance demonstrated that RNA levels are not necessarily predictive of the amount of protein abundance, therefore we tested whether SpoVG also binds to RNA associated with its gene. A labeled RNA that covered the same sequence as the DNA tested, on just the strand that gets transcribed was also used to test for SpoVG binding (Figure 3.7 B). Addition of SpoVG with this RNA resulted in a shifted band, consistent with SpoVG binding to this piece of RNA. Incubation of SpoVG with an unrelated labeled RNA did not result in a shift, indicating that SpoVG binds to specific RNA sequences, just as it does with DNA (Figure 3.7 C).

3.9 SpoVG expression in *B. burgdorferi* deficient for PlzA, or c-di-GMP

PlzA and SpoVG interact, and both PlzA and c-di-GMP have global impacts on gene expression (101, 144, 146-148). Therefore, we hypothesized that it is possible the PlzA and or c-di-GMP could regulate expression of SpoVG. In order to test this, we first measured *spoVG* expression levels in various mutants (Figure 3.9 A). Wild-type, Δ*plzA* mutant, and complemented Δ*plzA*+*plzA* were grown to mid-log phase at 34° C. Cells were harvested, RNA extracted and subjected to cDNA synthesis. cDNAs were subjected to analysis by qRT-PCR, using primers that amplified within the coding region of *spoVG*. *spoVG* transcript was measured to be nearly 3 $\log_2$ times lower in the Δ*plzA* strain as compared to the wild-type or Δ*plzA*+*plzA* strains.

Additionally, we measured SpoVG protein levels by Western Blot on several strains of *B. burgdorferi* (Figure 3.9 B). The Δ*plzA* strain was complemented with

exogenous *plzA* on a plasmid termed Δ*plzA*+*plzA* (101). The protein that synthesizes c-di-GMP is the response regulator of a two-component system, termed *rrp1* (188). Lysates were prepared from Wild-type, Δ*plzA*, Δ*plzA*+*plzA*, and Δ*rrp1* strains grown to mid-log phase at 34° C. FlaB was used as the loading control. SpoVG was readily detectable in both the wild-type and Δ*plzA*+*plzA* lysates, but undetectable in the Δ*plzA* and Δ*rrp1* lysates.

PlzA is the only known target of c-di-GMP in *B.* burgdorferi, therefore we hypothesize that PlzA needs to have c-di-GMP bound to it in order to regulate expression of SpoVG. It was previously known that both Δ*plzA* and Δ*rrp1* strains regulate expression of other genes. In order to determine if they do so only by regulating *spoVG,* we transformed both mutant strains with plasmid pCRS5 to introduce exogenous expression of SpoVG in these strains (Figure 3.9 C). Use of these strains in future studies will enable us to determine whether the effects on gene regulation observed in the Δ*plzA* and Δ*rrp1* strains are directly impacted by PlzA and or c-di-GMP, or if they are due to absence of SpoVG expression.

3.10 Discussion

Although fewer mouse bladders (14/17 for spoVG-ON compared to 10/10 for wild-type) were infected with the mutant strains of *B. burgdorferi,* all of the hearts were as assessed by qPCR. The fact that mice were successfully infected by strains constitutively expressing *spoVG* disproved our hypothesis that constitutive expression would render these strains entirely incapable of establishing infection in mice. Additionally, our collaborator Dr. Motaleb found that Δ*spoVG* strains are deficient in their ability to transmit between ticks and mice and establish persistent infections in mice, which disproves our hypothesis

that *spoVG* is dispensable for mouse infection (data unpublished). It is possible that constitutive expression of *spoVG* would be prohibitive in a direct competition infection study. Further studies will focus on quantifying bacterial loads in various organs (heart, bladder and ears are often used to demonstrate dissemination throughout the body), as well as quantifying whether wild-type *B. burgdorferi* are able to more efficiently infect and disseminate when co-infected with *spoVG*-ON and Δ*spoVG* mutants.

Transcriptomic analysis between *spoVG*-ON, Δ*spoVG* and wild-type demonstrated that numerous genes are differentially expressed in the mutant strains of *B. burgdorferi* compared to wild-type. The Δ*spoVG* strain had more transcripts differentially expressed on the chromosome, in contrast to the *spoVG*-ON strain, which had more transcripts differentially expressed on the chromosome than on the plasmids. Of the tRNAs that were differentially expressed, two of them were the same in both the *spoVG*-ON and Δ*spoVG* mutants compared to wild-type. Functional clustering analysis revealed that genes involved in numerous cell processes were differentially expressed. The group with the largest number of differentially expressed genes in both groups was membrane lipoproteins. This is unsurprising, given what we know about how important regulation of membrane proteins is for *B. burgdorferi* (116, 202). Apart from the membrane proteins, there are differences in how the differentially expressed genes cluster in the two mutant strains. This gives further indication that SpoVG acts broadly across the entire genome, and not on just a few specific transcripts.

Given that so many transcripts are differentially expressed between the wild-type and mutant strains, and the wide range of cell processes those genes are involved in, we hypothesize that SpoVG has a global effect on genome expression. It is possible that

SpoVG affects expression of a (or multiple) global regulator, however a couple of pieces of evidence counter this assumption, and point to the possibility that rather than working in a manner to specifically target certain genes, SpoVG exerts its influence by globally influencing the three-dimensional structure of the nucleoid. First, there is not significant overlap between those transcripts that are differentially expressed in the *spoVG*-ON mutant compared to wild-type than in the Δ*spoVG* mutant compared to wild-type. Other regulatory factors could be involved in the spoVG-ON mutant that are unchanged between wildtype and Δ*spoVG* mutant.

Recent debate in the scientific community has centered around the almost deification of the p-value (203). This test measures the statistical probability that a percentage of tests will be false-positives. False discovery rate adjusted p-values (by DESeq2) are used in instances where a large number of tests are being evaluated: for example, in RNA-sequencing data sets. Adjusted p-values provide the probability that a certain percentage of the statistically significant tests are false-positives. Many are currently arguing that in relying so heavily on using p-values as cutoffs to measure significance, it is possible that in so doing we miss biological relevance. For this reason, in addition to the curated tables presented that use both $\log_2$ fold-change and adjusted p-value of less than 0.05 to determine which transcripts are significantly differentially expressed between the mutant strains and wild-type, Tables A5.1 and A5.2 include all of the data from the Deseq analysis, which can be used for exploratory purposes.

That SpoVG showed impacts on expression of the *parA/parB* systems has broad implications for how plasmids are maintained. Although beyond the scope of this work, an intriguing hypothesis is that SpoVG has a critical role in the faithful replication and

maintenance of each plasmid during each point of the enzootic cycle. This could also partially explain why Δ*spoVG* cells are deficient in their ability to infect mice. One explanation for why so many *parA* transcripts were differentially expressed could be due to loss of copy number of individual plasmids, or individual cells within a population losing certain plasmids. It is not known how many copies of each plasmid are maintained within a single cell.

Just as there was circumstantial evidence that SpoVG could regulate its own expression in *B. subtilis,* it appears as though *B. burgdorferi* SpoVG also regulates its own protein production. We have seen evidence of another regulator in *B. burgdorferi*, BpuR, that also regulates its own expression (155, 156). Autoregulation of regulators in bacteria are beginning to be appreciated as a wide-spread evolutionary tactic (204-206). Additionally, it is recently appreciated that many classical DNA-binding proteins in bacteria may also bind RNA. The evidence that SpoVG binds both DNA and RNA makes sense for a bacterium with a reduced genome (156, 175, 207, 208). *B. burgdorferi* has limited coding capacity for unique proteins in contrast to other organisms. Using post-translational mechanisms of regulating activity of proteins allows the cell to perform all of the functions it needs to survive the enzootic cycle while limiting the resources it has to expend on maintaining the genome, and transcribing and translating individual genes.

Figure 3.1 pCRS5 (*spoVG*-ON) plasmid and Δ*spoVG* constructions

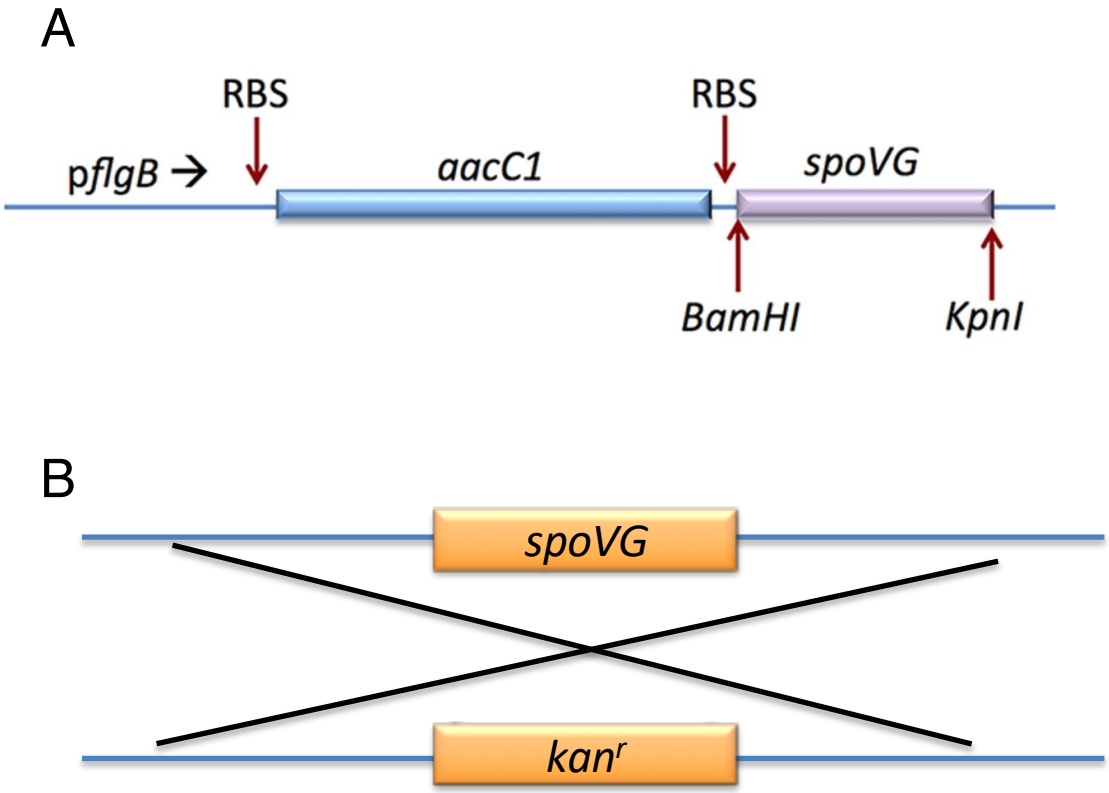

Adapted from Christina R. Savage et al. J. Bacteriol. 2018; doi:10.1128/JB.00033-18

A. pCRS5 (*spoVG*-ON) plasmid construction. *spoVG* was cloned into the BamHI and KpnI sites of our previously described pBLS715 plasmid. The parental construct was created to contain a consensus ribosome-binding site (RBS) appropriately placed 5′ of the insert. The constitutively expressed borrelial *flgB* promoter drives expression of both the gentamicin resistance gene (*aacC1*) and *spoVG*. The identically produced pBLS715*revA* produces elevated levels of both *revA* mRNA and RevA protein.

B. The *spoVG* gene was replaced in the chromosome with a Kanamycin resistance gene (Neomycin phosphotransferase II) to create the Δ*spoVG* strain.

Figure 3.2 Infection Study

A

Strain	Cultured bladders
WT1	6/6
CS8	5/6
CS9	5/6
WT2	4/4
GK1	4/5

WT	10/10
spoVG-ON	14/17

B

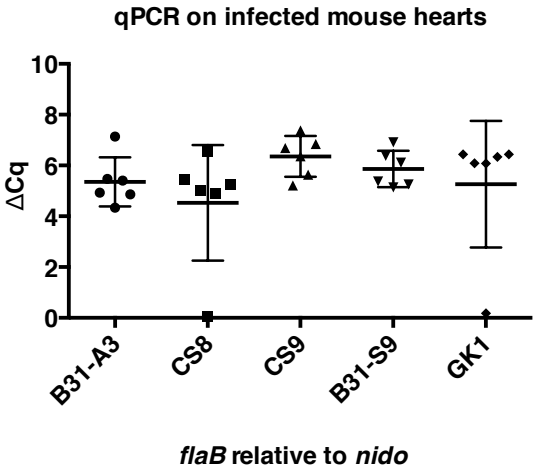

B31-A3 (WT1), CS8, CS9 (*spoVG*-ON), B31-S9 (WT2) and GK1 (*spoVG*-ON) were used to infect mice. 1 x 10^6 bacterial cells were used for each mouse. Infections were allowed to proceed for 3 weeks, after which time bladders were cultured in complete BSK-II media (A). 6 mice were infected with each strain, however a few of the cultured bladders became contaminated, so they were not included in the final counts. Cultures were examined by darkfield microscopy for the presence of *B. burgdorferi*. DNA was extracted from each mouse heart. DNA was analyzed by qPCR using primers that amplified the *nido* gene (present only in mice), and the *flaB* gene present only in *B. burgdorferi*). The difference in Cq value between *flaB* and *nido* was calculated for each mouse. *flaB* DNA was detectable in every mouse heart, indicating that every mouse was infected. The cohorts of hearts infected with each strain was analyzed by Tukeys Multiple comparisons statistical test. The infectious burden between strains was not different between any of the strains of *B. burgdorferi*.

Figure 3.3 RNA-seq transcripts

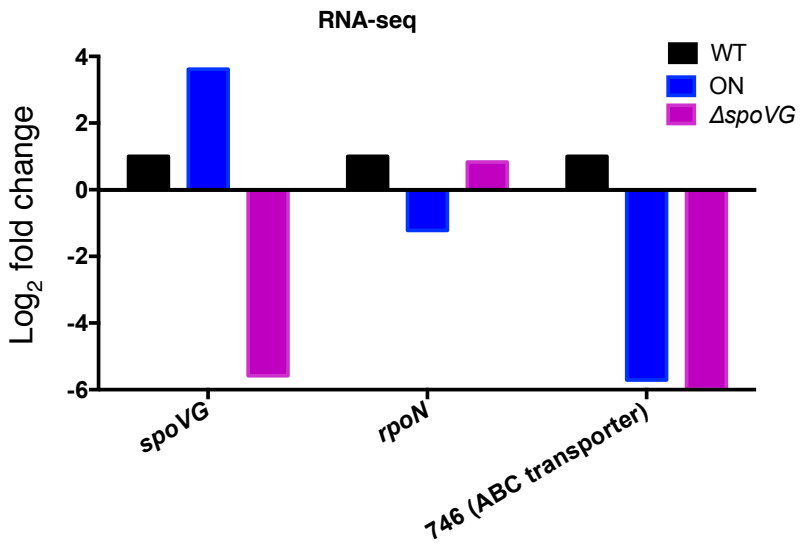

Examples from RNA sequencing that demonstrate that individual genes show different patterns of regulation between wild-type, *spoVG*-ON and Δ*spoVG* strains.

Figure 3.4 *parA* transcript abundance and plasmid quantification

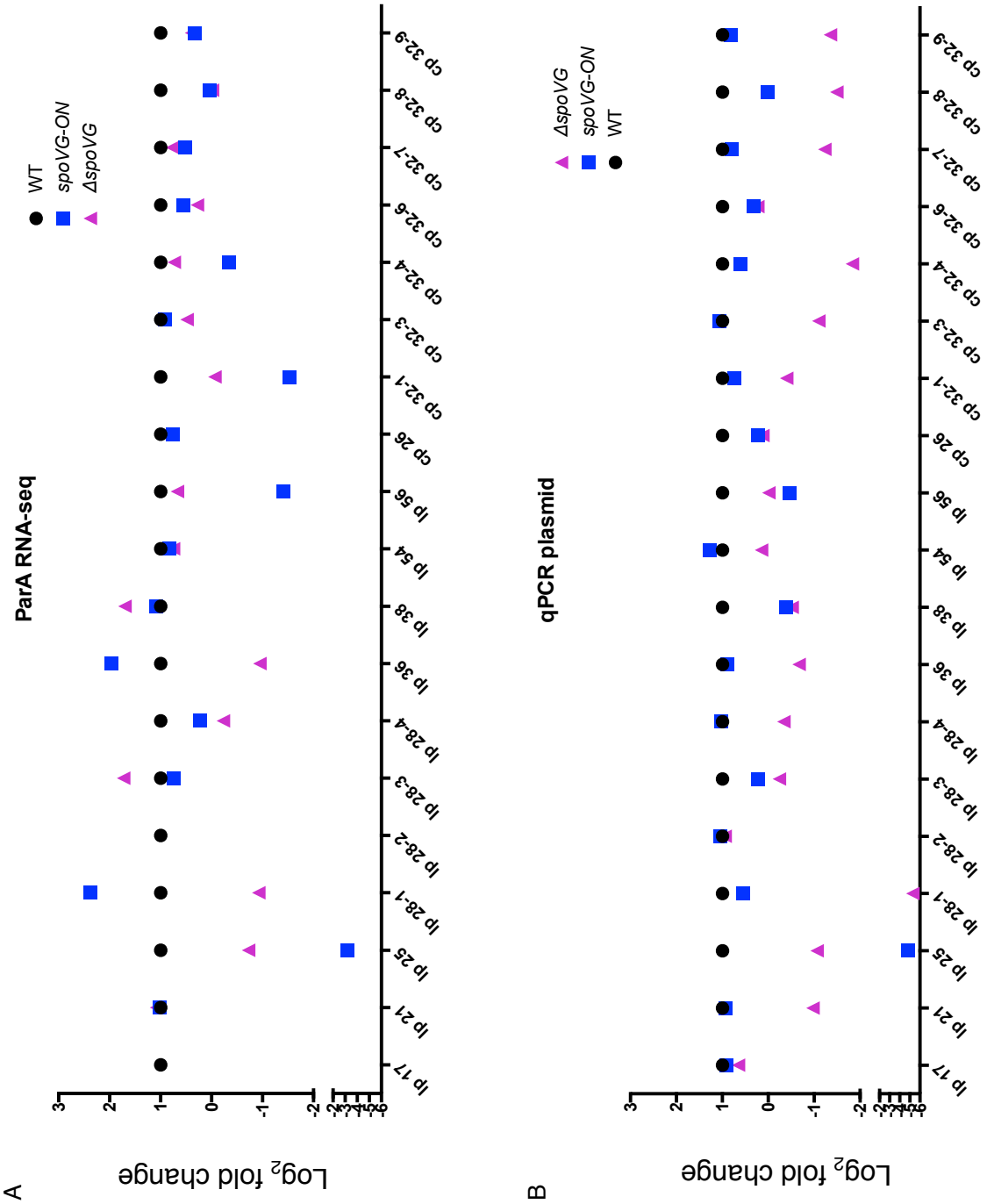

Log_2 differences in *parA* transcript abundance for individual plasmids, measured by RNA-seq (A). DNA was extracted from each strain, and plasmid quantity probed by qPCR using previously established primers unique to each plasmid (209). Log_2 differences in plasmid abundance, as measured by qPCR (B).

Figure 3.5 Effect of *spoVG* on growth rate of *B. burgdorferi*

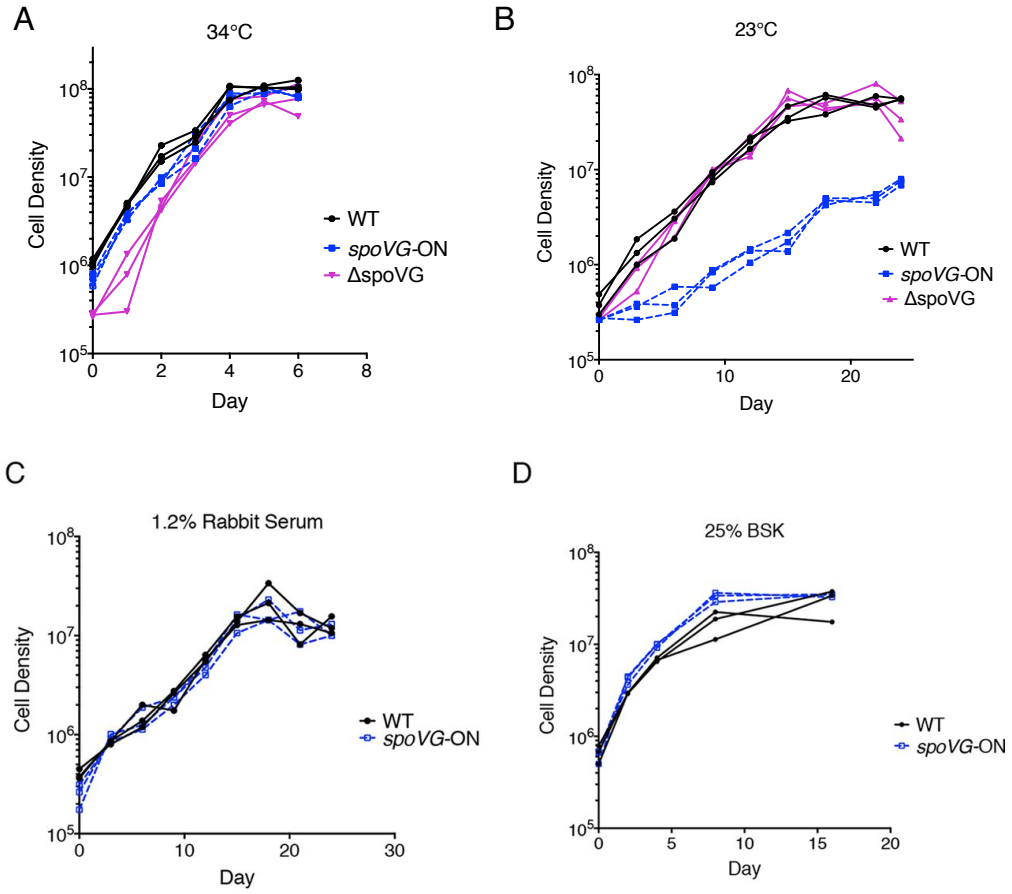

Adapted from Christina R. Savage et al. J. Bacteriol. 2018; doi:10.1128/JB.00033-18

(A and B) Cultured wild-type (WT) *spoVG*-ON and Δ*spoVG B. burgdorferi* strains were grown in complete medium at 34°C and counted every 24 h (A) or were grown in complete medium at 23°C and counted every 3 days (B).

(C and D) Cultured wild-type and *spoVG*-ON B. burgdorferi strains were also grown at 34°C in one of two deficient media, i.e., grown in 1.2% rabbit serum medium and counted every 3 days (C) or grown in 25% BSK medium and counted on days 2, 4, 8, and 16 (D).

Figure 3.6 SpoVG transcript and protein expression in culture

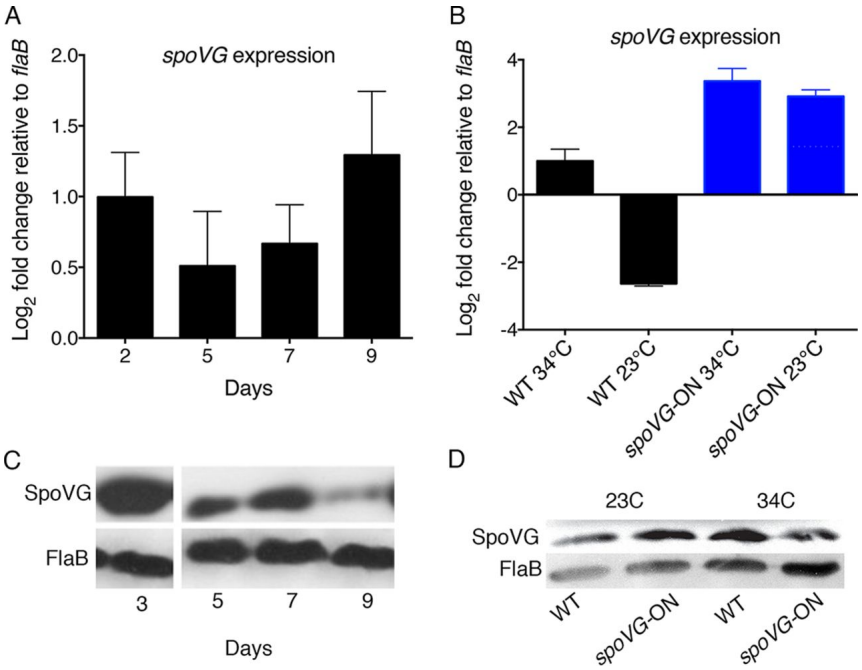

Christina R. Savage et al. J. Bacteriol. 2018; doi:10.1128/JB.00033-18

SpoVG transcript and protein expression in culture. (A) RNA extracted from cultured B. burgdorferi harvested on days 2, 5, 7, and 9 was analyzed by qRT-PCR. *spoVG* transcript levels were determined, relative to *flaB* transcripts, by the $\Delta\Delta C_T$ method. (B) RNAs extracted from cultured wild-type (WT) and *spoVG*-ON B. burgdorferi grown at 34°C and 23°C were analyzed by qRT-PCR. Relative *spoVG* transcript abundance was normalized to *flaB* transcript levels by the $\Delta\Delta C_T$ method. (C) Lysates from cultured B. burgdorferi harvested on days 3, 5, 7, and 9 were analyzed for SpoVG protein production. FlaB protein levels were used as a loading control. (D) Lysates from wild-type and *spoVG*-ON B. burgdorferi were harvested on day 3 from cultures grown at 34°C and on day 10 from cultures grown at 23°C and were analyzed by Western blotting. SpoVG abundance is shown with FlaB as the loading control.

Figure 3.7 SpoVG binds its own DNA and RNA

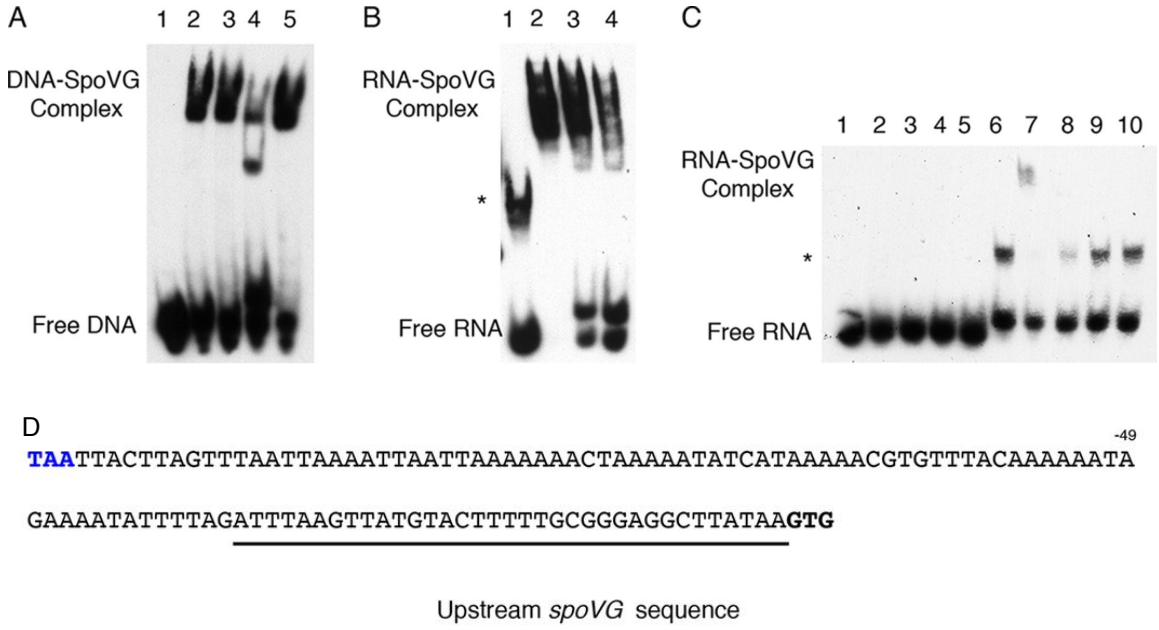

Christina R. Savage et al. J. Bacteriol. 2018; doi:10.1128/JB.00033-18

SpoVG binding of its own DNA and RNA. EMSAs were performed using either labeled DNA or RNA derived from the sequence 5′ of the *spoVG* translational start site or RNA derived from the sequence 5′ of the unrelated *erpAB* operon (23). The *spoVG* RNA probe formed a secondary structure in the absence of added protein (indicated by an asterisk). (A) Lane 1, 1 ng DNA probe; lane 2, 1 ng DNA probe with 2.4 μM rSpoVG; lane 3, 1 ng DNA probe with 4.8 μM rSpoVG; lane 4, 1 ng DNA probe with 4.8 μM rSpoVG and 100 ng unlabeled *spoVG* DNA; lane 5, 1 ng DNA probe with 4.8 μM rSpoVG and 100 ng unlabeled EMSA-pCR2.1 DNA. (B) Lane 1, 1 ng RNA probe (asterisk indicates a secondary structure of the RNA); lane 2, 1 ng RNA probe with 2.4 μM rSpoVG; lane 3, 1 ng RNA probe with 2.4 μM rSpoVG and 100 ng unlabeled *spoVG* DNA; lane 4, 1 ng RNA probe with 2.4 μM rSpoVG and 1,000 ng unlabeled *spoVG* DNA. (C) Lanes 1 to 5, 1 ng *erp* RNA; lanes 6 to 10, 1 ng *spoVG* RNA; lanes 1 and 6, no protein; lanes 2 and 7, 1.6 μM

r SpoVG; lanes 3 and 8, 160 nM rSpoVG; lanes 4 and 9, 16 nM rSpoVG; lanes 5 and 10, 1.6 nM rSpoVG. (D)

The sequence is shown as DNA, although SpoVG also bound to this site in single-stranded RNA. The DNA/RNA target region used for EMSAs are underlined. Intergenic region between the start of the *spoVG* open reading frame (ORF) and the gene located immediately upstream, *rsf*. The transcriptional start site of the *spoVG* ORF is highlighted in bold black type, and the stop codon of the *rsf* gene is highlighted in bold blue type.

Figure 3.8 Multiple SpoVG complexes bind to a single DNA

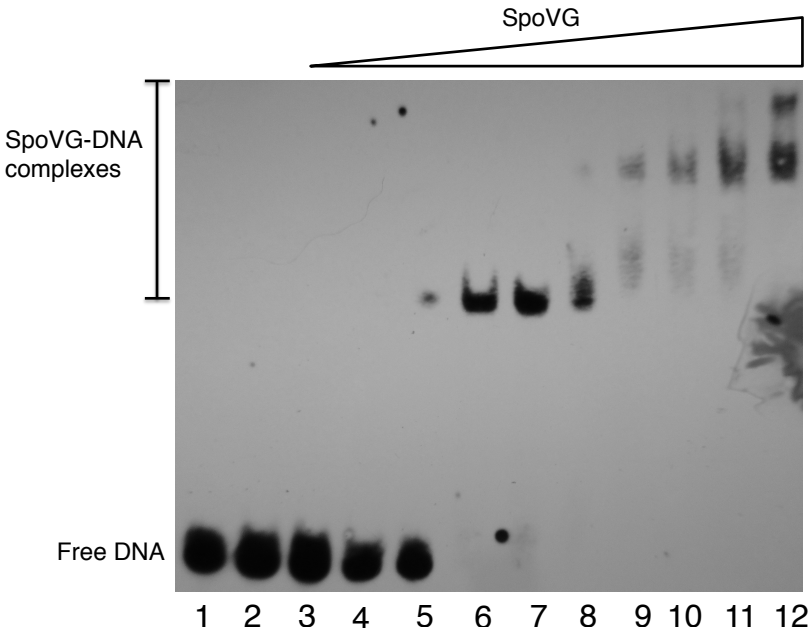

SpoVG protein was added in increasing amounts to a 100 bp DNA probe. Presence of multiple shifted bands indicate that multiple SpoVG proteins bind to a single DNA. Protein concentration ranged from 1-500x. All lanes contain 1 ng DNA. Lane 1: no protein. Lane 2: 1 µl of (1:1,00x) protein. Lane 3: 2 µl of (1:1,00x) protein. Lane 4: 5 µl of (1:1,00x) protein. Lane 6: 1 µl of (1:10x) protein. Lane 7: 2 µl of (1:10 x) protein. Lane 8: 5 µl of 1:10x protein). Lane 9: 1 µl of protein. Lane 10: 1 µl of protein. Lane 11: 2 µl of protein. Lane 12: 5 µl protein.

Figure 3.9 PlzA and c-di-GMP are necessary for expression of SpoVG

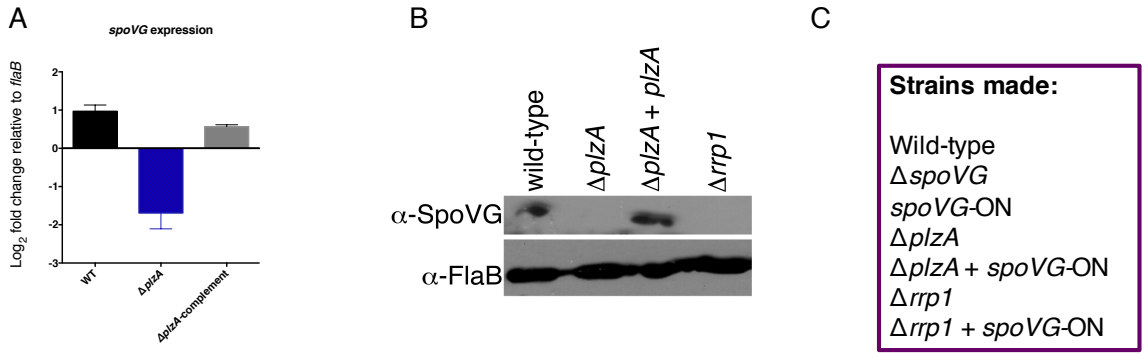

qRT-PCR on levels of *spoVG* transcript expressed by wild-type, Δ*plzA* and Δ*plzA*+*plzA* strains grown at 34° C. *spoVG* transcripts were normalized to *flaB* transcripts. Three biological replicates are graphed (A). Western Blot on wild-type, Δ*plzA*, Δ*plzA*+*plzA*, and Δ*rrp1* strains, probed for SpoVG and FlaB. Cultures were grown at 34° C, and lysates prepared at mid-log phase growth. Representative blot of at least three biological replicates (B). List of newly generated strains to study the impact that SpoVG has on expression of down-stream genes (C).

Figure 3.10 Distribution of differentially expressed RNAs

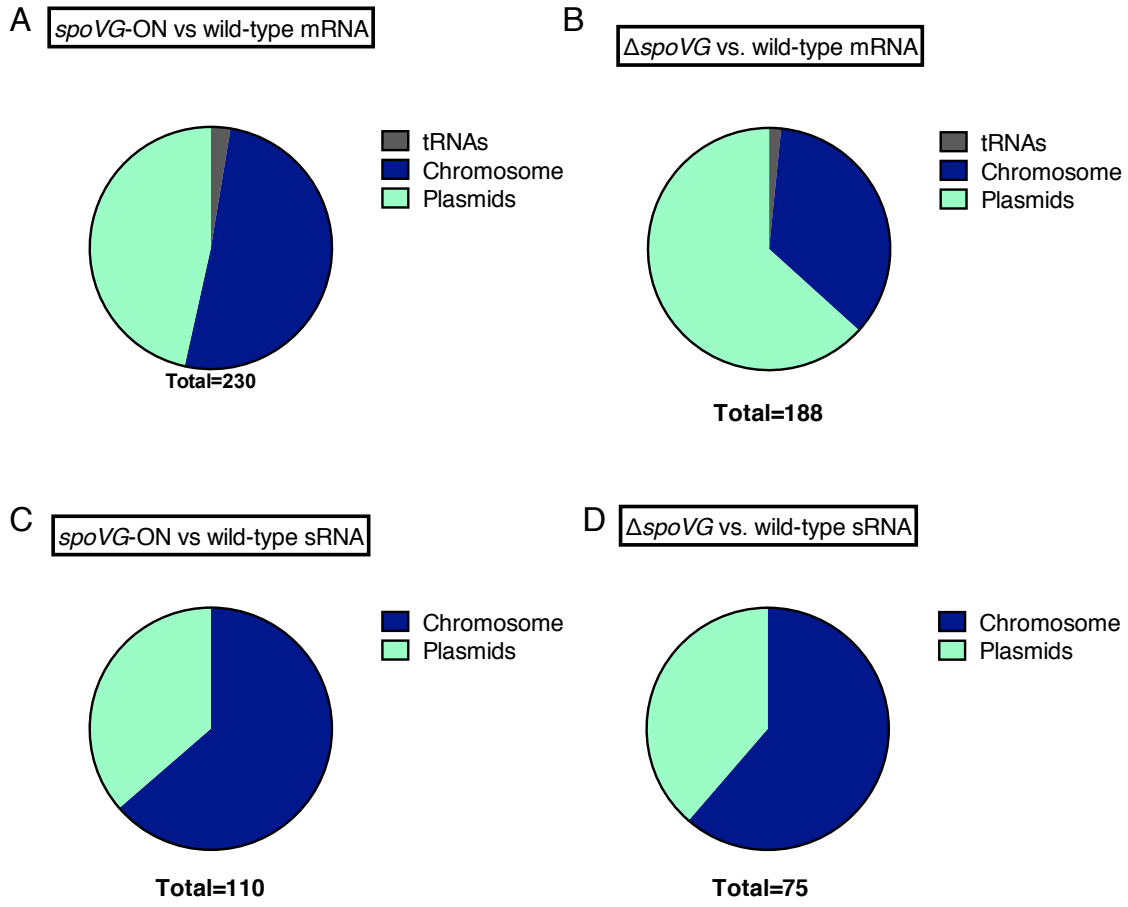

Distribution of differentially expressed RNAs across the main chromosome and plasmids. Each graph represents how many differentially expressed transcripts are found on the chromosome and how many are found on the various plasmids.

Figure 3.11 Functional clustering of differentially expressed transcripts

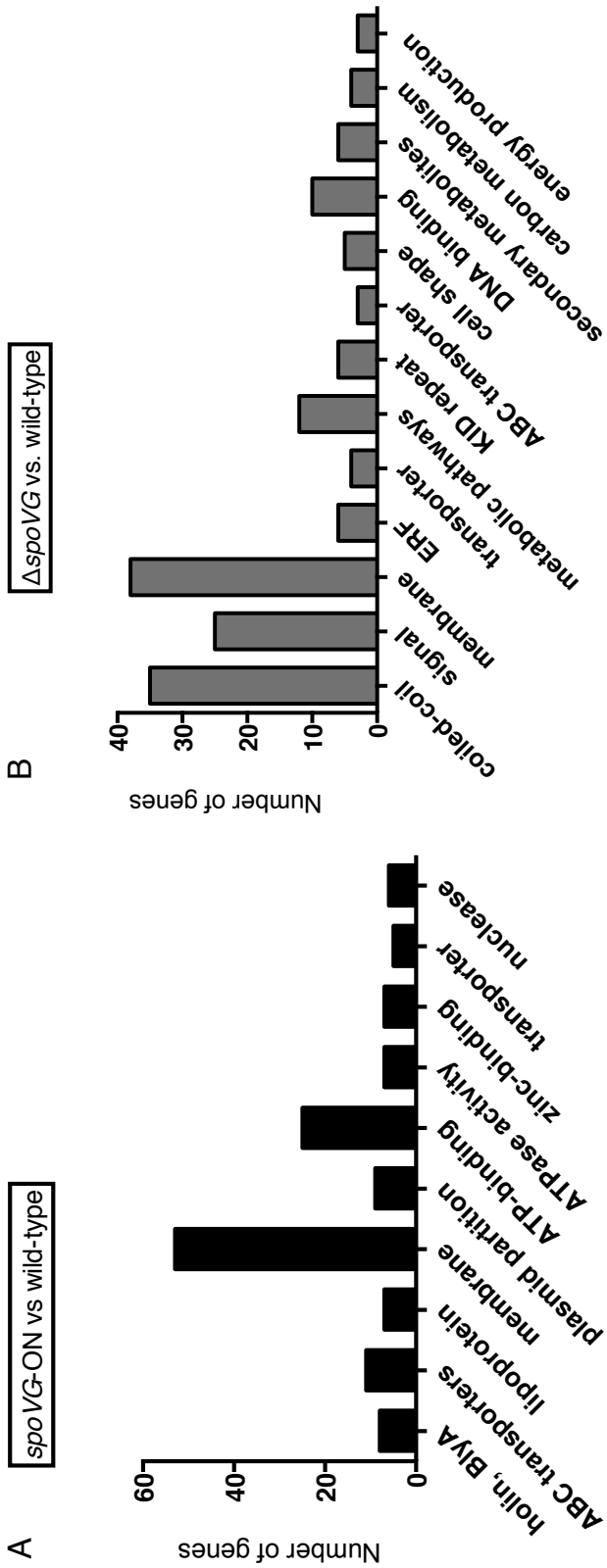

Functional classification for differentially expressed transcripts. A) *spoVG*-ON vs wild-type B) Δ*spoVG* vs wild-type. The height of each bar represents how many transcripts fall under that classification.

Table 3.1 Small RNAs differentially expressed between wild-type and *spoVG*-ON

SR ID		Start	Stop	Strand	log2FoldChange	padj
SR0001	chr	3151	3343	-	1.358484046	0.002241441
SR0014	chr	25903	25952	-	1.032088033	0.019764571
SR0028	chr	45908	45970	-	1.674028232	0.000643201
SR0042	chr	62874	62965	+	1.112696054	0.036858673
SR0067	chr	109635	109750	+	-1.267874699	0.021292417
SR0072	chr	115524	115593	+	-1.015940954	0.042829818
SR0089	chr	138320	138376	+	-1.302812659	0.000224418
SR0111	chr	164373	164418	+	1.34051063	0.000415857
SR0112	chr	164713	164837	-	1.304637546	0.03426588
SR0126	chr	176642	176691	+	-1.308248535	0.038847748
SR0165	chr	211234	211296	+	2.054932353	0.00017475
SR0168	chr	218334	218546	+	1.309936809	7.14E-05
SR0173	chr	223054	223124	-	-1.355726705	0.000196887
SR0186	chr	245945	246070	-	2.636228597	5.11E-24
SR0187	chr	246367	246464	-	2.349616463	5.02E-21
SR0196	chr	260581	260796	-	-1.218449775	0.00716771
SR0215	chr	295449	295594	-	12.3762417	1.22E-09
SR0233	chr	327895	328102	+	1.103912915	0.003147874
SR0246	chr	340302	340576	+	5.233280979	1.10E-92
SR0263	chr	369675	369724	-	-1.00333115	0.026546899
SR0264	chr	373474	373545	+	-1.690678454	0.03231015
SR0276	chr	394805	394853	+	1.284819642	3.57E-08
SR0277	chr	395312	395387	-	1.757089302	0.002885601
SR0278	chr	396334	396428	+	1.555158272	0.0085385
SR0279	chr	399917	400036	+	-1.11627616	0.036858673
SR0284	chr	408412	408480	-	1.609669841	0.00047551
SR0303	chr	421685	421769	-	-1.366458316	0.039063197
SR0305	chr	423518	423638	-	-1.698033543	0.002381768
SR0309	chr	428415	428516	-	-1.278242083	0.003342058
SR0324	chr	443571	443751	+	1.526204778	0.001062938
SR0341	chr	465040	465110	-	1.07500888	0.002993145
SR0345	chr	467849	467895	+	-1.892810192	0.000506069
SR0347	chr	472002	472086	+	-1.816307144	0.013983777
SR0359	chr	482082	482232	+	1.286200447	0.025638451
SR0392	chr	515629	515807	+	-2.183927843	2.70E-07
SR0395	chr	523418	523524	+	-1.006586325	0.009388403

SR0396	chr	526293	526449	+	-1.817469144	5.61E-06
SR0399	chr	531636	531704	-	1.680167476	0.021492887
SR0412	chr	551933	552192	+	2.411574701	0.000267652
SR0416	chr	559261	559321	+	-1.295063237	0.006823882
SR0457	chr	605915	605979	+	-1.019257396	0.010928101
SR0481	chr	631929	631984	-	1.074316651	0.000356408
SR0520	chr	662542	662591	+	-1.590596006	0.026316987
SR0524	chr	666067	666185	+	-2.300506847	1.22E-05
SR0540	chr	679320	679394	+	-1.68300255	0.000594103
SR0565	chr	708075	708215	-	-1.179179049	0.00077605
SR0568	chr	711583	711679	-	-1.152227018	0.011684339
SR0573	chr	714672	714720	+	1.127634628	0.034153959
SR0579	chr	722022	722071	-	-1.014394943	0.003784733
SR0582	chr	723012	723154	-	-1.018788592	0.001107488
SR0591	chr	731768	731852	+	2.233046335	0.001062938
SR0603	chr	742476	742541	+	1.586866727	0.000233071
SR0607	chr	745826	745919	-	-1.053451084	0.016961865
SR0620	chr	760922	760971	-	-1.294347604	0.014953278
SR0630	chr	769844	769938	+	-1.140244903	0.005389163
SR0635	chr	774458	774512	+	1.886801477	0.012248752
SR0643	chr	790233	790281	+	-2.61818306	1.44E-07
SR0648	chr	796463	796547	+	-1.015529348	0.000724873
SR0649	chr	797921	797971	+	-1.156381075	0.000191952
SR0655	chr	810040	810190	+	-1.77556561	3.41E-05
SR0657	chr	812265	812439	-	-1.748940548	0.002761958
SR0665	chr	822408	822454	-	-1.312375594	0.014941865
SR0666	chr	822940	822989	-	4.586636326	4.62E-50
SR0667	chr	823166	823231	+	1.018733002	0.000145481
SR0672	chr	831633	831683	+	1.26306113	0.035671486
SR0701	chr	871538	871606	+	-1.242085797	0.00260175
SR0708	chr	881440	881553	+	-1.69877351	5.82E-05
SR0709	chr	881987	882036	+	-1.617477403	0.006444542
SR0710	chr	883224	883285	+	-1.09376124	0.01455037
SR0715	chr	889701	889829	+	-1.109120463	0.004391075
SR0727	lp17	6593	6703	+	1.11827335	0.001338578
SR0728	lp17	8155	8220	+	1.237899082	0.011123802
SR0730	lp17	8407	8487	-	1.539037024	1.04E-05
SR0731	lp17	9414	9567	+	1.01345801	0.012086859
SR0734	lp17	10785	10832	+	1.881576623	0.00626945
SR0745	lp25	5310	5359	-	-4.784601894	0.000739504

SR0746	lp25	7036	7267	-	-2.981708151	1.86E-11
SR0747	lp25	9409	9553	-	-2.730403714	6.04E-11
SR0749	lp25	10817	10862	+	-3.096381485	0.003784733
SR0751	lp25	12423	12473	+	-3.732903036	6.04E-12
SR0752	lp25	13269	13417	-	-4.702350755	3.23E-07
SR0754	lp25	15673	15944	-	-4.537944456	2.92E-24
SR0755	lp25	15951	16076	+	-3.057487337	1.86E-09
SR0791	lp28-3	16481	16565	+	1.602897444	0.047405899
SR0793	lp28-3	19459	19508	+	1.021166642	0.029522634
SR0804	lp28-4	10785	10862	+	1.293920146	0.004680575
SR0805	lp28-4	12723	12840	-	-1.189420478	0.037148785
SR0811	lp28-4	18054	18137	+	2.100094268	0.001254413
SR0824	lp36	12209	12260	-	-1.358430595	0.045530176
SR0832	lp36	16149	16291	+	1.309117095	0.014449111
SR0836	lp36	22363	22451	+	-6.330188517	4.91E-06
SR0839	lp36	25584	25675	-	1.424315373	0.006382234
SR0840	lp36	25705	25783	+	1.837727784	0.030049609
SR0848	lp36	35057	35217	+	1.619337802	3.34E-06
SR0853	lp38	10402	10463	-	3.30339277	5.87E-15
SR0856	lp38	13386	13469	-	2.070162064	7.63E-08
SR0888	lp54	11715	11849	+	1.974205146	4.28E-07
SR0889	lp54	11974	12040	-	1.191854086	0.043761506
SR0900	lp54	29365	29422	-	-1.264039477	0.043761506
SR0907	lp54	41530	41649	+	-1.056680102	0.015541862
SR0922	lp56	19795	19847	-	-2.133046718	8.22E-09
SR0925	lp56	31737	31810	-	-3.215641219	0.010126645
SR0931	cp9	2128	2308	+	13.28855496	4.36E-25
SR0945	cp26	870	955	+	1.780785847	3.07E-09
SR0948	cp26	2376	2476	+	1.925642304	1.48E-05
SR0951	cp26	3191	3257	+	2.290735083	8.64E-11
SR0957	cp26	7794	7856	+	2.092446604	0.000348321
SR0958	cp26	8033	8111	-	1.032843739	0.035837546
SR0980	cp32-1	22671	22740	-	-1.422555192	0.002381768
SR0994	cp32-6	27219	27266	+	1.180157235	0.013416925

Table 3.2 Small RNAs differentially expressed between wild-type and Δ*spoVG*

		Start	Stop	Strand	log2FoldChange	padj
SR0006	chr	7249	7383	+	-1.159123135	0.004614012
SR0007	chr	7600	7661	+	-1.270580901	0.039173648
SR0021	chr	39498	39674	-	-1.643695488	0.049572294
SR0053	chr	80423	80539	-	-1.80540166	0.015018283
SR0078	chr	124199	124250	+	1.093696337	0.034904635
SR0122	chr	174087	174144	-	-5.896443438	0.030086279
SR0132	chr	181625	181673	+	-1.498631428	0.004865585
SR0186	chr	245945	246070	-	-2.497585903	2.16E-21
SR0187	chr	246367	246464	-	-3.153125812	3.01E-33
SR0189	chr	250385	250467	+	-1.159727406	0.004614012
SR0203	chr	269511	269626	+	-1.498171463	0.009379819
SR0244	chr	336511	336565	+	-1.024994359	0.047423471
SR0245	chr	338243	338293	+	-1.588537322	0.001486185
SR0246	chr	340302	340576	+	-1.02136926	0.002085611
SR0247	chr	340555	340650	-	-1.006465242	0.010664288
SR0254	chr	358532	358589	-	1.364565297	0.011245213
SR0273	chr	391800	391853	-	-1.190443551	0.015018283
SR0324	chr	443571	443751	+	-1.5775048	0.000988458
SR0326	chr	444712	444783	+	10.480605	3.57E-12
SR0332	chr	451393	451459	+	1.467490808	0.016587548
SR0389	chr	513193	513273	+	-1.225657468	0.000894501
SR0390	chr	514927	514976	-	-1.084538764	0.033792599
SR0417	chr	561897	561958	-	1.307866788	0.000440003
SR0429	chr	577156	577205	+	-1.832714092	0.011272339
SR0451	chr	600874	600966	+	-1.236582183	0.035067448
SR0459	chr	607624	607706	-	1.049962515	0.029441872
SR0472	chr	621854	621957	-	2.59978124	0.025861453
SR0513	chr	657818	657937	-	1.360417685	0.021798156
SR0514	chr	658746	658855	-	1.44876326	0.004573995
SR0520	chr	662542	662591	+	-2.930390418	6.62E-06
SR0521	chr	663063	663145	-	-3.645138546	1.16E-08
SR0537	chr	674835	674884	+	-1.954569165	1.86E-06
SR0538	chr	675672	675744	-	-1.340456717	0.000152096
SR0549	chr	688778	688888	-	1.059840465	0.046441965
SR0557	chr	696669	696840	+	-1.455782412	5.26E-07
SR0559	chr	699758	699987	-	7.802998976	2.03E-06

SR0616	chr	754389	754503	-	-1.579633071	0.013711721
SR0643	chr	790233	790281	+	-1.71542151	0.001400635
SR0644	chr	791442	791497	+	-1.640720176	0.032465907
SR0652	chr	803502	803604	-	-1.597307653	0.002085611
SR0657	chr	812265	812439	-	-2.320974658	6.31E-05
SR0666	chr	822940	822989	-	-7.064279447	9.11E-76
SR0667	chr	823166	823231	+	-1.181558845	1.18E-05
SR0692	chr	860131	860278	+	-1.730488146	0.007179662
SR0693	chr	860333	860544	-	-1.72865893	0.000957821
SR0697	chr	863477	863549	-	-1.489284025	0.005046202
SR0728	lp17	8155	8220	+	3.005385284	1.05E-13
SR0729	lp17	8211	8257	-	2.659286196	4.83E-05
SR0730	lp17	8407	8487	-	2.028182494	1.03E-09
SR0738	lp17	12902	12951	+	1.736504713	0.02204039
SR0751	lp25	12423	12473	+	-1.631260433	0.004865585
SR0752	lp25	13269	13417	-	-2.29987205	0.005232047
SR0755	lp25	15951	16076	+	-1.497872176	0.004940813
SR0766	lp28-1	10442	10547	-	-1.770008208	0.00095639
SR0768	lp28-1	13306	13355	+	-2.624185545	0.000125427
SR0779	lp28-2	26424	26497	+	2.223505386	0.004614012
SR0788	lp28-3	9510	9570	-	-2.018714944	5.60E-05
SR0805	lp28-4	12723	12840	-	-1.380152775	0.016637921
SR0812	lp28-4	19115	19207	-	1.335542101	0.034401719
SR0815	lp28-4	26351	26421	+	2.703553681	4.87E-07
SR0830	lp36	15735	15794	-	1.305942792	0.017463607
SR0837	lp36	22421	22583	-	-1.526193511	0.000443694
SR0841	lp36	26891	26940	-	1.270671751	0.013500781
SR0848	lp36	35057	35217	+	1.176672551	0.002180512
SR0852	lp38	6872	6947	+	-1.35492921	0.045065494
SR0865	lp38	26484	26597	+	1.65914682	0.029441872
SR0866	lp38	26536	26600	-	1.638570844	0.04052967
SR0879	lp38	38374	38508	-	3.405986738	2.67E-09
SR0896	lp54	23118	23236	+	1.349938919	0.000740556
SR0909	lp54	44646	44713	-	1.60009289	0.029441872
SR0911	lp54	45194	45286	+	1.727973613	0.007710031
SR0953	cp26	7013	7135	-	1.801787455	1.76E-05
SR0958	cp26	8033	8111	-	1.176239568	0.01770918
SR0980	cp32-1	22671	22740	-	-1.209487177	0.016598983
SR0996	cp32-7	18868	18934	-	-1.808827538	0.041740727

Table 3.3 mRNAs differentially expressed between wild-type and *spoVG*-ON

Gene	Log_2 Change	padj
BB_0008| conserved hypothetical protein0008|	-1.190	5.55E-05
BB_0009| conserved hypothetical protein0009|	-1.493	1.88E-10
BB_0013| conserved hypothetical protein0013|	-1.056	9.43E-03
BB_0014| priA| primosomal protein N'0014|	-1.527	4.28E-07
BB_0015| udk| uridine kinase0015|	-1.449	1.35E-06
BB_0023| ruvA| holliday junction DNA helicase RuvA0023|	1.149	3.52E-03
BB_0034| outer membrane protein P130034|	1.219	2.06E-03
BB_0043| conserved hypothetical protein0043|	1.824	2.74E-04
BB_0044| conserved hypothetical protein0044|	1.752	5.82E-04
BB_0047| conserved hypothetical protein0047|	2.071	4.46E-04
BB_0076| ftsY| signal recognition particle-docking protein	-1.098	6.20E-05
BB_0080| ABC transporter%2C ATP-binding protein0080|	-1.249	2.12E-03
BB_0081| efflux ABC transporter	-1.224	8.95E-03
BB_0098| MutS2 protein0098|	-1.113	1.46E-02
BB_0134| tetratricopeptide repeat domain protein0134|	-1.056	3.72E-03
BB_0184| csrA| carbon storage regulator0184|	-1.521	1.85E-03
BB_0189| rpmI| ribosomal protein L350189|	1.100	1.78E-03
BB_0211| DNA mismatch repair protein MutL0211|	-1.016	8.26E-04
BB_0212| borrelia ORF-A superfamily0212|	1.092	1.89E-02
BB_0217| pstA| phosphate ABC transporter	-1.166	3.16E-04
BB_0225| tRNA-dihydrouridine synthase A0225|	-1.348	1.43E-02
BB_0238| conserved hypothetical protein0238|	1.156	3.12E-03
BB_0240| glycerol uptake facilitator0240|	2.581	6.31E-25
BB_0241| glpK| glycerol kinase0241|	2.320	1.07E-12
BB_0242| conserved hypothetical protein0242|	2.370	5.89E-10
BB_0243| glycerol-3-phosphate dehydrogenase	2.409	1.30E-10
BB_0251| leuS| leucyl-tRNA synthetase0251|	-1.677	5.65E-05
BB_0273| fliR| flagellar biosynthetic protein FliR0273|	-1.070	2.51E-02
BB_0282| hypothetical protein0282|	1.015	1.41E-02
BB_0295| hslU| heat shock protein HslVU ATPase subunit	-1.057	5.06E-04
BB_0296| ATP-dependent protease HslV0296|	-1.202	5.94E-05
BB_0304| murF	-1.085	2.24E-03
BB_0305| conserved hypothetical protein0305|	-1.515	3.19E-09
BB_0306| mraW| S-adenosyl-methyltransferase MraW0306|	-1.190	1.11E-06
BB_0323| LysM domain protein0323|	1.103	1.46E-03

BB_0332| ABC transporter%2C permease protein0332|	-1.271	3.39E-04
BB_0334| oligopeptide transport ATP-binding protein OppD	-1.129	2.67E-02
BB_0355| transcription factor%2C putative0355|	1.019	2.09E-04
BB_0360| conserved hypothetical protein0360|	-1.054	1.33E-04
BB_0362| lgt| prolipoprotein diacylglyceryl transferase0362|	-1.038	2.30E-05
BB_0363| periplasmic protein0363|	-1.562	7.24E-11
BB_0366| vacuolar aminopeptidase I0366|	1.394	2.01E-03
BB_0367| phosphotransferase enzyme IIb component	1.687	4.63E-05
BB_0374| HD domain protein0374|	-1.621	7.32E-04
BB_0375| pfs| putative nucleosidase%2C Pfs protein0375|	-1.855	9.62E-10
BB_0376| metK| methionine adenosyltransferase0376|	-1.954	3.76E-08
BB_0377| luxS| S-ribosylhomocysteinase LuxS0377|	-1.520	4.72E-05
BB_0384| bmpC| basic membrane protein C (bmpC)0384|	1.088	8.45E-06
BB_0385| bmpD| basic membrane protein D (bmpD)0385|	1.255	1.53E-02
BB_0409| conserved hypothetical protein0409|	-1.884	2.90E-05
BB_0412| membrane protein%2C putative0412|	-1.065	1.61E-02
BB_0417| adenylate kinase (ATP-AMP transphosphorylase)	-1.357	1.24E-06
BB_0426| nucleoside 2-deoxyribosyltransferase superfamily	1.365	6.31E-04
BB_0445| fbaA| fructose-bisphosphate aldolase	1.115	6.27E-03
BB_0447| Na+/H+ antiporter0447|	-1.362	6.27E-03
BB_0450| rpoN| RNA polymerase sigma-54 factor0450|	-2.221	4.21E-05
BB_0451| chromate transport protein%2C putative0451|	-1.467	2.14E-02
BB_0452| chromate transporter superfamily0452|	-1.628	2.59E-02
BB_0472| murA|	-1.019	7.42E-05
BB_0475| lipoprotein%2C putative0475|	1.165	5.62E-03
BB_0507| conserved hypothetical protein0507|	-1.078	3.01E-02
BB_0512| conserved hypothetical protein0512|	-1.270	1.98E-03
BB_0535| conserved hypothetical protein0535|	1.257	7.76E-04
BB_0537| tetratricopeptide repeat domain protein0537|	-1.734	1.99E-06
BB_0538| hypothetical protein0538|	-1.506	6.68E-06
BB_0548| polA| DNA polymerase I superfamily0548|	-1.101	7.95E-05
BB_0555| conserved hypothetical protein0555|	-1.038	2.54E-03
BB_0577| conserved hypothetical protein0577|	1.290	2.25E-04
BB_0586| FemA protein0586|	-1.140	1.68E-03
BB_0592| caax amino protease family0592|	1.231	3.67E-03
BB_0603| p66| integral outer membrane protein P660603|	1.099	1.46E-03
BB_0617| conserved hypothetical protein0617|	1.401	7.25E-04
BB_0626| rnmV| ribonuclease M50626|	1.477	2.00E-04
BB_0633| recB| exodeoxyribonuclease	-1.440	3.57E-03
BB_0639| spermidine/putrescine ABC transporter0639|	-1.286	1.20E-02

BB_0640| binding-protein-dependent transport systems	-1.714	1.30E-04
BB_0641| putrescine transport system permease protein	-1.848	2.09E-05
BB_0642| potA| spermidine/putrescine ABC	-1.499	1.31E-03
BB_0649| groL| chaperonin GroL0649|	1.140	1.84E-02
BB_0661| conserved hypothetical protein0661|	1.540	4.24E-09
BB_0662| conserved hypothetical protein0662|	1.404	3.36E-04
BB_0671| CheC-like family protein0671|	-1.082	8.63E-05
BB_0672| CheY0672|	-1.268	6.77E-03
BB_0673| conserved hypothetical protein0673|	-1.006	3.69E-02
BB_0677| rbsA| sugar ABC transporter	-1.028	1.84E-02
BB_0679| ribose/galactose ABC transporter	-1.082	3.91E-02
BB_0690| napA| neutrophil activating protein A (napA)0690|	1.736	2.46E-03
BB_0712| RNA polymerase sigma factor RpoD	-1.341	3.71E-05
BB_0713| conserved hypothetical protein0713|	-1.759	6.02E-12
BB_0721| pgsA| 0721|	-1.055	3.06E-02
BB_0722| conserved hypothetical protein0722|	-1.270	1.07E-02
BB_0734| Sua5/YciO/YrdC/YwlC family protein	-1.060	3.41E-03
BB_0740| conserved hypothetical protein0740|	-1.724	1.12E-07
BB_0746| oligopeptide ABC transporter permease protein	-6.706	3.23E-06
BB_0754| ABC transporter%2C ATP-binding protein0754|	-1.229	1.22E-04
BB_0755| rnz| ribonuclease Z0755|	-1.208	1.76E-04
BB_0764| sensory transduction histidine kinase	-1.993	2.86E-07
BB_0765| conserved hypothetical protein0765|	-1.932	1.64E-04
BB_0766| cvpA| CvpA family protein0766|	-2.768	1.08E-07
BB_0767| murG| 0767|	-2.196	2.90E-05
BB_0768| pyridoxal kinase0768|	-2.056	5.69E-07
BB_0769| glycoprotease family0769|	-2.530	1.99E-08
BB_0770| divergent polysaccharide deacetylase superfamily	-2.116	1.33E-07
BB_0771a| hypothetical protein0771a|	-1.236	1.52E-02
BB_0782| nadD|	-1.198	1.68E-04
BB_0783| conserved hypothetical protein0783|	-1.051	2.38E-03
BB_0784| iojap-like ribosome-associated protein0784|	-1.062	8.47E-03
BB_0785| spoVG (Stage V sporulation protein G)0785|	2.617	3.67E-27
BB_0807| conserved hypothetical integral membrane protein	-1.510	4.23E-04
BB_0808| putative permease%2C YjgP/YjgQ family0808|	-1.196	7.37E-03
BB_0809| tgt| queuine tRNA-ribosyltransferase0809|	-1.095	1.01E-04
BB_0833| ileS| isoleucyl-tRNA synthetase0833|	-1.234	4.68E-03
BB_0837| uvrA| excinuclease ABC%2C A subunit0837|	-1.448	1.37E-04
BB_0838| conserved hypothetical protein0838|	-1.238	3.12E-03
BB_0841| arcA| arginine deiminase0841|	1.956	6.87E-12

BB_0842| argF| ornithine carbamoyltransferase0842|	1.752	6.16E-05
BB_0843| arginine-ornithine antiporter0843|	1.224	7.99E-07
BB_A08| conserved hypothetical proteinA08|	1.078	9.39E-03
BB_A38| putative phage portal protein%2C HI1409 familyA38|	-1.075	1.76E-02
BB_A40| lyme disease proteins of unknown functionA40|	-1.218	9.17E-04
BB_A41| conserved hypothetical proteinA41|	-1.320	1.34E-03
BB_A42| conserved hypothetical proteinA42|	-1.351	1.63E-03
BB_A53| Bbs27 proteinA53|	-1.352	4.38E-02
BB_A74| osm28| outer membrane porin OMS28A74|	-2.318	8.04E-04
BB_B01| acylphosphataseB01|	1.065	3.20E-03
BB_B03| resT| telomere resolvase ResTB03|	1.029	6.93E-03
BB_B04| chbC| chitibiose transporter protein chbCB04|	2.610	7.82E-14
BB_B10| borrelia ORF-A superfamilyB10|	1.243	8.57E-05
BB_B24| conserved hypothetical proteinB24|	-1.357	6.65E-05
BB_B29| pts system%2C iibc componentsB29|	1.287	8.21E-04
BB_C01| BBC01C01|	11.520	5.85E-19
BB_C03| BBC03C03|	10.782	2.25E-16
BB_C05| BBC05C05|	9.565	1.85E-12
BB_D14| borrelia ORF-A superfamilyD14|	1.670	5.61E-06
BB_E09| protein p23E09|	-3.640	8.11E-14
BB_E16| bptA| BptA proteinE16|	-3.894	2.50E-36
BB_E17| conserved hypothetical proteinE17|	-3.173	4.16E-23
BB_E18| PF-49 proteinE18|	-3.896	1.33E-20
BB_E19| PF-32 proteinE19|	-4.272	1.40E-26
BB_E20| borrelia family of unknown functionE20|	-4.332	5.15E-29
BB_E21| conserved hypothetical proteinE21|	-3.794	9.10E-39
BB_E22| pncA|	-4.970	2.44E-03
BB_E31| putative surface proteinE31|	-2.651	1.49E-19
BB_F23| PF49F23|	-1.556	1.33E-02
BB_G08| stage 0 sporulation protein JG08|	-1.073	4.02E-02
BB_H37| lipoprotein%2C putativeH37|	-1.481	1.62E-02
BB_I16| vraA|I16|	1.187	6.44E-03
BB_I22| PF-49 proteinI22|	-1.414	1.72E-02
BB_J08| putative surface proteinJ08|	1.263	4.38E-02
BB_J09| ospD| outer surface protein D (OspD)J09|	-1.693	3.48E-02
BB_J19| borrelia ORF-A superfamilyJ19|	1.225	7.40E-04
BB_K01| lipoprotein%2C putativeK01|	-2.160	6.10E-06
BB_K40| conserved hypothetical proteinK40|	1.712	3.34E-03
BB_K47| conserved hypothetical proteinK47|	-1.198	3.39E-02

BB_K49| conserved hypothetical proteinK49|	-1.095	4.59E-02
BB_K52| putative lipoproteinK52|	1.466	5.68E-05
BB_L20| conserved hypothetical proteinL20|	-1.174	1.31E-03
BB_L21| conserved hypothetical proteinL21|	-1.504	1.96E-04
BB_L22| conserved hypothetical proteinL22|	-1.170	8.35E-04
BB_L25| 2.9-6 ORF-CL25|	-1.730	9.88E-07
BB_L26| borrelia orf-D familyL26|	-1.785	7.92E-08
BB_L31| borrelia family of unknown functionL31|	-1.016	2.38E-03
BB_L32| PF-32 proteinL32|	-1.109	1.16E-03
BB_M20| conserved hypothetical proteinM20|	-1.393	1.46E-04
BB_M21| conserved hypothetical proteinM21|	-1.494	2.33E-04
BB_M25| 2.9-6 ORF-CM25|	-1.389	2.26E-04
BB_M30| BBC01M30|	1.161	3.62E-03
BB_M33| PF-49 proteinM33|	-1.812	2.58E-03
BB_M34| BdrKM34|	-1.456	1.98E-03
BB_N19| conserved hypothetical proteinN19|	1.036	1.75E-02
BB_N25| 2.9-6 ORF-CN25|	-1.112	2.22E-03
BB_N27| BdrRN27|	1.158	2.08E-02
BB_N28| lipoproteinN28|	1.683	1.23E-03
BB_N33| PF-49 proteinN33|	-1.532	4.75E-03
BB_N34| BdrQN34|	-1.177	1.35E-02
BB_O21| conserved hypothetical proteinO21|	-1.423	7.34E-04
BB_O22| conserved hypothetical proteinO22|	-1.151	1.03E-03
BB_O26| borrelia orf-D familyO26|	-1.127	3.56E-04
BB_O33| putative plasmid partition protein%3B Orf3O33|	-1.750	8.45E-03
BB_O34| BdrMO34|	-1.400	1.72E-02
BB_O39| erpL| ErpL proteinO39|	3.779	1.24E-02
BB_P20| conserved hypothetical proteinP20|	-1.393	1.46E-04
BB_P21| conserved hypothetical proteinP21|	-1.552	1.33E-04
BB_P22| conserved hypothetical proteinP22|	-1.152	1.07E-03
BB_P25| 2.9-7 ORF-CP25|	-1.490	1.63E-03
BB_P26| borrelia orf-D familyP26|	-1.384	4.75E-03
BB_P31| borrelia family of unknown functionP31|	-1.576	1.27E-04
BB_P32| PF-32 proteinP32|	-2.934	8.85E-07
BB_P33| PF-49 proteinP33|	-2.877	8.57E-08
BB_P34| BdrAP34|	-2.231	3.07E-06
BB_Q03| outer membrane proteinQ03|	-1.283	6.03E-03
BB_Q06| borrelia membrane protein P13Q06|	-1.188	1.62E-02
BB_Q09| borrelia family of unknown functionQ09|	-1.884	1.34E-03
BB_Q14| conserved hypothetical proteinQ14|	-5.022	4.38E-02

BB_Q23| conserved hypothetical proteinQ23|	-1.230	3.68E-02
BB_Q26| conserved hypothetical proteinQ26|	-1.083	3.34E-03
BB_Q27| conserved hypothetical proteinQ27|	-1.417	1.01E-04
BB_Q28| conserved hypothetical proteinQ28|	-1.768	2.90E-05
BB_Q29| conserved hypothetical proteinQ29|	-2.395	2.53E-13
BB_Q30| holin%2C BlyA familyQ30|	-1.092	1.63E-02
BB_Q31| hemolysin accessory proteinQ31|	-1.242	1.98E-03
BB_Q32| 2.9-6 ORF-CQ32|	-1.554	3.41E-05
BB_Q33| borrelia orf-D familyQ33|	-1.986	2.45E-10
BB_Q39| borrelia family of unknown functionQ39|	-1.132	3.07E-04
BB_Q40| PF-32 proteinQ40|	-2.722	3.41E-08
BB_Q48| conserved hypothetical proteinQ48|	-1.706	4.88E-05
BB_Q49| hypothetical proteinQ49|	-1.531	6.43E-04
BB_Q62| conserved hypothetical proteinQ62|	-2.884	2.09E-05
BB_Q67| adenine specific DNA methyltransferaseQ67|	-1.731	1.78E-03
BB_R05| lyme disease proteins of unknown functionR05|	-1.032	4.08E-02
BB_R20| conserved hypothetical proteinR20|	-1.240	5.60E-04
BB_R21| conserved hypothetical proteinR21|	-1.407	4.76E-04
BB_R22| conserved hypothetical proteinR22|	-1.521	3.25E-06
BB_R23| holin%2C BlyA familyR23|	-1.118	1.52E-02
BB_R25| 2.9-6 ORF-CR25|	-1.501	6.35E-05
BB_R26| borrelia orf-D familyR26|	-1.412	4.85E-05
BB_R27| BdrHR27|	1.187	4.93E-03
BB_R28| lipoproteinR28|	1.426	2.82E-03
BB_R32| borrelia family of unknown functionR32|	-1.037	6.44E-03
BB_R33| PF-32 proteinR33|	-1.579	6.65E-05
BB_R34| PF-49 proteinR34|	-1.569	9.06E-04
BB_S20| conserved hypothetical proteinS20|	-1.419	1.13E-04
BB_S21| conserved hypothetical proteinS21|	-1.278	1.34E-03
BB_S25| 2.9-6 ORF-CS25|	-1.497	5.82E-05
BB_S26| borrelia orf-D familyS26|	-1.293	5.02E-04
EBG00001182584| tRNA| biotype=tRNA00001182584	-1.124	1.70E-02
EBG00001182585| tRNA| biotype=tRNA00001182585	1.412	4.01E-02
EBG00001182601| tRNA| biotype=tRNA00001182601	1.144	4.23E-03
EBG00001182604| tRNA| biotype=tRNA00001182604	1.170	3.71E-02
EBG00001182606| tRNA| biotype=tRNA00001182606	1.772	5.46E-03
EBG00001182619| tRNA| biotype=tRNA00001182619	1.833	6.43E-04

Table 3.4 mRNAs differentially expressed between wild-type and Δ*spoVG*

gene	Log_2 Change	padj
BB_0006| membrane protein0006|	-1.161	4.61E-03
BB_0025| DNA-binding regulatory protein YebC/PmpR	1.507	1.07E-02
BB_0026| methylenetetrahydrofolate dehydrogenase0026|	1.338	8.69E-03
BB_0036| DNA topoisomerase II (N-region) domain protein	-1.474	6.59E-03
BB_0037| 1-acyl-sn-glycerol-3-phosphate acyltransferase	-1.464	2.18E-03
BB_0039| conserved hypothetical protein0039|	-1.320	2.31E-02
BB_0040| cheR| CheR methyltransferase	1.011	3.29E-02
BB_0084| aminotransferase%2C class V superfamily0084|	-1.849	1.09E-02
BB_0114| single-stranded DNA-binding protein	1.117	4.22E-03
BB_0115| 30S ribosomal protein S60115|	1.224	8.38E-04
BB_0138| conserved hypothetical protein0138|	-1.738	4.75E-03
BB_0168| DnaK suppressor%2C putative0168|	-1.092	6.83E-05
BB_0174| conserved hypothetical protein0174|	-1.081	2.97E-02
BB_0179| trmE| tRNA modification GTPase TrmE0179|	-1.170	9.97E-04
BB_0193| lipoprotein%2C putative0193|	-1.233	1.77E-02
BB_0240| glycerol uptake facilitator0240|	-3.036	3.31E-34
BB_0241| glpK| glycerol kinase0241|	-3.124	4.93E-23
BB_0242| conserved hypothetical protein0242|	-3.620	1.25E-22
BB_0243| glycerol-3-phosphate dehydrogenase	-2.348	5.13E-10
BB_0244| conserved hypothetical protein0244|	-1.303	3.32E-04
BB_0245| hypothetical protein0245|	-1.012	3.33E-03
BB_0246| M23 peptidase domain protein0246|	-1.582	1.12E-06
BB_0258| undecaprenol kinase0258|	-1.170	1.45E-02
BB_0275| fliP| flagellar biosynthetic protein FliP0275|	-1.152	4.58E-02
BB_0295| hslU|	1.073	5.71E-04
BB_0317| conserved hypothetical integral membrane prot	-1.001	4.20E-02
BB_0330| bacterial extracellular solute-binding protein	-1.755	8.65E-03
BB_0364| mgsA| methylglyoxal synthase0364|	-1.203	6.20E-03
BB_0426| nucleoside 2-deoxyribosyltransferase superfamily	1.001	2.45E-02
BB_0429| conserved hypothetical protein0429|	1.574	3.24E-03
BB_0434| spo0J| stage 0 sporulation protein J0434|	1.012	4.56E-02
BB_0438| dnaN| DNA polymerase III%2C beta subunit0438|	1.756	3.45E-04
BB_0439| conserved hypothetical protein0439|	1.395	3.19E-04
BB_0454| lipopolysaccharide biosynthesis-related protein	1.422	1.24E-02
BB_0470| conserved hypothetical protein0470|	-1.046	4.75E-03
BB_0508| engA| ribosome-associated GTPase EngA0508|	-1.569	2.03E-05

BB_0584| conserved hypothetical integral membrane prot	-1.730	8.49E-06
BB_0588| bgp| MTA/SAH nucleosidase Glycosaminoglycan binding	1.094	2.77E-02
BB_0592| caax amino protease family0592|	-1.185	8.01E-03
BB_0626| rnmV| ribonuclease M50626|	1.144	8.37E-03
BB_0631| conserved hypothetical protein0631|	-3.524	1.25E-26
BB_0636| zwf| glucose-6-phosphate 1-dehydrogenase	-1.229	9.97E-04
BB_0637| Na+/H+ antiporter family0637|	-1.047	6.31E-05
BB_0638| Na+/H+ antiporter0638|	-1.484	4.84E-07
BB_0639| spermidine/putrescine ABC transporter	-1.230	2.30E-02
BB_0656| oxygen-independent coproporphyrinogen III oxidase	-1.054	1.70E-04
BB_0657| rpiA| ribose 5-phosphate isomerase A0657|	-1.355	8.60E-06
BB_0658| phosphoglycerate mutase family protein	1.194	4.18E-03
BB_0678| ribose/galactose ABC transporter	-1.315	1.77E-03
BB_0679| ribose/galactose ABC transporter	-1.380	7.69E-03
BB_0689| lipoprotein%2C putative0689|	1.408	5.38E-05
BB_0691| fusA| translation elongation factor G0691|	1.321	3.50E-02
BB_0693| xylose operon regulatory protein0693|	1.020	1.36E-02
BB_0716| mreC| rod shape-determining protein MreC0716|	-1.134	4.62E-02
BB_0717| conserved hypothetical integral membrane protein	-1.709	5.99E-03
BB_0719| mrdB| rod shape-determining protein RodA0719|	-1.414	5.39E-03
BB_0737| histidine phosphokinase/phophatase	-1.230	4.38E-03
BB_0746| oligopeptide ABC transporter%2C permease	-6.982	1.34E-06
BB_0747| oligopeptide ABC transporter%2C permease	-1.448	2.79E-02
BB_0770| divergent polysaccharide deacetylase superfamily	-1.645	1.16E-04
BB_0776| conserved hypothetical protein0776|	1.453	8.95E-03
BB_0777| apt| adenine phosphoribosyltransferase0777|	1.497	1.35E-02
BB_0785| spoVG (Stage V sporulation protein G)0785|	-6.583	3.38E-167
BB_0814| panF| sodium/pantothenate symporter0814|	-1.675	1.06E-08
BB_0816| conserved hypothetical protein0816|	-1.154	7.42E-05
BB_0817| murC| UDP-N-acetylmuramate--alanine ligase0817|	-1.029	4.69E-02
BB_0844| lipoprotein%2C putative0844|	3.121	1.16E-08
BB_A24| dbpA| decorin-binding protein AA24|	2.807	2.17E-31
BB_A25| dbpB| decorin-binding protein BA25|	2.825	9.13E-27
BB_A32| conserved hypothetical proteinA32|	1.498	5.39E-03
BB_A34| bacterial extracellular solute-binding protein	1.980	2.19E-08
BB_A36| lipoproteinA36|	2.844	1.85E-16
BB_A37| conserved hypothetical proteinA37|	1.483	4.06E-02
BB_A52| outer membrane proteinA52|	-1.163	3.47E-02
BB_A53| Bbs27 proteinA53|	-1.508	2.82E-02

BB_A54| conserved hypothetical proteinA54|	-1.232	4.17E-02
BB_A58| conserved hypothetical proteinA58|	-1.991	1.40E-04
BB_A59| hypothetical proteinA59|	-2.335	7.42E-20
BB_A66| outer surface proteinA66|	1.603	2.27E-02
BB_A74| osm28| outer membrane porin OMS28A74|	-1.605	4.15E-02
BB_B09| lipoprotein%2C putativeB09|	1.569	7.71E-07
BB_D09| conserved hypothetical proteinD09|	1.485	2.49E-04
BB_D10| BBD10D10|	1.584	2.54E-03
BB_D13| conserved hypothetical proteinD13|	1.835	3.32E-04
BB_D14| borrelia ORF-A superfamilyD14|	2.154	1.15E-09
BB_D15| BBD15D15|	1.415	1.12E-02
BB_D21| CdsMD21|	1.453	5.15E-03
BB_E18| PF-49 proteinE18|	-1.410	4.61E-03
BB_E19| PF-32 proteinE19|	-1.657	2.93E-04
BB_E20| borrelia family of unknown functionE20|	-1.859	1.29E-05
BB_F14| borrelia family of unknown functionF14|	-2.407	1.00E-02
BB_F17| putative transmembrane proteinF17|	-2.082	1.77E-05
BB_F23| PF49F23|	-2.691	3.03E-06
BB_F24| PF32F24|	-2.636	5.38E-07
BB_F25| borrelia family of unknown functionF25|	-2.088	1.46E-04
BB_F26| borrelia ORF-A superfamilyF26|	-1.773	7.91E-04
BB_G16| conserved hypothetical proteinG16|	1.273	3.92E-02
BB_G17| conserved hypothetical proteinG17|	1.263	1.07E-02
BB_G18| conserved hypothetical proteinG18|	1.515	4.61E-03
BB_G19| putative phage terminaseG19|	1.665	2.63E-03
BB_G20| putative phage portal protein%2C HI1409 familyG20|	1.221	4.93E-02
BB_G26| conserved hypothetical proteinG26|	2.393	4.53E-02
BB_G29| borrelia ORF-A superfamilyG29|	2.103	1.16E-05
BB_G31| borrelia family of unknown functionG31|	1.510	1.03E-02
BB_G32| putative replicative helicaseG32|	1.040	4.87E-02
BB_G33| RepUG33|	1.614	1.76E-03
BB_H09| type I restriction enzyme r protein n terminus	1.624	1.27E-03
BB_H09a| conserved hypothetical proteinH09a|	1.401	2.92E-02
BB_H32| antigen%2C P35%2C putativeH32|	1.610	3.33E-03
BB_H41| borrelia membrane protein P13H41|	2.710	1.18E-07
BB_I20| borrelia family of unknown functionI20|	-1.085	8.52E-03
BB_I21| PF-32 proteinI21|	-1.075	2.59E-02
BB_I36| antigen%2C P35%2C putativeI36|	1.381	4.15E-02
BB_I41| conserved hypothetical proteinI41|	1.074	4.90E-02
BB_I42| outer membrane proteinI42|	2.276	2.36E-07

BB_J08| putative surface proteinJ08|	1.356	3.67E-02
BB_J09| ospD| outer surface protein D (OspD)J09|	-2.206	5.05E-03
BB_J19| borrelia ORF-A superfamilyJ19|	1.253	7.91E-04
BB_J23| tetratricopeptide repeat domain proteinJ23|	3.236	6.48E-16
BB_J24| conserved hypothetical proteinJ24|	2.349	4.02E-15
BB_J25| conserved hypothetical proteinJ25|	2.260	1.08E-08
BB_J26| ABC transporter%2C ATP-binding proteinJ26|	3.279	1.05E-09
BB_J27| efflux ABC transporter%2C permease proteinJ27|	2.743	2.41E-12
BB_J28| conserved hypothetical proteinJ28|	2.612	7.08E-21
BB_J29| conserved hypothetical proteinJ29|	1.997	5.58E-12
BB_J31| conserved hypothetical proteinJ31|	2.469	5.40E-12
BB_J43| conserved hypothetical proteinJ43|	1.884	5.66E-08
BB_J45| putative lipoproteinJ45|	2.462	7.46E-12
BB_J46| conserved hypothetical proteinJ46|	1.923	2.81E-10
BB_J47| conserved hypothetical proteinJ47|	1.191	6.59E-03
BB_J48| conserved hypothetical proteinJ48|	1.562	1.46E-04
BB_K0058| hypothetical proteinK0058|	2.267	7.55E-05
BB_K07| lipoprotein%2C putativeK07|	2.981	5.11E-06
BB_K17| adeC| adenine deaminaseK17|	1.239	5.39E-03
BB_K32| bbk32| fibronectin-binding protein BBK32K32|	2.191	1.58E-18
BB_K34| conserved hypothetical proteinK34|	-1.085	2.27E-02
BB_K35| conserved hypothetical proteinK35|	-2.055	4.57E-03
BB_K48| immunogenic protein P37%2C putativeK48|	2.060	3.57E-12
BB_K52| putative lipoproteinK52|	1.045	9.68E-03
BB_K53| outer membrane proteinK53|	2.055	3.95E-06
BB_K54| conserved hypothetical proteinK54|	2.413	2.72E-05
BB_L27| BdrPL27|	1.426	2.89E-03
BB_L28| lipoproteinL28|	1.929	1.13E-04
BB_L29| 2.9-5 36K%3B minus strand ORFL29|	1.064	7.45E-03
BB_L36| BppAL36|	1.300	4.03E-02
BB_L37| BppBL37|	1.277	1.43E-02
BB_L39| erpA8| ErpA8 proteinL39|	1.256	2.20E-02
BB_L40| erpB8| ErpB8 proteinL40|	1.448	1.25E-04
BB_M27| rev proteinM27|	2.717	2.79E-25
BB_M29| 2.9-5 36K%3B minus strand ORFM29|	1.145	7.94E-03
BB_M35| BppAM35|	1.283	3.50E-02
BB_M36| BppBM36|	1.078	4.57E-02
BB_M37| BppCM37|	1.059	4.24E-02
BB_M38| erpK| ErpK proteinM38|	3.120	6.96E-06
BB_N19| conserved hypothetical proteinN19|	1.450	5.44E-04

BB_N20| conserved hypothetical proteinN20|	1.040	1.47E-02
BB_N27| BdrRN27|	1.708	3.36E-04
BB_N28| lipoproteinN28|	1.376	1.50E-02
BB_N30| BBC01N30|	-1.011	4.83E-03
BB_N39| erpQ| ErpQ proteinN39|	1.344	3.17E-03
BB_O19| conserved hypothetical proteinO19|	1.759	8.69E-06
BB_O20| conserved hypothetical proteinO20|	1.531	3.83E-04
BB_O24| hemolysin accessory proteinO24|	1.271	5.65E-04
BB_O27| BdrNO27|	1.091	7.18E-03
BB_O28| lipoproteinO28|	1.443	4.70E-03
BB_O29| 2.9-5 36K%3B minus strand ORFO29|	1.251	1.40E-03
BB_O36| BppAO36|	1.293	4.41E-02
BB_O37| BppBO37|	1.283	1.47E-02
BB_O38| BppCO38|	1.080	4.24E-02
BB_O39| erpL| ErpL proteinO39|	5.358	2.11E-04
BB_O40| erpM| ErpM proteinO40|	2.795	1.14E-07
BB_P27| revA1| surface protein (RevA1)P27|	2.627	1.04E-23
BB_P29| 2.9-5 36K%3B minus strand ORFP29|	1.097	4.18E-03
BB_P38| erpA| ErpA proteinP38|	1.250	2.28E-02
BB_P39| erpB1| ErpB1 proteinP39|	1.446	1.25E-04
BB_Q03| outer membrane proteinQ03|	1.929	7.35E-06
BB_Q47| erpX| ErpX proteinQ47|	4.061	1.99E-13
BB_Q62| conserved hypothetical proteinQ62|	-2.089	4.37E-03
BB_R27| BdrHR27|	1.095	1.49E-02
BB_R29| 2.9-5 36K%3B minus strand ORFR29|	1.093	4.51E-02
BB_R44| hypothetical proteinR44|	1.052	1.47E-02
BB_S29| bdrF| KID repeat proteinS29|	1.287	9.81E-04
BB_S30| lipoproteinS30|	1.375	3.03E-02
BB_S31| 2.9-5 36K%3B minus strand ORFS31|	1.048	6.05E-03
BB_S41| erpG| ErpG proteinS41|	2.061	1.95E-08
BB_S42| bapA| BapA proteinS42|	2.338	2.54E-09
BB_U06| putative plasmid partition proteinU06|	1.195	3.20E-02
EBG00001182586| tRNA| biotype=tRNA	-1.710	4.75E-03
EBG00001182601| tRNA| biotype=tRNA	-1.181	4.87E-03
EBG00001182606| tRNA| biotype=tRNA	-1.608	4.15E-02

CHAPTER 4. SPOVG REGULATES EXPRESSION OF NUMEROUS GENES

4.1 Introduction

Our transcriptomic data identified numerous genes involved in many different cellular processes that were regulated at the RNA level in a *spoVG*-dependent manner. We sought to further identify whether several of these genes are regulated at the level of protein abundance, and whether SpoVG directly interacts with nucleic acids associated with these genes. We chose to investigate genes of known significance, involved in carbon metabolism, essential outer surface proteins, cell wall synthesis and post-translational modifications.

Borrelia burgdorferi must be able to metabolize glycerol to survive within a tick and efficiently transmit to a vertebrate (210). While other bacteria have more complex systems for bringing in glycerol, and regulation of how it is metabolized, *B. burgdorferi* encodes one three-gene operon termed *glpFKD* (211-218) (Figure 4.1). GlpF is a transport facilitator that brings glycerol across the cell membranes (216). GlpK phosphorylates glycerol (219). At this point, glycerol-3-P can be used to assemble phospholipids and lipoproteins, which are cell membrane components. Glycerol-3 phosphate can also be converted into di-hydroxy-acetone-phosphate (DHAP) by GlpD (220). GlpD shuttles *B. burgdorferi* into glycolysis, allowing glycerol to be used as a source to generate ATP.

Previously, several groups have demonstrated that PlzA and c-di-GMP have an impact on regulating expression of the *glpFKD* operon (144, 145, 147, 221). It has been known for some time that PlzA binds c-di-GMP, but apart from that interaction, and an indirect impact on regulation of several genes, no other function has been ascribed to PlzA.

It has been speculated that PlzA could interact with other proteins, or perhaps it could bind nucleic acids, but no studies have demonstrated either of these actions (147, 187, 222).

SpoVG was initially identified as a DNA-binding protein from previous studies on *vlsE* from the Stevenson lab (164). *vlsE* codes for an outer surface protein is unique in that the coding region of the gene undergoes antigenic variation when *B. burgdorferi* is in a vertebrate (Figure 4.6 A). *vlsE* is not expressed and does not undergo variation when *B. burgdorferi* is in a tick. The gene is proceeded by about 15 silent cassettes that can rearrange and slot into the coding portion guided by two identical direct repeat DNA sequences that are present on all of the cassettes and within the coding portion (139, 223-227). Although the mechanism of precisely how rearrangement takes place is unknown, the direct repeats act to guide rearrangement (223, 228-234).

A recent study on the acetylome in *Borrelia burgdorferi* reported that SpoVG is acetylated in the cell, and that global acetylation was dependent on growth rate (235). We hypothesized that acetylation could impact the activity of SpoVG, and that levels of acetylated SpoVG could be different in the different mutants, and grown under different conditions. *B. burgdorferi* does not have any dedicated acetyl-transferases, therefore proteins become acetylated due to an accumulation of free acetyl-phosphate, and this is directly dependent on AckA (235). It is hypothesized that global acetylation could be important in the tick, as a mechanism of inhibiting enzyme activity without expending energy to degrade proteins. *B. burgdorferi* brings in acetate from the environment, AckA phosphorylates it, then phosphotransacetylase (PTA) converts acetyl-P to Acetyl-CoA, which is used as a substrate for lipid II biosynthesis, a component of the cell wall material peptidoglycan (236, 237). In the absence of AckA, essentially no proteins in the cell were

acetylated. In the absence of PTA, however, in which an accumulation of Acetyl-P is present, even more proteins were acetylated, and on more sites, than in Wild-type *B. burgdorferi* (235).

4.2 SpoVG Regulates Expression of the *glpFKD* Operon

RNA-seq on wild-type, *spoVG*-ON, and Δ*spoVG* strains revealed that the entire *glpFKD* operon is expressed at different levels in the mutants as compared to the wild-type (Figure 4.2 A). The operon is arranged such that the first gene is *glpF*, followed by *glpK* then an un-characterized putative ORF of about 300 base pairs, and finally *glpD* (Figure 4.2 D). RNA-sequencing on triplicate cultures demonstrated that the amount of *glpFKD* RNA was approximately 3 $\log_2$ more abundant in the *spoVG*-ON strain than in wild-type, which was arbitrarily set to 1, while the amount of *glpFKD* RNA was approximately 3 $\log_2$ less abundant than in wild-type.

Two small, antisense non-coding RNAs are associated with *glpF*, one at the 5' end and the other near the 3' end (110, 195, 201). Both sRNAs overlap entirely with the coding region of the gene. These are designated SR00186 and SR00187. Anti-sense RNAs (asRNAs) can exhibit a variety of regulatory functions on their target RNAs, both at the levels of transcription and translation. For example, asRNAs that anneal to the 3' end of an mRNA transcript can increase stability of the transcript by inhibiting RNAse processing (238). asRNA can also inhibit translation by annealing the 5'UTR, and overlapping the ribosome-binding site (239). As these two anti-sense RNAs were only recently discovered, it is not known what impact they have on expression of *glpF* or the remainder of the operon. What makes their functions particularly unclear is that SR00186 does not overlap the

ribosome binding site. Both SR00186 and SR00187 are also differentially expressed in the *spoVG*-ON and Δ*spoVG* strains as compared to wild type (Figure 4.2 B). Just as the mRNA of the *glpFKD* operon is more abundant in the *spoVG*-ON strain than in wild-type, the two asRNA transcripts are also more abundant. The two asRNAs are also less abundant in the Δ*spoVG* strain compared to wild-type, as are the mRNA transcripts.

Because we had previously observed that SpoVG can affect gene regulation at both the levels of transcription and translation, we wanted to test whether the GlpD protein was also expressed at different levels in the mutant strains. GlpD protein was not appreciably altered in the *spoVG*-ON mutant as compared to wild-type, however the protein abundance is markedly decreased in the Δ*spoVG* strain as compared to both wild-type and *spoVG*-ON strains (Figure 4.2 C).

4.3 SpoVG binds to *glpFKD* DNA and RNA

Given that SpoVG impacts expression of the *glpFKD* operon, we tested whether SpoVG interacts directly with the DNA and RNA of the operon. *glpF* is transcribed with an approximately 200bp 5' UTR (untranslated region) (110, 145, 154). Previous work demonstrated that a 42bp region directly 3' of the transcriptional promoter has a positive impact on transcription (240). Using a 52bp DNA probe that spans this regulatory region, we demonstrated by EMSA that SpoVG binds directly (Figure 4.3 A). SpoVG also bound to RNA that contained the same sequence as the DNA probe (4.3 B). 1,000x unlabeled DNA of the same sequence was not sufficient to entirely compete away the shifted protein-RNA complex, indicating that SpoVG has a higher binding affinity for RNA than DNA.

This apparent higher affinity that SpoVG has for RNA over DNA is consistent with every probe tested.

Approximately 400bp separate the end of *glpK* and the start of *glpD*. Within this region lies a hypothetical ORF, which, if translated, would code for about a 100 amino acid protein. Within this region lies a promoter that drives expression of *glpD* independently of *glpFK* (110, 241). Being able to independently control expression of *glpD* could potentially drive whether glycerol is shuttled into glycolysis or used for membrane construction. We tested whether SpoVG can also bind to DNA associated with this region, as this could have consequences for how *B. burgdorferi* uses glycerol within different environments. We found that SpoVG specifically binds to a 38bp DNA just 3' of the transcriptional promoter, which we named *glpKD* (Figure 4.3 C). As with the *spoVG* and *glpF* sites, SpoVG also binds to RNA which contains the same sequence as *glpKD*, and 1,000x unlabeled *glpKD* DNA was unable to completely compete away the shifted SpoVG-RNA complex (Figure 4.3 D).

4.4 PlzA binds to *glpF* DNA

Given our knowledge that PlzA and SpoVG interact with one another, we hypothesized that PlzA would also bind to the sequence of *glpF* DNA that SpoVG does (MD Motaleb, personal communication). To test this, we performed an EMSA using labeled *glpF* DNA and recombinant PlzA protein (Figure 4.4). The presence of a shifted band when PlzA is present in the reaction demonstrates that PlzA does interact with the DNA. Increasing PlzA concentration resulted in a super-shift, indicating that multiple PlzA proteins were bound to each DNA. 100x unlabeled non-specific DNA was added to a

reaction with 40 nM PlzA. The addition of competitor DNA was insufficient to compete away the shifted band, indicating that the interaction between PlzA and DNA is specific.

4.5 Impact of Glycerol on Growth Rate

Previous work demonstrated that *B. burgdorferi* needs to use glycerol as a carbon source for maximum survival within the tick (210). *B. burgdorferi* essentially stops growing once the blood meal has been digested within the tick, and it has been speculated that perhaps *B. burgdorferi* senses glycerol, and it acts as a signal to slow growth (43, 242). Given that SpoVG regulates expression of the *glpFKD* operon, we hypothesized that cultured *B. burgdorferi* would grow more slowly when glycerol was added to the culture medium, and that this would be dependent in part, on expression of SpoVG.

Wild-type and *spoVG*-ON *B. burgdorferi* were cultured in triplicate in either complete BSK-II or complete BSK-II + 4% glycerol at 34° C (Figure 4.5 A). Cultures were counted once every 24 hours for density. Wild-type *B. burgdorferi* cultured in the presence of glycerol grew significantly more slowly, and reached a lower final density than those cultured in BSK-II without glycerol. In contrast, there was not a significant difference in growth rate or final density between *spoVG*-ON bacteria cultured in BSK-II with and without glycerol (Figure 4.5 B).

Given that there was a difference in growth rate in wild-type *B. burgdorferi* when exogenous glycerol was present or not, we tested by qRT-PCR whether transcript abundance of several genes was altered (Figure 4.5 C). We found that several genes were differentially expressed when glycerol is present, including *spoVG*, which was more highly expressed. A bit surprisingly, both *glpF* and *glpD* were less abundant when glycerol was

added to the media. This suggests that transcript abundance of other regulators may also be altered, and could compete with *spoVG* for impact on the *glpFKD* operon. Consistent with this, we found that *plzA*, and *hk1* (which encodes the histidine kinase that stimulates Rrp1 to produce c-di-GMP) were also more abundantly produced in the presence of glycerol. In addition, *dnaA*, which encodes the master regulator of DNA replication, and *recA*, which encodes a vital in DNA repair enzyme, were also more abundant when cultured in media containing glycerol (243, 244).

Previous studies from the Stevenson lab used BSK-Lite media to study the impact of different carbon sources on growth rate (245). BSK-Lite contains all of the components of complete BSK-II media, except that it lacks the 0.4% glucose (w/v). *B. burgdorferi* grows at the same rate in this media, however they reach a lower final density than they do in complete BSK-II. We hypothesized that wild-type *spoVG*-ON, and Δ*spoVG* strains would grow differently in BSK-Lite supplemented with glycerol, specifically that the *spoVG*-ON strain would reach a higher final density in BSK-II supplemented with glycerol than the Δ*spoVG* strain. To test this, we cultured all three strains at 34° C in BSK-Lite, BSK-Lite supplemented with 0.4% glucose (w/v) or 0.4% glycerol (v/v), then enumerated cell density once every 24 hours (Figure 4.6 A-C). All cultures were performed in triplicate. As expected, all three strains reached a lower final density in BSK-Lite than in BSK-Lite supplemented with glucose. Unexpectedly, all three strains reached the same final density grown in BSK-Lite supplemented with glycerol as BSK-Lite. This indicates that none of the strains were able to utilize glycerol to reach a higher density. This implies that *B. burgdorferi* cannot rely entirely on glycerol as an energy source, even when SpoVG is present and the *glpFKD* operon is abundantly expressed.

4.6 SpoVG and PlzA impact VlsE protein expression

We hypothesized that SpoVG could be involved in regulating expression of VlsE, given that SpoVG was initially identified as binding to DNA associated with the *vlsE* gene (Figure 4.7 A). To test this, wild-type and *spoVG*-ON cultures were grown at 34° C and 23° C to mid-log phase (Figure 4.7 B). Lysates were probed with polyclonal α-VlsE in rabbit serum. At 34° C, VlsE was less abundant in the *spoVG*-ON lysate than in wild-type (A3) lysate. As previously reported, VlsE is far more abundant in wild-type lysate grown at 23° C than at 34° C (246). Surprisingly, VlsE was more abundant in *spoVG*-ON lysate than wild-type when cultured at 23° C. Given the fact that SpoVG protein abundance did not appreciably change when either wild-type or *spoVG*-ON cells were cultured at 23° C versus 34° C, this indicates that some other cellular component(s) also regulate VlsE expression.

Given that we had demonstrated that SpoVG expression is undetectable in both Δ*plzA* (cannot respond to c-di-GMP) and Δ*rrp1* (cannot synthesize c-di-GMP), we hypothesized that VlsE would be significantly less abundant in these strains as well. To test this, B31-S9 (wild-type), Δ*plzA*, Δ*plzA*+*plzA* and Δ*rrp1* strains were grown to mid-log phase at 34°C (Figure 4.7 C). Lysates were probed with α-VlsE antibody. Although VlsE was readily detectable in both the wild-type and Δ*plzA*+*plzA* strains, it was greatly reduced in the Δ*plzA* and Δ*rrp1* strains. What is not immediately obvious is exactly what effect the reduction in SpoVG expression by these strains has on the expression of VlsE. Using the newly generated Δ*plzA*+*spoVG* and Δ*rrp1*+*spoVG* will allow us to probe the SpoVG-*vlsE* relationship more in-depth, by measuring VlsE protein abundance. If SpoVG is the

responsible for altered VlsE expression in the Δ*plzA* and Δ*rrp1* strains, then introducing SpoVG on the plasmid should restore wild-type VlsE expression.

4.7 SpoVG Does Not Impact *vlsE* Transcription

A significant hurdle to studying transcription of *vlsE* resides in the genomic location of the gene. *vlsE* is encoded on linear plasmid lp28-1 (247). *vlsE* is the last encoded before the right telomere, which is a closed hairpin loop. Sequencing through this region has historically been very difficult-when the genome of strain B31 was first sequenced in 1997, this region was not able to be resolved. Transcripts from our RNA-seq studies were not able to reliably map to this region, and multiple attempts to amplify cDNA by qRT-PCR using multiple primer pairs has proven fruitless.

In order to circumvent these obstacles, we took advantage of some GFP fusions previously generated by the Stevenson lab (246). Previously, Dr. Bykowski cloned the entire DNA region from the start of translation of *vlsE* up until the first silent cassette into a plasmid that contains a promoterless GFP gene (Figure 4.8 A). This includes the transcriptional promoter, as well as a unique large inverted repeat region that is hypothesized to be involved in region of expression and or recombination, although the mechanism of that has not been elucidated. He then created several additional plasmids by deleting sections of DNA all the way up until the -35 nucleotide of the transcriptional promoter. Dr. Bykowski then cloned each individual plasmid into B31-e2, an easily transformable, high-passage non-infectious strain of *B. burgdorferi.* B31-e2 is non-infectious because it has lost many plasmids. It is possible that loss of plasmids could have

an impact on *vlsE* expression, however since the background strain is the same in all cases, the effect of SpoVG on *vlsE* transcript abundance can still be measured.

We took advantage of these previously made strains by transforming them with plasmid pCRS5, the *spoVG*-ON construct. The strains used were TB3, which contained the longest transcriptional fusion, TB3+*spoVG*-ON, TB11, TB11+*spoVG*-ON, TB13 (which contains only the -35 nucleotide through start codon of GFP), and TB13+*spoVG*-ON. TB12 was not utilized in the subsequent studies because multiple attempts to transform the strain with pCRS5 failed (246). All six strains, including wild-type without GFP as a negative control were grown to mid-log phase at 34° C.

All six strains were subjected to analysis by Flow-cytometry (Figure 4.8 B-D). Each strain was directly compared to its sister strain that additionally carried *spoVG*-ON. The strains that contained *spoVG*-ON all exhibited less Green Fluorescence intensity than the parental strain without exogenous *spoVG* expression. This indicates the SpoVG-dependent expression of VlsE protein does not rely on DNA upstream of the transcriptional promoter. Given that the start of transcription of *vlsE* is only a few nucleotides upstream of the ribosomal binding site, this suggests that the effect of SpoVG on VlsE protein levels occurs on a post-transcriptional level.

4.8 SpoVG and PlzA bind DNA just up-stream of the *vlsE* gene

We hypothesized that since SpoVG regulates VlsE expression, that it likely binds to nucleic acids between the transcriptional start site and the start of translation (Figure 4.9 C). Even though SpoVG regulates expression post-transcriptionally, we started with a DNA probe given how prohibitively expensive RNA probes are (Figure 4.9 A). SpoVG

does indeed bind to this region of DNA. Future studies will test whether SpoVG also binds to RNA containing this same sequence.

Given that we had previously demonstrated that PlzA also binds to DNA, and that VlsE protein abundance is lower in a Δ*plzA* strain, we hypothesized that PlzA also binds to DNA upstream of the *vlsE* coding gene. We tested this hypothesis using recombinant PlzA and the same *vlsE* DNA probe used in the SpoVG-binding assay (Figure 4.9 B). PlzA did bind to this region of DNA, although its role in regulating VlsE expression and activity within the cell are still unclear.

4.9 Potential role for SpoVG in *vlsE* recombination

Given that SpoVG was initially identified using a piece of DNA near the recombination site of *vlsE* as a probe, we hypothesized that SpoVG could be involved in the process of recombination (164). Western blots probing for abundance of VlsE in wild-type and Δ*spoVG* protein lysates revealed an unusual pattern. A single, readily visible band of the correct size was observed in the lane loaded with wild-type lysate (Figure 4.10 A). The lane loaded with Δ*spoVG* lysate contains multiple bands, many of them smaller than that corresponding to the correct size. The source of antibody used is from rabbit serum, so it possible that other antibodies within the serum bind to other proteins in the lysate. If this were the case however, the multiple bands should be detected in both lanes, those loaded with wild-type lysates as well as Δ*spoVG* lysates.

We hypothesized that the multiple bands could be due to rearrangements at the *vlsE* locus. Perhaps SpoVG acts to stabilize the sites of recombination. These sites contain runs of guanosine nucleotides, which can potentially form G-quadruplex DNA structures, which

are unstable and prone to damage and breakages. We assayed by PCR across the coding region of *vlsE* using DNA extracted from wild-type and Δ*spoVG* cells (Figure 4.9 B). The product amplified from wild-type was the expected size-a little over 1 Kb. The amplified product from Δ*spoVG* was much smaller, just shy of 500 Kb. This suggests that DNA may have broken and been improperly repaired. For example, it is possible that the DNA between the recombination sites was lost without being replaced with another cassette.

4.10 SpoVG and acetylation

We hypothesized that the percentage of SpoVG that is acetylated in the cell could vary under different culture conditions, since the acetylome was altered at different growth rates (235). To test this, we separated lysates by SDS-PAGE from wild-type and *spoVG*-ON cultures grown at 34° C and 23° C. Cultures were grown in double for all strains and conditions. The gels were stained with Coomassie blue, the bands corresponding to the size of SpoVG were cut out, subjected to digestion by trypsin and analyzed by LC MS/MS (Figure 4.11 A). As expected, a very small percentage of SpoVG was acetylated in any condition. 0.3% of SpoVG was acetylated in wild-type and *spoVG*-ON cultures grown at 34° C. Approximately twice as much SpoVG was acetylated in both wild-type and *spoVG*-ON cultures grown at 34° C than those grown at 23° C. There was no difference in the amount of SpoVG that was acetylated in the wild-type and *spoVG*-ON cultures grown at either temperature.

RNA-sequencing revealed that the *ackA* transcript is less abundant in Δ*spoVG* than in wild-type or *spoVG*-ON strains (Figure 4.11 B). Transcript abundance of phosphotransacetylase (PTA) was unchanged in any strain. Given that deletion of *ackA*

resulted in almost no acetylated proteins in the cell, but deletion of PTA had no effect, we hypothesized that there would be reduced acetylated proteins in the Δ*spoVG* than in wild-type or *spoVG*-ON strains (235). Protein analysis of AckA revealed that that the abundance of protein was not appreciably altered in the Δ*spoVG* strain (Figure 4.11 C).

Given that SpoVG was identified as an acetylated protein in *B. burgdorferi,* and that we confirmed that a small percentage of SpoVG is acetylated in the cell, we wanted to test how acetylation affects the activity of SpoVG (235). The Stevenson lab previously demonstrated that SpoVG multimerizes, and binds DNA as a multimer (164). We hypothesized that acetylation would disrupt SpoVG multimerization. To test this, SpoVG was incubated either with or without 1 mM acetyl-phosphate for 60 minutes at 37° C. This method was used because *B. burgdorferi* does not encode any dedicated acetyl-transferases that acetylate individual proteins specifically (23). We confirmed by mass spec that after incubation with acetyl-phosphate that 100 % of SpoVG was acetylated. SpoVG that had been incubated with and without acetyl-phosphate was run on a Native-PAGE gel (Figure 4.12 A). Although SpoVG ran as a single band on SDS-PAGE gels, multiple bands were visible on the Native gel. This is likely due to different numbers of SpoVG proteins multimerizing together. The banding pattern did not differ when SpoVG was acetylated, indicating that acetylation does not disrupt multimerization.

Additionally, we tested the ability of acetylated SpoVG to bind nucleic acids. EMSA using RNA just upstream of the *ackA* gene and SpoVG pre-incubated with or without acetyl-phosphate (Figure 4.12 B). The only consistent motif across all known SpoVG-DNA binding sites is a run of at least four thymidine nucleotides. The *ackA* DNA probe was selected because it also contains a run of thymidine nucleotides. Two

concentrations of SpoVG protein were added: in one set only part of the RNA was shifted, and in the other, all of the RNA was shifted. Both acetylated and un-acetylated SpoVG bound the RNA, as evidenced by the shifted bands in both lanes. This indicates that, acetylation has no impact on SpoVG-RNA interactions. The same sequence was used as a DNA probe (Figure 4.12 C). As with the RNA, two concentrations of SpoVG protein was used, and at neither concentration was there a difference in Shifted DNA between acetylated and un-acetylated SpoVG protein. These assays were repeated twice with the same results. These studies demonstrate that acetylation has no impact on SpoVG binding to RNA or DNA.

4.11 Discussion

Glycolysis is the only mechanism by which *B. burgdorferi* generates ATP, therefore regulating this process is very important for survival (23, 210). Glycerol has only 3 carbons, and only 1 net molecule of ATP is generated per molecule of glycerol. Additionally, no net NADH molecules are generated, which are needed to keep the process of glycolysis going. This is all in contrast to the cell using glucose as the substrate for glycolysis. Glucose contains 6 carbons, and produces a net of 2 ATP and 1 NADH molecules. The means that glycerol is a pretty energy-poor way to generate ATP in an organism that is already severely limited in mechanisms for ATP production.

One can imagine that in an environment where nutrients are abundant that *B. burgdorferi* would not waste energy on using glycerol as a substrate for ATP. If glycerol is available, however, it would be expedient to use it for the purpose of membrane construction. This would eliminate the need to divert glucose away from glycolysis for this

purpose. When nutrients are very limited, say, when *B. burgdorferi* is in a tick that has completely digested the blood meal, and glucose is not readily available, using glycerol to generate ATP might provide just enough energy to survive until the next blood meal is taken.

The importance of *B. burgdorferi* metabolizing glycerol to survive within the tick has been established (210). A recent study using a Tn-Seq library of *B. burgdorferi* mutants did not identify Bb240-242 as unrecoverable from the tick (248). There are several reasons why this could by the case, including the fact that the library is not completely saturated, and it was not confirmed that those mutants were present in the library used. Understanding how the operon is regulated by *B. burgdorferi* is of considerable interest. The studies within this work present the first evidence of protein regulators interacting directly with DNA and RNA of the *glpFKD* operon. Additionally, although it has been postulated that PlzA is somehow involved in regulation of the operon, this is the first data demonstrating the PlzA binds to DNA upstream of *glpF*. It remains to be determined the exact effect that SpoVG and PlzA have on the protein abundance of each gene in the operon. This is particularly pertinent because of the two anti-sense RNAs that are associated with *glpF.*

In order to test these questions, antibodies should be raised against *glpF, glpK,* and potentially the ORF. (Our proteomics studies, which are currently in progress, will determine whether the ORF does get translated into a functional protein). The entire operon, from the transcriptional promoter could be cloned and transformed into *E. coli.* Since *E. coli* does not make either SpoVG or PlzA, the effect of each could be determined by transforming *E. coli* with additional plasmids that express SpoVG and PlzA. Using the

newly raised antibodies, the effects of SpoVG and PlzA on protein abundance of each individual gene on the *glpFKD* operon could be measured.

Finally, it is unknown the effect that expressing these proteins will have on glycerol metabolism. We hypothesize that SpoVG biases metabolism towards ATP production from glycerol, and that when SpoVG is very low or absent, that glycerol would still be used, but used for building cell membranes rather than ATP production.

Known interactions are enumerated as follows. PlzA binds to c-di-GMP, which is produced by cultured *B. burgdorferi.* PlzA interacts with SpoVG within the cell, although it is unknown if it binds to SpoVG when c-di-GMP is present or absent. It is not known what effect that the PlzA-SpoVG interaction has on the ability of SpoVG to bind DNA or the ability of SpoVG to bind RNA. It is not known what effect that c-di-GMP has on the ability of PlzA to bind DNA. It is also unknown what effect that interacting with SpoVG has on the ability of PlzA to bind to DNA. The interaction with SpoVG could be stabilizing, or it could be competitive. A significant hurdle we faced was the inability to purify recombinant PlzA from *E. coli* without c-di-GMP bound to it. *E. coli* encodes about 5 known/hypothesized c-di-GMP synthases, so deleting all of them from Rosetta-II strain that can express recombinant proteins would be rather difficult. We attempted to express recombinant PlzA in SF9 insect cell line designed to produce recombinant proteins, however the cells did not produce appreciable levels of PlzA.

Recombination at the *vlsE* locus has never been observed to occur in cultured *B. burgdorferi,* which has significantly hindered the Borrelial research community's ability to study the mechanism. Having a model to study the mechanism of recombination in culture would significantly move the field forward. Wild-type, *spoVG*-ON and Δ*spoVG*

cultures were first plated on BSK-II -agarose plates, in order to isolate individual colonies that gave rise from a single bacterium. Three individual colonies from each strain were grown at 34° C and passaged three times over the course of three weeks to allow ample time for recombination or DNA deterioration to occur. DNA was extracted from each culture for long-read PacBio sequencing. A particular hurdle that we currently face is the fact that *vlsE* can no longer be amplified from DNA extracted from Δ*spoVG* cultures. Multiple primer pairs were used, however we were limited in their design as the end of the *vlsE* gene is very near the hairpin telomere.

The importance and prevalence of post-translational modification by bacteria are only just beginning to be understood, not least in *B. burgdorferi.* We have identified that SpoVG can be phosphorylated, and confirmed that it can be acetylated, although the consequences of these modifications remain to be elucidated (Figure 4.13). It is possible that there is no biological impact of acetylation on how SpoVG acts in the cell. Because there are no specific acetyl-transferases in the cell, protein acetylation in *B. burgdorferi* is merely the consequence of accumulated acetyl-phosphate sticking to lysine residues that happen to be easily accessible.

It has been hypothesized that *B. burgdorferi* uses this strategy to survive within the tick: when ATP levels are low, flux through the lipid I biosynthesis pathway will be stalled, leading to accumulation of acetyl-phosphate. This acetyl-phosphate then acetylates all readily available lysine residues indiscriminately (235). This strategy may provide an evolutionary advantage of quickly stalling activity of enzymes within the cell, without spending energy to break down proteins. Additionally, these proteins are already made, and ready to be useful once the blood meal comes in. The influx of nutrients from the blood

meal would then allow flux through the lipid I pathway, reducing the amount of free acetyl-phosphate, which would then reduce acetylation on enzymes, instantly activating those enzymes. Multiple enzymes in the glycolysis pathway were demonstrated to be far less active when acetylated. Acetylation of SpoVG may simply be an accident of this strategy, with no real biological consequences.

It is also possible that acetylation of SpoVG influences how it interacts with PlzA, or the relative affinity that SpoVG has for DNA vs RNA, shifting its activity in that manner. In order to fully understand whether or not acetylation has an impact on activity within the cell, in *vitro* experiments could be done on SpoVG in both the Δ*ackA* and ΔPTA strains. Pull-downs to identify what proteins SpoVG is or is not interacting with, ChiP-seq and RIP-seq would identify whether there are any changes in these strains vs in wild-type *B. burgdorferi.*

Figure 4.1 Glycerol metabolism

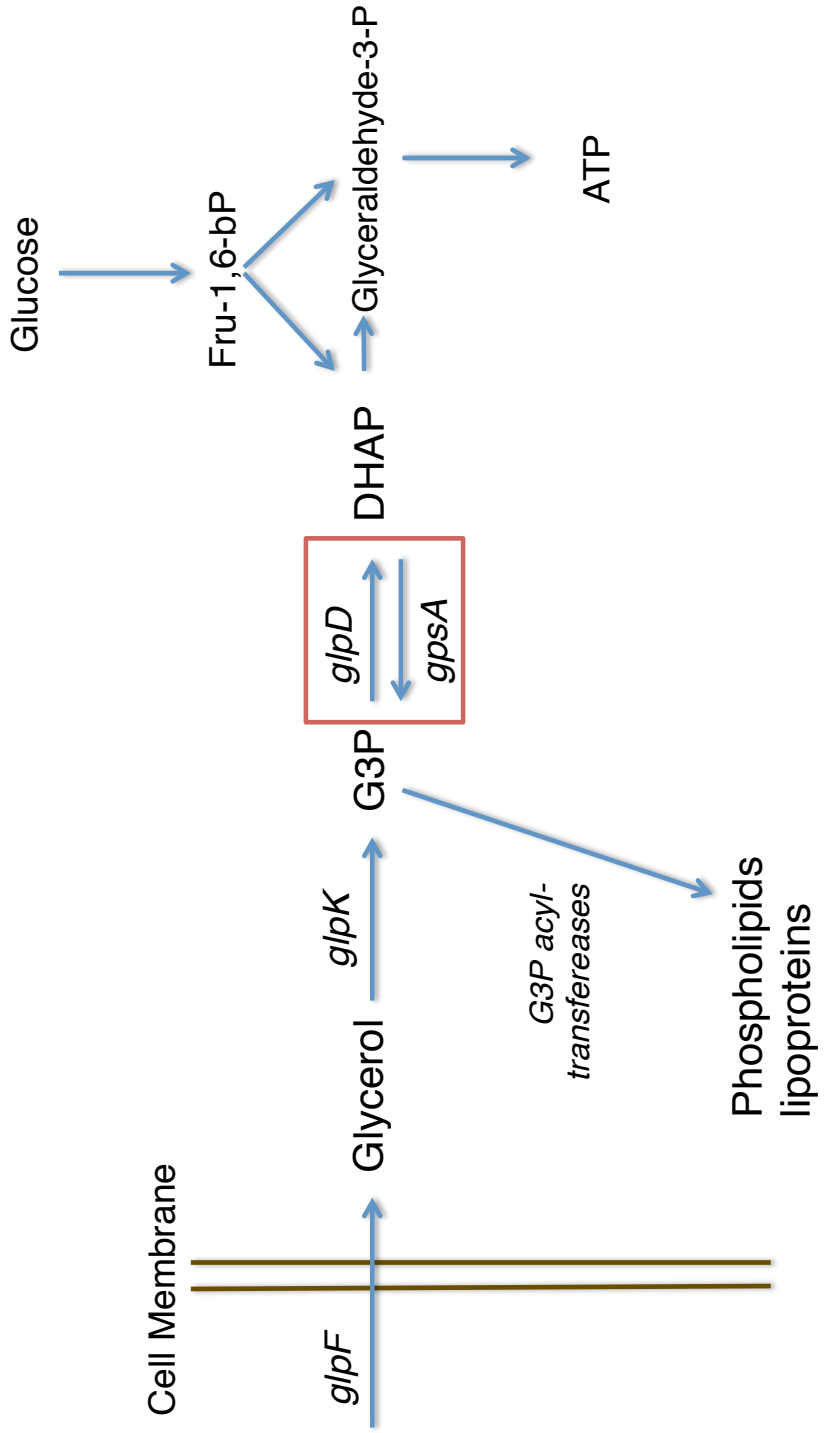

Diagram of how glycerol can be metabolized by *B. burgdorferi*. Glycerol is brought across the membrane by GlpF, then is phosphorylated by GlpK. Phosphorylated glycerol can either be used to assemble membrane components, or shuttled into glycolysis by GlpD for ATP production

Figure 4.2 SpoVG regulates expression of *glpFKD* operon

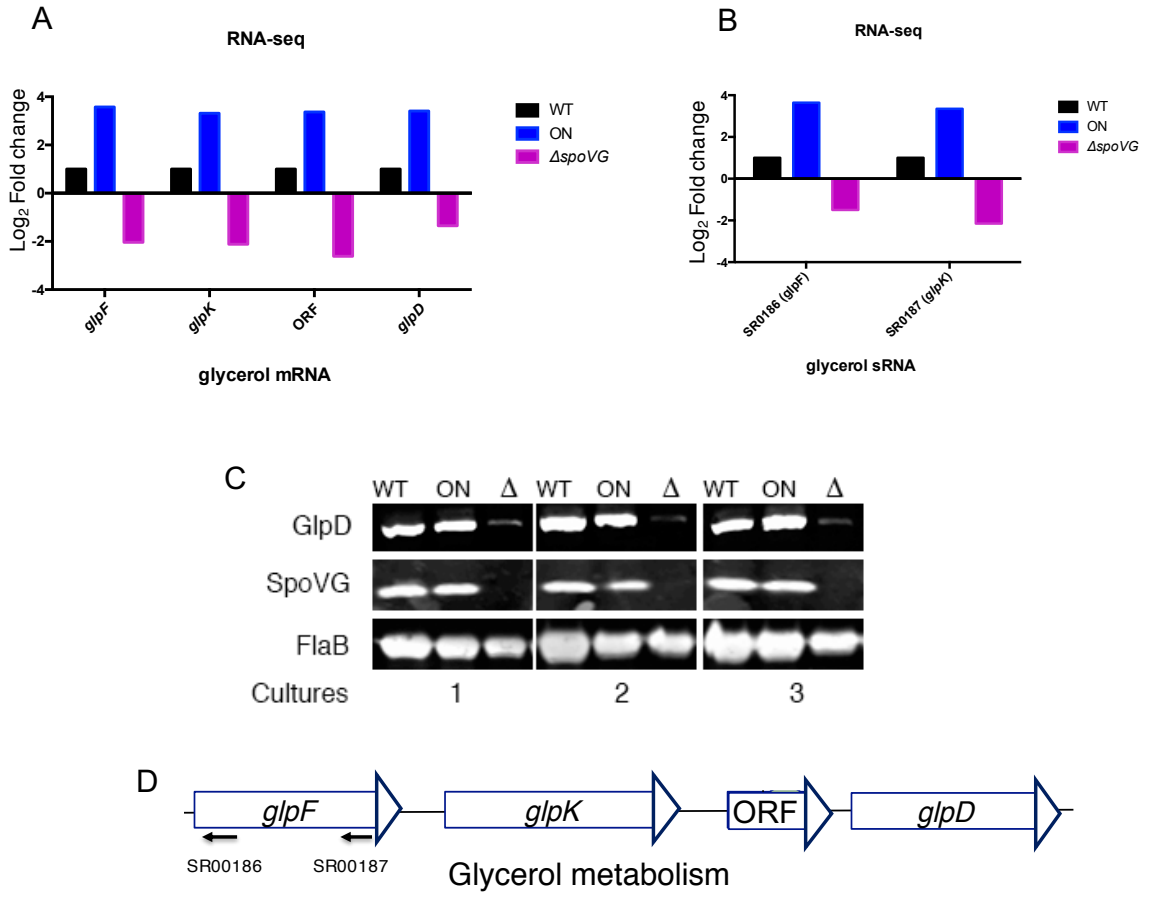

A. RNA-seq results depicting $\log_2$ differences in expression of each gene of the *glpFKD* operon between wild-type, *spoVG*-ON and Δ*spoVG*. Wild-type levels were arbitrarily set to 1, and the fold difference between mutants and wild-type added to, or subtracted from, 1. B. RNA-sequencing results depicting the $\log_2$ differences in expression of the two RNAs anti-sense to *glpF* between wild-type, *spoVG*-ON and Δ*spoVG*. C. Western Blots on wild-type, *spoVG*-ON, and Δ*spoVG* protein lysates from cultures grown at 34° C. Shown are three biological replicates. Blots were probed for GlpD, SpoVG, and FlaB. D. Schematic of the layout of *glpFKD* including location of the two anti-sense RNAs.

Figure 4.3 SpoVG binds to *glpFKD* DNA and RNA

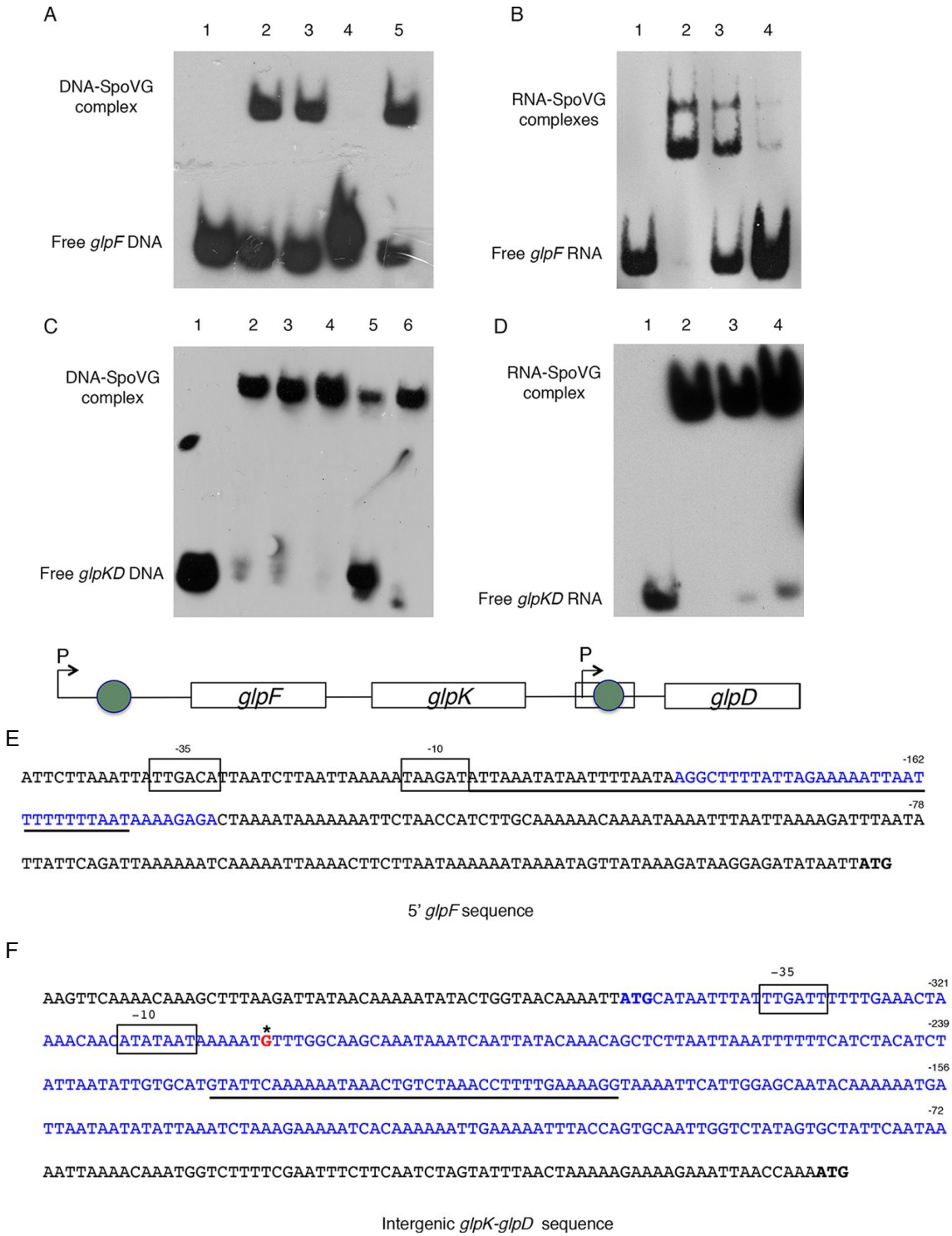

Christina R. Savage et al. J. Bacteriol. 2018; doi:10.1128/JB.00033-18

SpoVG binding to DNA and RNA at two sites in the *glpFKD* operon. (A and B) Sequence 5′ of *glpF*. (C and D) Region between *glpK* and *glpD*. EMSAs were performed using either labeled DNA or RNA. (A) Lane 1, 1 ng *glpF* DNA; lane 2, 1 ng *glpF* DNA with 2.4 μM rSpoVG; lane 3, 1 ng *glpF* DNA with 4.8 μM rSpoVG; lane 4, 1 ng *glpF* DNA with 4.8 μM rSpoVG and 100 ng unlabeled *glpF* DNA; lane 5, 1 ng *glpF* DNA with 4.8 μM rSpoVG and 100 ng unlabeled EMSA-pCR2.1 DNA. (B) Lane 1, 1 ng *glpF* RNA; lane 2, 1 ng *glpF* RNA with 2.4 μM rSpoVG; lane 3, 1 ng *glpF* RNA with 2.4 μM rSpoVG and 100 ng unlabeled *glpF* DNA; lane 4, 1 ng *glpF* RNA with 2.4 μM rSpoVG and 1,000 ng unlabeled *glpF* DNA. (C) Lane 1, 1 ng *glpKD* DNA; lane 2, 1 ng *glpKD* DNA with 0.73 μM rSpoVG; lane 3, 1 ng *glpKD* DNA with 1.47 μM rSpoVG; lane 4, 1 ng *glpKD* DNA with 3 μM rSpoVG; lane 5, 1 ng *glpKD* DNA with 3 μM rSpoVG and 100 ng unlabeled *glpKD* DNA; lane 6, 1 ng *glpKD* DNA with 3 μM rSpoVG and 100 ng unlabeled EMSA-pCR2.1 DNA. (D) Lane 1, 1 ng *glpKD* RNA; lane 2, 1 ng *glpKD* RNA with 2.4 μM rSpoVG; lane 3, 1 ng *glpKD* RNA with 2.4 μM rSpoVG and 100 ng unlabeled *glpKD* DNA; lane 4, 1 ng *glpKD* RNA with 2.4 μM rSpoVG and 1,000 ng unlabeled *glpKD* DNA. A graphic representation of SpoVG-binding sites and promoters, relative to the *glpFKD* operon, is shown at the bottom.

Nucleic acid sequences that contain SpoVG binding sites. The sequences are shown as DNA, although SpoVG also bound to these sites in single-stranded RNA. The DNA/RNA target regions used for EMSAs are underlined. (E) Sequence 5′ of the *glpFKD* operon. The −35 and −10 sequences of the probable transcriptional promoter are boxed, and the translational initiation codon of *glpF* is in bold black type. The maximal sequence bound by SpoVG is underlined. The region previously identified as having a stimulatory

effect on transcript levels is shown in blue type. (F) Sequence of the intergenic region between *glpK* and *glpD*. The maximal sequence bound by SpoVG is underlined. The −35 and −10 sequences of the predicted transcriptional promoter are boxed. The transcription start site is marked with an asterisk. The translational initiation codon of *glpD* is in bold type. A small ORF of unknown function, *bb0242*, is indicated in blue.

Figure 4.4 PlzA binds to *glpF* DNA

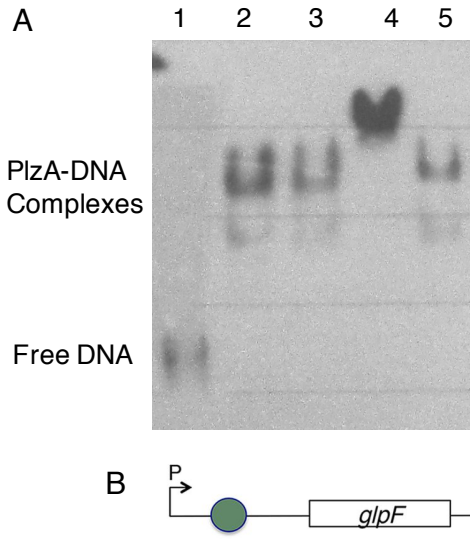

EMSA demonstrating that PlzA protein binds to DNA upstream of *glpF* gene (A). Lane 1 contains just *glpF* DNA. Lane 2 and 3 contain DNA and 40 nM PlzA. Lane 4 contains DNA and 400 nM PlzA. Lane 5 contains DNA, 40 nM PlzA, and 100x unlabeled non-specific DNA. PlzA binds to the same DNA sequence as SpoVG (B).

Figure 4.5 Complete BSK + glycerol

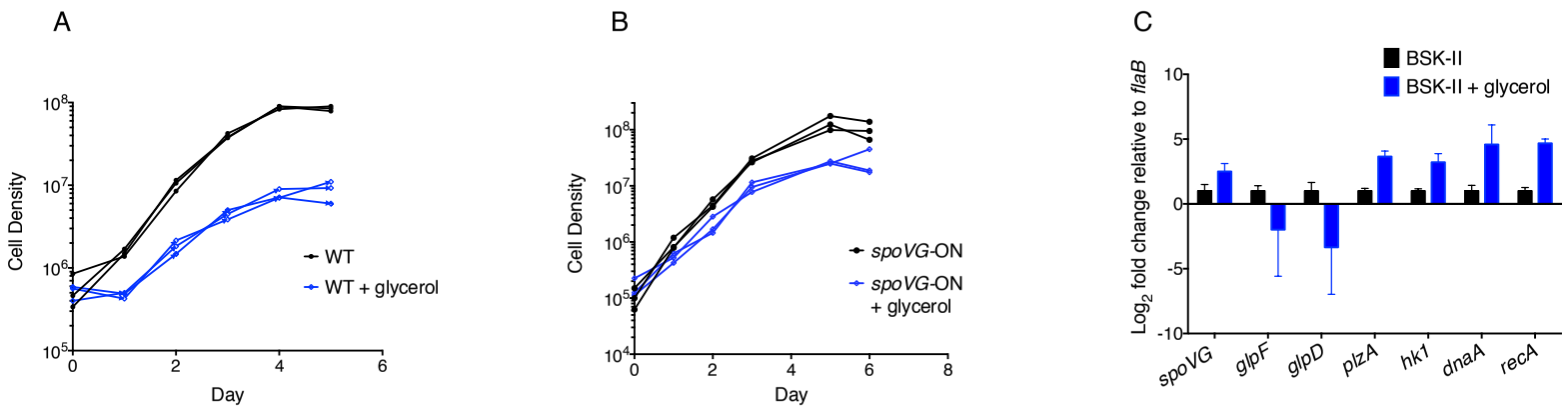

A. Growth curve of independent triplicate cultures of wild-type *B. burgdorferi* grown with and without 4% added glycerol. Cells were enumerated by Petroff-Hauser counter once every 24 hours. B. Growth curve of triplicate cultures of *spoVG*-ON *B. burgdorferi* grown with and without 4% added glycerol. C. qRT-PCR of several genes from wild-type grown with and without glycerol. All Cq values have been normalized to *flab* Cq values for each culture condition.

Figure 4.6 BSK-Lite + glycerol

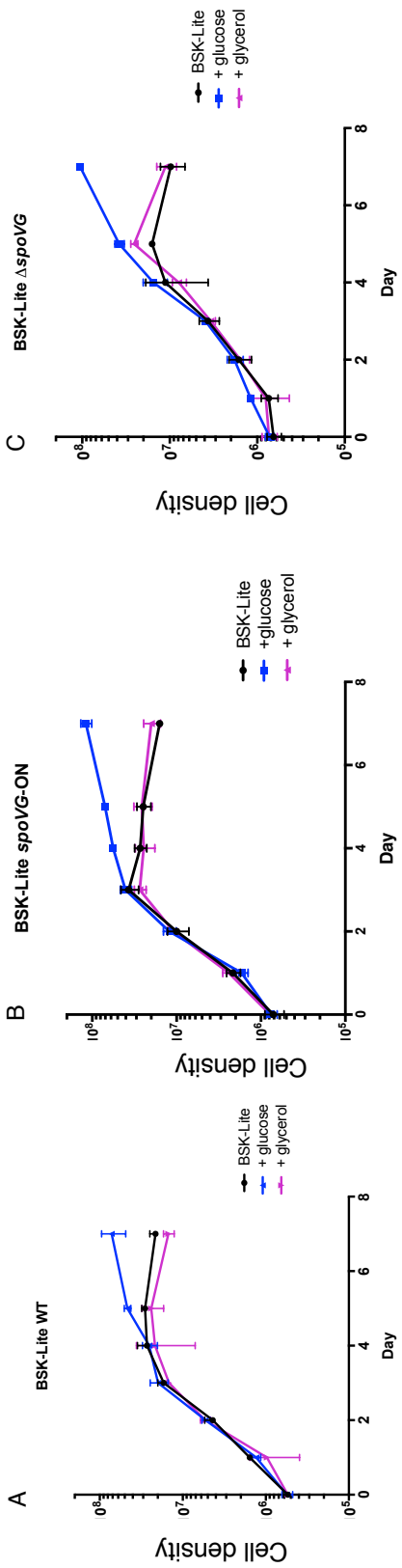

Growth curves of triplicate cultures of wild-type (A), spoVG-ON (B) and Δ*spoVG* (C) B. *burgdorferi* grown in BSK-Lite, BSK-Lite supplemented with 0.4% glucose (w/v) and BSK-Lite supplemented with glycerol (v/v). Cell were enumerated once every 24 hours by Petroff-Hauser counter.

Figure 4.7 VlsE expression

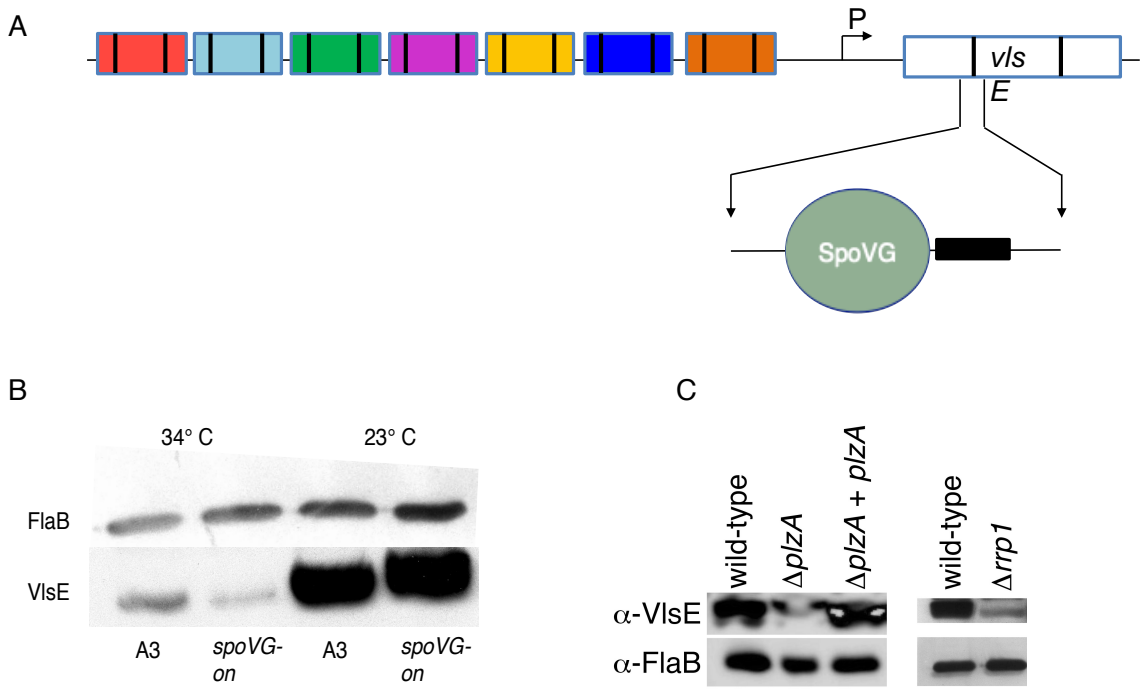

Schematic (A) of the *vlsE* gene locus. The coding region is white. The colored boxes represent some of the silent cassettes upstream of the gene. The black bars represent the direct repeat sequences that are present in the coding region and each of the silent cassettes. SpoVG was found to bind a portion of DNA near one of the Direct repeats within the coding region. (B) Western Blots of FlaB and VlsE. A3, which is the wild-type, and *spoVG*-ON cultures were grown to mid-log phase at 34° C and 23° C. This experiment was repeated three times with similar results. (C) Western Blots of FlaB and VlsE. Wild-type, Δ*plzA*, Δ*plzA*+*plzA* and Δ*rrp1* were grown to mid-log phase at 34° C. This experiment was repeated three times with similar results.

Figure 4.8 Transcriptional GFP fusions

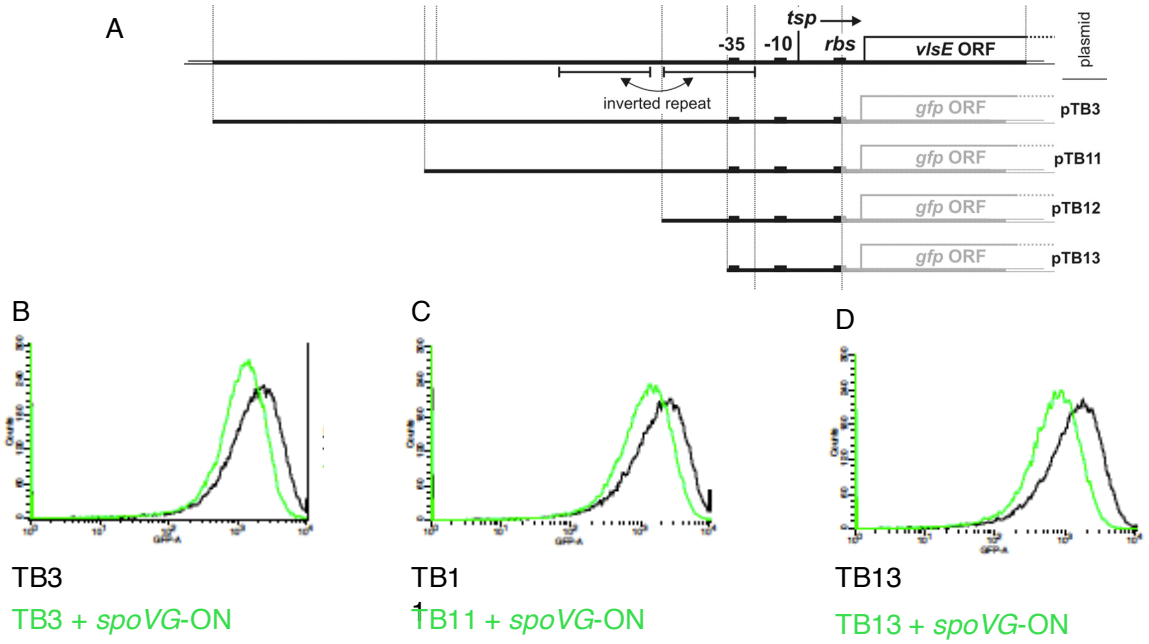

Schematic (A) of vlsE promoter fusions to GFP. A version of this figure originally appeared in Bykowski et al 2006. pTB3, pTB11 and pTB13 were transformed with the *spoVG*-ON plasmid (246). (B-D) Flow cytometry analysis of GFP intensity of original fusions (black), and strains harboring *spoVG*-ON as well (green). This experiment was repeated twice with similar results.

Figure 4.9 SpoVG and PlzA bind to *vlsE* DNA

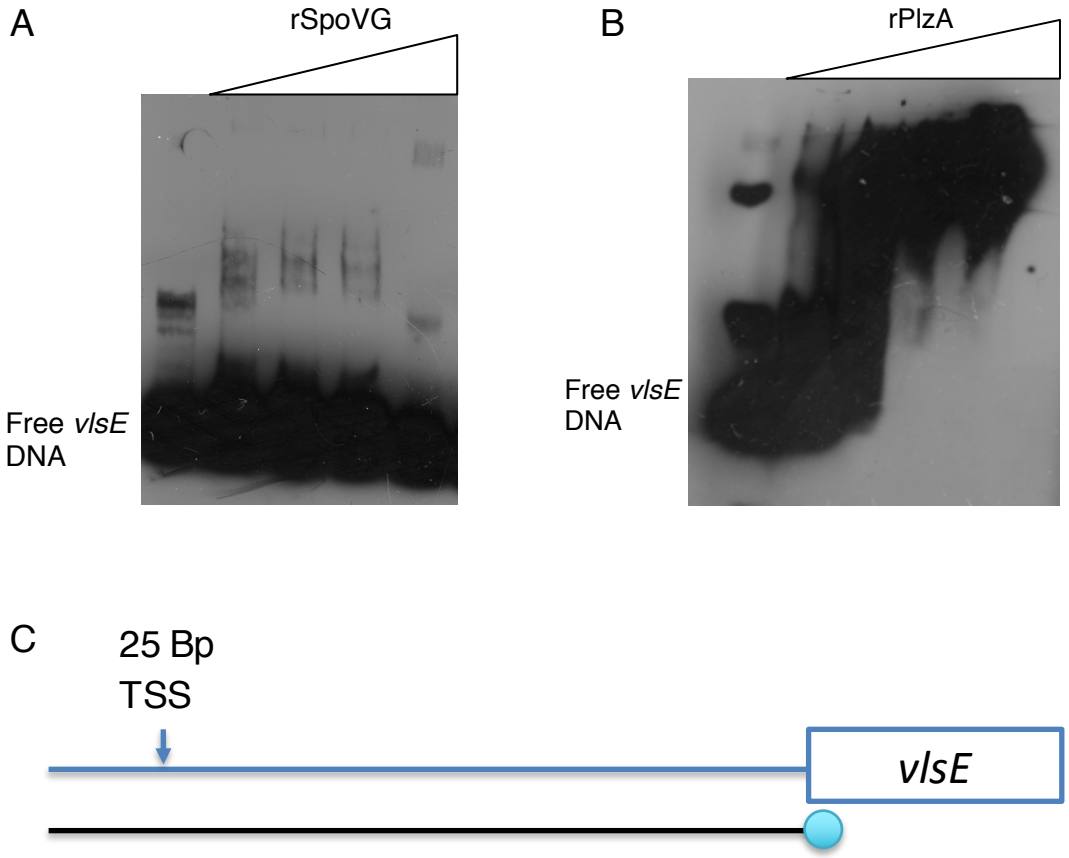

EMSA (A) demonstrating the SpoVG binds to *vlsE* DNA. Multiple shifted bands appear with increasing amounts of SpoVG protein added. (B) EMSA demonstrating that PlzA also binds to *vlsE* DNA. (C) Location of the DNA probe used in relation to the coding portion of *vlsE*.

Figure 4.10 Potential role for SpoVG in *vlsE* recombination

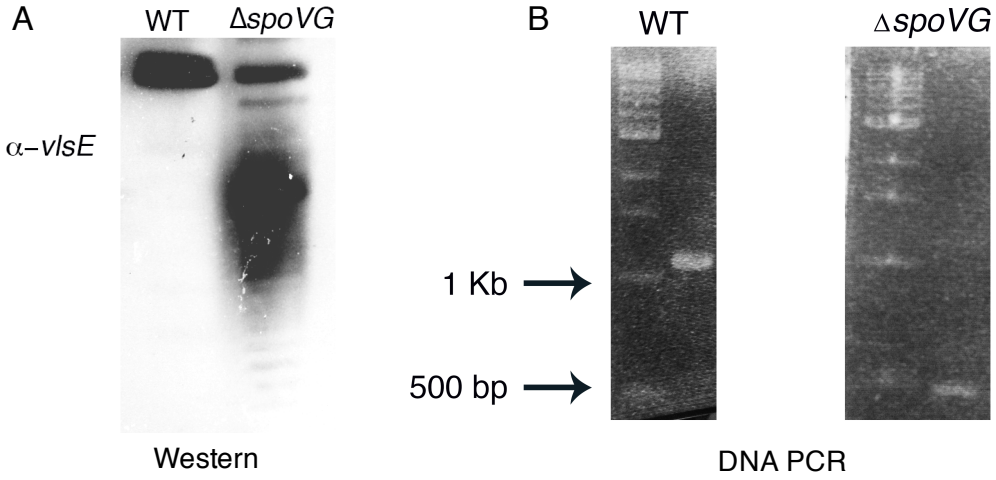

Western Blot (A) of VlsE from wild-type and Δ*spoVG* protein lysates. Multiple bands were recognized in the Δ*spoVG* lysates. (B) PCR amplification of the *vlsE* coding gene from DNA extracted from wild-type and Δ*spoVG*.

Figure 4.11 Acetylation and *ackA* expression

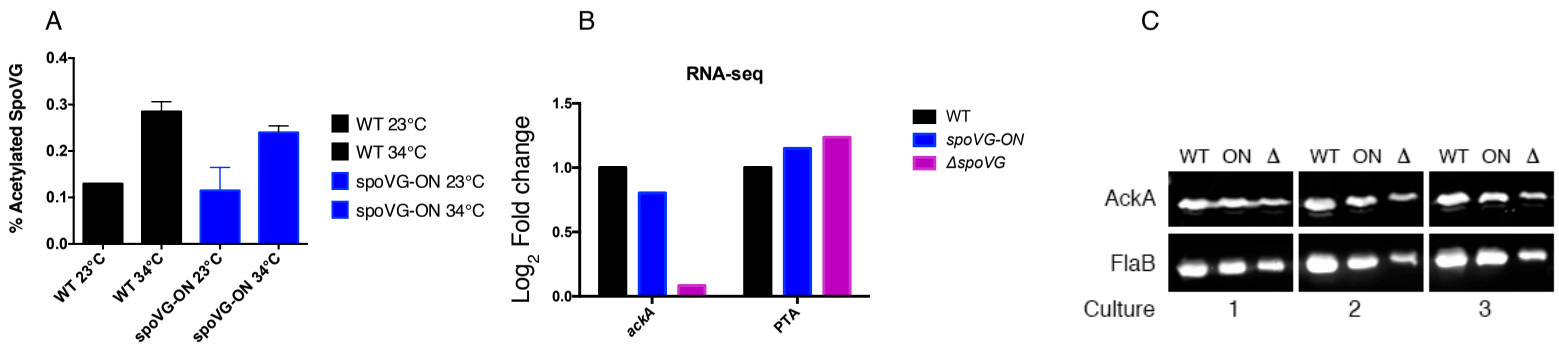

Lysates from wild-type and *spoVG*-ON cultures grown at 23° C and 34° C were separated on an SDS-polyacrylamide gel, and stained with Coomassie. The bands corresponding to SpoVG were excised, digested with trypsin and subjected to analysis by Mass spec (A). The percent of acetylated SpoVG was calculated based on the percent of missed cleavages. By one-way Anova, the difference between 23° and 34° C was statistically significant. (B) RNA-seq data of relative *ackA* and PTA expression within wild-type, *spoVG*-ON and Δ*spoVG* strains. (C) Western Blot probed with antibodies against AckA and FlaB. Shown are biological triplicate cultures for wild-type, *spoVG*-ON and Δ*spoVG* strains.

Figure 4.12 Effect of Acetylation on SpoVG activity

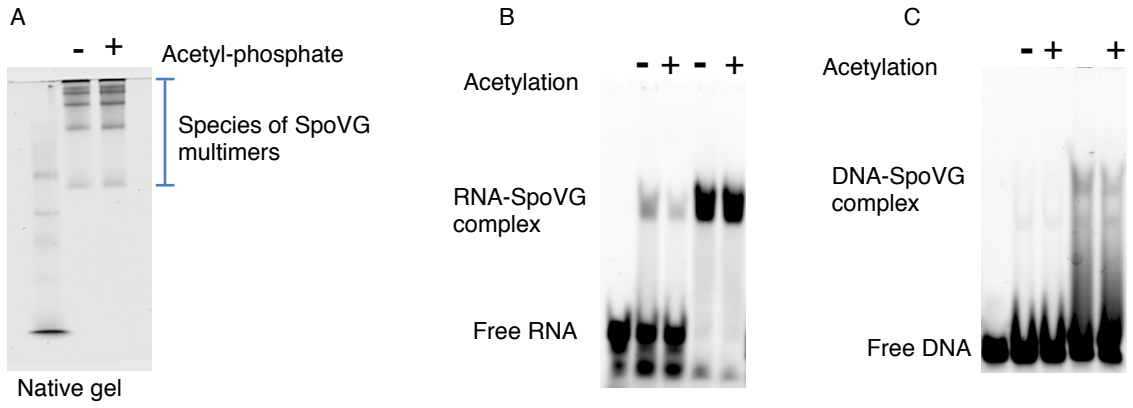

SpoVG purified from *E. coli* was incubated with and without acetyl-phosphate at 37° C for 1 hour, then separated on a Native gel (A). EMSA using *ackA* RNA and purified SpoVG incubated with or without acetyl-phosphate (B). EMSA using *ackA* DNA and SpoVG incubated with and without acetyl-phosphate.

Figure 4.13 SpoVG alignments

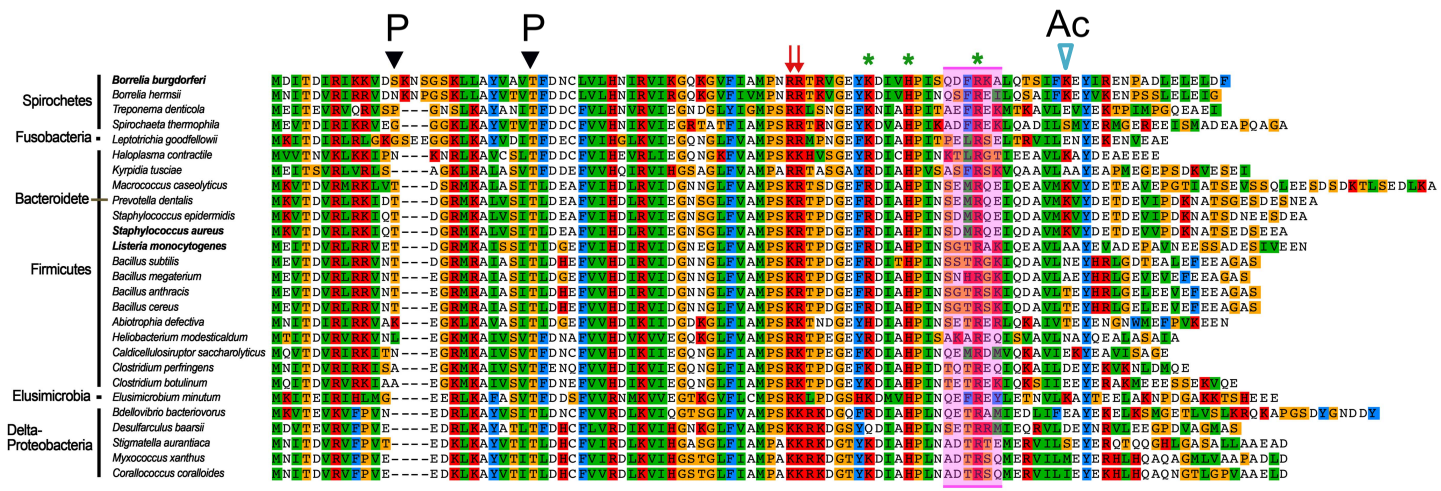

Adapted from Jutras et al. Plos One. 2013

A version of this figure originally appeared in Jutras et al 2013. Amino acid sequence alignments of SpoVG from *B. burgdorferi* and several other Gram-positive bacteria. Black arrows indicate residues that can be phosphorylated. The teal arrow indicates the lysine residue that can be acetylated.

CHAPTER 5. SPOVG AND CYCLIC-DI-AMP REGULATE OSPC TRANSLATION INDEPENDENTLY OF TRANSCRIPTION

5.1 Introduction

There are few defined or hypothetical regulators in the *B. burgdorferi* genome (23, 247). Use of nucleotide second messengers as regulators is useful, because they can work at multiple levels of regulation. RNA riboswitches can bind them, in order to regulate expression of specific genes at specific times (249, 250). Nucleotides can bind protein partners, which may have distinct functions whether the nucleotide is present or not, conserving energy that would have gone into transcription and translation. Most recently, ppGpp has been found to bind DNA near the *E. coli oriC,* thus directly impacting DNA replication (251)

Although new discoveries and mechanisms of action of signaling through the second-messenger c-di-GMP continues to occur, its importance has been well established in most laboratory-studied bacteria (252-256). More recently, newly described nucleotides as signaling messengers in bacteria have emerged (257-260). The synthesis of cyclic-di-adenosine monophosphate (cyclic di-AMP) by several members of gram-positive bacteria has also been described (261). This molecule has a demonstrated role in gene regulation, potassium transport, biofilm formation and eliciting an immune response from eukaryotic organisms (262-269).

Before I began my studies, the presence of c-di-GMP and ppGpp had already been demonstrated in *B. burgdorferi* (144, 148, 187, 188, 221, 241). We sought to examine whether *B. burgdorferi* can also synthesize another modified nucleotide messenger, c-di-AMP, and establish a functional role for the molecule within the cell. Establishing another

nucleotide second messenger in *B. burgdorferi* would expand our repertoire of known regulatory factors, allowing us to gain further insight into how *B. burgdorferi* controls its cellular processes at each point along the enzootic cycle.

OspC is an outer-surface protein, expressed by *B. burgdorferi* during transmission from tick to vertebrate, and during the early stages of establishing infection in the vertebrate (270-272). Regulation of this gene is very tightly controlled, and absolutely essential for *B. burgdorferi* to survive (273-275). Some upstream DNA elements have been demonstrated to have an effect on expression. *ospC* is transcribed from an RpoD-dependent promoter, but there is evidence that RpoS-mediated proteins are involved in regulation of *ospC* (276-280).

The prevailing hypothesis states that OspC is under transcriptional control of the alternative sigma factor RpoS. This model states that RpoS is expressed once the blood meal comes in, then is responsible for *ospC* expression (200, 274, 276, 281-283). This model leaves much to be desired, and several remaining questions. For one, *ospC* is still expressed (albeit at lower levels) in a Δ*rpoS* strain of *B. burgdorferi* (284, 285). Two, RpoS is expressed throughout vertebrate infection, yet OspC expression gets repressed early after infection has been established. The *ospC* gene is likely regulated at the levels of transcription, translation and post-translation. Any insight into the intricate regulatory mechanism of this essential protein will be valuable for understanding how *B. burgdorferi* is able to transition between transmitting from a tick to infecting a vertebrate.

5.2 Bb0008 Encodes a Cyclic-di-AMP synthase

Although *Borrelia burgdorferi* is technically classified as a gram-negative bacterium due to the presence of an outer membrane, many of the proteins it possesses are more closely related to those found in gram-positive organisms (recall that SpoVG is only present in gram-positive bacteria and spirochetes). Protein-BLAST (BLAST-P) analysis revealed that the gene Bb0008 is predicted to encode a c-di-AMP synthase based on the fact that it contains a putative di-adenylate-cyclase domain (DAC) domain (Figure 5.1). *E. coli* does not naturally make c-di-AMP, therefore the gene Bb0008 was cloned and expressed in *E.* coli in order to determine if it does make a functional c-di-AMP synthase (266, 286).

Bb0008 was amplified from the genome, cloned into plasmid pCR2.1, and transformed into DH5α *E. coli* cells. This plasmid was named pCRS0. pCR 2.1 allows transcription of the cloned product from the *lac* promoter Using an *E. coli* cell line that contains the *lacI* repressor was essential, otherwise the cells used available ATP, and were unable to grow. Overnight cultures of pCRS0 were passaged 1:1000 with 1 mM IPTG, and allowed to grow for 3 hours. The nucleotide fraction was extracted, and analyzed by LC-MS/MS by our collaborator Dr. Chris Waters, for the presence of c-di-AMP. C-di-AMP was readily detected, indicating that the gene does in fact encode a functional c-di-AMP synthase (Figure 5.2). Gene Bb0008 was thus named *cdaA* after the similar genes in *Bacillus* and *Listeria* (287, 288).

5.3 Overexpression of CdaA does not alter intracellular levels of c-di-AMP

C-di-AMP has been demonstrated in other bacteria to be essential for growth (288, 289). For this reason, we elected to study the effects of overexpressing *cdaA* rather than deleting the gene from the chromosome. The *cdaA* gene was amplified from *B. burgdorferi* genomic DNA and cloned into plasmid pSZW53-4 in which the *cdaA* gene is transcribed from a TetR-regulated hybrid P*ost* promoter, which is inducible with anhydrous tetracycline (ATc) (162, 290). This construct was named pAG1. pAG1 was transformed into non-infectious, high passage B31-e2 and low-passage, infectious B31-A3 strains of *B. burgdorferi*. The strain created in the B31-e2 background was named AG1. pSZW53-4 without *cdaA* cloned into it was transformed into B31-e2, and named KS50. The strain created in the low-passage, B31-A3 background was named *cdaA*-ON.

AG1 was grown without ATc at 34° C to early-log phase, then split into two cultures. Final concentration of 0.5 μg/ml ATc was added to one culture, and both were incubated for an additional 24 hours at 34° C. Nucleotide fractions were purified from AG1 with and without ATc, flash frozen in liquid nitrogen and shipped on dry ice to Dr. Chris Waters at Michigan State University for analysis. This group is expert at identifying and quantifying small nucleotide second messengers. The concentration of c-di-AMP was very low in the wild-type strains, and not detectably different in the cultures that were induced with ATc to overexpress *cdaA* (Figure 5.3 A). This was repeated with similar results. Protein lysates were prepared from AG1 and KS50 strains, grown with and without 0.5 μg/ml final concentration of ATc at 34° C. Although FlaB is readily detectable in all strains, CdaA was undetectable in both KS50 cultures as well as the uninduced AG1

cultures. CdaA was abundantly produced in AG1 induced with 0.5 μg/ml ATc (Figure 5.3 B).

RNA was also extracted from KS50 and AG1 grown with and without ATc, and subjected to qRT-PCR. The difference in Cq value between ATc uninduced and induced cultures was calculated for each gene transcript. *flaB* is the gene usually used to normalize qRT-PCR and Western Blot data, as it is consistently expressed in culture. To ensure that our data were not skewed in the event that *flaB* is regulated by c-di-AMP, we normalized all Cq values to *flaB* and *recA*. Cq values for each gene were normalized to *flaB* (Figure 5.3 C) or *recA* (Figure 5.3 D) transcripts. Plotted on the graph are the normalized Cq values for both AG1 and KS50 strains. *cdaA* from AG1 culture was the only transcript differentially expressed. This indicates that the action of c-di-AMP within *B. burgdorferi* is not at the level of transcription.

5.4 CdaA affects expression levels of OspC protein

Given the fact that overexpression of CdaA did not alter any of the transcripts we examined apart from *cdaA*, we hypothesized that it could influence gene regulation at the level of translation. *cdaA*-ON was cultured with 0, 0.5, 1.0 or 2.0 μg/ml final concentration of ATc at 34° C to mid-log phase. Protein lysates were separated by SDS-PAGE and probed with α-OspC, α-SpoVG and α-FlaB antibodies (Figure 5.4). FlaB is readily detectable in all lanes, and SpoVG abundance is not altered from the different lysates, indicating that SpoVG is not regulated by CdaA. OspC expression decreases as increasing amounts of ATc inducer was added to the culture medium. In protein lysates from cultures induced with 2.0 μg/ml ATc, OspC is not detectable at all. This indicates the CdaA does

regulate expression of OspC protein in a SpoVG-independent manner that is independent of *ospC* transcriptional regulation.

5.5 SpoVG regulates OspC protein but not transcript

RNA-sequencing revealed that the *cdaA* transcript was about 2 times less abundant in the *spoVG*-ON strain compared to wild-type (Figure 5.5 A). The *cdaA* transcript was not altered in the Δ*spoVG* strain compared to wild-type. Since the *spoVG*-ON strain alters transcript abundance of *cdaA*, and we demonstrated that increasing CdaA protein results in less OspC protein, we hypothesized that levels of OspC protein would also be altered. In order to understand the level of regulation at which SpoVG may be acting, we looked at *ospC* transcript abundance from our RNA-sequencing. The *ospC* transcript was not altered in either *spoVG*-ON compared to wild-type, nor Δ*spoVG* compared to wild-type (Figure 5.5A).

We next tested whether levels of OspC protein was altered by over expression of *spoVG* or temperature (Figure 5.5 B). Predictably, OspC was detectable, but not highly abundant in protein lysates from wild-type bacteria grown at 34° C (291). OspC has been shown to be expressed at very low levels at both 23° C and 34° C, but expression increases dramatically when cultures grown at 23° C are shifted to 34° C (200, 271, 291, 292). As we hypothesized, OspC is significantly more abundant in *spoVG*-ON cultures than wild-type when grown at 34° C. OspC is less abundant in *spoVG*-ON cultures grown at 23° C than *spoVG*-ON cultures grown at 34° C.

As we had previously observed that *spoVG* transcript increases when glycerol is added to the culture medium, we hypothesized that OspC protein expression would also

increase when glycerol was added to culture medium (Figure 5.5 C). As hypothesized, OspC was more abundant in wild-type cultures grown with glycerol. Counterintuitively, OspC protein was less abundant when *spoVG*-ON cells were cultured with glycerol than without. We previously saw that the *spoVG*-ON strain responded differently to the addition of glycerol than did wild-type.

Finally, we tested whether OspC would be differentially expressed in the Δ*spoVG* strain compared to wild-type (Figure 5.5 D). Wild-type, *spoVG*-ON and Δ*spoVG* were cultured at 34° C to mid-log phase. OspC was not detectable in the lysates from either the wild-type or Δ*spoVG* strains. OspC was highly abundant in the lysate from *spoVG*-ON cells, which skews the ability to detect protein in cultures expressing significantly less OspC protein. In order to determine if OspC is differentially expressed in the Δ*spoVG* strain as compared to wild-type, lysates from these two strains will need to be analyzed in the future on a blot without *spoVG*-ON lysate.

5.6 SpoVG binds to RNA associated with *ospC* gene

OspC protein expression, but not mRNA expression, is regulated by *B. burgdorferi* that overexpress *spoVG*. We hypothesized that SpoVG protein binds directly to RNA associated with the *ospC* gene. There are numerous ways that an RNA transcript can regulate translation of the gene associated with it (250, 293). The start of transcription for *ospC* was identified just a few nucleotides upstream of the ribosomal binding site (276, 294). This eliminates the possibility of a long 5' untranslated region (UTR) that could be involved. Riboswitches are ubiquitous across the bacterial kingdom as a mechanism of posttranscriptional control by binding small molecules (249, 250, 295, 296). To date, no

riboswitches have been identified or even predicted for *B. burgdorferi*, although they have been identified in other Spirochetes (249, 295, 297), {and personal communication with Dr. McCown}. Additionally, we looked for anti-sense RNAs that may be associated with the mRNA transcript: none were identified (110, 195, 201).

A unique feature of the DNA sequence that codes for OspC, is that the first few amino acids (less than 20) are absolutely conserved across all known *B. burgdorferi* species and subspecies, but a large portion of the gene codes for highly variable amino acids (298-300). We hypothesized that the sequence that codes for the first few amino acids could be essential for translational regulation of the *ospC* gene. We predicted the structure of a 50 bp RNA that spans from the transcriptional start site through the first 10 coded amino acids using http://rnaanalyzer.bioapps.biozentrum.uni-wuerzburg.de/ (Figure 5.6 A). This RNA is predicted with high certainty to be highly structured (Figure 5.6 B). It is conceivable that the RNA folds into this structure, and needs some other interacting molecule to enable RNA polymerase to break the long stem loop that is predicted to form. Or perhaps regulation works by a molecule stabilizing the stem loop, and only when that molecule is not present or able to bind does translation occur.

To answer these questions, we ordered a 49 bp RNA labeled with Alexa/488 from IDT DNA Inc. We hypothesized that since SpoVG and c-di-AMP regulate OspC protein but not transcription that one or both bind to the RNA. SpoVG binds to this RNA by evidence of a shifted band in the reaction that included SpoVG (Figure 5.6 C). Addition of c-di-AMP to a reaction that contains SpoVG and RNA did not disrupt the higher-order complex, indicating that c-di-AMP does not interrupt SpoVG-RNA binding. A reaction containing RNA and c-di-AMP did not yield a shifted band. In order to test for c-di-AMP-

RNA interaction, an RNase experiment will need to be done. In this experiment, RNA is treated with RNase and in different reactions, RNase plus increasing amounts of c-di-AMP. Different cleavage patterns would be expected if c-di-AMP binds to the RNA.

It is unknown if SpoVG recognizes a specific sequence, or if SpoVG binds to a particular structure. To test this, we designed four additional labeled RNAs that are the same length as the original RNA, but a few nucleotides are mutated at various locations (Figure 5.7 B). We used the same RNA prediction software to predict the structure of each RNA (Figure 5.7 A). Some of these structurally look more similar to the original sequence, and others look structurally very different. SpoVG bound to all of the RNAs using the highest concentration of protein (Figure 5.8). This is seen in the third lane for each panel. The second lane in each panel contains 1/10 as much SpoVG protein as the third lanes in each panel. Some of RNA A was shifted in the second lane, which suggests that SpoVG binds to this RNA with a slightly higher affinity than RNA B or RNA C. RNA A contains an additional UUUU site, which we hypothesize SpoVG recognizes.

5.7 Discussion

Very little is known about mechanisms of post-transcriptional regulation in *B. burgdorferi*. Growing evidence suggests that regulating protein production independently from transcriptional restraints plays an important role in the ability of *B. burgdorferi* to survive throughout the enzootic cycle (191, 195, 201, 301, 302). From an evolutionary perspective, this makes sense, as both transcription and translation require an enormous amount of energy. *B. burgdorferi* must both survive the nutrient-poor environment of the tick mid-gut, and quickly respond to the incoming blood meal in order to survive. The

evidence presented here, of an additional cyclic-di-nucleotide, and the example of a gene that is regulated post-transcriptionally by c-di-AMP provides a significant advance to our understanding of how *B. burgdorferi* regulates gene expression.

The exact role that c-di-AMP has on *B. burgdorferi* physiology remains to be determined. No knockout of the *cdaA* gene has been generated, and overproduction of the enzyme does not result in altered intracellular levels of c-di-AMP. Additionally, no protein or RNA partners have been identified for c-di-AMP in *B. burgdorferi.*

It is tempting to postulate how c-di-AMP could serve as a sensor for intracellular ATP levels within the cell. Bacteria that are unable to slow growth in the presence of antibiotics are far less likely to survive in the presence of, and develop resistance to, antibiotics. In the same way, one can imagine that if *B. burgdorferi* within a tick is unable to slow those cellular processes that require large amounts of ATP before the blood meal has been digested, they would be far more likely to die. Perhaps depletion of c-di-AMP acts as a sensor that intracellular levels of ATP are running low. Or perhaps it serves as a reserve, to store ATP, until absolutely necessary.

The identification of the predicted highly structured RNA associated with *ospC*, and the subsequent demonstration of two systems that affect only OspC protein but not transcription provides substantial insight into additional mechanisms involved in gene regulation. The prevailing dogma of the *Borrelia* field states that Hk1/Rrp1 govern survival in the tick, then Hk2/Rrp2 govern transition to, and infection within, vertebrates. There has been strong evidence over the years that this simplistic model, with all regulation lying under one of the two two-component systems is not sufficient to describe the complexity

of regulation and survival. Here we present evidence for additional mechanisms of regulation distinct from classical two-component systems.

The fact that SpoVG binds to the structured RNA associated with *ospC* could have one of a number of effects. Binding of SpoVG could stabilize or disrupt the structure of the RNA. The fact that SpoVG was still able to bind to a (mostly similar) sequence of RNA that was predicted to have a very different structure indicates that SpoVG does not interact with unique structures per se, but rather with sequences within that RNA. SpoVG binding with higher affinity to an RNA with an added UUUU site gives further support for this hypothesis. This binding could have the effect of either blocking the ribosome binding site, thus inhibiting translation or opening the ribosome binding site to be available, thus allowing translation to proceed. It is also possible that if SpoVG bound to double-stranded RNA, that it could stall the RNA polymerase, thus prevent the complete RNA from being transcribed in the first place.

Finally, although there have been no identified or predicted riboswitches in *B. burgdorferi*, here we present evidence of a structured RNA involved in regulation of translation of *ospC*, but not transcription. It remains to be elucidated exactly how this RNA structure functions. Can c-di-AMP interact with the RNA, thus providing an entirely new class of riboswitches that could have implications for other organisms in addition to *B. burgdorferi*? Is this RNA stable during, and after transcription, or is there some form of processing that occurs that regulates whether the protein will be expressed or not? And finally, what is the direct effect of SpoVG binding to the RNA? Does SpoVG effectively hide the ribosomal binding site, thus preventing translation, or does it work to open and stabilize the RNA in a way that allows ribosomes access?

Figure 5.1 *cdaA* alignments

```
Bb  MI--DINDLNQIKDTFSRILDLSLISILVYYIYKNVINSYSTNLLKGMLIIISVGIISYYLNLYTISWLLN
Bs  MAFE----DIPFLQYLGNAVDILLVWYVIYKLIMVIRGTKAVQLLKGIVVIVLVRMASQYLGLSTLQWLMD
Lm  MDFS----NMSILHYLANIVDILVVWFVIYKVIMLIRGTKAVQLLKGIFIIIAVKLLSGFFGLQTVEWITD
Sa  MDFSNFFQNLSTLKIVTSILDLLIVWYVLYLLITVFKGTKAIQLLKGILVIVIGQQISMILNLTATSKLFD
Ct  MD----------------------------------------LVFGLLSFLCLFVLAEKLHLPVIRNLML
    *..                 :.. .. . :  .    .... .*: *.. :. .   :  : * .  .: .

Bb  YIANILPIAIVILFNQEIKKIIMQIGNFNLAFKLSN--KKEETLKVISEILKAVKHLSENKSGSLICIEKK
Bs  QAITWGFLAIIIIFQPELRRALEQLGRGRFFSRSGT-PVEEAQQKTIEAITKAINYMAKRRIGALLTIERD
Lm  QMLTWGFLAIIIIFQPELRRALETLGRGNIFTRYGS-RIEREQHHLIESIEKSTQYMAKRRIGALISVARD
Sa  IVIQWGVLALIVIFQPEIRRALEQLGRGSFLKRYTSNTYSKDEEKLIQSVSKAVQYMAKRRIGALIVFEKE
Ct  HVVNIAAIVVFIIFQPEIRLALSRIR-----LRRGK-FVINMQDEFIDHLTACIYRMAERQIGALIVLENE
        .. .:..::*::*:: ::..:...    : .     . . . *    :.  .::.:.:*:*: .:..

Bb  IQLEQIINK-GTKIDALISSELLISLFERETPLHDGAVIISKNKLKYAGSFLPLS-NVDSISKAFGTRHRA
Bs  TGMGDYIET-GIPLNAKVSSELLINIFIPNTPLHDGAVIMKNNEIAAAACYLPLS-ESPFISKELGTRHRA
Lm  TGMDDYIET-GIPLNAKISSQLLINIFIPNTPLHDGAVIIKGNEIASAASYLPLS-DSPFLSKELGTRHRA
Sa  TGLQDYIET-GIAMDSNISQELLINVFIPNTPLHDGAMIIQGTKIAAAASYLPLS-DSPKISKSLGTRHRA
Ct  RLLNDLLNLSAVKINADFSEELLEAIFEPSSHLHDGAVLMRGETISYARVILPLAHDTTQLSRSMGTRHRA
    ... :.:.. :. ..: .*::**:..*.:.::*****:::  . :. *. .***: .....*: .******

Bb  GLGISENSDAITIITSEETGSISITINAKLEYNLSLSEIRNKLNLELIE
Bs  AVGISEVTDSLTIIVSEETGGVSVAKNGDLHRELTEEALKEMLEAEFKKNTRDTSSNRWYWRGKKNG
Lm  ALGISEVTDSITIVVSEETGGISLTKGGELFRDVSEEELHKILLKELVTVTAKKPSIFSKWKGGKSE
Sa  AVGISEVSDAFTVIVSEETGDISVTFDGKLRRDISNEIFEELLAEHWFGTRFQKKGVK
Ct  ALGASQRTDALVIVVSEETGAVSLARDGILTRGVKMDRFKAILRSILTRNERKTNPIISWMRKK
    :.*:*:..*. .:.:***** .*    . *    . .     *
```

Savage CR, et al. doi.org/10.1371/journal.pone.0125440

The two regions of conserved residues that constitute the DAC domain are boxed in blue. Residues found in all 5 proteins are indicated by an asterisk (*), residues in 4 proteins by a colon (:), and those in 3 proteins by a period (.). Enzyme sequences are identified as: Bb, *B. burgdorferi* CdaA; Bs, *Bacillus subtilis* CdaA (formerly YbbP); Lm, *Listeria monocytogenes* CdaA/DacA

Figure 5.2 *B. burgdorferi* synthesizes c-di-AMP

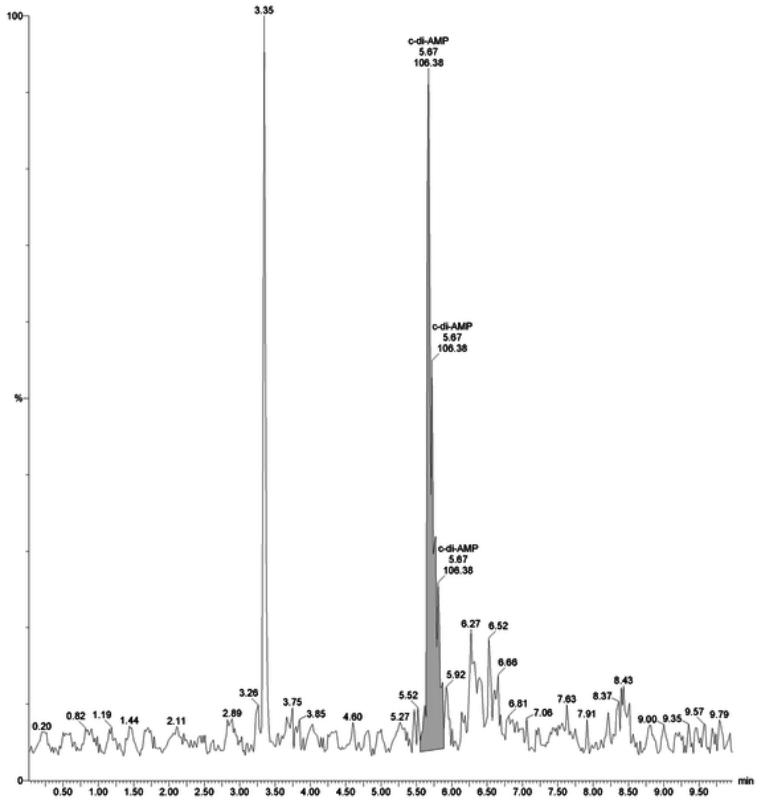

Savage CR, et al. doi.org/10.1371/journal.pone.0125440

Representative mass spectrometric analysis of cytoplasmic extract from IPTG-induced *E. coli* strain CRS-0, which expresses *B. burgdorferi* CdaA from a chimeric plasmid. The identity of the peak at 3.35 min was not determined.

Figure 5.3 Effects of overexpression *cdaA* in *B. burgdorferi*

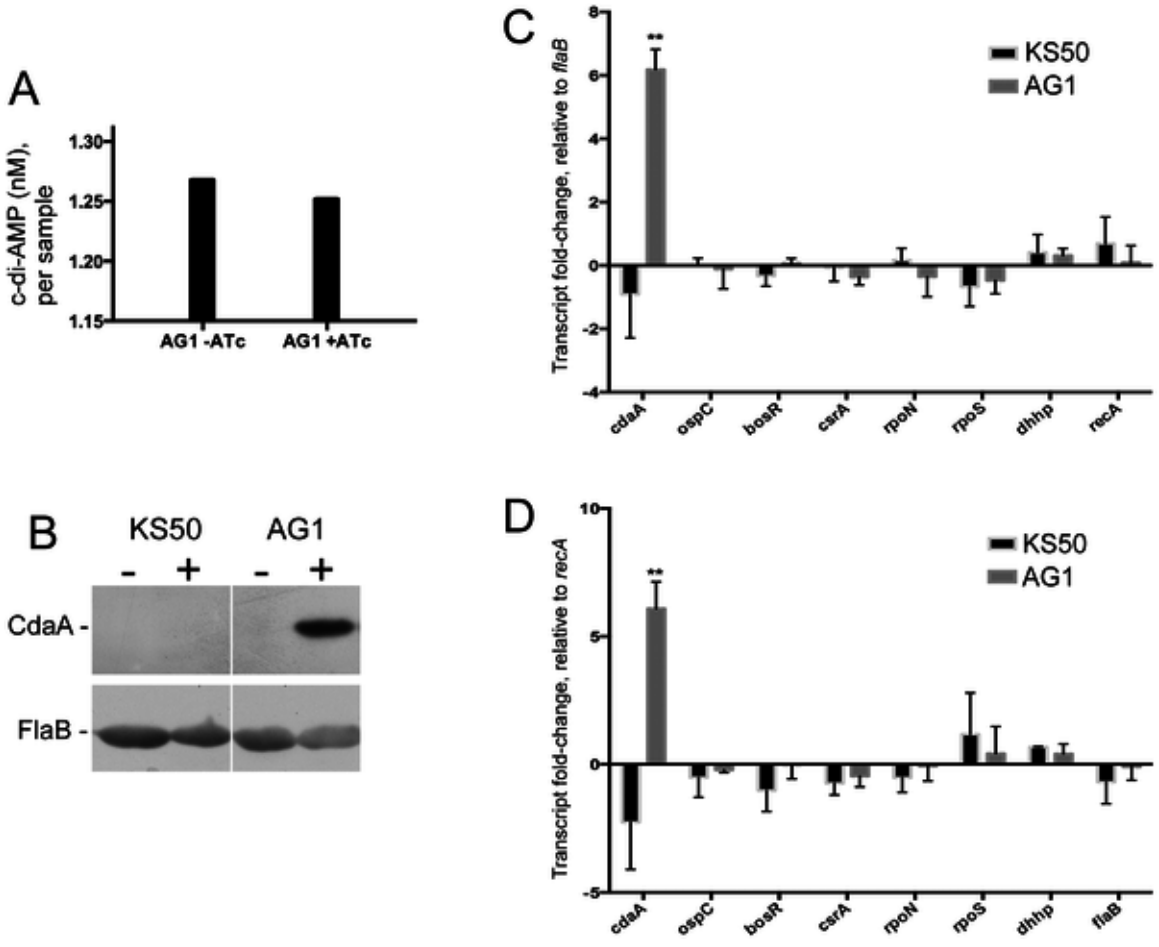

Savage CR, et al. doi.org/10.1371/journal.pone.0125440

A. Measurements of *B. burgdorferi* cytoplasmic c-di-AMP levels in samples of uninduced and induced AG1. Bacteria were cultured to mid-exponential phase (approximately 10^7 bacteria/ml), divided equally divided into two tubes, then *cdaA* transcription was induced by addition of 0.5 μg/ml (final concentration) anhydrotetracycline (ATc) to one tube, and both were incubated for 24h at 34°C. Equal volumes of borrelial cell extracts were analyzed. B. Immunoblot analyses of KS50 and

AG1, without and with inclusion of 0.5 μg/ml anhydrotetracycline (ATc) inducer (- and +, respectively). Membranes were probed with antibodies directed against CdaA or the constitutively-expressed FlaB subunit of the flagella. Wild-type and uninduced AG1 bacteria produced substantially less CdaA than did induced AG1, and the immunoblot signal was not detectable for those strains/conditions at the illustrated exposure. Analyses of mRNA levels also indicated that *cdaA* is expressed at low levels by uninduced AG1 (data not shown). C and D. Q-RT-PCR analyses of the effects of CdaA hyperexpression on transcription of select *B. burgdorferi* mRNAs. Transcript fold changes are shown as the difference between uninduced and induced cultures for both strains KS50 and AG1, relative to control *flaB* or *recA*, respectively. Multiple t tests were performed for each strain and examined transcript. Only the differences in levels of *cdaA* transcripts in induced cultures of AG1 were significant (indicated by **, $p = 0.0012$ when compared with *flaB*, and $p = 0.0023$ when compared with *recA*)

Figure 5.4 Impact of cdaA on OspC and SpoVG expression

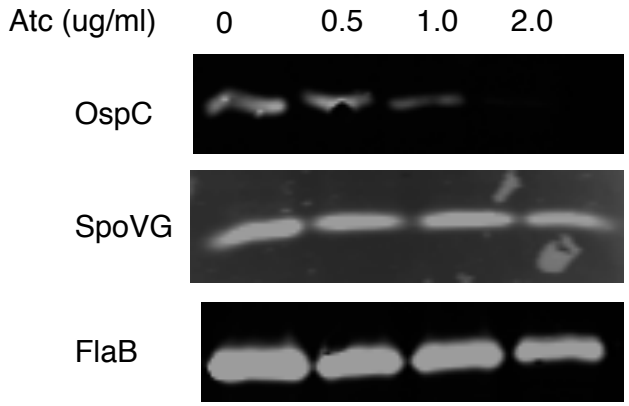

Western Blots of OspC, SpoVG and FlaB. *cdaA*-ON was cultured at 34° C with 0, 0.5, 1.0 or 2.0 μg/ml ATc to induce CdaA at varying levels. Cultures were grown to mid-log, and protein lysates separated by SDS-PAGE. α-rabbit (SpoVG) conjugated to IRD700 and α-mouse (FlaB and OspC) conjugated to IRD800 were used for secondary antibodies.

Figure 5.5 Impact of SpoVG on *cdaA* and OspC expression

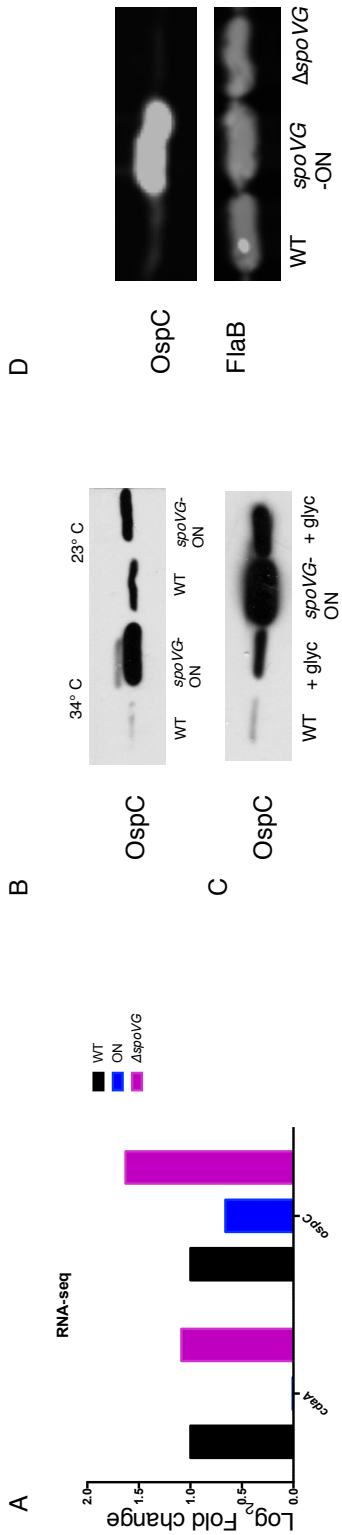

RNA-seq of *cdaA* and *ospC* transcripts in wild-type, *spoVG*-ON and Δ*spoVG* cultures. (B) Western blots of OspC from wild-type and *spoVG*-ON lysates grown at 34° C and 23° C. (C) Western Blot of OspC from wild-type and *spoVG*-ON cultures grown with and without addition of 4% glycerol. D. Western Blot of OspC and FlaB from wild-type, *spoVG*-ON and Δ*spoVG* lysates Cultured at 34° C.

Figure 5.6 SpoVG binds to *ospC* RNA

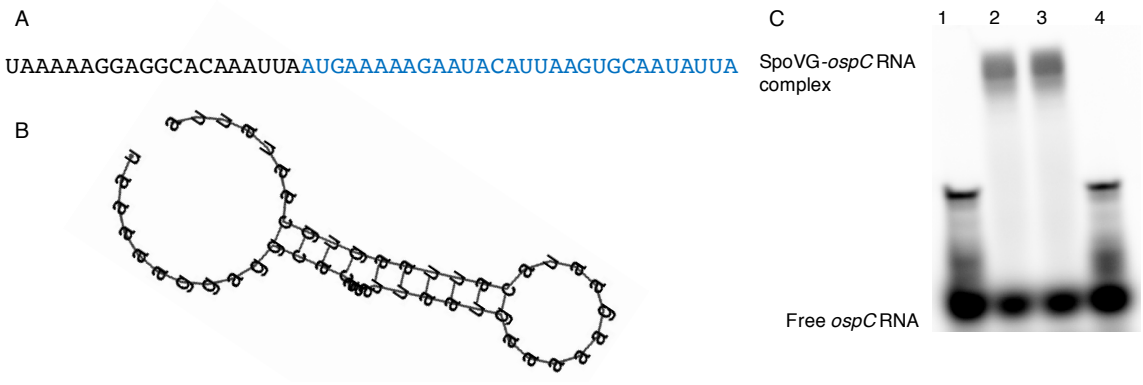

The sequence of RNA used for SpoVG-RNA EMSA spans from just upstream of the ribosomal binding site through the coding region for the first several amino acids for OspC (A). The predicted structure of the *ospC* RNA (B). The sequence listed in A was run through http://rnaanalyzer.bioapps.biozentrum.uni-wuerzburg.de/ prediction software. EMSA using the *ospC* RNA and SpoVG protein (C). Lane 1 contains RNA, Lane 2 contains RNA and SpoVG protein, Lane 3 contains RNA, SpoVG protein and c-di-AMP, Lane 4 contains RNA and c-di-AMP.

Figure 5.7 Mutated *ospC* RNAs to test SpoVG-RNA binding

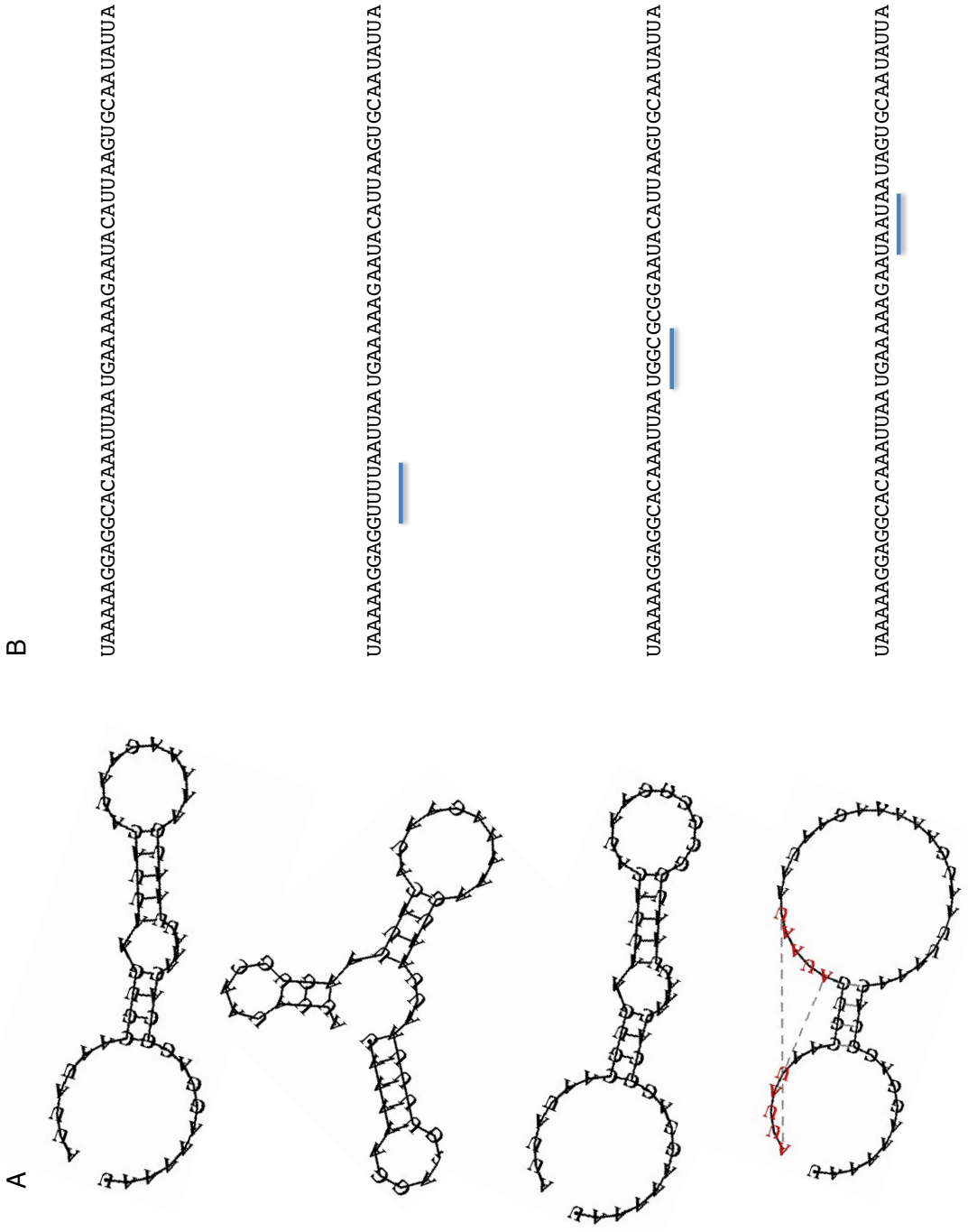

The predicted structures for all RNAs ordered to test SpoVG binding to (A). All structures were predicted using http://rnaanalyzer.bioapps.biozentrum.uni-wuerzburg.de/ software. The sequences for all mutated RNAs (B).

Figure 5.8 SpoVG binding to mutated RNAs

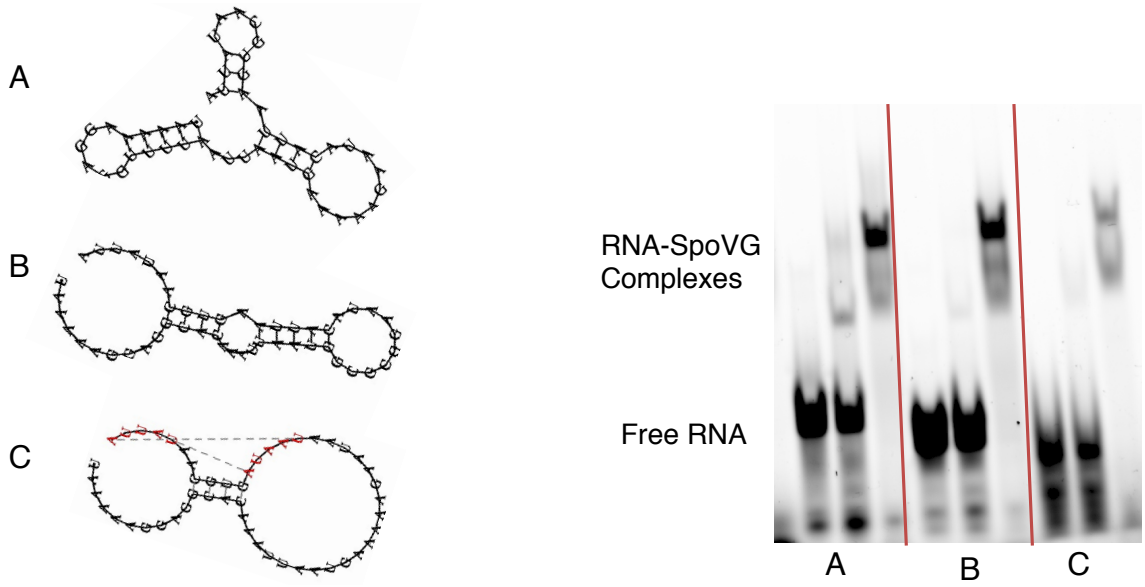

EMSA using purified SpoVG protein and mutated *ospC* RNAs. Panel A contains RNA A, panel B contains RNA B, and Panel C contains RNA C. For each Panel, the first lane contains no protein, the second lane contains RNA and SpoVG, and the third lane contains RNA and 10x more SpoVG protein.

CHAPTER 6. DISCUSSION

6.1 SpoVG in B. burgdorferi

The studies presented in this work shed light on the importance of SpoVG within the cell, and the ways in which it impacts regulation of numerous genes, both at the level of transcription and translation. We had hypothesized the SpoVG would be dispensable for *B. burgdorferi* to survive within a mouse, given the fact that *spoVG* transcript abundance is very low. We further hypothesized that over-expressing SpoVG would render *B. burgdorferi* incapable of infecting mice. Our infection studies, using multiple strains of *B. burgdorferi* that overexpress *spoVG* demonstrated that this was not the case. In infection studies conducted by our collaborator Dr. Motaleb demonstrated that deletion of the *spoVG* gene made the bacteria non-infectious in mice.

This could be due to one of a number of reasons, including that even a small amount of SpoVG is necessary for survival. Our studies on cultured *B. burgdorferi* revealed that RNA levels do not necessarily predict protein abundance, and furthermore, SpoVG appears to regulate itself at the level of translation. Simply because RNA levels of *spoVG* are low when *B. burgdorferi* is inside a mouse, does not indicate that protein levels are necessarily low as well.

6.2 Transcriptomics on *spoVG*-ON, Δ*spoVG* and wild-type

Transcriptomics on mutant strains of *B. burgdorferi* in which *spoVG* had either been deleted or over-expressed revealed that numerous transcripts are differentially expressed within these mutants compared to wild-type. Differentially expressed genes were

distributed across both the chromosome and the various plasmids. Additionally, functional clustering analysis revealed that genes involved in a wide variety of processes are involved, including DNA repair, carbon metabolism, and ABC transporters. The most abundant group for both *spoVG*-ON vs. wild-type and Δ*spoVG* vs wild-type was membrane lipoproteins. Even looking at differentially expressed genes by how they cluster into functional groups, there was great overlap between the genes that were differentially expressed in the *spoVG*-ON mutant compared to the genes that were differentially expressed in the Δ*spoVG* mutant. These data suggest that SpoVG has wide-ranging effects on gene-regulation in *B. burgdorferi,* rather than regulating a very specific set of genes.

Some might argue that in order to be defined as a regulator, that a particular gene must regulate a defined set of genes, and demonstrate that there is high specificity for those genes. It might also be argued that nucleoid-associated proteins cannot be defined as regulators. To these points, I would make a counter-argument, specifically with regard to SpoVG. We provide evidence that *SpoVG* is regulated at the levels of transcription and translation, and evidence that the *spoVG* gene is regulated in culture as well as in the enzootic cycle. The evidence that we present that SpoVG acts broadly does not disprove our hypothesis that SpoVG serves a necessary function for fitness throughout the enzootic cycle, and that it is a regulator in that it enables *B. burgdorferi* to express the right genes at the appropriate levels when needed.

Nearly all of the plasmid *parA* genes were differentially expressed, which could not be explained away by differential plasmid abundance. In addition to gene regulation, this has broad implications for plasmid replication and segregation. It is still unknown how *B. burgdorferi* manages to faithfully maintain 20 extra-chromosomal plasmids. We

demonstrated that the differences in *parA* transcript abundance could not be explained simply by a difference in plasmid copy number. Regulating expression of *parA/B* genes could have effects in multiple ways. Regulating expression of the genes could have impacts on plasmid replication and segregation over time. It may be possible that *B. burgdorferi* employs different plasmid maintenance programs when it is inside the tick versus inside the vertebrate. For example, previous work has demonstrated that *B. burgdorferi* can exchange plasmids with other *Borrelia* when inside a tick (303). Perhaps SpoVG plays a role in this by regulating how plasmids replicate, particularly when inside the tick.

6.3 Regulation of *ospC* gene by SpoVG and c-di-AMP

SpoVG interacts directly with DNAs and RNAs associated with genes that it regulates. We found examples where SpoVG impacted the transcript of a gene but not the protein, and examples where SpoVG regulated protein abundance of a gene but not the transcript. Understanding the why SpoVG interacts with certain DNAs and RNAs, and the factors that impact the relative affinity SpoVG has for one or the other may provide insight into these observed differences in regulation.

We demonstrated for the first time that *B. burgdorferi* synthesizes cyclic-di-AMP. Both c-di-AMP and SpoVG have impacts on expression of the outer surface protein OspC that is necessary only during transmission from tick to mouse. Both of these regulators influence only OspC protein abundance, but not transcript abundance. SpoVG interacts directly with the RNA transcript, although the detailed mechanism of how it influences protein abundance remains to be determined. Likewise, the mechanism of how c-di-AMP regulates OspC remains to be determined. Although c-di-AMP riboswitches are ubiquitous

in other bacteria that also synthesize c-di-AMP, no riboswitch has been found in the Borrelial genome. It is possible that this represents a new class of riboswitch that has never been experimentally confirmed before now. It is also possible that c-di-AMP binds to a protein that only interacts with the *ospC* RNA when c-di-AMP is present, or not. Our EMSAs with SpoVG and *ospC* RNA with and without c-di-AMP indicate that SpoVG does not interact with c-di-AMP, or at least that it does not impact whether or not SpoVG interacts with the RNA. Studies that determine cellular components that c-di-AMP interacts with would be very useful.

6.4 Structural insights into SpoVG

The structure of SpoVG from *B. burgdorferi* has not been solved, however it models with high confidence on the solved structure of *Bacillus subtilis* subsp. subtilis str. 168 (2IA9) SpoVG (Figure 4.13). Shown in grey is the *B. subtilis* SpoVG, as a hexamer. In orange is one subunit of SpoVG modeled from *B. burgdorferi*. Putting together everything we know about the different residues, in lilac are the residues required for interacting with the DNA back-bone. These residues are delineated by two red arrows on the sequence alignment, and are highly conserved across all SpoVG homologues. In dark blue are the residues involved in recognizing specific sequences, and are delineated by the magenta box on the sequence alignments, which are highly divergent between different species (164). The residue in red is the one that can be acetylated, and in turquoise are the residues that can be phosphorylated.

6.5 SpoVG as a potential nucleoid-associated protein

It remains to be determined if *B. burgdorferi* SpoVG forms hexamers, and if this is the active unit that binds nucleic acid. Observing how one unit of SpoVG models onto the hexameric structure of *B. subtilis*, reveals some intriguing insight. All of the residues involved in non-specific interactions with the DNA backbone are on one face of the SpoVG hexamer, and all of the residue involved in sequence-specific interactions are on the opposite face. By definition, bacteria, as prokaryotes do not have a membrane-bound nucleus, however they package their DNA into nucleoid like structures within the cell, packaged by nucleoid-associated proteins (159, 304-308). We hypothesize that SpoVG is one such nucleoid-associated protein. It is tempting to think of a SpoVG hexamer almost as analogous to a histone, with the DNA wrapping around the faces-one one side anchoring DNA via interactions with its backbone, and on the other, pulling in recognized sequences.

Studies on nucleoid structure in bacteria are possible, and widely observed in many species of bacteria (306, 307, 309, 310). Studies involving intracellular imaging on *Borrelia burgdorferi* are particularly challenging for a number of reasons. For one, *B. burgdorferi* is very thin, even for a bacterium. Their diameter is about 200 nm, which is smaller than the wavelength of visible light. Even using high-resolution microscopy, it is very difficult to accurately resolve cell membranes-cytoplasm-cell membranes. Secondly, it has been widely observed using stains such as DAPI that nucleic acid material runs throughout the majority of the length of the bacteria (159, 307).

There are two distinct states that have been seen: one in which essentially the entire bacterium stains consistently, and one in which “beads on a string” (to borrow terminology from Eukaryotes) is visible (307). No one has been able to effectively determine what

causes one state over the other. Associations with growth rate, or the presence or absence of regulatory factors does not provide consistent insight. Attempts to stain fixed bacteria with α-SpoVG antibodies did not yield any consistent results. In a newly-published paper, the Jacobs-Wagner lab profiled nucleoid size across a vast array of different bacteria, they did not include any Spirochetes in their analyses because they were unable to consistently define nucleoid size or shape. (38, 306, 311) (Personal correspondence with Dr. Jutras).

Moving forward, there are a number of studies that could be employed to discern whether or not SpoVG actually influences the three-dimensional structure of the DNA. More recently, we have hypothesized that perhaps SpoVG only gets expressed at a certain time in the cell cycle. In order to test this, a fusion of the SpoVG promoter to GFP could determine if cells only some cells in a population express GFP at a given time. This could help determine whether there is any correlation between SpoVG expression and nucleoid shape with in *B. burgdorferi*.

Approaches that do not require light microscopy could also be employed to probe whether SpoVG helps shape the nucleoid. Atomic force microscopy has been employed to determine if bacterial chromosomes develop a different conformation with or without the presence of a protein of interest. This method directly probes purified chromosome in an in vitro environment, free of the cell. Hi-C sequencing could also be employed. This approach essentially sequencing regions of DNA that are in close physical proximity to one another, and has been employed to demonstrate that when a specific protein of interest is absent within a cell, that the regions of DNA close to one another drastically change, thus indicating a conformational role of the protein of interest.

6.6 Presence of Poly-T sites

The only motif consistent with every identified DNA sequence that SpoVG interacts with is a run of poly-Thymidine. This is not an uncommon motif in the *B. burgdorferi* genome, which is composed of approximately 70% A-T. In this genome, a run of 5 Thymidines in a row occurs 23,869 times on the main chromosome alone. Keeping in mind that the main chromosome is only about 910 KB, this represents a substantial percentage of the chromosome. The ubiquitous poly-Ts are not surprising given then A-T content of the genome, however, it could offer a reason why *B. burgdorferi* SpoVG evolved to bind the nucleotide residues that it does. Our data indicate that SpoVG influences regulation of numerous genes throughout the genome. It could be that rather than specifically targeting a set of genes to hold under its control, that SpoVG acts in a more general manner to influence the overall structure of the chromosome within the cell.

Poly-U sites are present in each of the RNAs that SpoVG binds to as well. Throughout the studies described in this work, focus was placed on studying the 5' ends of genes, to understand how SpoVG has an impact on transcription and translation. Bacteria have two mechanisms for transcription termination: intrinsic and rho-dependent terminators (312). Intrinsic transcriptional terminators contain a sequence that forms a stem loop when transcribed into RNA, followed by a poly-U sequence. It is possible that SpoVG exerts its global effects, not just by regulating the start of transcription and translation, but also by regulating transcription termination. Another possibility is that perhaps SpoVG binds to these pol-U sites on the 3'ends of transcripts, and protects them from degradation. The half-life of RNA transcripts in *B. burgdorferi* is unusually long for a bacterium, at 45

minutes (313). The mechanism of how the half-life of transcripts is so long is not known. Perhaps SpoVG has a role in the regulation of the half-life of transcripts in *B. burgdorferi.*

6.7 Post-translational modification of SpoVG

It is still unclear what role, if any the post-translational modifications of acetylation and phosphorylation has on SpoVG activity. Each individually, or both, may impact the relative affinity of SpoVG for DNA vs RNA. Our studies demonstrated that SpoVG appears to possess a higher affinity for RNA than DNA, and this would be consistent with what was observed in *L. monocytogenes* (175). It has been reported that phosphorylation of *S. aureus* SpoVG impacts its ability to bind DNA (174). There was no indication that acetylation had an impact on SpoVG multimerization, however it remains to be tested whether it has an impact on the interaction between SpoVG and PlzA. Additionally, phosphorylation of SpoVG remains to be tested. There are two putative serine/threonine kinases encoded in the genome that have not been studied at all (23).

6.8 Model of SpoVG network in *B. burgdorferi*

Putting together everything we know of how SpoVG is regulated, and how it acts within the cell, it becomes clear that SpoVG is central to numerous processes (Figure 6.2). SpoVG is regulated by numerous regulatory factors including CsrA, PlzA, BadR, RpoS and the stringent response regulator ppGpp (154, 221, 284, 314, 315). These factors include DNA-RNA binding proteins, an alternative sigma factor, and nucleotide second messengers. Each of these factors has been reported to be necessary at different stages of

the enzootic cycle. Perhaps SpoVG acts as a sensor for the current environment, and what is present within the cell.

SpoVG acts in multiple ways, including binding DNA, binding RNA and interacting with at least one other protein. Although the effect of post-translational modifications on SpoVG activity has yet to be elucidated, it is possible that they modulate how SpoVG acts in the cell. In this way, *B. burgdorferi*, with its reduced genome, could conserve energy on translating multiple different proteins, and instead re-purpose the same protein to behave differently when the environment changes.

6.9 SpoVG as potentially analogous to a eukaryotic cell-cycle checkpoint protein

The studies on *Bacillus subtilis* SpoVG from the 1980s and 1990s appear to present conflicting results. In one scenario, when SpoVG was absent, sporulation was halted in almost every cell, and in another scenario, a non-sense mutation in SpoVG restored the ability of cells to continue sporulation (165, 166, 169, 316). It is important to remember that SpoVG is expressed during stage 1 of sporulation, even when SpoVG was deleted on its own, it halted sporulation at stage 5. These data suggest that perhaps SpoVG serves a purpose in monitoring the progress of sporulation. Rather than regulating a certain set of genes necessary for advancement through the different stages of sporulation, it acts to ensure fidelity of the process, and to halt proceeding if something is not right.

Bacteria do not have a programed cell cycle in the same way that eukaryotes do, but they still have to coordinate different processes such as DNA replication, cell growth and cell division. If a cell were to divide without properly replicating and segregating their chromosome(s), those cells would not survive. The process of sporulation offers insight

into a more organized cell program, but the notion of true checkpoint proteins in sporulating and non-sporulating bacteria is still rather a foreign concept.

Even though *Borrelia burgdorferi* does not form spores, the rigidity of the enzootic cycle they traverse confers external cell program constraints. There are very specific times when *B. burgdorferi* must be highly motile, times when they must replicate rapidly, and times when they must essentially lie quiescent-within the unfed tick. Not only this, but they must be prepared to rapidly alter their cellular functions when new cues come in. Perhaps SpoVG acts to ensure that cell processes are progressing as they should, thereby serving as a type of prokaryotic cell cycle checkpoint protein.

Figure 6.1 Modeled SpoVG structure

Borrelia burgdorferi SpoVG protein sequence (orange) modeled on the solved crystal structure of *Bacillus subtilis* SpoVG protein (grey). The grey represents a hexamer of SpoVG, the orange depicts a monomer of SpoVG. In light purple are the residues necessary for interacting with DNA backbone. Nucleotides in dark blue depict those necessary for interacting with specific sequences. In red is the Lysine residue that can be acetylated. In turquoise are the residues that can be phosphorylated.

Figure 6.2 Model of SpoVG activities

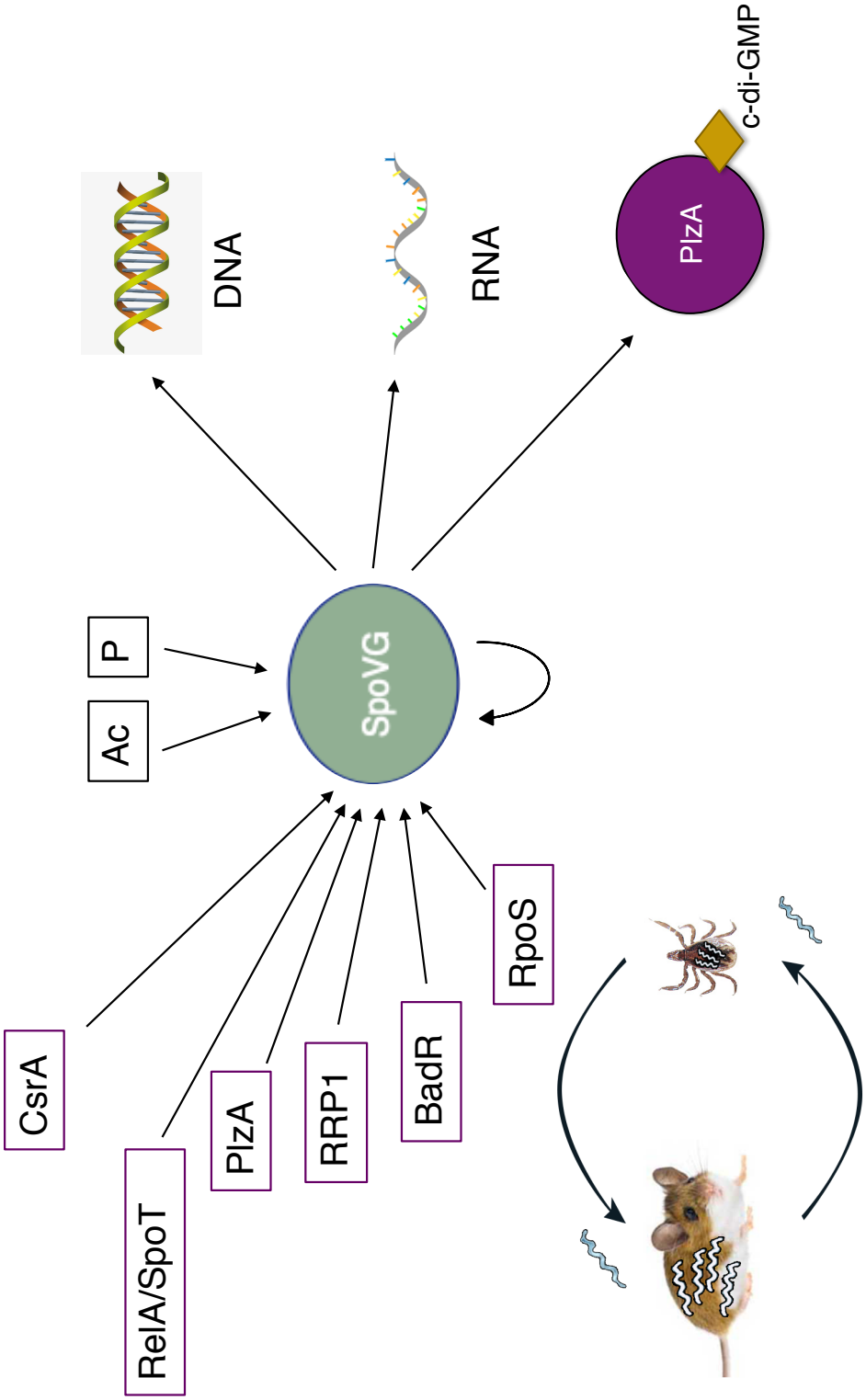

APPENDICES

APPENDIX 1. *CHEA* MUTANTS RESPOND TO GLYCEROL DIFFERENTLY THAN WILD-TYPE *B. BURGDORFERI*

A.1.1 Introduction

Wild-type *B. burgdorferi* responds to the presence of glycerol added to BSK media by reducing growth rate and altering transcription of genes involved in various cellular processes such as growth rate, DNA replication, and DNA repair. Cells over-expressing *spoVG* did not respond in the same manner. We wondered how the cells recognized glycerol, and how that recognition was transduced to transcriptional outputs. As previously stated, *B. burgdorferi* has very few known regulatory proteins.

The process of chemotaxis by bacteria has been extensively studied. At the core of how the system works, MCP (methyl-accepting chemotactic proteins) are receptors that span the outer and inner membrane of the cell wall and can bind different molecules. The cytoplasmic portion of the protein interacts with the histidine-kinase (CheA) of a two-component system. The response regulator, CheY can be phosphorylated by CheA and can interact with the flagellar motor. This system was first studied in laboratory strains of *E. coli*, which encodes one gene for *cheA* and one gene for *cheY*. This was used as the model system to study chemotaxis for a number of decades (317).

Most bacteria that are not *E. coli* have multiple proteins that are homologous to CheA, and multiple proteins that are homologous to CheY (318). Under the classical chemotaxis assay, many of these additional systems served no apparent role, thus were dismissed for several decades as unnecessary, and unworthy of pursuit. Recently, studies

within a few bacteria have revealed that these additional systems are necessary for chemotaxis in different conditions, for example transition in and out of biofilms, and have additional signaling roles distinct from chemotaxis, such as gene regulation, and cell division(255, 319-322). *B. burgdorferi* has two CheA proteins, and three CheY proteins. Only one of each is necessary for chemotaxis. The function of the other proteins is unknown (80, 99, 102, 323-325).

A.1.2 Δ*cheA1* and Δ*cheA2* growth response to glycerol

We hypothesized that perhaps glycerol was sensed through the Che system, thus potentially linking nutrient availability to growth rate and gene regulation. For this, we obtained both CheA mutants: Δ*cheA1* and Δ*cheA2* from Dr. Chris Li. These mutants form massive clumps in liquid culture, making it impossible to conduct growth curves by counting cell density (Figure A1.1 A) (80).

For this reason, we relied on a previously-published method to circumvent this obstacle (326). BSK-II media contains the pH indicator phenol Red. As *B. burgdorferi* produces ATP, lactic acid is secreted from the cells, and the once red media turns yellow. This color change can be measured by a spectrophotometer by calculating the absorbance at 562 nm divided by the absorbance at 630 nm. In cultures grown in BSK without glycerol, the media from both Δ*cheA1* and Δ*cheA2* strains acidified significantly more slowly that wild-type (Figure A1.1 B and C). This indicates that there is a difference in how both of the mutant strains are able to metabolize available sugars and produce ATP.

There is a slight difference in media acidification between wild-type grown in BSK with and without glycerol. This difference is significantly greater in both Δ*cheA1* and

Δ*cheA2* cultures (Figure A1.1 B and C). This indicates that both CheA proteins may be involved in carbon metabolism as well as chemotaxis, and potentially other processes as well.

A.1.3 Δ*cheA1* and Δ*cheA2* transcriptional response to glycerol

We next sought to test whether there were transcriptional differences in how wild-type, Δ*cheA* and Δ*cheA2* respond to glycerol. We first compared relative transcript abundance from wild-type, Δ*cheA1* and Δ*cheA2* grown in BSK without glycerol (Figure A1.2 A). The only transcript that was differentially expressed was *dnaA* in the Δ*che1* strain. The implication for regulation of DNA replication is intriguing, but was not pursued further.

We next compared the differences in transcript abundance in response to 4% glycerol added to BSK media for each strain (Figure A1.2 B). For example, we had previously reported that *spoVG* transcript is more abundant when glycerol is added to the medium. *spoVG* transcript was unaltered in either Δ*cheA1* or Δ*cheA2*. Additionally, *dnaA* transcript was more abundant in both wild-type and Δ*cheA2* when glycerol was added to the media, but remained unchanged in Δ*cheA1*. These data indicate that both CheA1 and CheA2 are involved in cellular processes beyond chemotaxis.

Figure A1.1 Differences in growth rate in response to glycerol

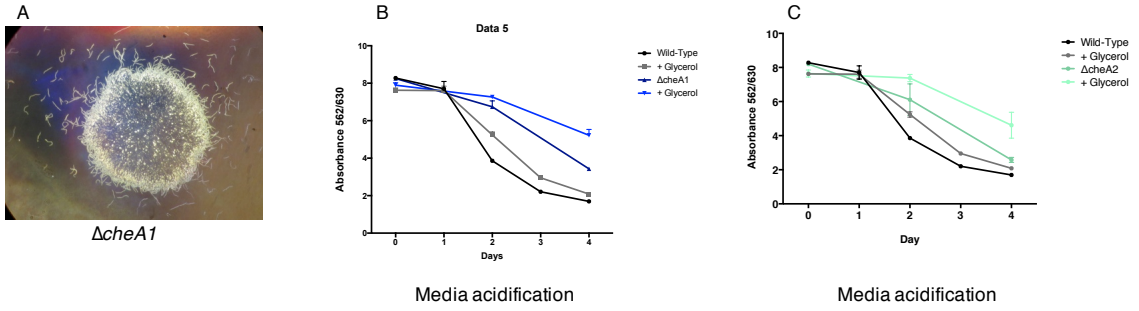

Representative clump of bacteria that both *cheA* mutants form in culture (A). (B) Wild-type (B31-A), and *cheA1* cultured with and without 4% glycerol. (C) Wild-type (B31-A), and *cheA2* cultured with and without 4% glycerol. Media acidification was measured using a spectrophotometer. Wild-type (black and grey) is plotted on each graph to demonstrate the differences between the *cheA* mutants and wild-type.

Figure A1.2 Differences in Transcriptional response to glycerol

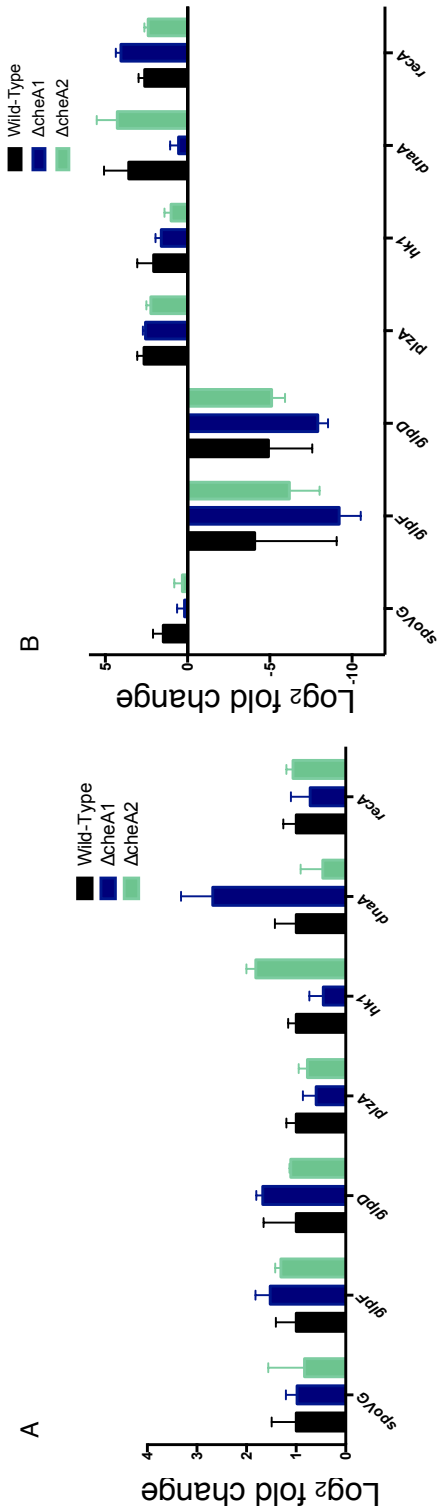

qRT-PCR of various transcripts from *B. burgdorferi* grown with and without 4% glycerol. (A) Transcripts from wild-type, Δ*cheA1* and Δ*cheA1* grown in BSK without glycerol. (B) Differences in how each strain responds to glycerol. What is plotted is the Cq of each transcript from cultures grown in BSK + glycerol subtracted from Cq value of that transcript grown in BSK without added glycerol.

APPENDIX 2 . Intracellular c-di-GMP analysis by FRET

The ability to synthesize cyclic-di-GMP is essential for *B. burgdorferi* to survive within a tick, and successfully transmit to a mouse. As with many other bacteria, it also has a role in motility and chemotaxis. C-di-GMP is synthesized by the response regulator *rrp1* of a two-component signaling system in *B. burgdorferi* (Figure A2.1 A). Both the Histidine Kinase (Hk1) and Rrp1 are produced in culture, but it is unclear what Hk1 responds to in culture or in the enzootic cycle in order to stimulate c-di-GMP synthesis. Given the newly discovered link between c-di-GMP signaling pathway with gene regulation by SpoVG (via interacting with PlzA), we were particularly motivated to develop a method that would allow us to gain insight into this system.

We took advantage of a newly developed FRET sensor for c-di-GMP inside living bacterial cells. A few other systems have been developed for studying c-di-GMP, each with their own limitations for application in *B. burgdorferi* (327-329). This system is ideal, because the FRET sensor is always expressed by *B. burgdorferi*, and FRET is dependent on c-di-GMP binding. Using this method, we will be able to visualize c-di-GMP synthesis/degradation in real time, and in mouse infection/tick colonization studies.

Christen et al linked the gene for a Pilz-domain protein (binds c-di-GMP) to the gene for CFP on one end, and the gene for YFP on the other (figure A2.1 C). They tested numerous c-di-GMP proteins, and settled on the one the underwent the largest structural change, and thus the clearest distinction with FRET signal (330).

We had the DNA for the entire CFP-PilZ-YFP construct synthesized using optimized codons for *B. burgdorferi* end a BamH1 restriction site on the CFP end and a Kpn1 restriction site on the YFP end. This was then cloned into pBLS715 and transformed into B31-A3 cells (Figure A2.1 D).

A Zeiss LSM 880 upright multiphoton microscope was used to image *B. burgdorferi* expressing the FRET plasmid (Figure A2.2A). The initial images confirmed that the construct is expressed well, and that FRET can be detected. Current work in progress is to transform additional strains for analysis (Figure A2.2 B). The Δ*rrp1* strain will serve as c-di-GMP negative control, and the Δ*pdeA*Δ*pdeB* will serve as a c-di-GMP positive control, since PdeA and PdeB both degrade c-di-GMP (Figure A2.1 A).

Figure A2.1 Construction of FRET sensor for c-di-GMP

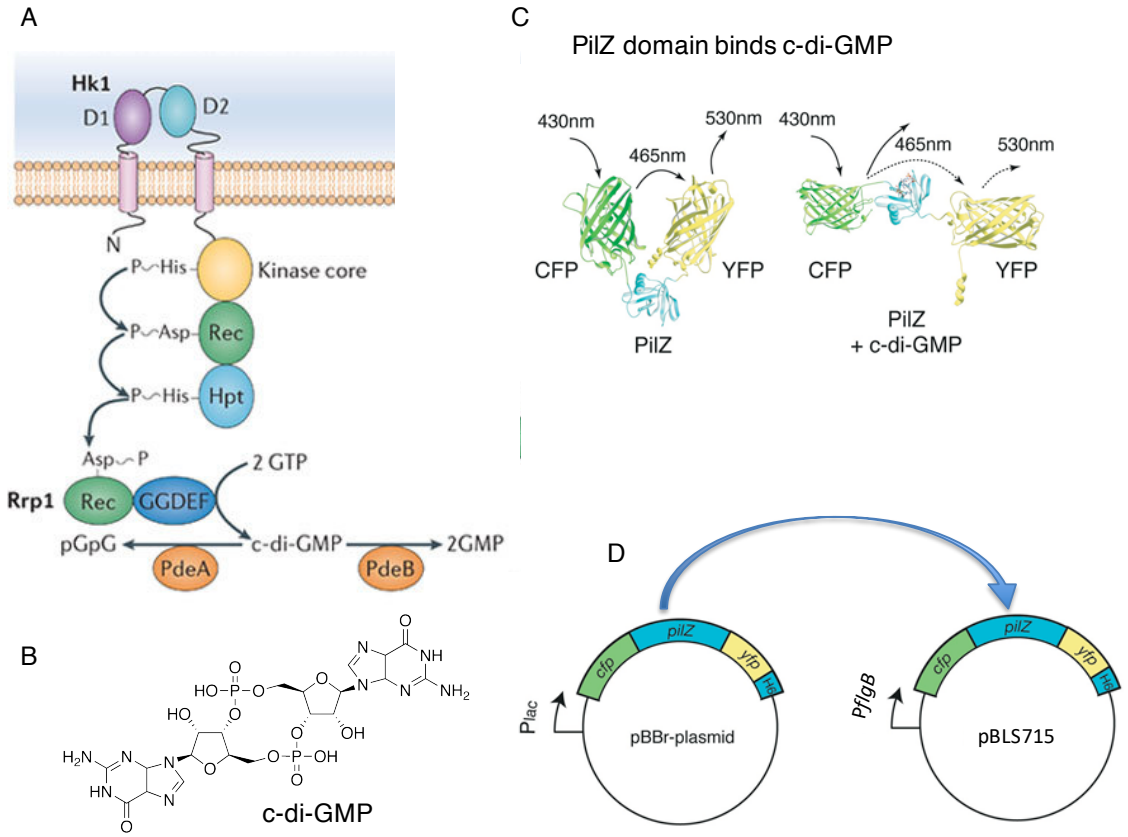

Figure adapted from Radolf et al. Nature Reviews. 2012. And

C-di-GMP is synthesized by one protein in *B. burgdorferi*: the response regulator Rrp1 of a two-component system (A). (B) Structure of c-di-GMP. (C) Structure of the FRET construct. C-di-GMP binds to PilZ domains.

Figure A2.2 *B. burgdorferi* expressing the FRET sensor

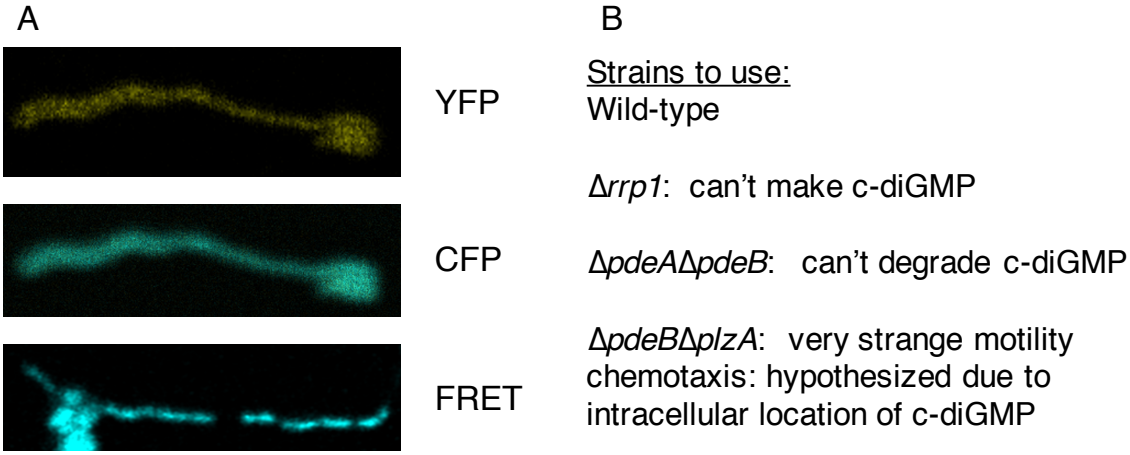

B. burgdorferi B31-A3 expressing FRET sensor (A). Demonstrates that YFP and CFP are expressed and visualized well. Also, able to detect FRET, indicating the sensor does fold correctly. (B). Will transform additional strains with the same sensor for positive and negative controls.

APPENDIX 3: Additional binding interactions

A3.1 C-di-GMP inhibits SpoVG binding to DNA.

In our initial studies to determine how the interaction between SpoVG and PlzA impacted the binding affinity of SpoVG for DNA, c-di-GMP was included in these studies. It was observed that when c-di-GMP was added, the interaction between SpoVG and DNA was competed away (Figure A3.1). The SpoVG-DNA complex is evidenced by the presence of a shifted band in lane 3 of the EMSA. Lane 4 contains the same concentration of DNA and SpoVG, as well as 1 mM c-di-GMP. The band seen in lane 3 is almost entirely shifted back down. This result was seen numerous times, every time c-di-GMP was added to a reaction with SpoVG and DNA. We know that SpoVG has a higher affinity for RNA than DNA, although it is not yet clear what RNA motif SpoVG interacts with. Knowing this, it is not entirely surprising that c-di-GMP would interrupt SpoVG-DNA interactions: c-di-GMP essentially looks like an RNA. Additionally, neither c-di-GMP nor c-di-AMP are able to compete away SpoVG-RNA interactions.

The biological significance of this remains to be elucidated. It is not known if either c-di-GMP nor c-di-AMP are ever produced in within *B. burgdorferi* when their canonical binding partners are not also produced. If they were, is it possible that they would act as sponges to essentially "soak up" any SpoVG that may be binding to DNA, thus ensuring that SpoVG exerts its effects at only post-transcriptionally?

A3.2 SpoVG binds to DNA upstream of the *ospA* promoter

Every identified DNA sequence that SpoVG binds to contains a run of poly-Ts. Previous work had identified a region of DNA with runs of poly-Ts upstream of the *ospA* transcriptional promoter involved in regulation of the gene (Figure A3.2 B) (274, 331).

OspA is an outer surface protein that is expressed during, and absolutely essential, for *B. burgdorferi* to colonize ticks. This protein interacts with the receptor TROSPA, which is expressed on the outer surface of tick mid-gut cells. The interaction between OspA and TROSPA allows *B. burgdorferi* to attach to the midgut through the molt. Expression of this protein gets turned off during the blood meal, allowing *B. burgdorferi* to detach and transmit into the vertebrate (117-119, 332).

Knowing that regulation of this gene is tightly controlled, and that the upstream region contains two runs of poly-Ts, we hypothesized that SpoVG could bind to this sequence of DNA. An EMSA using *ospA* DNA and SpoVG demonstrates that SpoVG does interact with this region (Figure A3.2 A). Lanes 2 and 3 contain increasing amounts of SpoVG. Lane 4 contains the same concentration of SpoVG as Lane 3, as well as 100x unlabeled *ospA* DNA.

A3.3 PlzA binds to DNA associated with its own gene

There is evidence to suggest that PlzA regulates its own expression (144, 148, 333). We therefore hypothesized that PlzA binds to DNA associated with its own gene. To test this, we used a DNA probe that spans the approximately 300 base pairs between it and the down-stream gene (Figure A3.3 C). Addition of PlzA protein to the DNA probe resulted in a shifted band, indicating that PlzA does in fact, bind its own DNA (Figure A3.3 A). Although PlzA regulates expression of SpoVG, RNA-sequencing from our *spoVG*-mutant strains revealed that SpoVG does not impact *plzA* transcription. It remains to be tested whether SpoVG influences PlzA translation.

Figure A3.1 c-di-GMP inhibits SpoVG binding to DNA

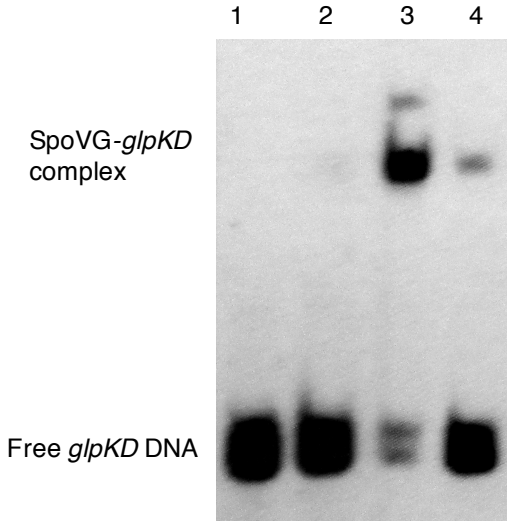

As previously demonstrated, SpoVG binds to the *glpKD* DNA. Lane 1: *glpKD* DNA. Lane 2 *glpKD* DNA and diluted SpoVG protein. Lane 3: *glpKD* DNA and more SpoVG. Lane 4: *glpKD* DNA, the same concentration of SpoVG as in lane 3, and c-di-GMP.

Figure A3.2: SpoVG binds to *ospA* DNA

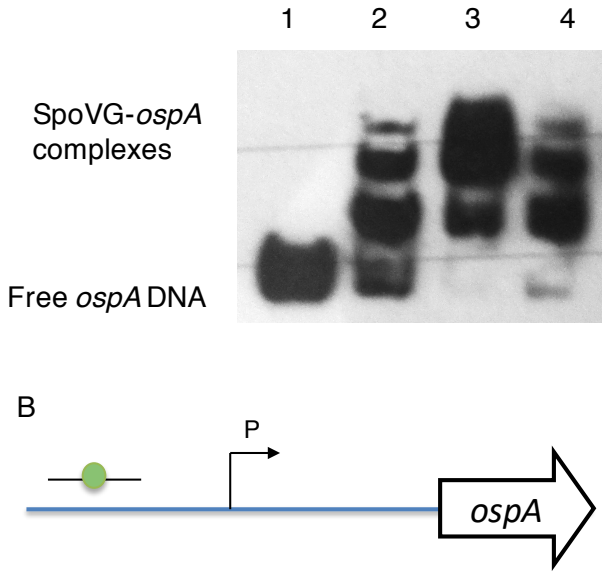

SpoVG binds to DNA upstream of the transcriptional promoter of *ospA* (A). Lane 1: *ospA* DNA. Lanes 2 and 3: *ospA* DNA and SpoVG. Lane 4: *ospA* DNA, SpoVG (amount used in Lane 3), unlabeled specific competitor. The sequence of DNA that *ospA* binds to (B).

A3.3: PlzA binds to its own promoter DNA

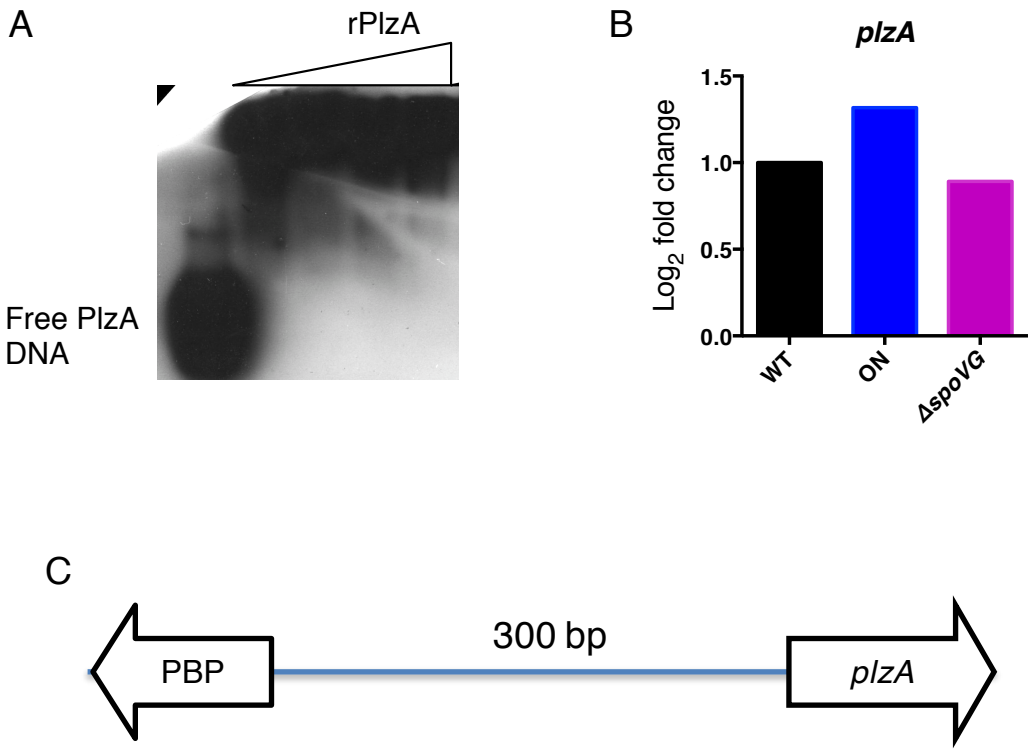

PlzA protein binds to DNA in the intergenic region between the upstream PBP gene and *plzA* (A). RNA-seq results demonstrating that SpoVG does not regulate *plzA* at the level of transcription (B). Schematic of DNA probe used for EMSA (C).

APPENDIX 4: Proteomics

RNA-sequencing revealed that numerous transcripts are altered when *spoVG* is dysregulated. We hypothesized that our *spoVG* mutant strains would reveal differences in numerous protein abundances as well. Furthermore, given the fact that SpoVG binds RNA in addition to DNA, we hypothesized that some proteins would be differentially regulated without differences in their transcript abundance. We already have two examples of this: VlsE and OspC, however we set out to identify more examples.

Additionally, post-translational modifications on proteins can impact their activity. We have already discussed acetylation above (235, 334, 335). Another common modification employed by all forms of life, including bacteria, is phosphorylation (336). Apart from work on the two-component systems, no one has studied the potential phosphorylome of *B. burgdorferi*. A group studying SpoVG in *Staphylococcus aureus* discovered that SpoVG can be phosphorylated by *S. aureus*, and furthermore, that SpoVG nucleic acid-binding activity is dependent on phosphorylation (174).

We hypothesized that SpoVG could be phosphorylated in *B. burgdorferi* as well, and that its activity could be dependent on phosphorylation states as well. Furthermore, we hypothesized that it is possible that SpoVG not only regulates the abundance of numerous transcripts and proteins, but that perhaps the overall phosphorylome of *B. burgdorferi* is also differentially regulated. SpoVG from *B. burgdorferi* was phosphorylated, as demonstrated by MS/MS.

To address these questions, we conducted 2-dimensional gel electrophoresis to compare overall proteomes and phosphorylomes between wild-type, *spoVG*-ON and Δ*spoVG* strains of *B. burgdorferi*. Each strain was grown to mid-log phase in 10 ml

cultures. Proteins were extracted, and separated by isoelctric focusing on strips containing a pH gradient from 3 to 10. Proteins were then separated by size on 20% polyacrylamide gels. Gels were first stained with Pro-Q diamond to detect phosphorylated proteins, then stained with Coomassie in order to visualize all proteins.

Although none of the spots were subjected to mass-spec for analysis (the gels were handled with bare hands by someone who should have known better), these gels did serve as preliminary data that the full proteomes of these strains should be analyzed. Rather than wasting more time running 2-D gels, we are moving forward with full proteomics with our collaborator Dr. Wolfram Zückert.

Figure A4 2-D gel analysis of total and phosphorylated proteins

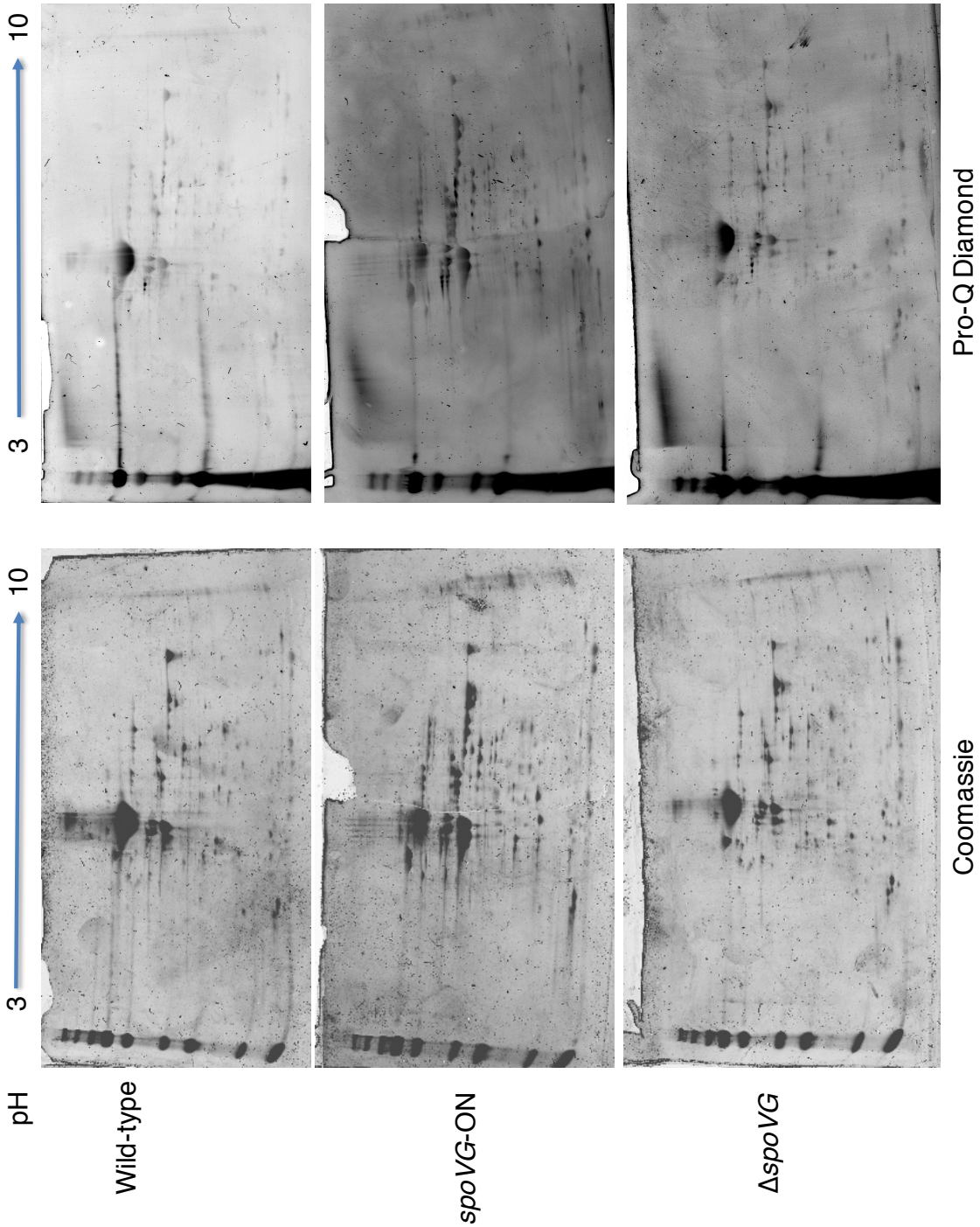

2-Dimensional gels, each separated by pH horizontally, and size vertically. Each gel was first stained with Pro-Q Diamond, to visualize phosphorylated proteins, and imaged on a typhoon. The same gels were then stained with Coomassie to visualize total protein and imaged on an Odyssey imager.

APPENDIX 5: Full transcriptomic tables

Figure A5.1 WT vs *spoVG*-ON and WT vs Δ*spoVG* mRNA Full table

gene	WT vs ON log2	WT vs ON padj	WT vs Δ log2	WT vs Δ padj
BB_0001| hypothetical protein	0.02	9.78E-01	-0.65	1.27E-01
BB_0002| glycosyl hydrolase family 3 N domain protein	0.82	2.94E-02	-0.10	9.37E-01
BB_0004| phosphoglucomutase	-0.05	9.59E-01	-0.10	8.78E-01
BB_0005| trpS| tryptophanyl-tRNA synthetase	-0.40	2.85E-01	-0.45	2.42E-01
BB_0006| membrane protein	-0.01	9.95E-01	-1.16	4.61E-03
BB_0007| hypothetical protein	0.46	4.46E-01	-0.88	7.78E-02
BB_0008| hypothetical protein	-1.19	5.55E-05	0.16	7.85E-01
BB_0009| hypothetical protein	-1.49	1.88E-10	0.22	5.55E-01
BB_0010| holo-(acyl-carrier-protein) synthase	0.32	5.45E-01	0.32	5.41E-01
BB_0011| hypothetical protein	-0.78	6.27E-03	-0.16	7.57E-01
BB_0012| truA| tRNA pseudouridine synthase A	-0.90	1.43E-02	-0.40	4.07E-01
BB_0013| hypothetical protein	-1.06	9.43E-03	-0.29	6.52E-01
BB_0014| priA| primosomal protein N'	-1.53	4.28E-07	-0.44	2.91E-01
BB_0015| udk| uridine kinase	-1.45	1.35E-06	-0.50	2.10E-01
BB_0016| GlpE protein	-0.97	3.41E-03	-0.22	6.77E-01
BB_0017| hypothetical integral membrane protein	-0.62	2.27E-01	-0.73	1.55E-01
BB_0019| hypothetical protein	0.01	9.84E-01	-0.33	3.95E-01
BB_0022| ruvB| holliday junction DNA helicase RuvB	0.95	4.05E-03	0.25	6.28E-01
BB_0023| ruvA| holliday junction DNA helicase RuvA	1.15	3.52E-03	0.98	2.25E-02
BB_0024| hypothetical protein	0.88	9.75E-03	-0.58	1.41E-01
BB_0025| DNA-binding regulatory protein YebC/PmpR family	-0.08	9.59E-01	1.51	1.07E-02
BB_0026| methylenetetrahydrofolate dehydrogenase 0026|	0.40	5.93E-01	1.34	8.69E-03
BB_0027| hypothetical protein 0027|	0.98	2.61E-02	0.04	9.89E-01
BB_0028| lipoprotein 0028|	0.09	9.59E-01	0.21	8.40E-01
BB_0029| YaiI/YqxD family protein 0029|	-0.64	2.35E-01	-0.56	3.35E-01
BB_0030| lepB| signal peptidase I 0030|	-0.78	4.36E-02	-0.11	9.29E-01
BB_0031| lepB| signal peptidase I 0031|	0.26	6.19E-01	0.38	3.95E-01
BB_0032| hypothetical protein 0032|	-0.36	3.18E-01	0.20	6.52E-01
BB_0033| smpB| SsrA-binding protein 0033|	-0.21	7.21E-01	0.73	6.22E-02
BB_0034| outer membrane protein P13 0034|	1.22	2.06E-03	-0.13	9.12E-01
BB_0035| DNA gyrase/topoisomerase IV	5.56	NA	5.77	NA
BB_0036| DNA topoisomerase II (N-region)	-0.43	5.87E-01	-1.47	6.59E-03
BB_0037| 1-acyl-sn-glycerol-3-phosphate acyltransferase	-0.36	6.26E-01	-1.46	2.18E-03
BB_0039| hypothetical protein 0039|	-0.66	3.27E-01	-1.32	2.31E-02
BB_0040| cheR| CheR methyltransferase	0.07	9.59E-01	1.01	3.29E-02
BB_0042| phoU| phosphate transport system	0.73	1.09E-01	-0.09	9.64E-01
BB_0043| hypothetical protein 0043|	1.82	2.74E-04	0.72	2.76E-01
BB_0044| hypothetical protein 0044|	1.75	5.82E-04	0.34	6.89E-01
BB_0045| P115 protein 0045|	-0.13	9.06E-01	0.11	9.32E-01
BB_0046| rnhB| ribonuclease HII 0046|	0.63	4.68E-02	-0.31	4.51E-01
BB_0047| hypothetical protein 0047|	2.07	4.46E-04	0.60	4.73E-01
BB_0048| hypothetical protein 0048|	0.70	3.11E-01	0.60	4.20E-01
BB_0050| transporter 0050|	-0.26	7.61E-01	-0.66	2.70E-01
BB_0051| integral membrane protein	-0.24	5.87E-01	-0.03	9.89E-01
BB_0052| tRNA/rRNA methyltransferase 0052|	-0.05	9.59E-01	-0.59	1.81E-01
BB_0053| ung| uracil-DNA glycosylase 0053|	-0.07	9.59E-01	-0.88	7.69E-03
BB_0054| protein-export membrane protein SecG	0.41	5.39E-01	0.19	8.47E-01
BB_0055| tpiA| triose-phosphate isomerase 0055|	-0.04	9.61E-01	0.27	6.68E-01
BB_0056| pgk| phosphoglycerate kinase 0056|	-0.16	8.30E-01	0.15	8.51E-01
BB_0057| gap| glyceraldehyde-3-phosphate dehydrogenase	0.10	8.98E-01	-0.05	9.89E-01
BB_0058| tetratricopeptide repeat domain protein 0058|	-0.11	9.59E-01	-0.79	1.40E-01
BB_0059| CBS domain pair protein 0059|	-0.18	8.07E-01	-0.30	5.86E-01
BB_0060| hypothetical protein 0060|	0.17	8.32E-01	-0.25	6.75E-01
BB_0061| trx| thioredoxin 0061|	0.68	2.41E-01	0.85	1.40E-01
BB_0062| RNA methyltransferase RsmE family 0062|	0.22	7.07E-01	-0.26	6.27E-01
BB_0063| pasta domain protein 0063|	-0.12	8.91E-01	-0.13	8.78E-01
BB_0064| fmt| methionyl-tRNA formyltransferase 0064|	0.24	7.42E-01	0.28	6.76E-01

BB_0065| def| peptide deformylase 0065|	-0.03	9.59E-01	0.21	6.69E-01
BB_0066| hypothetical protein 0066|	0.52	9.63E-02	0.36	3.35E-01
BB_0068| haloacid dehalogenase-like hydrolase 0068|	-0.20	7.51E-01	0.63	1.31E-01
BB_0069| aminopeptidase II 0069|	-0.43	4.60E-01	0.86	6.68E-02
BB_0070| hypothetical protein 0070|	-0.27	7.25E-01	0.64	2.64E-01
BB_0072| membrane protein 0072|	-0.90	2.26E-04	0.36	2.63E-01
BB_0073| hypothetical protein 0073|	-0.86	7.43E-03	0.60	9.94E-02
BB_0074| prfB| peptide chain release factor 2 0074|	-0.12	8.27E-01	0.47	1.15E-01
BB_0075| hypothetical protein 0075|	-0.68	3.37E-02	0.54	1.36E-01
BB_0076| ftsY| signal recognition particle-docking protein	-1.10	6.20E-05	0.71	2.15E-02
BB_0080| ABC transporter ATP-binding protein 0080|	-1.25	2.12E-03	-0.01	9.89E-01
BB_0081| efflux ABC transporter permease protein	-1.22	8.95E-03	0.03	9.89E-01
BB_0082| hypothetical protein 0082|	-0.58	2.57E-01	-0.22	7.77E-01
BB_0083| hypothetical protein 0083|	0.06	9.59E-01	-0.13	8.66E-01
BB_0084| aminotransferase class V superfamily 0084|	-0.88	3.03E-01	-1.85	1.09E-02
BB_0085| hypothetical protein 0085|	0.37	4.48E-01	0.05	9.89E-01
BB_0086| Mg chelatase homolog 0086|	0.01	9.90E-01	-0.24	6.59E-01
BB_0087| L-lactate dehydrogenase 0087|	0.83	1.76E-02	0.03	9.89E-01
BB_0088| lepA| GTP-binding protein LepA 0088|	0.00	9.95E-01	-0.27	5.76E-01
BB_0089| hypothetical protein 0089|	-0.09	9.35E-01	-0.44	2.34E-01
BB_0090| V-type ATPase subunit K 0090|	0.52	2.33E-01	0.07	9.80E-01
BB_0092| V-type ATPase D subunit 0092|	-0.53	2.37E-01	-0.27	6.46E-01
BB_0093| ATP synthase beta chain (V-type ATPase subunitB)	-0.35	3.38E-01	-0.16	7.47E-01
BB_0095| hypothetical protein 0095|	-0.33	5.45E-01	-0.21	7.49E-01
BB_0096| ATP synthase subunit E (V-type ATPase subunit E)	0.02	9.84E-01	-0.50	3.85E-01
BB_0097| hypothetical protein 0097|	0.37	6.01E-01	-0.44	5.05E-01
BB_0098| MutS2 protein 0098|	-1.11	1.46E-02	-0.36	5.87E-01
BB_0099| rsgA| ribosome small subunit-dependent GTPase A	0.02	9.76E-01	-0.14	8.60E-01
BB_0100| murI| glutamate racemase 0100|	0.57	7.88E-02	0.07	9.55E-01
BB_0101| asnS| asparaginyl-tRNA synthetase 0101|	-0.17	7.00E-01	0.24	5.49E-01
BB_0102| hypothetical protein 0102|	-0.16	7.82E-01	0.26	5.63E-01
BB_0103| phosphoribosyl transferase domain protein 0103|	-0.17	7.81E-01	0.23	6.69E-01
BB_0104| periplasmic serine protease DO 0104|	0.49	3.64E-01	0.25	7.31E-01
BB_0105| map| methionine aminopeptidase type I	-0.25	7.15E-01	0.09	9.73E-01
BB_0106| tetratricopeptide repeat domain protein 0106|	-0.80	1.43E-02	-0.43	2.83E-01
BB_0107| nusB| transcription antitermination factor NusB	-0.67	6.89E-02	-0.12	8.97E-01
BB_0108| basic membrane protein 0108|	0.04	9.59E-01	-0.46	1.80E-01
BB_0109| acetyl-CoA acetyltransferases subfamily 0109|	-0.25	5.74E-01	-0.54	1.24E-01
BB_0110| hypothetical protein 0110|	0.07	9.59E-01	-0.17	7.99E-01
BB_0111| dnaB| replicative DNA helicase 0111|	-0.43	3.09E-01	-0.15	8.40E-01
BB_0112| rplI| ribosomal protein L9 0112|	0.14	8.99E-01	0.52	2.91E-01
BB_0113| rpsR| ribosomal protein S18 0113|	0.25	7.00E-01	0.61	2.12E-01
BB_0114| single-stranded DNA-binding protein (SSB)	0.27	6.55E-01	1.12	4.22E-03
BB_0115| 30S ribosomal protein S6 0115|	0.53	2.28E-01	1.22	8.38E-04
BB_0116| pts system glucose-specific iiabc component	0.04	9.59E-01	0.71	1.36E-01
BB_0117| membrane protein 0117|	0.03	9.63E-01	-0.14	8.07E-01
BB_0118| rseP| RIP metalloprotease RseP 0118|	0.00	9.98E-01	-0.25	6.69E-01
BB_0120| uppS| di-transpoly-cis-decaprenylcistransferase	0.27	5.73E-01	-0.35	4.07E-01
BB_0121| frr| ribosome recycling factor 0121|	0.28	5.21E-01	0.02	9.89E-01
BB_0122| tsf| translation elongation factor Ts 0122|	0.42	3.37E-01	0.24	6.62E-01
BB_0123| rpsB| ribosomal protein S2 0123|	0.51	2.73E-01	0.56	2.39E-01
BB_0124| hypothetical protein 0124|	-0.24	7.00E-01	0.24	6.99E-01
BB_0125| hypothetical protein 0125|	0.06	9.59E-01	0.26	6.62E-01
BB_0126| hypothetical protein 0126|	0.24	7.60E-01	0.12	9.38E-01
BB_0127| ribosomal protein S1 0127|	0.33	5.69E-01	0.62	1.87E-01
BB_0128| cmk| cytidylate kinase 0128|	0.45	4.15E-01	0.65	1.99E-01
BB_0129| RNA pseudouridine synthase	-0.79	4.53E-02	-0.38	4.43E-01
BB_0130| hypothetical protein 0130|	-0.60	3.66E-01	-0.64	3.39E-01
BB_0131| recA| protein RecA 0131|	-0.29	6.19E-01	-0.55	2.42E-01
BB_0132| transcription elongation factor GreA	-0.30	6.06E-01	-0.46	3.53E-01
BB_0133| tetratricopeptide repeat domain protein 0133|	0.53	1.30E-01	-0.25	5.78E-01
BB_0134| tetratricopeptide repeat domain protein 0134|	-1.06	3.72E-03	-0.31	5.59E-01
BB_0135| hisS| histidyl-tRNA synthetase 0135|	0.00	9.99E-01	-0.10	9.36E-01
BB_0136| penicillin-binding protein 0136|	-0.14	7.42E-01	-0.20	5.87E-01

BB_0137| long-chain-fatty-acid CoA ligase 0137|	0.85	2.74E-02	-0.18	7.93E-01
BB_0138| hypothetical protein 0138|	0.13	9.59E-01	-1.74	4.75E-03
BB_0139| hypothetical protein 0139|	-0.83	1.48E-02	0.15	8.24E-01
BB_0141| membrane fusion protein 0141|	0.17	7.27E-01	-0.47	1.73E-01
BB_0142| outer membrane efflux protein 0142|	0.61	6.26E-02	-0.75	1.99E-02
BB_0143| hypothetical protein YidD 0143|	0.05	9.61E-01	0.46	5.45E-01
BB_0144| glycine betaine L-proline ABC transporter	0.16	9.11E-01	0.24	7.85E-01
BB_0145| glycine betaine L-proline ABC transporter permease protein	0.41	4.74E-01	0.33	5.89E-01
BB_0146| glycine betaine L-proline ABC transporter ATP-binding protein	0.67	2.49E-01	0.44	5.35E-01
BB_0147| p41 0147|	0.50	3.58E-01	0.21	8.01E-01
BB_0151| nagA| N-acetylglucosamine-6-phosphate deacetylase 0151|	-0.51	3.48E-01	0.35	5.78E-01
BB_0152| nagB| glucosamine-6-phosphate isomerase 0152|	-0.76	5.56E-02	0.08	9.73E-01
BB_0153| superoxide dismutase (Mn) (General stress protein 24)	-0.80	9.16E-02	-0.55	3.14E-01
BB_0154| secA| preprotein translocase SecA subunit 0154|	-0.11	8.62E-01	-0.63	3.91E-02
BB_0155| lipoprotein 0155|	0.25	6.29E-01	0.51	2.12E-01
BB_0156| hypothetical protein 0156|	-0.01	9.94E-01	0.41	4.11E-01
BB_0157| hypothetical protein 0157|	0.31	7.19E-01	0.95	1.02E-01
BB_0158| S2 lipoprotein 0158|	0.20	7.66E-01	0.31	5.80E-01
BB_0159| hypothetical protein 0159|	-0.30	6.60E-01	0.44	4.51E-01
BB_0160| alr| alanine racemase 0160|	0.17	7.00E-01	0.53	8.37E-02
BB_0161| hypothetical protein 0161|	-0.11	9.04E-01	-0.69	5.58E-02
BB_0162| hypothetical protein 0162|	-0.11	9.57E-01	-0.65	2.05E-01
BB_0163| hypothetical protein 0163|	0.65	9.30E-02	-0.24	6.62E-01
BB_0164| K+-dependent Na+/Ca+ exchanger homolog 0164|	-0.52	2.08E-01	-0.53	2.21E-01
BB_0165| hypothetical protein 0165|	-0.66	1.36E-01	-0.87	4.41E-02
BB_0166| malQ| 4-alpha-glucanotransferase 0166|	0.60	2.43E-01	0.02	9.89E-01
BB_0167| outer membrane protein 0167|	-0.16	8.27E-01	-0.93	1.66E-02
BB_0168| DnaK suppressor 0168|	0.23	5.99E-01	-1.09	6.83E-05
BB_0169| infA| translation initiation factor IF-1 0169|	-0.74	1.13E-01	-0.72	1.45E-01
BB_0170| hypothetical protein 0170|	-0.18	8.59E-01	-0.76	1.46E-01
BB_0171| tetratricopeptide repeat domain protein 0171|	0.08	9.59E-01	-0.05	9.89E-01
BB_0172| von Willebrand factor type A domain protein 0172|	-0.33	4.53E-01	-0.33	4.43E-01
BB_0174| hypothetical protein 0174|	-0.67	2.17E-01	-1.08	2.97E-02
BB_0175| hypothetical protein 0175|	-0.75	8.89E-02	-0.81	6.92E-02
BB_0176| ATPase family associated with various cellular activities (AAA)	-0.21	7.26E-01	-0.86	1.86E-02
BB_0177| gidB| 16S rRNA methyltransferase GidB 0177|	-0.82	2.23E-02	-0.67	9.48E-02
BB_0178| gidA| tRNA uridine 5-carboxymethylaminomethyl modification	-0.45	1.69E-01	-0.76	1.10E-02
BB_0179| trmE| tRNA modification GTPase TrmE 0179|	-0.05	9.59E-01	-1.17	9.97E-04
BB_0180| FlbF protein 0180|	0.01	9.84E-01	0.20	6.99E-01
BB_0183| hypothetical protein 0183|	-0.79	9.11E-02	0.22	7.77E-01
BB_0184| csrA| carbon storage regulator 0184|	-1.52	1.85E-03	-0.38	6.06E-01
BB_0185| glycoprotease family 0185|	-0.75	2.07E-01	-0.24	8.07E-01
BB_0186| ATPase YjeE family 0186|	0.40	4.52E-01	0.32	5.81E-01
BB_0187| hypothetical protein 0187|	0.40	4.04E-01	0.14	8.71E-01
BB_0189| rpmI| ribosomal protein L35 0189|	1.10	1.78E-03	0.40	3.96E-01
BB_0190| infC| translation initiation factor IF-3 0190|	0.82	2.83E-02	0.38	4.31E-01
BB_0192| hypothetical protein 0192|	0.17	8.30E-01	-0.72	9.28E-02
BB_0193| lipoprotein 0193|	0.51	4.36E-01	-1.23	1.77E-02
BB_0194| hydrolase TatD family 0194|	-0.04	9.59E-01	-0.60	1.55E-01
BB_0195| TPR domain protein 0195|	-0.12	9.13E-01	-0.59	1.94E-01
BB_0197| protoporphyrinogen oxidase 0197|	0.71	1.04E-01	-0.52	2.92E-01
BB_0198| ((ppGpp)ase)	0.60	1.74E-01	-0.43	3.95E-01
BB_0200| D-alanine--D-alanine ligase	-0.01	9.91E-01	0.97	8.89E-02
BB_0201| UDP-MurNAc-tripeptide synthetase	0.63	1.13E-01	0.65	1.14E-01
BB_0202| hemolysin 0202|	0.52	1.92E-01	-0.04	9.89E-01
BB_0203| hflK| HflK protein 0203|	-0.54	2.37E-01	-0.85	4.17E-02
BB_0204| hflC| HflC protein 0204|	-0.52	3.23E-01	0.11	9.46E-01
BB_0205| hypothetical protein 0205|	-0.09	9.59E-01	0.34	6.01E-01
BB_0206| methyltransferase 0206|	-0.39	6.40E-01	-0.21	8.71E-01
BB_0209| tetratricopeptide repeat domain protein 0209|	0.73	5.11E-02	0.22	7.08E-01
BB_0211| DNA mismatch repair protein MutL 0211|	-1.02	8.26E-04	0.84	1.07E-02
BB_0212| borrelia ORF-A superfamily 0212|	1.09	1.89E-02	0.15	9.07E-01
BB_0213| lipoprotein 0213|	0.94	7.11E-04	-0.20	6.69E-01
BB_0214| efp| translation elongation factor P 0214|	-0.42	4.79E-01	-0.13	9.19E-01

BB_0215| phosphate ABC transporter	0.68	1.67E-02	0.02	9.89E-01
BB_0216| pstC| phosphate ABC transporter permease protein PstC	-0.87	2.18E-03	-0.41	2.61E-01
BB_0217| pstA| phosphate ABC transporter permease protein PstA	-1.17	3.16E-04	-0.28	5.78E-01
BB_0218| pstB| phosphate ABC transporter ATP-binding protein	0.12	9.14E-01	-0.49	2.62E-01
BB_0219| zinc (Zn2+)-iron (Fe2+) permease (ZIP) family	0.31	5.73E-01	-0.58	1.86E-01
BB_0220| alanyl-tRNA synthetase 0220|	-0.49	2.47E-01	-0.06	9.89E-01
BB_0221| flagellar motor switch protein 0221|	0.01	9.82E-01	0.46	2.03E-01
BB_0222| 6-phosphogluconolactonase (6PGL) 0222|	-0.31	5.40E-01	-0.42	3.50E-01
BB_0225| tRNA-dihydrouridine synthase A 0225|	-1.35	1.43E-02	-0.68	3.27E-01
BB_0226| serS| seryl-tRNA synthetase 0226|	-0.45	5.02E-01	-0.80	1.60E-01
BB_0227| hypothetical protein 0227|	0.09	9.59E-01	-0.24	7.69E-01
BB_0228| peptidase M16 inactive domain family 0228|	-0.41	5.48E-01	-0.37	5.81E-01
BB_0229| rpmE| ribosomal protein L31 0229|	0.19	7.97E-01	-0.12	9.27E-01
BB_0230| rho| transcription termination factor Rho 0230|	-0.67	1.20E-01	-0.40	4.43E-01
BB_0231| hypothetical protein 0231|	-0.31	6.40E-01	-0.33	6.03E-01
BB_0232| hbb| small DNA-binding protein Hbb 0232|	-0.25	6.54E-01	-0.66	1.00E-01
BB_0233| rpsT| ribosomal protein S20 0233|	0.18	8.31E-01	-0.68	1.69E-01
BB_0234| hypothetical integral membrane protein 0234|	0.07	9.59E-01	-0.29	7.12E-01
BB_0235| ychF| GTP-binding protein YchF 0235|	-0.02	9.79E-01	-0.10	9.27E-01
BB_0236| tetratricopeptide repeat domain protein 0236|	0.52	1.74E-01	-0.66	8.18E-02
BB_0237| lnt| apolipoprotein N-acyltransferase 0237|	-0.10	9.59E-01	-0.32	6.59E-01
BB_0238| hypothetical protein 0238|	1.16	3.12E-03	0.32	5.81E-01
BB_0239| deoxyguanosine/deoxyadenosine kinase 0239|	-0.14	8.28E-01	-0.14	8.38E-01
BB_0240| glycerol uptake facilitator 0240|	2.58	6.31E-25	-3.04	3.31E-34
BB_0241| glpK| glycerol kinase 0241|	2.32	1.07E-12	-3.12	4.93E-23
BB_0242| hypothetical protein 0242|	2.37	5.89E-10	-3.62	1.25E-22
BB_0243| glycerol-3-phosphate dehydrogenase anaerobic 0243|	2.41	1.30E-10	-2.35	5.13E-10
BB_0244| hypothetical protein 0244|	0.15	8.53E-01	-1.30	3.32E-04
BB_0245| hypothetical protein 0245|	-0.11	9.13E-01	-1.01	3.33E-03
BB_0246| M23 peptidase domain protein 0246|	-0.09	9.50E-01	-1.58	1.12E-06
BB_0247| rdgB| non-canonical purine NTP pyrophosphatase	0.02	9.78E-01	0.07	9.57E-01
BB_0248| pepF| oligoendopeptidase F 0248|	-0.57	8.92E-02	-0.42	2.73E-01
BB_0249| phosphatidyltransferase 0249|	-0.64	9.75E-02	-0.60	1.53E-01
BB_0250| DedA protein 0250|	0.02	9.76E-01	-0.57	1.28E-01
BB_0251| leuS| leucyl-tRNA synthetase 0251|	-1.68	5.65E-05	0.32	6.44E-01
BB_0253| lon| ATP-dependent protease La 0253|	0.92	2.94E-02	0.41	4.51E-01
BB_0254| recJ| single-stranded-DNA-specific exonuclease RecJ 0254|	-0.57	5.05E-01	-1.04	1.36E-01
BB_0255| M23 peptidase domain protein 0255|	-0.45	5.71E-01	-0.97	1.19E-01
BB_0256| rpsU| ribosomal protein S21 0256|	-0.03	9.76E-01	0.05	9.89E-01
BB_0258| undecaprenol kinase 0258|	-0.63	2.39E-01	-1.17	1.45E-02
BB_0259| transglycosylase SLT domain protein 0259|	-0.90	8.06E-02	-0.94	7.87E-02
BB_0260| hypothetical protein 0260|	0.70	2.40E-01	-0.86	1.49E-01
BB_0261| tetratricopeptide repeat domain protein 0261|	0.09	9.59E-01	0.20	8.14E-01
BB_0262| M23 peptidase domain protein 0262|	-0.26	6.10E-01	-0.30	5.27E-01
BB_0263| lepB| signal peptidase I 0263|	-0.53	4.62E-01	-0.57	4.09E-01
BB_0264| heat shock protein 70 0264|	-0.56	1.74E-01	-0.17	8.10E-01
BB_0265| hypothetical protein 0265|	-0.22	7.97E-01	0.13	9.26E-01
BB_0266| hypothetical protein 0266|	0.38	4.79E-01	0.01	9.91E-01
BB_0267| hypothetical protein 0267|	0.75	1.79E-01	0.05	9.89E-01
BB_0268| hypothetical protein 0268|	0.79	1.28E-01	-0.16	9.07E-01
BB_0269| ATP-binding protein 0269|	0.43	2.87E-01	-0.17	7.81E-01
BB_0270| flagellar biosynthesis protein FlhF	-0.83	3.22E-02	-0.54	2.39E-01
BB_0271| flhA| flagellar biosynthesis protein FlhA 0271|	0.05	9.59E-01	-0.61	7.23E-02
BB_0272| flhB| flagellar biosynthetic protein FlhB 0272|	0.98	1.27E-02	0.14	8.81E-01
BB_0273| fliR| flagellar biosynthetic protein FliR 0273|	-1.07	2.51E-02	-0.86	1.03E-01
BB_0274| fliQ| flagellar biosynthetic protein FliQ 0274|	-0.89	1.69E-01	-1.19	5.63E-02
BB_0275| fliP| flagellar biosynthetic protein FliP 0275|	-0.72	2.51E-01	-1.15	4.58E-02
BB_0276| flagellar protein FliZ 0276|	0.04	9.67E-01	-0.83	2.01E-01
BB_0277| flagellar switch protein FliY 0277|	0.24	6.64E-01	-0.09	9.44E-01
BB_0278| fliM| flagellar motor switch protein FliM 0278|	-0.18	7.59E-01	-0.25	6.26E-01
BB_0279| fliL| flagellar basal body-associated protein FliL 0279|	-0.27	6.16E-01	-0.30	5.57E-01
BB_0280| flagellar motor apparatus 0280|	-0.20	7.11E-01	-0.21	6.85E-01
BB_0281| chemotaxis protein MotA (Motility protein A) 0281|	-0.26	5.96E-01	-0.28	5.55E-01
BB_0282| hypothetical protein 0282|	1.01	1.41E-02	0.22	7.63E-01

BB_0283| flagellar hook protein FlgE 0283|	0.03	9.59E-01	0.00	1.00E+00
BB_0284| flgD| flagellar hook capping protein 0284|	0.19	8.40E-01	-0.03	9.89E-01
BB_0285| flagellar protein 0285|	-0.26	7.27E-01	-0.14	9.20E-01
BB_0286| flagellar protein 0286|	-0.05	9.59E-01	0.05	9.89E-01
BB_0287| flagellar protein 0287|	-0.17	8.71E-01	0.14	9.19E-01
BB_0288| fliI| flagellar protein export ATPase FliI 0288|	0.23	7.00E-01	0.03	9.89E-01
BB_0289| flagellar assembly protein FliH 0289|	-0.20	7.59E-01	-0.02	9.89E-01
BB_0290| fliG| flagellar motor switch protein FliG 0290|	-0.45	1.69E-01	-0.23	5.76E-01
BB_0291| fliF| flagellar M-ring protein FliF 0291|	0.01	9.92E-01	-0.35	3.06E-01
BB_0292| fliE| flagellar hook-basal body complex protein (FliE)	0.52	2.02E-01	-0.53	2.12E-01
BB_0293| flgC| flagellar basal-body rod protein FlgC 0293|	0.32	4.44E-01	-0.37	3.43E-01
BB_0294| flgB| flagellar basal-body rod protein FlgB 0294|	0.31	4.87E-01	-0.19	7.34E-01
BB_0295| hslU| heat shock protein HslVU ATPase subunit HslU	-1.06	5.06E-04	1.07	5.71E-04
BB_0296| ATP-dependent protease HslV	-1.20	5.94E-05	0.32	4.57E-01
BB_0297| protein smf 0297|	-0.82	8.47E-03	-0.03	9.89E-01
BB_0298| tetratricopeptide repeat domain protein 0298|	-0.10	9.58E-01	-0.22	7.39E-01
BB_0299| ftsZ| cell division protein FtsZ 0299|	0.56	1.24E-01	0.17	7.69E-01
BB_0300| ftsA| cell division protein FtsA 0300|	0.17	7.96E-01	0.17	7.74E-01
BB_0301| DivIB 0301|	0.23	7.14E-01	0.24	6.94E-01
BB_0302| ftsW| cell division protein FtsW 0302|	-0.84	1.06E-03	-0.48	1.15E-01
BB_0303| mraY| phospho-N-acetylmuramoyl-pentapeptide-transferase	-0.85	5.59E-03	-0.72	3.14E-02
BB_0304| UDP-N-acetylmuramoyl-tripeptide--D-alanyl-D-alanine ligase	-1.08	2.24E-03	-0.68	1.04E-01
BB_0305| hypothetical protein 0305|	-1.52	3.19E-09	-0.03	9.89E-01
BB_0306| mraW| S-adenosyl-methyltransferase MraW 0306|	-1.19	1.11E-06	-0.14	7.69E-01
BB_0307| hypothetical protein 0307|	-0.90	1.73E-03	-0.46	1.98E-01
BB_0308| hypothetical protein 0308|	-0.07	9.59E-01	-0.73	1.14E-01
BB_0309| hypothetical protein 0309|	0.23	6.15E-01	-0.23	6.16E-01
BB_0311| inorganic polyphosphate/ATP-NAD kinase	-0.01	9.94E-01	-0.07	9.79E-01
BB_0312| purine-binding chemotaxis protein 0312|	0.18	6.85E-01	0.29	4.26E-01
BB_0313| rrmJ| ribosomal RNA large subunit methyltransferase J	0.26	5.29E-01	0.40	2.57E-01
BB_0314| octaprenyl-diphosphate synthase 0314|	-0.27	7.33E-01	-0.07	9.89E-01
BB_0315| hypothetical protein 0315|	-0.64	1.85E-01	-0.55	2.88E-01
BB_0316| hypothetical integral membrane protein 0316|	0.05	9.59E-01	-0.90	5.46E-02
BB_0317| hypothetical integral membrane protein 0317|	-0.56	3.11E-01	-1.00	4.20E-02
BB_0318| ABC transporter ATP-binding protein 0318|	-4.22	NA	-4.38	NA
BB_0319| exported protein 0319|	0.11	8.99E-01	-0.66	4.62E-02
BB_0321| hypothetical protein 0321|	-0.17	7.82E-01	-0.80	2.10E-02
BB_0322| hypothetical protein 0322|	0.04	9.59E-01	-0.55	2.76E-01
BB_0323| LysM domain protein 0323|	1.10	1.46E-03	-0.52	2.40E-01
BB_0324| hypothetical protein 0324|	0.05	9.59E-01	-0.78	2.63E-02
BB_0325| hypothetical protein 0325|	-0.39	2.40E-01	-0.10	8.80E-01
BB_0326| tetratricopeptide repeat domain protein	-0.45	3.52E-01	-0.83	4.87E-02
BB_0327| glycerol-3-phosphate O-acyltransferase	0.25	7.14E-01	-0.88	5.35E-02
BB_0328| bacterial extracellular solute-binding protein family 5	0.69	1.13E-01	-0.74	9.52E-02
BB_0330| bacterial extracellular solute-binding protein family 5	-0.16	9.58E-01	-1.75	8.65E-03
BB_0331| Hypothetical protein 0331|	-0.98	3.73E-01	-1.79	6.66E-02
BB_0332| ABC transporter permease protein 0332|	-1.27	3.39E-04	-0.85	3.47E-02
BB_0333| oligopeptide transport system permease protein OppC 0333|	-0.55	3.73E-01	-0.58	3.48E-01
BB_0334| oligopeptide transport ATP-binding protein OppD 0334|	-1.13	2.67E-02	-0.97	7.97E-02
BB_0335| OppF 0335|	-1.00	7.93E-02	-0.68	3.10E-01
BB_0337| eno| phosphopyruvate hydratase 0337|	0.28	7.34E-01	-0.28	7.30E-01
BB_0338| rpsI| ribosomal protein S9 0338|	0.17	8.31E-01	-0.52	2.92E-01
BB_0339| rplM| ribosomal protein L13 0339|	-0.07	9.59E-01	-0.17	7.79E-01
BB_0340| hypothetical protein 0340|	-0.99	4.63E-02	-0.90	9.46E-02
BB_0341| glu-trnagln amidotransferase suBunit b 0341|	-0.63	1.69E-01	-0.77	8.89E-02
BB_0342| glutamyl-tRNA(Gln) amidotransferase subunit A	-0.32	5.87E-01	-0.52	2.79E-01
BB_0343| gatC| glutamyl-tRNA(Gln) amidotransferase C subunit	0.77	3.50E-01	-0.46	6.57E-01
BB_0344| DNA helicase 0344|	-0.20	8.14E-01	-0.96	3.78E-02
BB_0345| hypothetical protein 0345|	0.72	1.69E-01	-0.66	2.43E-01
BB_0346| export chaperone 0346|	0.78	4.22E-02	-0.23	6.95E-01
BB_0347| fibronectin/fibrinogen-binding protein 0347|	0.18	7.82E-01	-0.74	6.14E-02
BB_0348| pyk| pyruvate kinase 0348|	0.04	9.69E-01	0.95	8.12E-02
BB_0349| hypothetical protein 0349|	-0.13	8.27E-01	0.34	3.87E-01
BB_0350| rpmB| ribosomal protein L28 0350|	-0.39	4.50E-01	-0.13	8.98E-01

BB_0351| hypothetical protein 0351|	-0.52	9.35E-02	0.03	9.89E-01
BB_0352| hypothetical protein 0352|	-0.58	9.59E-01	-2.58	6.44E-01
BB_0353| membrane protein 0353|	-0.50	3.46E-01	-0.76	1.22E-01
BB_0354| hypothetical protein 0354|	0.69	1.29E-01	-0.26	6.85E-01
BB_0355| transcription factor 0355|	1.02	2.09E-04	-0.38	3.04E-01
BB_0358| RNA methyltransferase RsmE family 0358|	-0.18	8.40E-01	-0.65	2.12E-01
BB_0360| hypothetical protein 0360|	-1.05	1.33E-04	-0.46	1.92E-01
BB_0361| ATP-binding protein 0361|	-0.40	7.47E-01	0.10	9.89E-01
BB_0362| lgt| prolipoprotein diacylglyceryl transferase 0362|	-1.04	2.30E-05	-0.35	2.92E-01
BB_0363| periplasmic protein 0363|	-1.56	7.24E-11	-0.47	1.42E-01
BB_0364| mgsA| methylglyoxal synthase 0364|	-0.56	2.80E-01	-1.20	6.20E-03
BB_0365| la7| outer surface 22 kda lipoprotein (antigen IpLA7) 0365|	-1.44	NA	-1.51	NA
BB_0366| vacuolar aminopeptidase I 0366|	1.39	2.01E-03	0.55	3.58E-01
BB_0367| phosphotransferase enzyme IIb component 0367|	1.69	4.63E-05	0.46	4.32E-01
BB_0368| glycerol-3-phosphate dehydrogenase	0.40	2.10E-01	-0.63	3.15E-02
BB_0369| ATP-dependent Clp protease subunit A 0369|	-0.82	1.52E-01	-0.73	2.36E-01
BB_0370| tyrS| tyrosyl-tRNA synthetase 0370|	-0.66	2.23E-01	-0.82	1.28E-01
BB_0371| glyS| glycyl-tRNA synthetase 0371|	0.05	9.59E-01	-0.61	2.45E-01
BB_0372| gltX| glutamyl-tRNA synthetase 0372|	-0.17	8.67E-01	-0.56	3.14E-01
BB_0373| P31-23 protein 0373|	0.86	1.39E-01	-0.87	1.55E-01
BB_0374| HD domain protein 0374|	-1.62	7.32E-04	-0.86	1.40E-01
BB_0375| pfs| nucleosidase Pfs protein 0375|	-1.86	9.62E-10	-0.82	2.45E-02
BB_0376| metK| methionine adenosyltransferase 0376|	-1.95	3.76E-08	-0.62	1.99E-01
BB_0377| luxS| S-ribosylhomocysteinase LuxS 0377|	-1.52	4.72E-05	-0.55	2.70E-01
BB_0378| hypothetical protein 0378|	-0.20	7.55E-01	0.04	9.89E-01
BB_0379| protein kinase C1 inhibitor 0379|	0.48	2.20E-01	-0.25	6.19E-01
BB_0380| mgtE| magnesium transporter 0380|	0.45	1.63E-01	-0.55	8.68E-02
BB_0381| trehalase 0381|	-0.07	9.59E-01	-0.65	1.45E-01
BB_0382| bmpB| basic membrane protein B (bmpB) 0382|	0.24	6.62E-01	-0.82	2.44E-02
BB_0383| bmpA| basic membrane protein A (bmpA)	0.53	2.21E-01	-0.54	2.31E-01
BB_0384| bmpC| basic membrane protein C (bmpC) 0384|	1.09	8.45E-06	0.77	4.61E-03
BB_0385| bmpD| basic membrane protein D (bmpD) 0385|	1.25	1.53E-02	0.39	6.16E-01
BB_0386| rpsG| ribosomal protein S7 0386|	0.42	2.63E-01	-0.06	9.83E-01
BB_0387| rpsL| ribosomal protein S12 0387|	0.35	4.20E-01	-0.19	7.23E-01
BB_0388| rpoC| DNA-directed RNA polymerase beta' subunit 0388|	-0.82	6.72E-02	-0.37	5.27E-01
BB_0390| rplL| ribosomal protein L7/L12 0390|	-0.34	6.23E-01	0.13	9.29E-01
BB_0391| ribosomal protein L10 0391|	0.10	9.48E-01	0.15	8.63E-01
BB_0392| rplA| ribosomal protein L1 0392|	0.18	8.07E-01	-0.29	6.08E-01
BB_0393| rplK| ribosomal protein L11 0393|	0.14	8.53E-01	-0.04	9.89E-01
BB_0394| nusG| transcription termination/antitermination factor	0.89	1.76E-02	0.54	2.32E-01
BB_0395| secE| preprotein translocase SecE subunit 0395|	0.92	7.70E-02	0.22	8.28E-01
BB_0396| rpmG| ribosomal protein L33 0396|	0.89	7.02E-02	0.52	3.90E-01
BB_0397| hypothetical protein 0397|	0.39	3.39E-01	0.12	8.90E-01
BB_0398| lipoprotein 0398|	0.21	6.76E-01	0.15	7.94E-01
BB_0399| ankyrin repeat protein 0399|	0.44	9.17E-01	1.14	5.69E-01
BB_0400| hypothetical protein 0400|	-0.98	4.14E-03	0.99	5.46E-03
BB_0401| glutamate transporter 0401|	-0.10	8.67E-01	-0.21	5.91E-01
BB_0402| proS| prolyl-tRNA synthetase 0402|	-0.35	3.70E-01	0.35	3.86E-01
BB_0403| hypothetical protein 0403|	0.44	4.36E-01	-0.30	6.42E-01
BB_0404| hypothetical protein 0404|	-0.75	2.46E-01	0.47	5.45E-01
BB_0405| hypothetical protein 0405|	-0.97	8.82E-01	2.24	5.47E-01
BB_0406| hypothetical protein 0406|	-0.12	8.88E-01	0.42	3.11E-01
BB_0407| manA| mannose-6-phosphate isomerase class I 0407|	0.07	9.59E-01	-0.49	5.33E-01
BB_0408| pts system fructose-specific iiabc component 0408|	-0.58	4.67E-01	-0.65	3.94E-01
BB_0409| hypothetical protein 0409|	-1.88	2.90E-05	-0.99	6.41E-02
BB_0412| membrane protein 0412|	-1.07	1.61E-02	-0.88	6.90E-02
BB_0413| hypothetical integral membrane protein 0413|	0.19	7.07E-01	-0.70	3.48E-02
BB_0414| chemotaxis protein methyltransferase 0414|	-0.57	2.11E-01	0.17	8.27E-01
BB_0415| protein-glutamate methylesterase 0415|	-0.46	2.70E-01	0.78	3.92E-02
BB_0416| pheromone shutdown protein 0416|	-0.82	5.43E-02	-0.56	2.59E-01
BB_0417| adenylate kinase (ATP-AMP transphosphorylase)	-1.36	1.24E-06	-0.08	9.46E-01
BB_0418| hypothetical protein 0418|	-0.76	7.04E-02	0.45	3.69E-01
BB_0419| response regulatory protein 0419|	-0.26	6.64E-01	-0.27	6.41E-01
BB_0420| sensory transduction histidine kinase 0420|	-0.22	6.96E-01	-0.27	5.92E-01

BB_0421| haloacid dehalogenase-like hydrolase 0421|	-0.23	7.66E-01	-0.95	4.17E-02
BB_0422| DNA-3-methyladenine glycosylase 0422|	0.10	9.35E-01	-0.66	7.13E-02
BB_0426| nucleoside 2-deoxyribosyltransferase superfamily 0426|	1.37	6.31E-04	1.00	2.45E-02
BB_0427| hypothetical protein 0427|	0.34	3.96E-01	0.03	9.89E-01
BB_0428| hypothetical protein 0428|	0.46	3.38E-01	0.39	4.57E-01
BB_0429| hypothetical protein 0429|	-0.13	9.59E-01	1.57	3.24E-03
BB_0430| hypothetical protein 0430|	0.79	7.81E-02	0.80	8.66E-02
BB_0431| CobQ/CobB/MinD/ParA nucleotide binding domain	-0.31	6.39E-01	-0.43	4.43E-01
BB_0434| spo0J| stage 0 sporulation protein J 0434|	-0.14	9.35E-01	1.01	4.56E-02
BB_0435| gyrA| DNA gyrase A subunit 0435|	0.60	1.09E-01	0.20	7.34E-01
BB_0436| gyrB| DNA gyrase B subunit 0436|	0.42	4.27E-01	-0.05	9.89E-01
BB_0437| dnaA| chromosomal replication initiator protein DnaA 0437|	-0.68	6.89E-02	-0.24	6.55E-01
BB_0438| dnaN| DNA polymerase III beta subunit 0438|	0.36	6.46E-01	1.76	3.45E-04
BB_0439| hypothetical protein 0439|	-0.02	9.79E-01	1.40	3.19E-04
BB_0440| rpmH| ribosomal protein L34 0440|	0.78	1.29E-01	0.78	1.53E-01
BB_0441| rnpA| ribonuclease P protein component 0441|	0.44	6.30E-01	0.06	9.89E-01
BB_0443| spoiiij-associtated protein 0443|	-0.73	5.59E-02	0.12	9.15E-01
BB_0444| WbnF 0444|	-0.62	5.68E-02	-0.36	3.69E-01
BB_0445| fbaA| fructose-bisphosphate aldolase class II 0445|	1.11	6.27E-03	0.44	4.18E-01
BB_0446| aspS| aspartyl-tRNA synthetase 0446|	-0.90	7.93E-03	0.15	8.36E-01
BB_0447| Na+/H+ antiporter 0447|	-1.36	6.27E-03	-0.75	2.21E-01
BB_0448| phosphocarrier protein HPr 0448|	-1.00	8.28E-02	-0.71	2.83E-01
BB_0449| hypothetical protein 0449|	-0.77	5.05E-02	-0.86	3.14E-02
BB_0450| rpoN| RNA polymerase sigma-54 factor 0450|	-2.22	4.21E-05	-0.17	9.33E-01
BB_0451| chromate transport protein 0451|	-1.47	2.14E-02	-0.35	7.47E-01
BB_0452| chromate transporter superfamily 0452|	-1.63	2.59E-02	-0.54	6.06E-01
BB_0453| transporter small conductance mechanosensitive ion channel	0.04	9.59E-01	-0.41	3.83E-01
BB_0454| lipopolysaccharide biosynthesis-related protein 0454|	0.19	8.98E-01	1.42	1.24E-02
BB_0455| DNA polymerase III delta subunit superfamily 0455|	-0.21	8.80E-01	-0.19	8.97E-01
BB_0456| hypothetical protein 0456|	-0.61	3.51E-01	-0.31	7.24E-01
BB_0457| uvrC| excinuclease ABC C subunit 0457|	-0.67	2.06E-02	-0.22	5.89E-01
BB_0459| tetratricopeptide repeat domain protein 0459|	0.03	9.74E-01	-0.73	2.12E-01
BB_0460| lipoprotein 0460|	0.65	7.91E-02	-0.44	3.11E-01
BB_0461| DNA polymerase III subunits gamma and tau 0461|	-0.75	1.44E-01	-0.76	1.65E-01
BB_0462| efbC| DNA-binding protein ebfC protein 0462|	-0.64	4.20E-02	-0.44	2.34E-01
BB_0463| nucleoside diphosphate kinase (NDK) (NDP kinase)	0.18	7.12E-01	0.01	9.89E-01
BB_0464| hypothetical protein 0464|	0.12	8.40E-01	-0.30	4.18E-01
BB_0465| hypothetical protein 0465|	0.66	1.93E-01	0.52	3.56E-01
BB_0466| ABC transporter ATP-binding protein 0466|	0.05	9.59E-01	0.40	4.37E-01
BB_0467| hypothetical protein 0467|	0.23	8.35E-01	0.31	7.26E-01
BB_0468| hypothetical protein 0468|	-0.06	9.59E-01	-0.49	4.14E-01
BB_0469| lspA| signal peptidase II 0469|	-0.34	6.02E-01	-0.47	4.04E-01
BB_0470| hypothetical protein 0470|	-0.27	6.30E-01	-1.05	4.75E-03
BB_0471| hypothetical protein 0471|	-0.46	3.56E-01	-0.54	2.66E-01
BB_0472| murA| UDP-N-acetylglucosamine 1-carboxyvinyltransferase	-1.02	7.42E-05	0.29	4.32E-01
BB_0473| hypothetical integral membrane protein 0473|	0.26	6.91E-01	-0.59	2.24E-01
BB_0475| lipoprotein 0475|	1.16	5.62E-03	0.12	9.32E-01
BB_0476| tuf| translation elongation factor Tu 0476|	-0.30	6.54E-01	-0.48	3.95E-01
BB_0477| rpsJ| ribosomal protein S10 0477|	-0.24	7.38E-01	-0.61	2.17E-01
BB_0478| rplC| ribosomal protein L3 0478|	-0.25	7.00E-01	-0.61	1.92E-01
BB_0479| rplD| ribosomal protein L4/L1 family 0479|	-0.42	3.89E-01	-0.51	2.79E-01
BB_0480| rplW| ribosomal protein L23 0480|	-0.58	2.52E-01	-0.71	1.55E-01
BB_0481| rplB| ribosomal protein L2 0481|	-0.79	1.20E-01	-0.67	2.35E-01
BB_0482| rpsS| ribosomal protein S19 0482|	-0.62	1.89E-01	-0.67	1.69E-01
BB_0483| rplV| ribosomal protein L22 0483|	-0.73	1.43E-01	-0.61	2.74E-01
BB_0484| rpsC| ribosomal protein S3 0484|	-0.55	2.02E-01	-0.54	2.37E-01
BB_0485| rplP| ribosomal protein L16 0485|	-0.39	4.10E-01	-0.24	6.65E-01
BB_0486| rpmC| ribosomal protein L29 0486|	-0.21	7.33E-01	-0.06	9.89E-01
BB_0487| rpsQ| ribosomal protein S17 0487|	-0.19	7.93E-01	-0.20	7.71E-01
BB_0488| rplN| ribosomal protein L14 0488|	-0.26	7.00E-01	-0.09	9.68E-01
BB_0489| rplX| ribosomal protein L24 0489|	-0.25	7.05E-01	-0.28	6.42E-01
BB_0490| ribosomal L5P family C-terminus protein 0490|	-0.28	6.38E-01	-0.19	7.85E-01
BB_0491| rpsN| ribosomal protein S14p/S29e 0491|	-0.07	9.59E-01	0.18	7.75E-01
BB_0492| rpsH| ribosomal protein S8 0492|	0.03	9.74E-01	0.04	9.89E-01

BB_0493| ribosomal protein L6 0493|	-0.11	9.16E-01	0.04	9.89E-01
BB_0494| rplR| ribosomal protein L18 0494|	-0.13	8.67E-01	-0.23	6.51E-01
BB_0495| rpsE| ribosomal protein S5 0495|	0.23	6.75E-01	-0.13	8.71E-01
BB_0496| ribosomal protein L30 0496|	-0.28	7.33E-01	-0.21	8.22E-01
BB_0497| rplO| ribosomal protein L15 0497|	-0.25	6.70E-01	-0.49	2.87E-01
BB_0498| preprotein translocase SecY subunit 0498|	-0.21	7.00E-01	-0.44	2.79E-01
BB_0499| rpmJ| ribosomal protein L36 0499|	0.60	3.05E-01	0.44	5.26E-01
BB_0500| rpsM| ribosomal protein S13p/S18e 0500|	0.23	7.02E-01	0.25	6.75E-01
BB_0501| rpsK| ribosomal protein S11 0501|	0.02	9.77E-01	-0.21	6.82E-01
BB_0502| rpoA| DNA-directed RNA polymerase alpha subunit 0502|	-0.31	5.45E-01	-0.27	6.07E-01
BB_0503| rplQ| ribosomal protein L17 0503|	-0.01	9.88E-01	-0.11	9.04E-01
BB_0504| hypothetical protein 0504|	-0.14	8.65E-01	-0.61	1.49E-01
BB_0505| hypothetical protein 0505|	-0.43	3.18E-01	-0.73	6.13E-02
BB_0507| hypothetical protein 0507|	-1.08	3.01E-02	-0.50	4.37E-01
BB_0508| engA| ribosome-associated GTPase EngA 0508|	-0.86	3.61E-02	-1.57	2.03E-05
BB_0509| hypothetical protein 0509|	-0.69	6.07E-02	-0.87	1.66E-02
BB_0512| hypothetical protein 0512|	-1.27	1.98E-03	-0.37	5.41E-01
BB_0514| pheT| phenylalanyl-tRNA synthetase beta subunit 0514|	-0.65	2.36E-01	-0.46	4.57E-01
BB_0517| dnaJ| chaperone protein DnaJ 0517|	-0.85	3.89E-01	0.25	8.91E-01
BB_0518| dnaK| chaperone protein DnaK 0518|	-1.24	6.61E-02	-0.18	9.35E-01
BB_0519| grpE| co-chaperone GrpE 0519|	-0.76	1.85E-01	-0.11	9.64E-01
BB_0524| Inositol monophosphatase family protein 0524|	0.58	2.59E-01	-0.45	4.32E-01
BB_0525| hypothetical protein 0525|	0.98	1.98E-03	0.08	9.57E-01
BB_0526| hypothetical protein 0526|	0.31	4.48E-01	-0.40	2.79E-01
BB_0527| transcriptional activator Baf family 0527|	-0.96	2.28E-02	0.01	9.89E-01
BB_0528| aldose reductase 0528|	0.52	1.12E-01	-0.05	9.89E-01
BB_0533| PhnP protein 0533|	0.60	1.07E-01	-0.35	4.45E-01
BB_0534| xth| exodeoxyribonuclease III 0534|	0.92	2.07E-02	-0.10	9.50E-01
BB_0535| hypothetical protein 0535|	1.26	7.76E-04	-0.22	7.42E-01
BB_0536| zinc protease 0536|	0.65	2.83E-02	-0.34	3.59E-01
BB_0537| tetratricopeptide repeat domain protein 0537|	-1.73	1.99E-06	-0.72	1.15E-01
BB_0538| hypothetical protein 0538|	-1.51	6.68E-06	-0.65	1.23E-01
BB_0539| membrane protein 0539|	-0.32	4.88E-01	-0.11	9.07E-01
BB_0540| fusA| translation elongation factor G 0540|	-0.58	1.26E-01	-0.36	4.14E-01
BB_0543| hypothetical protein 0543|	-0.09	9.59E-01	-0.64	1.92E-01
BB_0544| phosphoribosyl pyrophosphate synthetase 0544|	-0.42	3.58E-01	-0.14	8.75E-01
BB_0545| xylulokinase 0545|	-0.39	2.70E-01	-0.64	4.74E-02
BB_0546| hypothetical protein 0546|	0.49	1.99E-01	0.06	9.89E-01
BB_0547| coaE| dephospho-CoA kinase 0547|	-0.45	4.50E-01	0.32	6.20E-01
BB_0548| polA| DNA polymerase I superfamily 0548|	-1.10	7.95E-05	0.53	1.26E-01
BB_0549| hypothetical protein 0549|	-0.79	1.18E-01	0.17	8.78E-01
BB_0550| fliS| flagellar protein FliS 0550|	-0.20	6.40E-01	0.57	5.38E-02
BB_0551| CheY 0551|	0.82	8.23E-03	0.81	1.36E-02
BB_0552| ligA| DNA ligase NAD-dependent 0552|	-0.49	2.80E-01	-0.01	9.91E-01
BB_0554| hypothetical protein 0554|	-0.58	9.22E-02	-0.13	8.44E-01
BB_0555| hypothetical protein 0555|	-1.04	2.54E-03	-0.05	9.89E-01
BB_0556| hypothetical protein 0556|	-0.36	6.02E-01	-0.60	2.92E-01
BB_0557| phosphocarrier protein HPr 0557|	0.21	6.81E-01	-0.13	8.63E-01
BB_0558| ptsP| phosphoenolpyruvate-protein phosphotransferase	0.29	5.23E-01	-0.23	6.26E-01
BB_0559| PTS system glucose-specific IIA component 0559|	0.64	8.06E-02	0.04	9.89E-01
BB_0560| chaperone protein HtpG 0560|	-0.09	9.59E-01	0.06	9.89E-01
BB_0561| gnd| 6-phosphogluconate dehydrogenase decarboxylating	-0.55	4.36E-01	-0.99	9.30E-02
BB_0562| hypothetical protein 0562|	-0.01	9.91E-01	-0.28	5.59E-01
BB_0563| hypothetical protein 0563|	-0.62	3.78E-02	0.69	2.35E-02
BB_0564| hypothetical protein 0564|	-0.01	9.94E-01	0.28	7.18E-01
BB_0565| purine-binding chemotaxis protein 0565|	-0.67	4.46E-02	0.52	1.72E-01
BB_0566| hypothetical protein 0566|	-0.67	4.54E-02	0.33	4.36E-01
BB_0567| chemotaxis histidine kinase 0567|	-0.85	1.51E-03	0.53	9.28E-02
BB_0568| CheB	-0.06	9.59E-01	0.43	2.75E-01
BB_0569| hypothetical protein 0569|	0.10	9.33E-01	0.39	3.53E-01
BB_0570| chemotaxis response regulator 0570|	0.52	4.13E-01	0.92	8.94E-02
BB_0571| uridylate kinase 0571|	-0.95	1.35E-02	0.08	9.72E-01
BB_0572| glycosyl transferase 0572|	0.05	9.59E-01	-0.57	3.06E-02
BB_0574| hypothetical integral membrane protein 0574|	0.79	4.84E-02	-0.34	5.33E-01

BB_0575| pyrG| CTP synthase 0575|	0.33	4.62E-01	0.00	1.00E+00
BB_0576| hypothetical protein 0576|	-0.09	9.59E-01	0.18	7.81E-01
BB_0577| hypothetical protein 0577|	1.29	2.25E-04	0.38	4.49E-01
BB_0578| methyl-accepting chemotaxis protein 0578|	0.02	9.84E-01	0.44	3.13E-01
BB_0579| DNA polymerase III subunit alpha 0579|	-0.47	1.36E-01	0.35	3.31E-01
BB_0580| hypothetical integral membrane protein 0580|	-0.23	5.66E-01	0.23	5.66E-01
BB_0581| recG| ATP-dependent DNA helicase RecG 0581|	-0.80	1.68E-03	0.79	2.64E-03
BB_0582| carboxypeptidase 0582|	0.46	4.85E-01	-0.87	1.09E-01
BB_0583| hypothetical integral membrane protein 0583|	0.26	4.97E-01	-0.78	5.46E-03
BB_0584| hypothetical integral membrane protein 0584|	-0.41	4.74E-01	-1.73	8.49E-06
BB_0585| murD| UDP-N-acetylmuramoylalanine--D-glutamate ligase	0.05	9.59E-01	0.49	3.29E-01
BB_0586| FemA protein 0586|	-1.14	1.68E-03	-0.04	9.89E-01
BB_0587| metG| methionyl-tRNA synthetase 0587|	-0.94	1.39E-02	-0.33	5.46E-01
BB_0588| bgp| MTA/SAH nucleosidase Glycosaminoglycan binding	0.97	4.53E-02	1.09	2.77E-02
BB_0590| ksgA| dimethyladenosine transferase 0590|	-0.87	1.41E-01	-0.65	3.35E-01
BB_0591| competence locus E 0591|	0.27	6.54E-01	0.08	9.72E-01
BB_0592| caax amino protease family 0592|	1.23	3.67E-03	-1.19	8.01E-03
BB_0593| long-chain-fatty-acid CoA ligase 0593|	0.55	2.11E-01	-0.81	5.07E-02
BB_0594| argS| arginyl-tRNA synthetase 0594|	-0.38	4.36E-01	0.09	9.51E-01
BB_0595| hypothetical protein 0595|	-0.48	3.90E-01	-0.53	3.30E-01
BB_0596| methyl-accepting chemotaxis protein 0596|	-0.15	8.45E-01	-0.40	3.79E-01
BB_0597| methyl-accepting chemotaxis protein 0597|	0.55	1.19E-01	0.29	5.32E-01
BB_0598| murB| UDP-N-acetylenolpyruvoylglucosamine reductase	-0.32	4.91E-01	0.57	1.42E-01
BB_0599| cysS| cysteinyl-tRNA synthetase 0599|	0.12	9.32E-01	-0.87	5.23E-02
BB_0600| IPT/TIG domain protein 0600|	-0.13	9.59E-01	-0.36	7.78E-01
BB_0601| glyA| serine hydroxymethyltransferase 0601|	-0.26	5.48E-01	-0.79	9.76E-03
BB_0602| chaperonin 0602|	0.13	8.95E-01	-0.91	1.86E-02
BB_0603| p66| integral outer membrane protein P66 0603|	1.10	1.46E-03	-0.50	2.63E-01
BB_0604| L-lactate permease 0604|	-0.91	1.43E-01	-0.17	9.25E-01
BB_0605| serine-type D-Ala-D-Ala carboxypeptidase 0605|	0.52	7.95E-02	-0.28	4.45E-01
BB_0606| CheD family 0606|	0.45	2.46E-01	0.04	9.89E-01
BB_0607| pcrA| ATP-dependent DNA helicase PcrA 0607|	-0.55	2.81E-01	-0.67	1.94E-01
BB_0608| aminoacyl-histidine dipeptidase 0608|	-0.63	1.76E-01	-0.37	5.25E-01
BB_0610| tig| trigger factor 0610|	-0.01	9.92E-01	0.38	2.61E-01
BB_0611| clpP| ATP-dependent Clp protease proteolytic subunit	-0.22	6.86E-01	0.15	8.23E-01
BB_0612| clpX| ATP-dependent Clp protease ATP-binding subunit	-0.47	3.01E-01	0.04	9.89E-01
BB_0613| lon| ATP-dependent protease La 0613|	-0.33	4.92E-01	-0.27	6.01E-01
BB_0614| hypothetical protein 0614|	0.77	2.35E-01	-0.02	9.89E-01
BB_0615| rpsD| ribosomal protein S4 0615|	0.85	5.46E-03	0.57	1.05E-01
BB_0616| hypothetical integral membrane protein 0616|	0.16	9.04E-01	-0.19	8.42E-01
BB_0617| hypothetical protein 0617|	1.40	7.25E-04	0.75	1.41E-01
BB_0618| cdd| cytidine deaminase 0618|	0.10	9.51E-01	-0.07	9.88E-01
BB_0619| DHH family 0619|	0.26	7.14E-01	0.50	3.63E-01
BB_0620| beta-glucosidase 0620|	0.11	9.06E-01	0.28	5.68E-01
BB_0621| 4-methyl-5 0621|	-0.07	9.59E-01	-0.14	9.49E-01
BB_0622| ackA| acetate kinase 0622|	-0.39	5.67E-01	-0.87	9.64E-02
BB_0623| mfd| transcription-repair coupling factor 0623|	-0.83	1.39E-01	-0.70	2.54E-01
BB_0624| hypothetical protein 0624|	0.88	2.16E-03	-0.39	2.92E-01
BB_0625| N-acetylmuramoyl-L-alanine amidase 0625|	-0.14	8.80E-01	-0.80	4.97E-02
BB_0626| rnmV| ribonuclease M5 0626|	1.48	2.00E-04	1.14	8.37E-03
BB_0628| lipoprotein 0628|	0.09	9.59E-01	-0.10	9.55E-01
BB_0629| pts system fructose-specific iiabc component 0629|	0.72	8.44E-02	0.21	7.49E-01
BB_0630| pfkB| 1-phosphofructokinase 0630|	0.05	9.59E-01	-0.17	8.71E-01
BB_0631| hypothetical protein 0631|	0.86	3.46E-02	-3.52	1.25E-26
BB_0632| recD| exodeoxyribonuclease V alpha subunit 0632|	-0.83	1.20E-01	-0.04	9.89E-01
BB_0633| recB| exodeoxyribonuclease V beta subunit 0633|	-1.44	3.57E-03	0.14	9.38E-01
BB_0635| pncB| nicotinate phosphoribosyltransferase 0635|	-0.95	7.02E-02	-0.49	4.55E-01
BB_0636| zwf| glucose-6-phosphate 1-dehydrogenase 0636|	-0.24	7.00E-01	-1.23	9.97E-04
BB_0637| Na+/H+ antiporter family 0637|	0.28	4.48E-01	-1.05	6.31E-05
BB_0638| Na+/H+ antiporter 0638|	0.48	2.05E-01	-1.48	4.84E-07
BB_0639| spermidine/putrescine ABC transporter	-1.29	1.20E-02	-1.23	2.30E-02
BB_0640| binding-protein-dependent transport systems	-1.71	1.30E-04	-0.69	2.34E-01
BB_0641| putrescine transport system permease protein PotH 0641|	-1.85	2.09E-05	-0.79	1.49E-01
BB_0642| potA| spermidine/putrescine ABC transporter	-1.50	1.31E-03	-0.29	7.26E-01

BB_0643| ylqF| ribosome biogenesis GTP-binding protein YlqF 0643|	0.24	5.99E-01	0.81	7.58E-03
BB_0644| N-acetylmannosamine-6-P epimerase 0644|	-0.69	5.23E-01	-1.18	1.94E-01
BB_0645| pts system iibc components 0645|	-0.30	8.10E-01	-1.18	9.57E-02
BB_0646| hypothetical protein 0646|	0.43	4.04E-01	-0.49	3.39E-01
BB_0647| bosR| Borrelia oxidative stress regulator protein BosR 0647|	0.34	4.15E-01	0.18	7.49E-01
BB_0649| groL| chaperonin GroL 0649|	1.14	1.84E-02	0.90	9.77E-02
BB_0650| hypothetical protein 0650|	0.49	4.33E-01	0.63	2.79E-01
BB_0651| yajC| preprotein translocase YajC subunit 0651|	0.80	9.42E-02	0.43	4.63E-01
BB_0652| secD| protein-export membrane protein SecD 0652|	0.42	3.70E-01	-0.20	7.60E-01
BB_0653| secF| protein-export membrane protein SecF 0653|	0.35	3.90E-01	-0.21	6.72E-01
BB_0654| hypothetical protein 0654|	-0.99	3.17E-03	-0.84	2.20E-02
BB_0655| heat shock protein 0655|	0.00	9.95E-01	-0.26	5.66E-01
BB_0656| oxygen-independent coproporphyrinogen III oxidase	0.81	4.05E-03	-1.05	1.70E-04
BB_0657| rpiA| ribose 5-phosphate isomerase A 0657|	0.61	8.78E-02	-1.36	8.60E-06
BB_0658| phosphoglycerate mutase family protein 0658|	0.08	9.59E-01	1.19	4.18E-03
BB_0659| lysS| lysyl-tRNA synthetase 0659|	-1.03	1.61E-01	-0.83	3.12E-01
BB_0660| era| GTP-binding protein Era 0660|	-0.12	9.39E-01	-0.06	9.89E-01
BB_0661| hypothetical protein 0661|	1.54	4.24E-09	0.65	4.24E-02
BB_0662| hypothetical protein 0662|	1.40	3.36E-04	0.42	4.46E-01
BB_0663| hypothetical protein 0663|	0.82	1.48E-02	-0.01	9.89E-01
BB_0664| lipoprotein 0664|	0.78	4.56E-02	0.79	5.58E-02
BB_0665| hypothetical protein 0665|	1.10	NA	0.64	NA
BB_0666| N-acetylmuramoyl-L-alanine amidase domain protein	0.06	9.84E-01	-1.00	6.33E-01
BB_0667| hypothetical protein 0667|	-0.44	5.59E-01	-0.98	8.89E-02
BB_0668| flagellar filament outer layer protein 0668|	-0.40	3.93E-01	-0.42	3.61E-01
BB_0669| CheA 0669|	-0.80	5.70E-02	-0.38	4.85E-01
BB_0670| purine-binding chemotaxis protein 0670|	-0.75	1.43E-02	0.13	8.38E-01
BB_0671| CheC-like family protein 0671|	-1.08	8.63E-05	0.46	1.94E-01
BB_0672| CheY 0672|	-1.27	6.77E-03	0.08	9.89E-01
BB_0673| hypothetical protein 0673|	-1.01	3.69E-02	-0.24	7.64E-01
BB_0674| membrane protein 0674|	-0.58	6.81E-02	0.14	8.18E-01
BB_0675| hypothetical protein 0675|	-0.87	1.07E-01	-0.60	3.39E-01
BB_0676| phosphoglycolate phosphatase 0676|	-0.26	8.30E-01	-0.65	3.96E-01
BB_0677| rbsA| sugar ABC transporter ATP-binding protein 0677|	-1.03	1.84E-02	-0.83	8.64E-02
BB_0678| ribose/galactose ABC transporter permease protein 0678|	-0.87	4.88E-02	-1.32	1.77E-03
BB_0679| ribose/galactose ABC transporter permease protein 0679|	-1.08	3.91E-02	-1.38	7.69E-03
BB_0680| methyl-accepting chemotaxis protein 0680|	-0.81	4.68E-02	-0.03	9.89E-01
BB_0681| methyl-accepting chemotaxis protein 0681|	-0.89	4.31E-03	-0.26	5.69E-01
BB_0682| trmU| tRNA methyltransferase	-0.71	9.63E-02	-0.52	2.86E-01
BB_0683| hydroxymethylglutaryl-CoA synthase 0683|	-0.35	5.89E-01	0.56	2.92E-01
BB_0684| fni| isopentenyl-diphosphate delta-isomerase type 2 0684|	-0.45	2.93E-01	-0.03	9.89E-01
BB_0685| hydroxymethylglutaryl-CoA reductase degradative 0685|	-0.59	1.61E-01	-0.33	5.25E-01
BB_0686| mvaD| diphosphomevalonate decarboxylase 0686|	0.10	9.19E-01	-0.23	5.98E-01
BB_0687| phosphomevalonate kinase 0687|	0.45	2.70E-01	-0.01	9.89E-01
BB_0688| mvk| mevalonate kinase 0688|	0.70	9.59E-02	0.07	9.85E-01
BB_0689| lipoprotein 0689|	-0.03	9.62E-01	1.41	5.38E-05
BB_0690| napA| neutrophil activating protein A (napA) 0690|	1.74	2.46E-03	1.19	6.87E-02
BB_0691| fusA| translation elongation factor G 0691|	0.91	1.69E-01	1.32	3.50E-02
BB_0693| xylose operon regulatory protein 0693|	0.31	6.02E-01	1.02	1.36E-02
BB_0694| ffh| signal recognition particle protein 0694|	0.00	9.98E-01	0.46	2.74E-01
BB_0695| rpsP| ribosomal protein S16 0695|	0.69	3.07E-01	1.03	1.03E-01
BB_0696| hypothetical protein 0696|	0.94	1.77E-01	1.10	1.15E-01
BB_0697| rimM| 16S rRNA processing protein RimM 0697|	-0.05	9.59E-01	0.47	3.35E-01
BB_0698| trmD| tRNA (guanine-N1)-methyltransferase 0698|	0.14	7.82E-01	0.58	5.54E-02
BB_0699| rplS| ribosomal protein L19 0699|	0.49	2.18E-01	0.59	1.36E-01
BB_0701| hypothetical protein 0701|	0.31	5.37E-01	0.17	7.85E-01
BB_0702| coaD| pantetheine-phosphate adenylyltransferase 0702|	0.09	9.47E-01	0.40	3.05E-01
BB_0703| rpmF| ribosomal protein L32 0703|	-0.06	9.59E-01	0.11	9.12E-01
BB_0704| acpP| acyl carrier protein 0704|	6.37	NA	0.20	NA
BB_0705| rnc| ribonuclease III 0705|	-0.43	2.86E-01	-0.01	9.91E-01
BB_0706| polynucleotide adenylyltransferase 0706|	-0.53	2.20E-01	-0.23	7.04E-01
BB_0707| hypothetical protein 0707|	0.98	3.73E-02	0.32	6.55E-01
BB_0708| hypothetical protein 0708|	0.88	1.50E-01	-1.16	5.43E-02
BB_0709| hypothetical protein 0709|	-0.81	4.67E-02	-0.49	3.25E-01

BB_0712| RNA polymerase sigma factor RpoD (Sigma-70) 0712|	-1.34	3.71E-05	-0.28	5.81E-01
BB_0713| hypothetical protein 0713|	-1.76	6.02E-12	0.17	7.43E-01
BB_0714| tetratricopeptide repeat domain protein 0714|	0.60	1.83E-01	-0.95	2.28E-02
BB_0715| cell division protein FtsA 0715|	0.71	2.74E-02	-0.66	5.46E-02
BB_0716| mreC| rod shape-determining protein MreC 0716|	0.06	9.59E-01	-1.13	4.62E-02
BB_0717| hypothetical integral membrane protein 0717|	-0.03	9.84E-01	-1.71	5.99E-03
BB_0718| penicillin-binding protein 0718|	-0.39	6.54E-01	-1.19	5.02E-02
BB_0719| mrdB| rod shape-determining protein RodA 0719|	-0.49	4.67E-01	-1.41	5.39E-03
BB_0721| pgsA|	-1.06	3.06E-02	-0.84	1.25E-01
BB_0722| hypothetical protein 0722|	-1.27	1.07E-02	-0.81	1.69E-01
BB_0725| lectin 0725|	-0.01	9.86E-01	0.37	3.04E-01
BB_0726| ATP-binding protein 0726|	-0.34	5.65E-01	0.51	3.10E-01
BB_0727| phosphofructokinase 0727|	-0.31	5.30E-01	0.32	5.12E-01
BB_0728| cdr| CoA-disulfide reductase 0728|	-0.86	2.62E-03	0.10	9.12E-01
BB_0729| (na+ or H+) symporter (daacs) family	-0.50	1.46E-01	0.28	5.08E-01
BB_0730| pgi| glucose-6-phosphate isomerase 0730|	-0.93	7.34E-03	0.00	9.99E-01
BB_0731| hypothetical protein 0731|	-1.00	4.26E-02	-0.69	2.32E-01
BB_0732| penicillin-binding protein 0732|	-0.58	1.18E-01	-0.56	1.53E-01
BB_0733| hypothetical protein 0733|	0.32	5.21E-01	-0.11	9.20E-01
BB_0734| Sua5/YciO/YrdC/YwlC family protein 0734|	-1.06	3.41E-03	-0.31	5.57E-01
BB_0735| rare lipoprotein A 0735|	0.23	6.67E-01	-0.09	9.51E-01
BB_0737| histidine phosphokinase/phophatase 0737|	-0.23	7.63E-01	-1.23	4.38E-03
BB_0738| valS| valyl-tRNA synthetase 0738|	-0.34	5.59E-01	-0.84	5.20E-02
BB_0740| hypothetical protein 0740|	-1.72	1.12E-07	-0.70	8.00E-02
BB_0741| groS| chaperonin GroS 0741|	0.22	7.38E-01	0.23	7.19E-01
BB_0742| ABC transporter ATP-binding protein 0742|	-0.06	9.59E-01	-0.25	5.65E-01
BB_0743| hypothetical protein 0743|	-0.46	3.25E-01	-0.38	4.55E-01
BB_0744| p83/100| Borrelia P83/P100 antigen 0744|	0.34	4.45E-01	0.50	2.12E-01
BB_0745| endonuclease III 0745|	0.33	3.17E-01	0.37	2.56E-01
BB_0746| oligopeptide ABC transporter permease protein 0746|	-6.71	3.23E-06	-6.98	1.34E-06
BB_0747| oligopeptide ABC transporter permease protein 0747|	-1.21	6.58E-02	-1.45	2.79E-02
BB_0748| septum formation initiator subfamily 0748|	-0.09	9.59E-01	-0.61	3.54E-01
BB_0749| hypothetical protein 0749|	0.91	5.74E-04	-0.11	8.71E-01
BB_0751| hypothetical protein 0751|	-0.85	4.93E-02	-0.16	8.75E-01
BB_0754| ABC transporter ATP-binding protein 0754|	-1.23	1.22E-04	-0.14	8.62E-01
BB_0755| rnz| ribonuclease Z 0755|	-1.21	1.76E-04	-0.38	3.96E-01
BB_0756| FAD dependent oxidoreductase 0756|	0.39	4.08E-01	0.66	1.02E-01
BB_0757| clpP| Clp protease 0757|	-0.49	3.58E-01	-0.16	8.79E-01
BB_0758| hypothetical protein 0758|	-0.84	2.04E-01	-0.33	7.26E-01
BB_0759| membrane protein 0759|	0.12	9.57E-01	-0.53	3.83E-01
BB_0760| gene 37 protein (Gp37) 0760|	0.10	9.59E-01	-0.42	5.87E-01
BB_0764| sensory transduction histidine kinase 0764|	-1.99	2.86E-07	-0.53	3.39E-01
BB_0765| hypothetical protein 0765|	-1.93	1.64E-04	-0.82	2.10E-01
BB_0766| cvpA| CvpA family protein 0766|	-2.77	1.08E-07	-0.80	2.52E-01
BB_0767| murG|	-2.20	2.90E-05	-0.63	3.95E-01
BB_0768| pyridoxal kinase 0768|	-2.06	5.69E-07	-0.72	1.90E-01
BB_0769| glycoprotease family 0769|	-2.53	1.99E-08	-0.88	1.36E-01
BB_0770| divergent polysaccharide deacetylase superfamily 0770|	-2.12	1.33E-07	-1.65	1.16E-04
BB_0771| rpoS| RNA polymerase sigma factor (rpoS) 0771|	-0.41	5.67E-01	0.58	3.43E-01
BB_0771a| hypothetical protein 0771a|	-1.24	1.52E-02	-0.97	8.68E-02
BB_0772| flagellar P-ring protein (Basal body P-ring protein) 0772|	0.12	8.99E-01	-0.27	6.06E-01
BB_0773| hypothetical protein 0773|	-0.97	1.00E-01	-0.60	3.93E-01
BB_0774| flgG| flagellar basal-body rod protein FlgG 0774|	-0.26	7.00E-01	0.47	3.95E-01
BB_0775| flagellar hook-basal body complex protein 0775|	-0.02	9.78E-01	0.36	3.76E-01
BB_0776| hypothetical protein 0776|	-0.47	5.44E-01	1.45	8.95E-03
BB_0777| apt| adenine phosphoribosyltransferase 0777|	-0.59	4.48E-01	1.50	1.35E-02
BB_0778| rplU| ribosomal protein L21 0778|	0.08	9.46E-01	0.49	1.41E-01
BB_0779| hypothetical protein 0779|	-1.56	6.14E-01	0.79	8.71E-01
BB_0780| rpmA| ribosomal protein L27 0780|	0.39	5.99E-01	1.05	5.20E-02
BB_0781| GTP-binding protein Obg/CgtA 0781|	0.30	6.29E-01	0.86	5.07E-02
BB_0782| nadD| nicotinamide nucleotide adenylyltransferase	-1.20	1.68E-04	0.02	9.89E-01
BB_0783| hypothetical protein 0783|	-1.05	2.38E-03	-0.26	6.40E-01
BB_0784| iojap-like ribosome-associated protein 0784|	-1.06	8.47E-03	-0.47	3.77E-01
BB_0785| spoVG (	2.62	3.67E-27	-6.58	3.38E-167

BB_0786| ribosomal protein L25 Ctc-form 0786|	-0.26	6.29E-01	-0.50	2.48E-01
BB_0787| pth| peptidyl-tRNA hydrolase 0787|	0.00	9.96E-01	-0.28	4.57E-01
BB_0788| tilS| tRNA(Ile)-lysidine synthetase 0788|	0.60	2.09E-01	0.14	8.97E-01
BB_0789| cell division protein FtsH 0789|	0.57	2.30E-01	0.14	8.89E-01
BB_0790| hypothetical protein 0790|	-0.17	8.57E-01	-0.48	3.95E-01
BB_0791| thymidine kinase 0791|	-0.48	1.85E-01	-0.05	9.89E-01
BB_0792| hypothetical protein 0792|	-0.24	6.31E-01	-0.07	9.63E-01
BB_0793| tmk| thymidylate kinase 0793|	0.06	9.59E-01	-0.40	4.67E-01
BB_0795| outer membrane protein 0795|	0.37	2.47E-01	-0.93	4.72E-04
BB_0796| hypothetical protein 0796|	0.14	8.95E-01	-0.87	3.98E-02
BB_0797| mutS| DNA mismatch repair protein MutS 0797|	-0.57	2.78E-01	-0.60	2.73E-01
BB_0798| competence protein F 0798|	-0.85	1.24E-01	-0.87	1.36E-01
BB_0799| hypothetical protein 0799|	0.36	6.18E-01	-0.01	9.89E-01
BB_0800| transcription elongation protein NusA 0800|	0.34	6.32E-01	-0.17	8.76E-01
BB_0801| translation initiation factor IF-2 0801|	-0.19	8.56E-01	-0.41	5.26E-01
BB_0802| rbfA| ribosome-binding factor A 0802|	0.40	5.28E-01	0.29	6.85E-01
BB_0803| truB| tRNA pseudouridine synthase B 0803|	0.15	9.35E-01	0.02	9.89E-01
BB_0804| rpsO| ribosomal protein S15 0804|	0.32	6.33E-01	0.57	2.88E-01
BB_0805| polyribonucleotide nucleotidyltransferase	0.16	8.20E-01	0.19	7.54E-01
BB_0806| lipoprotein 0806|	-0.59	1.92E-01	0.05	9.89E-01
BB_0807| hypothetical integral membrane protein 0807|	-1.51	4.23E-04	0.11	9.52E-01
BB_0808| permease YjgP/YjgQ family 0808|	-1.20	7.37E-03	-0.37	5.66E-01
BB_0809| tgt| queuine tRNA-ribosyltransferase 0809|	-1.09	1.01E-04	0.02	9.89E-01
BB_0810| mviN| integral membrane protein MviN 0810|	-0.71	1.25E-01	-0.16	8.71E-01
BB_0811| hypothetical protein 0811|	-0.55	9.05E-02	0.04	9.89E-01
BB_0812| coaBC|	0.10	9.25E-01	0.60	1.15E-01
BB_0814| panF| sodium/pantothenate symporter 0814|	0.16	8.07E-01	-1.68	1.06E-08
BB_0816| hypothetical protein 0816|	-0.11	8.95E-01	-1.15	7.42E-05
BB_0817| murC| UDP-N-acetylmuramate--alanine ligase 0817|	-0.17	8.95E-01	-1.03	4.69E-02
BB_0818| hypothetical protein 0818|	-0.63	2.47E-01	-0.63	2.76E-01
BB_0819| cytidylate kinase 0819|	-0.47	3.46E-01	-0.64	1.85E-01
BB_0820| rpoZ| DNA-directed RNA polymerase omega subunit	0.14	9.47E-01	0.03	9.89E-01
BB_0821| miaA| tRNA delta(2)-isopentenylpyrophosphate transferase	0.29	6.54E-01	-0.41	4.57E-01
BB_0823| lipoprotein 0823|	0.43	4.37E-01	-0.62	2.19E-01
BB_0824| hypothetical protein 0824|	0.53	1.09E-01	-0.82	8.59E-03
BB_0825| hypothetical protein 0825|	-0.26	5.98E-01	-0.43	2.88E-01
BB_0826| hypothetical protein 0826|	0.11	9.61E-01	0.91	5.76E-01
BB_0827| ATP-dependent helicase HrpA 0827|	-1.00	2.59E-02	-0.26	7.30E-01
BB_0828| topA| DNA topoisomerase I 0828|	-0.29	6.02E-01	-0.14	8.75E-01
BB_0829| Exonuclease SbcD homolog 0829|	-0.64	4.08E-01	-0.78	2.88E-01
BB_0830| exonuclease SbcC 0830|	-1.14	8.93E-02	-0.90	2.34E-01
BB_0831| xylose operon regulatory protein 0831|	0.16	8.31E-01	0.34	5.12E-01
BB_0832| lipoprotein 0832|	-0.58	1.01E-01	-0.45	2.50E-01
BB_0833| ileS| isoleucyl-tRNA synthetase 0833|	-1.23	4.68E-03	-0.35	5.97E-01
BB_0834| ATP-dependent Clp protease subunit C 0834|	-0.46	4.45E-01	-0.23	7.80E-01
BB_0835| phosphomannomutase 0835|	-0.47	6.19E-01	-0.19	9.26E-01
BB_0837| uvrA| excinuclease ABC A subunit 0837|	-1.45	1.37E-04	0.03	9.89E-01
BB_0838| hypothetical protein 0838|	-1.24	3.12E-03	-0.14	9.15E-01
BB_0838a| hypothetical protein 0838a|	-0.26	7.53E-01	-0.11	9.61E-01
BB_0839| hypothetical protein 0839|	0.44	3.18E-01	0.48	2.79E-01
BB_0840| lipoprotein 0840|	0.16	7.96E-01	-0.23	6.41E-01
BB_0841| arcA| arginine deiminase 0841|	1.96	6.87E-12	-0.70	5.02E-02
BB_0842| argF| ornithine carbamoyltransferase 0842|	1.75	6.16E-05	-0.03	9.89E-01
BB_0843| arginine-ornithine antiporter 0843|	1.22	7.99E-07	-0.32	3.57E-01
BB_0844| lipoprotein 0844|	-0.64	4.37E-01	3.12	1.16E-08
BB_0852| type I restriction enzyme r protein n terminus (hsdr_n)	0.07	9.59E-01	0.80	2.09E-02
BB_A0078| lipoprotein A0078|	-0.57	4.31E-01	-0.79	2.29E-01
BB_A03| outer membrane protein A03|	-1.06	2.33E-01	-1.09	2.39E-01
BB_A04| S2 antigen A04|	-0.11	9.56E-01	0.30	6.69E-01
BB_A05| S1 antigen A05|	0.08	9.59E-01	-0.04	9.89E-01
BB_A07| chpAI protein A07|	0.11	9.59E-01	-0.65	5.10E-01
BB_A08| hypothetical protein A08|	1.08	9.39E-03	0.74	1.22E-01
BB_A09| hypothetical protein A09|	0.47	3.50E-01	0.94	3.07E-02
BB_A10| hypothetical protein A10|	-0.02	9.79E-01	0.58	2.42E-01

BB_A11| hypothetical protein A11|	0.51	2.05E-01	0.71	6.26E-02
BB_A12| holin BlyA family A12|	-0.19	9.01E-01	0.65	3.29E-01
BB_A13| hypothetical protein A13|	-0.14	9.35E-01	0.48	4.34E-01
BB_A15| ospA| outer surface protein A (OspA) A15|	0.30	6.91E-01	-0.23	7.93E-01
BB_A16| ospB| outer surface protein B (OspB) A16|	0.51	3.77E-01	-0.11	9.58E-01
BB_A19| borrelia family of unknown function A19|	-0.02	9.76E-01	0.08	9.68E-01
BB_A20| PF-32 protein A20|	-0.39	2.15E-01	-0.25	5.02E-01
BB_A21| PF-49 protein A21|	-0.56	1.59E-01	-0.61	1.37E-01
BB_A23| BppB A23|	0.86	8.97E-03	0.99	2.79E-03
BB_A24| dbpA| decorin-binding protein A A24|	-0.56	7.02E-02	2.81	2.17E-31
BB_A25| dbpB| decorin-binding protein B A25|	-0.83	8.52E-03	2.83	9.13E-27
BB_A30| hypothetical protein A30|	-0.35	7.09E-01	-0.31	7.55E-01
BB_A31| phage terminase pbsx family A31|	-0.92	1.03E-01	-0.62	3.53E-01
BB_A32| hypothetical protein A32|	-0.24	8.31E-01	1.50	5.39E-03
BB_A33| lipoprotein A33|	0.15	9.59E-01	1.29	6.20E-02
BB_A34| bacterial extracellular solute-binding protein family 5	-0.56	2.31E-01	1.98	2.19E-08
BB_A36| lipoprotein A36|	0.06	9.59E-01	2.84	1.85E-16
BB_A37| hypothetical protein A37|	-0.30	8.26E-01	1.48	4.06E-02
BB_A38| phage portal protein HI1409 family A38|	-1.08	1.76E-02	0.02	9.89E-01
BB_A40| lyme disease proteins of unknown function A40|	-1.22	9.17E-04	0.38	4.59E-01
BB_A41| hypothetical protein A41|	-1.32	1.34E-03	0.45	4.20E-01
BB_A42| hypothetical protein A42|	-1.35	1.63E-03	0.37	5.60E-01
BB_A43| hypothetical protein A43|	-0.04	9.63E-01	0.32	6.51E-01
BB_A45| hypothetical protein A45|	-0.51	2.78E-01	0.64	1.70E-01
BB_A46| hypothetical protein A46|	-0.71	7.86E-02	0.67	1.22E-01
BB_A47| hypothetical protein A47|	-0.70	1.94E-01	0.72	1.99E-01
BB_A48| hypothetical protein A48|	-0.49	3.86E-01	0.91	5.84E-02
BB_A49| hypothetical protein A49|	-0.42	6.17E-01	1.10	6.56E-02
BB_A51| hypothetical protein A51|	-0.09	9.59E-01	0.93	1.45E-02
BB_A52| outer membrane protein A52|	-0.66	2.83E-01	-1.16	3.47E-02
BB_A53| Bbs27 protein A53|	-1.35	4.38E-02	-1.51	2.82E-02
BB_A54| hypothetical protein A54|	-0.97	1.15E-01	-1.23	4.17E-02
BB_A57| P45-13 A57|	-0.14	9.59E-01	0.52	5.33E-01
BB_A58| hypothetical protein A58|	-0.73	2.63E-01	-1.99	1.40E-04
BB_A59| hypothetical protein A59|	0.07	9.59E-01	-2.33	7.42E-20
BB_A60| surface lipoprotein P27 A60|	0.42	5.16E-01	-0.91	7.03E-02
BB_A61| hypothetical protein A61|	-0.87	5.27E-02	-0.86	6.69E-02
BB_A62| lp6.6| 6.6 kDa lipoprotein (Lp6.6 protein) A62|	0.61	5.23E-01	0.58	5.41E-01
BB_A64| P35 antigen A64|	1.04	7.54E-02	0.96	1.27E-01
BB_A65| lipoprotein A65|	1.54	5.89E-02	1.07	2.60E-01
BB_A66| outer surface protein A66|	0.24	8.90E-01	1.60	2.27E-02
BB_A68| cspA| (CRASP-1)	0.36	3.72E-01	0.53	1.56E-01
BB_A69| surface protein A69|	0.19	7.80E-01	-0.15	8.71E-01
BB_A73| antigen P35 A73|	0.26	8.31E-01	-1.04	1.37E-01
BB_A74| osm28| outer membrane porin OMS28 A74|	-2.32	8.04E-04	-1.61	4.15E-02
BB_A76| thyX| thymidylate synthase flavin-dependent A76|	-0.73	1.58E-01	-0.90	7.92E-02
BB_B01| acylphosphatase B01|	1.07	3.20E-03	-0.22	7.30E-01
BB_B02| hypothetical protein B02|	0.13	7.97E-01	0.24	5.39E-01
BB_B03| resT| telomere resolvase ResT B03|	1.03	6.93E-03	-0.46	3.50E-01
BB_B04| chbC| chitibiose transporter protein chbC B04|	2.61	7.82E-14	-0.47	3.64E-01
BB_B05| chbA| chitibiose transporter protein chbA B05|	0.86	3.62E-03	0.27	5.35E-01
BB_B06| chbB| chitibiose transporter protein chbB B06|	0.06	9.59E-01	-0.19	8.96E-01
BB_B07| alpha3-beta1 integrin-binding protein B07|	0.05	9.59E-01	-0.40	5.97E-01
BB_B09| lipoprotein B09|	0.68	6.98E-02	1.57	7.71E-07
BB_B10| borrelia ORF-A superfamily B10|	1.24	8.57E-05	0.89	1.07E-02
BB_B12| PF-32 protein B12|	-0.33	3.33E-01	0.02	9.89E-01
BB_B13| plasmid partition protein B13|	-0.11	9.54E-01	0.29	6.77E-01
BB_B14| hypothetical protein B14|	-0.19	8.02E-01	0.14	8.91E-01
BB_B16| oppAIV| oligopeptide ABC transporter OppAIV B16|	0.93	5.27E-02	0.72	1.88E-01
BB_B17| guaB| inosine-5'-monophosphate dehydrogenase B17|	-0.26	6.74E-01	-0.35	5.27E-01
BB_B18| guaA| GMP synthase B18|	-0.33	6.13E-01	-0.65	2.03E-01
BB_B19| ospC| outer surface protein C (OspC) B19|	-0.48	3.61E-01	0.75	1.11E-01
BB_B22| guanine/xanthine permease B22|	0.06	9.59E-01	0.63	2.17E-01
BB_B23| guanine/xanthine permease B23|	-0.78	4.83E-02	-0.50	2.90E-01

BB_B24| hypothetical protein B24|	-1.36	6.65E-05	-0.79	4.56E-02
BB_B25| hypothetical protein B25|	-0.24	7.31E-01	-0.48	3.79E-01
BB_B26| hypothetical protein B26|	0.38	3.20E-01	-0.35	3.95E-01
BB_B27| lipoprotein B27|	-0.08	9.59E-01	-0.69	2.11E-01
BB_B28| ankyrin repeat protein B28|	-0.56	4.75E-01	-0.46	5.81E-01
BB_B29| pts system iibc components B29|	1.29	8.21E-04	0.17	8.41E-01
BB_C01| BBC01 C01|	11.52	5.85E-19	0.95	8.07E-01
BB_C02| borrelia family of unknown function C02|	NA	NA	NA	NA
BB_C03| BBC03 C03|	10.78	2.25E-16	0.00	1.00E+00
BB_C05| BBC05 C05|	9.56	1.85E-12	1.01	8.11E-01
BB_C06| eppA| exported protein A (eppA) C06|	NA	NA	NA	NA
BB_C07| BBC07 C07|	NA	NA	NA	NA
BB_C10| revB| rev protein C10|	NA	NA	NA	NA
BB_C11| BBC11 C11|	NA	NA	NA	NA
BB_D001| lipoprotein D001|	0.44	9.14E-01	1.85	2.24E-01
BB_D0027| hypothetical protein D0027|	0.81	2.84E-01	-0.06	9.89E-01
BB_D0031| hypothetical protein D0031|	0.75	6.62E-01	1.81	1.28E-01
BB_D01| hypothetical protein D01|	0.24	9.33E-01	0.47	7.23E-01
BB_D04| hypothetical protein D04|	0.76	6.46E-01	1.30	3.12E-01
BB_D09| hypothetical protein D09|	-0.31	6.39E-01	1.49	2.49E-04
BB_D10| BBD10 D10|	0.38	6.37E-01	1.58	2.54E-03
BB_D13| hypothetical protein D13|	0.41	6.17E-01	1.84	3.32E-04
BB_D14| borrelia ORF-A superfamily D14|	1.67	5.61E-06	2.15	1.15E-09
BB_D15| BBD15 D15|	-0.61	3.74E-01	1.42	1.12E-02
BB_D18| hypothetical protein D18|	-0.36	7.00E-01	0.07	9.89E-01
BB_D21| CdsM D21|	-0.31	7.15E-01	1.45	5.15E-03
BB_D22| hypothetical protein D22|	-0.86	1.50E-01	1.05	7.13E-02
BB_D24| hypothetical protein D24|	-2.20	4.42E-01	1.74	4.03E-01
BB_E09| protein p23 E09|	-3.64	8.11E-14	-0.59	4.03E-01
BB_E16| bptA| BptA protein E16|	-3.89	2.50E-36	0.25	6.51E-01
BB_E17| hypothetical protein E17|	-3.17	4.16E-23	0.24	6.89E-01
BB_E18| PF-49 protein E18|	-3.90	1.33E-20	-1.41	4.61E-03
BB_E19| PF-32 protein E19|	-4.27	1.40E-26	-1.66	2.93E-04
BB_E20| borrelia family of unknown function E20|	-4.33	5.15E-29	-1.86	1.29E-05
BB_E21| hypothetical protein E21|	-3.79	9.10E-39	-0.95	7.94E-03
BB_E22| pncA| pyrazinamidase/nicotinamidase PncA protein E22|	-4.97	2.44E-03	-0.80	8.07E-01
BB_E31| surface protein E31|	-2.65	1.49E-19	0.59	1.43E-01
BB_F0034| hypothetical protein F0034|	0.87	1.98E-01	0.20	8.97E-01
BB_F0039| hypothetical protein F0039|	-0.35	9.59E-01	-0.47	9.60E-01
BB_F0040| hypothetical protein F0040|	-0.32	9.59E-01	-2.10	4.34E-01
BB_F0041| outer surface protein VlsE1 F0041|	0.52	5.99E-01	0.03	9.89E-01
BB_F01| hypothetical protein F01|	0.00	9.99E-01	0.64	5.49E-01
BB_F02| hypothetical protein F02|	1.30	3.61E-01	-1.19	5.35E-01
BB_F03| RepU F03|	0.78	4.35E-01	-1.08	3.06E-01
BB_F06| hypothetical protein F06|	1.25	4.64E-01	0.54	8.46E-01
BB_F08| hypothetical protein F08|	1.19	3.41E-01	-0.17	9.89E-01
BB_F14| borrelia family of unknown function F14|	0.92	3.39E-01	-2.41	1.00E-02
BB_F17| transmembrane protein F17|	0.91	6.89E-02	-2.08	1.77E-05
BB_F20| BBF20 F20|	-0.50	6.13E-01	-0.72	3.97E-01
BB_F23| PF49 F23|	-1.56	1.33E-02	-2.69	3.03E-06
BB_F24| PF32 F24|	-0.88	1.82E-01	-2.64	5.38E-07
BB_F25| borrelia family of unknown function F25|	0.13	9.59E-01	-2.09	1.46E-04
BB_F26| borrelia ORF-A superfamily F26|	0.90	1.21E-01	-1.77	7.91E-04
BB_G0036| hypothetical protein G0036|	0.79	3.20E-01	0.90	2.52E-01
BB_G01| lipoprotein G01|	-0.88	2.98E-01	1.09	1.91E-01
BB_G02| adenine specific DNA methyltransferase G02|	0.06	9.63E-01	0.13	9.73E-01
BB_G07| borrelia family of unknown function G07|	-0.86	1.09E-01	0.25	7.76E-01
BB_G08| stage 0 sporulation protein J G08|	-1.07	4.02E-02	0.27	7.54E-01
BB_G09| plasmid partition protein G09|	-0.87	1.35E-01	0.56	4.08E-01
BB_G12| hypothetical protein G12|	-0.37	6.56E-01	0.87	1.59E-01
BB_G13| hypothetical protein G13|	-0.46	5.90E-01	1.04	1.09E-01
BB_G14| hypothetical protein G14|	-0.02	9.91E-01	1.25	8.17E-02
BB_G15| hypothetical protein G15|	-0.45	6.80E-01	0.91	2.73E-01
BB_G16| hypothetical protein G16|	0.37	7.00E-01	1.27	3.92E-02

BB_G17| hypothetical protein G17|	0.05	9.59E-01	1.26	1.07E-02
BB_G18| hypothetical protein G18|	0.29	7.56E-01	1.52	4.61E-03
BB_G19| phage terminase G19|	0.12	9.59E-01	1.66	2.63E-03
BB_G20| phage portal protein HI1409 family G20|	0.67	3.50E-01	1.22	4.93E-02
BB_G21| phage terminase large subunit pbsx family G21|	0.46	5.96E-01	0.90	1.94E-01
BB_G22| hypothetical protein G22|	0.41	7.50E-01	1.16	1.92E-01
BB_G23| hypothetical protein G23|	0.60	5.37E-01	1.33	7.47E-02
BB_G24| hypothetical protein G24|	0.52	6.33E-01	1.35	9.21E-02
BB_G25| borrelia orf-D family G25|	0.10	9.59E-01	1.26	1.44E-01
BB_G26| hypothetical protein G26|	1.47	2.80E-01	2.39	4.53E-02
BB_G27| hypothetical protein G27|	0.52	8.29E-01	2.37	5.63E-02
BB_G28| hypothetical protein G28|	0.73	5.29E-01	1.23	1.98E-01
BB_G29| borrelia ORF-A superfamily G29|	0.45	5.47E-01	2.10	1.16E-05
BB_G30| hypothetical protein G30|	0.05	9.66E-01	1.20	1.11E-01
BB_G31| borrelia family of unknown function G31|	-0.14	9.59E-01	1.51	1.03E-02
BB_G32| replicative helicase G32|	-0.86	1.09E-01	1.04	4.87E-02
BB_G33| RepU G33|	0.50	4.83E-01	1.61	1.76E-03
BB_G34| hypothetical protein G34|	0.06	9.59E-01	0.40	4.03E-01
BB_H0042| hypothetical protein H0042|	-0.65	9.59E-01	-0.91	9.33E-01
BB_H02| CdsC H02|	0.37	8.24E-01	0.53	6.85E-01
BB_H04| hypothetical protein H04|	0.65	4.53E-01	1.02	1.81E-01
BB_H05| hypothetical protein H05|	1.22	4.45E-01	1.32	3.88E-01
BB_H06| cspZ| (CRASP-2)	-0.81	1.12E-01	0.75	1.73E-01
BB_H09| type I restriction enzyme r protein n terminus (hsdr_n)	-0.04	9.68E-01	1.62	1.27E-03
BB_H09a| hypothetical protein H09a|	-0.34	7.69E-01	1.40	2.92E-02
BB_H13| RepU H13|	0.30	6.14E-01	0.08	9.73E-01
BB_H17| hypothetical protein H17|	0.87	4.74E-01	0.38	8.46E-01
BB_H26| borrelia ORF-A superfamily H26|	1.24	7.13E-01	0.88	8.38E-01
BB_H27| borrelia family of unknown function H27|	-0.38	6.38E-01	0.44	5.59E-01
BB_H28| PF-32 protein H28|	-0.52	5.66E-01	0.53	5.47E-01
BB_H29| plasmid partition protein H29|	-0.53	4.44E-01	0.56	4.02E-01
BB_H32| antigen P35 H32|	-1.07	6.43E-02	1.61	3.33E-03
BB_H33| adenine deaminase (Adenase) (Adenine aminase) H33|	-0.33	5.33E-01	0.60	1.54E-01
BB_H37| lipoprotein H37|	-1.48	1.62E-02	0.21	8.97E-01
BB_H39| hypothetical protein H39|	1.20	2.20E-01	0.88	4.30E-01
BB_H40| transposase family H40|	0.50	7.66E-01	0.85	5.05E-01
BB_H41| borrelia membrane protein P13 H41|	-0.88	1.98E-01	2.71	1.18E-07
BB_I0044| hypothetical protein I0044|	0.84	1.55E-01	0.78	2.17E-01
BB_I01| hypothetical protein I01|	1.21	9.22E-02	0.14	9.72E-01
BB_I06| mtnN| MTA/SAH nucleosidase I06|	0.10	9.59E-01	0.68	1.76E-01
BB_I12| hypothetical protein I12|	0.19	8.63E-01	0.46	5.06E-01
BB_I15| Borrelia burgdorferi virulent strain associated lipoprotein	0.05	9.70E-01	0.52	6.08E-01
BB_I16| vraA| virulent strain-associated repetitive antigen A	1.19	6.44E-03	0.09	9.73E-01
BB_I18| hypothetical protein I18|	0.08	9.59E-01	-0.91	4.96E-02
BB_I19| BBC01 I19|	0.76	8.40E-01	-0.67	8.78E-01
BB_I20| borrelia family of unknown function I20|	-0.57	2.25E-01	-1.09	8.52E-03
BB_I21| PF-32 protein I21|	-0.92	5.25E-02	-1.08	2.59E-02
BB_I22| PF-49 protein I22|	-1.41	1.72E-02	-1.25	5.23E-02
BB_I26| transporter major facilitator family I26|	1.87	6.99E-01	2.64	5.26E-01
BB_I29| virulent strain associated lipoprotein I29|	0.18	9.04E-01	0.63	3.57E-01
BB_I34| virulent strain associated lipoprotein I34|	1.01	2.21E-01	0.19	9.39E-01
BB_I36| antigen P35 I36|	-0.04	9.78E-01	1.38	4.15E-02
BB_I38| surface antigen I38|	-0.04	9.78E-01	1.32	5.11E-02
BB_I39| surface antigen I39|	-0.57	4.62E-01	0.62	4.09E-01
BB_I41| hypothetical protein I41|	0.41	5.87E-01	1.07	4.90E-02
BB_I42| outer membrane protein I42|	-0.67	2.47E-01	2.28	2.36E-07
BB_J0056| hypothetical protein J0056|	0.45	9.50E-01	0.47	9.37E-01
BB_J0058| hypothetical protein J0058|	0.11	9.59E-01	0.60	5.35E-01
BB_J08| surface protein J08|	1.26	4.38E-02	1.36	3.67E-02
BB_J09| ospD| outer surface protein D (OspD) J09|	-1.69	3.48E-02	-2.21	5.05E-03
BB_J11| hypothetical protein J11|	0.49	4.47E-01	0.69	2.29E-01
BB_J13| hypothetical protein J13|	0.71	3.64E-01	1.11	1.15E-01
BB_J16| plasmid partition protein J16|	-0.52	2.17E-01	0.76	5.40E-02
BB_J17| PF-32 protein J17|	-0.03	9.59E-01	0.76	5.46E-03

BB_J18| borrelia family of unknown function J18|	0.76	1.20E-01	0.72	1.67E-01
BB_J19| borrelia ORF-A superfamily J19|	1.22	7.40E-04	1.25	7.91E-04
BB_J23| tetratricopeptide repeat domain protein J23|	-0.20	8.42E-01	3.24	6.48E-16
BB_J24| hypothetical protein J24|	-0.23	6.89E-01	2.35	4.02E-15
BB_J25| hypothetical protein J25|	0.27	7.16E-01	2.26	1.08E-08
BB_J26| ABC transporter ATP-binding protein J26|	0.69	3.76E-01	3.28	1.05E-09
BB_J27| efflux ABC transporter permease protein J27|	0.11	9.57E-01	2.74	2.41E-12
BB_J28| hypothetical protein J28|	-0.46	2.47E-01	2.61	7.08E-21
BB_J29| hypothetical protein J29|	-0.47	2.56E-01	2.00	5.58E-12
BB_J31| hypothetical protein J31|	0.28	6.64E-01	2.47	5.40E-12
BB_J34| lipoprotein J34|	-0.15	8.99E-01	-0.44	4.57E-01
BB_J36| lipoprotein J36|	-0.39	6.82E-01	1.22	5.63E-02
BB_J37| hypothetical protein J37|	0.42	6.91E-01	0.64	4.52E-01
BB_J41| antigen P35 J41|	-0.29	7.90E-01	0.33	7.30E-01
BB_J42| hypothetical protein J42|	1.56	5.37E-01	0.40	9.68E-01
BB_J43| hypothetical protein J43|	-0.23	7.42E-01	1.88	5.66E-08
BB_J45| lipoprotein J45|	0.30	6.39E-01	2.46	7.46E-12
BB_J46| hypothetical protein J46|	0.06	9.59E-01	1.92	2.81E-10
BB_J47| hypothetical protein J47|	-0.84	6.90E-02	1.19	6.59E-03
BB_J48| hypothetical protein J48|	-0.42	4.88E-01	1.56	1.46E-04
BB_K0058| hypothetical protein K0058|	0.28	8.17E-01	2.27	7.55E-05
BB_K0059| hypothetical protein K0059|	1.65	1.43E-01	1.08	4.25E-01
BB_K01| lipoprotein K01|	-2.16	6.10E-06	-0.26	7.87E-01
BB_K07| lipoprotein K07|	-0.92	2.80E-01	2.98	5.11E-06
BB_K09| hypothetical protein K09|	0.76	6.03E-01	1.07	3.95E-01
BB_K13| hypothetical protein K13|	-0.25	6.91E-01	-0.15	8.75E-01
BB_K15| antigen P35 K15|	-0.58	3.30E-01	-0.31	6.89E-01
BB_K17| adeC| adenine deaminase K17|	-0.98	2.97E-02	1.24	5.39E-03
BB_K19| lipoprotein K19|	0.45	5.13E-01	0.40	5.65E-01
BB_K21| PF-32 protein K21|	0.11	9.59E-01	0.42	5.91E-01
BB_K22| borrelia family of unknown function K22|	-0.08	9.59E-01	0.51	5.33E-01
BB_K23| borrelia ORF-A superfamily K23|	0.42	5.77E-01	0.58	3.69E-01
BB_K24| PF-49 protein K24|	0.87	NA	-0.75	NA
BB_K32| bbk32| fibronectin-binding protein BBK32 K32|	-0.26	5.53E-01	2.19	1.58E-18
BB_K33| hypothetical protein K33|	0.85	4.25E-01	0.36	8.38E-01
BB_K34| hypothetical protein K34|	0.75	1.20E-01	-1.08	2.27E-02
BB_K35| hypothetical protein K35|	1.17	1.29E-01	-2.06	4.57E-03
BB_K40| hypothetical protein K40|	1.71	3.34E-03	0.90	2.12E-01
BB_K41| hypothetical protein K41|	0.55	2.20E-01	-0.17	8.38E-01
BB_K42| hypothetical protein K42|	0.79	6.40E-02	0.77	8.49E-02
BB_K45| immunogenic protein P37 K45|	-0.16	8.14E-01	-0.54	1.86E-01
BB_K47| hypothetical protein K47|	-1.20	3.39E-02	-1.15	5.43E-02
BB_K48| immunogenic protein P37 K48|	-0.45	2.71E-01	2.06	3.57E-12
BB_K49| hypothetical protein K49|	-1.09	4.59E-02	-1.00	9.17E-02
BB_K50| immunogenic protein P37 K50|	-0.37	7.07E-01	0.86	2.39E-01
BB_K52| lipoprotein K52|	1.47	5.68E-05	1.04	9.68E-03
BB_K53| outer membrane protein K53|	-0.90	8.92E-02	2.06	3.95E-06
BB_K54| hypothetical protein K54|	1.04	1.36E-01	2.41	2.72E-05
BB_L01| hypothetical protein L01|	-0.29	6.39E-01	0.53	2.74E-01
BB_L02| hypothetical protein L02|	-0.30	7.15E-01	0.55	3.96E-01
BB_L03| lyme disease proteins of unknown function L03|	-0.32	6.51E-01	0.53	3.62E-01
BB_L04| lyme disease proteins of unknown function L04|	-0.56	4.01E-01	0.35	6.59E-01
BB_L06| hypothetical protein L06|	-0.92	1.02E-01	0.55	4.04E-01
BB_L07| hypothetical protein L07|	-0.31	6.62E-01	0.35	5.81E-01
BB_L08| hypothetical protein L08|	-0.32	6.91E-01	0.33	6.59E-01
BB_L09| hypothetical protein L09|	-0.36	6.44E-01	0.37	6.09E-01
BB_L10| hypothetical protein L10|	-0.70	2.46E-01	0.30	7.23E-01
BB_L11| hypothetical protein L11|	-0.64	2.92E-01	0.29	7.37E-01
BB_L12| hypothetical protein L12|	-0.63	3.18E-01	0.50	4.54E-01
BB_L13| hypothetical protein L13|	-0.78	2.10E-01	0.29	7.48E-01
BB_L14| hypothetical protein L14|	-0.05	9.76E-01	0.42	7.30E-01
BB_L15| hypothetical protein L15|	-0.28	7.12E-01	0.32	6.50E-01
BB_L16| hypothetical protein L16|	-0.74	1.20E-01	0.13	9.19E-01
BB_L17| hypothetical protein L17|	0.13	8.85E-01	0.23	6.80E-01

BB_L18| hypothetical protein L18|	-0.44	5.62E-01	0.51	4.44E-01
BB_L19| hypothetical protein L19|	-0.85	1.84E-02	0.40	3.96E-01
BB_L20| hypothetical protein L20|	-1.17	1.31E-03	0.31	5.67E-01
BB_L21| hypothetical protein L21|	-1.50	1.96E-04	0.36	5.55E-01
BB_L22| hypothetical protein L22|	-1.17	8.35E-04	0.37	4.36E-01
BB_L23| holin BlyA family L23|	-0.46	2.92E-01	0.41	3.65E-01
BB_L24| BlyB L24|	-0.60	1.91E-01	0.25	6.92E-01
BB_L25| 2.9-6 ORF-C L25|	-1.73	9.88E-07	-0.29	6.21E-01
BB_L26| borrelia orf-D family L26|	-1.78	7.92E-08	0.00	9.99E-01
BB_L27| BdrP L27|	0.78	1.40E-01	1.43	2.89E-03
BB_L28| lipoprotein L28|	0.84	1.57E-01	1.93	1.13E-04
BB_L29| 2.9-5 36K%3B minus strand ORF L29|	0.30	6.19E-01	1.06	7.45E-03
BB_L30| BBC01 L30|	0.64	1.46E-01	-0.44	3.92E-01
BB_L31| borrelia family of unknown function L31|	-1.02	2.38E-03	-0.24	6.59E-01
BB_L32| PF-32 protein L32|	-1.11	1.16E-03	-0.97	7.69E-03
BB_L35| BdrO L35|	-0.90	2.46E-02	-0.61	1.96E-01
BB_L36| BppA L36|	0.01	9.92E-01	1.30	4.03E-02
BB_L37| BppB L37|	-0.10	9.59E-01	1.28	1.43E-02
BB_L38| BppC L38|	-0.33	5.94E-01	0.54	2.87E-01
BB_L39| erpA8| ErpA8 protein L39|	0.95	8.95E-02	1.26	2.20E-02
BB_L40| erpB8| ErpB8 protein L40|	0.31	5.99E-01	1.45	1.25E-04
BB_L41| hypothetical protein L41|	-0.82	4.50E-02	0.00	9.97E-01
BB_L42| hypothetical protein L42|	-0.26	7.51E-01	0.55	3.39E-01
BB_L43| phage terminase large subunit pbsx family L43|	-0.21	8.40E-01	0.19	8.71E-01
BB_M01| hypothetical protein M01|	-0.33	5.92E-01	0.49	3.39E-01
BB_M02| hypothetical protein M02|	-0.27	7.54E-01	0.65	2.76E-01
BB_M03| lyme disease proteins of unknown function M03|	-0.43	5.03E-01	0.65	2.34E-01
BB_M04| lyme disease proteins of unknown function M04|	-0.37	4.78E-01	0.54	2.40E-01
BB_M05| lyme disease proteins of unknown function M05|	-0.92	1.14E-01	0.27	7.66E-01
BB_M06| hypothetical protein M06|	-0.40	5.23E-01	0.48	3.94E-01
BB_M07| hypothetical protein M07|	-0.20	8.25E-01	0.24	7.38E-01
BB_M08| hypothetical protein M08|	-0.29	7.14E-01	0.62	2.88E-01
BB_M09| hypothetical protein M09|	-0.01	9.92E-01	0.57	3.66E-01
BB_M10| hypothetical protein M10|	-0.72	3.39E-01	0.47	5.79E-01
BB_M11| hypothetical protein M11|	-0.68	2.64E-01	0.43	5.60E-01
BB_M12| hypothetical protein M12|	-0.64	3.18E-01	0.52	4.37E-01
BB_M13| hypothetical protein M13|	-0.79	2.07E-01	0.31	7.18E-01
BB_M14| hypothetical protein M14|	-1.00	2.11E-01	0.42	6.81E-01
BB_M15| hypothetical protein M15|	-0.15	9.22E-01	0.43	5.18E-01
BB_M16| hypothetical protein M16|	-0.49	3.98E-01	0.27	7.13E-01
BB_M17| hypothetical protein M17|	0.48	2.03E-01	0.09	9.44E-01
BB_M18| hypothetical protein M18|	0.16	9.42E-01	0.60	3.96E-01
BB_M19| hypothetical protein M19|	-0.94	1.17E-02	0.58	1.94E-01
BB_M20| hypothetical protein M20|	-1.39	1.46E-04	0.67	1.37E-01
BB_M21| hypothetical protein M21|	-1.49	2.33E-04	0.42	4.59E-01
BB_M23| holin BlyA family M23|	-0.48	2.55E-01	0.41	3.69E-01
BB_M24| hemolysin accessory protein M24|	-0.38	4.71E-01	0.35	5.24E-01
BB_M25| 2.9-6 ORF-C M25|	-1.39	2.26E-04	0.07	9.85E-01
BB_M26| borrelia orf-D family M26|	-0.78	5.07E-02	0.36	4.76E-01
BB_M27| rev protein M27|	-0.33	4.47E-01	2.72	2.79E-25
BB_M28| lipoprotein M28|	-0.57	1.85E-01	-0.27	6.33E-01
BB_M29| 2.9-5 36K%3B minus strand ORF M29|	0.06	9.59E-01	1.15	7.94E-03
BB_M30| BBC01 M30|	1.16	3.62E-03	0.46	3.95E-01
BB_M31| borrelia family of unknown function M31|	-0.84	3.69E-02	0.19	7.85E-01
BB_M32| PF-32 protein M32|	-0.95	2.23E-02	-0.29	6.39E-01
BB_M33| PF-49 protein M33|	-1.81	2.58E-03	0.27	8.38E-01
BB_M34| BdrK M34|	-1.46	1.98E-03	0.33	6.62E-01
BB_M35| BppA M35|	0.07	9.59E-01	1.28	3.50E-02
BB_M36| BppB M36|	0.03	9.82E-01	1.08	4.57E-02
BB_M37| BppC M37|	0.47	4.79E-01	1.06	4.24E-02
BB_M38| erpK| ErpK protein M38|	1.02	2.49E-01	3.12	6.96E-06
BB_M39| hypothetical protein M39|	0.90	1.56E-02	0.69	9.94E-02
BB_M41| hypothetical protein M41|	0.00	9.98E-01	0.72	2.76E-01
BB_M42| phage terminase large subunit pbsx family M42|	-0.05	9.59E-01	0.58	3.41E-01

BB_N01| hypothetical protein N01|	0.52	2.17E-01	0.50	2.61E-01
BB_N02| hypothetical protein N02|	0.55	2.90E-01	0.46	4.11E-01
BB_N03| lyme disease proteins of unknown function N03|	0.02	9.78E-01	0.48	3.23E-01
BB_N04| lyme disease proteins of unknown function N04|	-0.14	8.53E-01	0.30	5.36E-01
BB_N07| hypothetical protein N07|	-0.14	9.10E-01	0.02	9.89E-01
BB_N08| hypothetical protein N08|	-0.33	7.00E-01	0.33	6.81E-01
BB_N09| hypothetical protein N09|	0.04	9.63E-01	0.09	9.73E-01
BB_N10| hypothetical protein N10|	-0.48	4.45E-01	0.04	9.89E-01
BB_N12| hypothetical protein N12|	-0.79	1.39E-01	0.39	5.55E-01
BB_N14| hypothetical protein N14|	0.23	9.42E-01	0.51	6.92E-01
BB_N15| hypothetical protein N15|	-0.15	9.14E-01	0.25	7.59E-01
BB_N17| hypothetical protein N17|	0.26	6.54E-01	0.21	7.33E-01
BB_N19| hypothetical protein N19|	1.04	1.75E-02	1.45	5.44E-04
BB_N20| hypothetical protein N20|	-0.30	6.46E-01	1.04	1.47E-02
BB_N23| holin BlyA family N23|	0.65	5.72E-01	0.12	9.89E-01
BB_N24| BlyB N24|	-0.60	1.98E-01	0.22	7.54E-01
BB_N25| 2.9-6 ORF-C N25|	-1.11	2.22E-03	0.03	9.89E-01
BB_N26| borrelia orf-D family N26|	0.39	7.12E-01	0.50	5.87E-01
BB_N27| BdrR N27|	1.16	2.08E-02	1.71	3.36E-04
BB_N28| lipoprotein N28|	1.68	1.23E-03	1.38	1.50E-02
BB_N30| BBC01 N30|	0.07	9.59E-01	-1.01	4.83E-03
BB_N31| borrelia family of unknown function N31|	-0.75	3.68E-02	-0.22	6.96E-01
BB_N32| PF-32 protein N32|	-0.82	4.26E-02	-0.59	2.10E-01
BB_N33| PF-49 protein N33|	-1.53	4.75E-03	-0.64	3.74E-01
BB_N34| BdrQ N34|	-1.18	1.35E-02	-0.36	6.10E-01
BB_N35| BppA N35|	0.12	9.59E-01	1.08	7.94E-02
BB_N36| BppB N36|	0.27	7.71E-01	0.45	5.27E-01
BB_N38| erpP| ErpP protein N38|	0.49	5.09E-01	1.01	9.16E-02
BB_N39| erpQ| ErpQ protein N39|	0.45	4.62E-01	1.34	3.17E-03
BB_N41| hypothetical protein N41|	0.02	9.82E-01	-0.32	5.47E-01
BB_N42| hypothetical protein N42|	0.19	8.26E-01	0.46	4.04E-01
BB_N43| phage terminase large subunit pbsx family N43|	-0.22	7.71E-01	0.05	9.89E-01
BB_O01| hypothetical protein O01|	-0.34	5.48E-01	0.61	1.87E-01
BB_O02| hypothetical protein O02|	-0.25	7.82E-01	0.73	2.31E-01
BB_O03| lyme disease proteins of unknown function O03|	-0.31	6.77E-01	0.55	3.50E-01
BB_O04| lyme disease proteins of unknown function O04|	-0.14	9.38E-01	0.82	1.46E-01
BB_O06| hypothetical protein O06|	-0.91	1.11E-01	0.64	3.23E-01
BB_O07| hypothetical protein O07|	-0.34	5.65E-01	0.63	1.86E-01
BB_O08| hypothetical protein O08|	-0.30	7.04E-01	0.61	2.94E-01
BB_O09| hypothetical protein O09|	-0.16	9.13E-01	0.61	3.07E-01
BB_O10| hypothetical protein O10|	-0.79	3.28E-01	0.51	5.76E-01
BB_O11| hypothetical protein O11|	-0.77	2.01E-01	0.55	4.11E-01
BB_O12| hypothetical protein O12|	-0.99	1.19E-01	0.76	2.61E-01
BB_O13| hypothetical protein O13|	-0.67	4.48E-01	0.93	2.13E-01
BB_O14| hypothetical protein O14|	0.40	8.14E-01	0.65	6.00E-01
BB_O15| hypothetical protein O15|	-0.52	3.40E-01	0.41	5.06E-01
BB_O16| hypothetical protein O16|	-0.72	3.09E-01	0.43	5.98E-01
BB_O17| hypothetical protein O17|	-0.64	2.86E-01	0.49	4.57E-01
BB_O18| hypothetical protein O18|	-0.33	7.12E-01	0.16	9.30E-01
BB_O19| hypothetical protein O19|	0.12	9.44E-01	1.76	8.69E-06
BB_O20| hypothetical protein O20|	-0.51	3.76E-01	1.53	3.83E-04
BB_O21| hypothetical protein O21|	-1.42	7.34E-04	0.67	2.04E-01
BB_O22| hypothetical protein O22|	-1.15	1.03E-03	0.38	4.18E-01
BB_O23| holin BlyA family O23|	-0.46	2.82E-01	0.40	3.69E-01
BB_O24| hemolysin accessory protein O24|	0.40	4.33E-01	1.27	5.65E-04
BB_O25| 2.9-7 ORF-C O25|	-0.55	2.43E-01	0.59	2.05E-01
BB_O26| borrelia orf-D family O26|	-1.13	3.56E-04	0.14	8.46E-01
BB_O27| BdrN O27|	0.98	1.35E-02	1.09	7.18E-03
BB_O28| lipoprotein O28|	0.79	1.68E-01	1.44	4.70E-03
BB_O29| 2.9-5 36K%3B minus strand ORF O29|	0.54	2.55E-01	1.25	1.40E-03
BB_O30| BBC01 O30|	0.28	5.38E-01	-0.28	5.27E-01
BB_O31| borrelia family of unknown function O31|	-0.45	2.35E-01	0.23	6.42E-01
BB_O32| PF-32 protein O32|	-0.77	7.04E-02	-0.22	7.51E-01
BB_O33| plasmid partition protein%3B Orf3 O33|	-1.75	8.45E-03	-0.20	9.22E-01

BB_O34| BdrM O34|	-1.40	1.72E-02	-0.04	9.89E-01
BB_O36| BppA O36|	-0.03	9.79E-01	1.29	4.41E-02
BB_O37| BppB O37|	-0.09	9.59E-01	1.28	1.47E-02
BB_O38| BppC O38|	0.47	4.96E-01	1.08	4.24E-02
BB_O39| erpL| ErpL protein O39|	3.78	1.24E-02	5.36	2.11E-04
BB_O40| erpM| ErpM protein O40|	0.89	1.88E-01	2.80	1.14E-07
BB_O43| hypothetical protein O43|	-2.61	1.83E-01	2.11	3.14E-01
BB_O44| phage terminase large subunit pbsx family O44|	-0.39	5.45E-01	0.52	3.69E-01
BB_P01| phage portal protein P01|	-0.29	6.39E-01	0.53	2.79E-01
BB_P02| hypothetical protein P02|	-0.30	7.15E-01	0.55	3.98E-01
BB_P03| lyme disease proteins of unknown function P03|	-0.32	6.54E-01	0.53	3.63E-01
BB_P04| lyme disease proteins of unknown function P04|	-0.56	3.98E-01	0.35	6.58E-01
BB_P06| hypothetical protein P06|	-0.92	1.02E-01	0.56	4.01E-01
BB_P07| hypothetical protein P07|	-0.31	6.54E-01	0.37	5.58E-01
BB_P08| hypothetical protein P08|	-0.35	6.39E-01	0.32	6.66E-01
BB_P09| hypothetical protein P09|	-0.35	6.54E-01	0.41	5.59E-01
BB_P10| hypothetical protein P10|	-0.69	2.52E-01	0.30	7.28E-01
BB_P11| hypothetical protein P11|	-0.65	2.81E-01	0.29	7.30E-01
BB_P12| hypothetical protein P12|	-0.65	2.94E-01	0.48	4.67E-01
BB_P13| hypothetical protein P13|	-0.88	1.45E-01	0.33	6.85E-01
BB_P14| hypothetical protein P14|	-0.19	9.54E-01	0.36	7.80E-01
BB_P15| hypothetical protein P15|	-0.28	7.15E-01	0.32	6.55E-01
BB_P16| hypothetical protein P16|	-0.73	1.20E-01	0.13	9.12E-01
BB_P17| hypothetical protein P17|	0.12	9.13E-01	0.23	6.91E-01
BB_P18| hypothetical protein P18|	-0.39	6.19E-01	0.52	4.29E-01
BB_P19| hypothetical protein P19|	-0.64	1.60E-01	0.55	2.63E-01
BB_P20| hypothetical protein P20|	-1.39	1.46E-04	0.48	3.14E-01
BB_P21| hypothetical protein P21|	-1.55	1.33E-04	0.35	5.65E-01
BB_P22| hypothetical protein P22|	-1.15	1.07E-03	0.38	4.32E-01
BB_P23| blyA1| holin protein (BlyA1) P23|	-0.46	2.73E-01	0.40	3.69E-01
BB_P24| blyB1| hemolysin accessory protein P24|	-0.84	7.46E-02	0.16	8.83E-01
BB_P25| 2.9-7 ORF-C P25|	-1.49	1.63E-03	-0.21	8.31E-01
BB_P26| borrelia orf-D family P26|	-1.38	4.75E-03	-0.62	3.31E-01
BB_P27| revA1| surface protein (RevA1) P27|	-0.35	3.95E-01	2.63	1.04E-23
BB_P28| mlpA| surface protein mlp lipoprotein family P28|	-0.58	1.74E-01	-0.20	7.69E-01
BB_P29| 2.9-5 36K%3B minus strand ORF P29|	0.32	5.67E-01	1.10	4.18E-03
BB_P30| BBC01 P30|	0.32	4.79E-01	-0.79	2.25E-02
BB_P31| borrelia family of unknown function P31|	-1.58	1.27E-04	-0.81	1.03E-01
BB_P32| PF-32 protein P32|	-2.93	8.85E-07	-1.12	1.42E-01
BB_P33| PF-49 protein P33|	-2.88	8.57E-08	-0.91	2.05E-01
BB_P34| BdrA P34|	-2.23	3.07E-06	-0.90	1.37E-01
BB_P35| bppA1| BppA protein P35|	-0.25	8.27E-01	1.01	1.07E-01
BB_P36| bppB1| BppB protein P36|	-0.58	2.78E-01	0.43	4.61E-01
BB_P37| bppC1| site-specific recombinase phage integrase family	-0.44	4.05E-01	0.42	4.32E-01
BB_P38| erpA| ErpA protein P38|	0.95	9.26E-02	1.25	2.28E-02
BB_P39| erpB1| ErpB1 protein P39|	0.31	6.02E-01	1.45	1.25E-04
BB_P40| hypothetical protein P40|	-0.83	3.78E-02	0.03	9.89E-01
BB_P41| hypothetical protein P41|	-0.25	7.57E-01	0.55	3.43E-01
BB_P42| phage terminase large subunit pbsx family P42|	-0.10	9.59E-01	0.27	7.85E-01
BB_Q0091| hypothetical protein Q0091|	0.00	9.98E-01	0.86	4.07E-01
BB_Q03| outer membrane protein Q03|	-1.28	6.03E-03	1.93	7.35E-06
BB_Q05| antigen P35 Q05|	-0.19	8.24E-01	0.13	9.22E-01
BB_Q06| borrelia membrane protein P13 Q06|	-1.19	1.62E-02	-0.06	9.89E-01
BB_Q07| plasmid partition protein Q07|	-0.03	9.68E-01	-0.05	9.89E-01
BB_Q08| PF-32 protein Q08|	-1.84	5.68E-01	0.14	9.89E-01
BB_Q09| borrelia family of unknown function Q09|	-1.88	1.34E-03	-0.19	9.03E-01
BB_Q12| lyme disease proteins of unknown function Q12|	-0.68	2.20E-01	0.35	6.03E-01
BB_Q13| hypothetical protein Q13|	-0.40	5.26E-01	0.50	3.86E-01
BB_Q14| hypothetical protein Q14|	-5.02	4.38E-02	-0.55	9.51E-01
BB_Q15| hypothetical protein Q15|	-0.12	9.59E-01	0.59	5.36E-01
BB_Q17| hypothetical protein Q17|	-0.38	7.45E-01	0.60	5.14E-01
BB_Q18| hypothetical protein Q18|	-0.81	2.00E-01	0.29	7.64E-01
BB_Q19| hypothetical protein Q19|	-0.43	7.15E-01	0.77	3.95E-01
BB_Q20| hypothetical protein Q20|	-0.83	2.41E-01	0.33	7.30E-01

BB_Q21| hypothetical protein Q21|	0.42	8.80E-01	1.37	3.32E-01
BB_Q22| hypothetical protein Q22|	-0.59	3.25E-01	0.27	7.39E-01
BB_Q23| hypothetical protein Q23|	-1.23	3.68E-02	0.04	9.89E-01
BB_Q24| hypothetical protein Q24|	-0.21	7.97E-01	0.25	7.26E-01
BB_Q25| hypothetical protein Q25|	-0.23	8.14E-01	0.28	7.47E-01
BB_Q26| hypothetical protein Q26|	-1.08	3.34E-03	0.57	2.07E-01
BB_Q27| hypothetical protein Q27|	-1.42	1.01E-04	0.65	1.42E-01
BB_Q28| hypothetical protein Q28|	-1.77	2.90E-05	0.27	7.14E-01
BB_Q29| hypothetical protein Q29|	-2.40	2.53E-13	0.48	2.91E-01
BB_Q30| holin BlyA family Q30|	-1.09	1.63E-02	0.67	1.98E-01
BB_Q31| hemolysin accessory protein Q31|	-1.24	1.98E-03	0.42	4.35E-01
BB_Q32| 2.9-6 ORF-C Q32|	-1.55	3.41E-05	0.04	9.89E-01
BB_Q33| borrelia orf-D family Q33|	-1.99	2.45E-10	0.08	9.63E-01
BB_Q34| BdrW Q34|	-0.31	4.97E-01	0.98	2.84E-03
BB_Q35| MlpJ Q35|	0.24	7.26E-01	0.77	9.17E-02
BB_Q37| 2.9-5 36K%3B minus strand ORF Q37|	0.03	NA	-0.11	NA
BB_Q38| BBC01 Q38|	-0.42	2.92E-01	-0.40	3.47E-01
BB_Q39| borrelia family of unknown function Q39|	-1.13	3.07E-04	-0.36	3.98E-01
BB_Q40| PF-32 protein Q40|	-2.72	3.41E-08	-0.44	5.85E-01
BB_Q42| BdrV Q42|	-0.92	4.00E-02	-0.48	3.94E-01
BB_Q43| BppA Q43|	-0.11	9.59E-01	1.12	6.16E-02
BB_Q44| BppB Q44|	-0.96	1.43E-01	0.79	2.34E-01
BB_Q45| BppC Q45|	-0.65	2.87E-01	0.25	7.81E-01
BB_Q47| erpX| ErpX protein Q47|	-0.30	8.10E-01	4.06	1.99E-13
BB_Q48| hypothetical protein Q48|	-1.71	4.88E-05	0.04	9.89E-01
BB_Q49| hypothetical protein Q49|	-1.53	6.43E-04	-0.02	9.89E-01
BB_Q50| phage terminase large subunit pbsx family Q50|	-1.02	8.92E-02	0.12	9.72E-01
BB_Q52| hypothetical protein Q52|	-0.12	9.59E-01	0.52	4.43E-01
BB_Q53| hypothetical protein Q53|	-0.43	5.16E-01	0.50	4.03E-01
BB_Q54| hypothetical protein Q54|	-0.33	6.15E-01	0.59	2.67E-01
BB_Q62| hypothetical protein Q62|	-2.88	2.09E-05	-2.09	4.37E-03
BB_Q67| adenine specific DNA methyltransferase Q67|	-1.73	1.78E-03	-0.01	9.89E-01
BB_Q85| hypothetical protein Q85|	0.76	6.46E-01	1.30	3.12E-01
BB_Q88| CdsC Q88|	0.15	9.59E-01	0.37	8.01E-01
BB_Q89| hypothetical protein Q89|	0.44	9.13E-01	1.91	2.01E-01
BB_R01| hypothetical protein R01|	-0.20	8.14E-01	0.41	4.58E-01
BB_R03| lyme disease proteins of unknown function R03|	-0.56	3.34E-01	0.62	2.83E-01
BB_R04| lyme disease proteins of unknown function R04|	-0.38	5.62E-01	0.19	8.41E-01
BB_R05| lyme disease proteins of unknown function R05|	-1.03	4.08E-02	0.56	3.39E-01
BB_R06| hypothetical protein R06|	-0.80	9.05E-02	0.39	5.21E-01
BB_R07| hypothetical protein R07|	-0.44	4.53E-01	0.28	6.89E-01
BB_R08| hypothetical protein R08|	-0.41	6.62E-01	0.50	5.42E-01
BB_R09| hypothetical protein R09|	-0.33	6.82E-01	0.44	5.27E-01
BB_R10| hypothetical protein R10|	-0.46	5.30E-01	0.12	9.60E-01
BB_R11| hypothetical protein R11|	-0.45	5.38E-01	0.41	5.76E-01
BB_R12| hypothetical protein R12|	-0.65	3.11E-01	0.61	3.52E-01
BB_R13| hypothetical protein R13|	-0.88	1.84E-01	0.36	6.85E-01
BB_R14| hypothetical protein R14|	-0.13	9.59E-01	0.59	6.99E-01
BB_R15| hypothetical protein R15|	-0.37	5.80E-01	0.29	6.75E-01
BB_R16| hypothetical protein R16|	-0.59	3.98E-01	0.13	9.53E-01
BB_R17| hypothetical protein R17|	0.46	2.15E-01	0.13	8.62E-01
BB_R18| hypothetical protein R18|	-0.54	4.74E-01	-0.02	9.89E-01
BB_R19| hypothetical protein R19|	-0.93	1.24E-02	0.60	1.68E-01
BB_R20| hypothetical protein R20|	-1.24	5.60E-04	0.63	1.45E-01
BB_R21| hypothetical protein R21|	-1.41	4.76E-04	0.55	2.90E-01
BB_R22| hypothetical protein R22|	-1.52	3.25E-06	0.34	4.59E-01
BB_R23| holin BlyA family R23|	-1.12	1.52E-02	0.64	2.34E-01
BB_R24| hemolysin accessory protein R24|	-0.86	7.02E-02	0.14	9.20E-01
BB_R25| 2.9-6 ORF-C R25|	-1.50	6.35E-05	0.05	9.89E-01
BB_R26| borrelia orf-D family R26|	-1.41	4.85E-05	0.26	6.55E-01
BB_R27| BdrH R27|	1.19	4.93E-03	1.10	1.49E-02
BB_R28| lipoprotein R28|	1.43	2.82E-03	0.78	1.86E-01
BB_R29| 2.9-5 36K%3B minus strand ORF R29|	-0.47	5.08E-01	1.09	4.51E-02
BB_R31| BBC01 R31|	0.33	4.59E-01	-0.68	5.77E-02

BB_R32| borrelia family of unknown function R32|	-1.04	6.44E-03	-0.09	9.64E-01
BB_R33| PF-32 protein R33|	-1.58	6.65E-05	-0.29	6.55E-01
BB_R34| PF-49 protein R34|	-1.57	9.06E-04	-0.21	8.45E-01
BB_R36| BppA R36|	-0.07	9.59E-01	1.05	8.39E-02
BB_R37| BppB R37|	-0.23	8.65E-01	0.61	4.10E-01
BB_R38| BppC R38|	-0.01	9.92E-01	0.43	5.92E-01
BB_R41| borrelia outer surface protein E R41|	-0.08	9.59E-01	0.84	4.06E-02
BB_R42| erpY| ErpY protein R42|	0.09	9.59E-01	0.92	1.13E-02
BB_R43| hypothetical protein R43|	0.06	9.59E-01	0.08	9.83E-01
BB_R44| hypothetical protein R44|	-0.20	8.07E-01	1.05	1.47E-02
BB_R45| phage terminase large subunit pbsx family R45|	-0.61	1.69E-01	0.48	3.39E-01
BB_S01| hypothetical protein S01|	-0.05	9.59E-01	0.57	2.76E-01
BB_S02| hypothetical protein S02|	-0.25	7.97E-01	0.61	3.40E-01
BB_S03| lyme disease proteins of unknown function S03|	-0.31	6.79E-01	0.55	3.52E-01
BB_S04| lyme disease proteins of unknown function S04|	0.01	9.92E-01	0.79	2.05E-01
BB_S06| hypothetical protein S06|	-0.91	1.01E-01	0.54	4.09E-01
BB_S07| hypothetical protein S07|	-0.30	6.62E-01	0.41	4.97E-01
BB_S08| hypothetical protein S08|	-0.35	6.40E-01	0.31	6.80E-01
BB_S09| hypothetical protein S09|	-0.14	9.35E-01	0.52	3.99E-01
BB_S10| hypothetical protein S10|	-0.62	3.25E-01	0.33	6.75E-01
BB_S11| hypothetical protein S11|	-0.65	2.81E-01	0.29	7.30E-01
BB_S12| hypothetical protein S12|	-0.61	3.39E-01	0.52	4.37E-01
BB_S13| hypothetical protein S13|	-0.77	2.20E-01	0.31	7.23E-01
BB_S14| hypothetical protein S14|	-0.12	9.59E-01	0.39	7.51E-01
BB_S15| hypothetical protein S15|	-0.37	5.92E-01	0.27	7.30E-01
BB_S16| hypothetical protein S16|	-0.86	1.24E-01	0.12	9.51E-01
BB_S17| hypothetical protein S17|	0.16	8.33E-01	0.24	6.85E-01
BB_S18| hypothetical protein S18|	-0.39	6.31E-01	0.51	4.52E-01
BB_S19| hypothetical protein S19|	-0.63	1.69E-01	0.55	2.62E-01
BB_S20| hypothetical protein S20|	-1.42	1.13E-04	0.48	3.11E-01
BB_S21| hypothetical protein S21|	-1.28	1.34E-03	0.30	6.26E-01
BB_S23| holin BlyA family S23|	-0.47	2.77E-01	0.41	3.73E-01
BB_S24| hemolysin accessory protein S24|	-0.86	6.80E-02	0.14	9.19E-01
BB_S25| 2.9-6 ORF-C S25|	-1.50	5.82E-05	-0.09	9.58E-01
BB_S26| borrelia orf-D family S26|	-1.29	5.02E-04	0.02	9.89E-01
BB_S27| Bbs27 protein S27|	-0.70	6.20E-01	0.36	8.62E-01
BB_S29| bdrF| KID repeat protein S29|	0.82	5.11E-02	1.29	9.81E-04
BB_S30| lipoprotein S30|	0.97	1.41E-01	1.38	3.03E-02
BB_S31| 2.9-5 36K%3B minus strand ORF S31|	0.38	4.50E-01	1.05	6.05E-03
BB_S33| BBC01 S33|	0.52	1.50E-01	-0.67	5.58E-02
BB_S34| borrelia family of unknown function S34|	-0.38	3.11E-01	-0.32	4.27E-01
BB_S35| PF-32 protein S35|	-0.19	7.69E-01	-0.48	2.74E-01
BB_S37| BdrE S37|	-0.27	6.29E-01	-0.50	2.76E-01
BB_S38| BppA S38|	0.10	9.59E-01	1.11	6.27E-02
BB_S39| BppB S39|	0.06	9.59E-01	0.87	1.94E-01
BB_S40| BppC S40|	0.08	9.59E-01	0.46	5.69E-01
BB_S41| erpG| ErpG protein S41|	0.70	1.23E-01	2.06	1.95E-08
BB_S42| bapA| BapA protein S42|	0.87	6.61E-02	2.34	2.54E-09
BB_S44| hypothetical protein S44|	0.33	7.69E-01	0.85	2.79E-01
BB_S45| phage terminase large subunit pbsx family S45|	-0.18	8.63E-01	0.58	3.11E-01
BB_T0008| Borrelia ORF-A superfamily protein T0008|	0.50	5.32E-01	0.51	5.14E-01
BB_T01| hypothetical protein T01|	0.62	4.73E-01	0.52	5.67E-01
BB_T02| hypothetical protein T02|	0.00	1.00E+00	1.01	9.77E-01
BB_T03| hypothetical protein T03|	1.21	5.89E-01	0.53	8.97E-01
BB_T06| Sua5/YciO/YrdC/YwlC family protein T06|	-0.52	6.62E-01	-0.34	8.22E-01
BB_T07| outer membrane protein T07|	-0.13	9.59E-01	1.57	2.87E-01
BB_U01| hypothetical protein U01|	0.69	3.39E-01	0.57	4.57E-01
BB_U02| hypothetical protein U02|	0.94	7.45E-03	0.40	3.95E-01
BB_U04| BBC01 U04|	0.49	5.13E-01	0.38	6.41E-01
BB_U05| PF-32 protein U05|	-0.21	8.35E-01	0.18	8.75E-01
BB_U06| plasmid partition protein U06|	0.22	8.36E-01	1.19	3.20E-02
BB_U07| BBC01 U07|	-0.08	9.59E-01	0.92	2.25E-02
BB_U08| SUA5 domain subfamily U08|	-0.42	7.39E-01	0.88	3.05E-01
BB_U09| TM2 domain family U09|	0.31	8.07E-01	0.59	5.11E-01

BB_U10| BBC01 U10|	-1.17	6.64E-01	-0.59	8.87E-01
BB_U11| Sua5/YciO/YrdC/YwlC family protein U11|	-0.49	6.81E-01	0.01	9.97E-01
EBG00001182576| tRNA G00001182576	0.54	7.11E-01	-0.80	5.59E-01
EBG00001182577| tRNA G00001182577	-0.02	9.88E-01	-0.13	9.37E-01
EBG00001182578| tRNA G00001182578	1.25	2.49E-01	0.78	5.59E-01
EBG00001182579| 5_8S_rRNA| biotype=rRNA	0.18	9.59E-01	-0.57	8.66E-01
EBG00001182580| tRNA G00001182580	0.44	6.46E-01	-0.55	5.45E-01
EBG00001182581| Bacteria_small_SRP| biotype=ncRNA	-0.08	9.59E-01	-0.60	4.36E-01
EBG00001182582| tRNA G00001182582	0.00	9.98E-01	0.22	7.81E-01
EBG00001182583| tRNA G00001182583	-2.13	NA	-2.45	NA
EBG00001182584| tRNA G00001182584	-1.12	1.70E-02	-0.14	9.14E-01
EBG00001182585| tRNA G00001182585	1.41	4.01E-02	-0.95	2.50E-01
EBG00001182586| tRNA G00001182586	0.33	7.11E-01	-1.71	4.75E-03
EBG00001182587| 5_8S_rRNA| biotype=rRNA	0.18	9.59E-01	-0.57	8.66E-01
EBG00001182588| tRNA G00001182588	0.66	2.82E-01	-0.05	9.89E-01
EBG00001182589| tRNA G00001182589	0.13	9.59E-01	-1.44	2.92E-01
EBG00001182590| tRNA G00001182590	-0.32	9.59E-01	-0.28	9.73E-01
EBG00001182591| 5S_rRNA| biotype=rRNA	0.15	9.59E-01	-0.56	6.76E-01
EBG00001182592| PK-G12rRNA| biotype=rRNA	0.21	9.59E-01	0.28	9.83E-01
EBG00001182593| PK-G12rRNA| biotype=rRNA	0.22	9.59E-01	0.05	9.89E-01
EBG00001182594| LSU_rRNA_bacteria| biotype=rRNA	0.54	8.67E-01	1.65	3.53E-01
EBG00001182595| LSU_rRNA_bacteria| biotype=rRNA	0.54	8.67E-01	1.66	3.52E-01
EBG00001182596| tRNA G00001182596	-0.07	9.59E-01	-0.30	7.56E-01
EBG00001182597| tRNA G00001182597	0.51	5.48E-01	-0.57	5.04E-01
EBG00001182598| tRNA G00001182598	-0.61	4.47E-01	-1.08	1.18E-01
EBG00001182599| tRNA G00001182599	3.11	1.20E-01	0.46	9.62E-01
EBG00001182600| tRNA G00001182600	0.66	2.56E-01	0.05	9.89E-01
EBG00001182601| tRNA G00001182601	1.14	4.23E-03	-1.18	4.87E-03
EBG00001182602| tRNA G00001182602	1.06	3.00E-01	0.19	9.68E-01
EBG00001182603| tRNA G00001182603	0.60	2.15E-01	0.62	2.25E-01
EBG00001182604| tRNA G00001182604	1.17	3.71E-02	-0.79	2.77E-01
EBG00001182605| tRNA G00001182605	1.03	3.81E-01	-0.37	8.78E-01
EBG00001182606| tRNA G00001182606	1.77	5.46E-03	-1.61	4.15E-02
EBG00001182607| 5S_rRNA| biotype=rRNA	0.15	9.59E-01	-0.57	6.65E-01
EBG00001182608| tRNA G00001182608	0.94	4.29E-01	-0.29	9.19E-01
EBG00001182609| tRNA G00001182609	0.00	9.98E-01	-0.85	1.45E-01
EBG00001182610| tRNA G00001182610	1.10	7.64E-02	-0.42	6.58E-01
EBG00001182611| SSU_rRNA_archaea| biotype=rRNA	2.73	1.09E-01	2.49	1.77E-01
EBG00001182612| tRNA G00001182612	0.53	3.89E-01	-0.05	9.89E-01
EBG00001182613| tRNA G00001182613	0.88	5.56E-01	-0.01	9.99E-01
EBG00001182614| tRNA G00001182614	-0.95	6.22E-01	1.34	3.94E-01
EBG00001182615| tRNA G00001182615	0.84	5.83E-01	0.25	9.55E-01
EBG00001182616| tmRNA| biotype=ncRNA	0.00	9.98E-01	0.47	5.89E-01
EBG00001182617| tRNA G00001182617	0.64	6.29E-01	-0.61	6.74E-01
EBG00001182618| RNaseP_bact_a| biotype=ribozyme	0.80	1.42E-01	0.56	3.76E-01
EBG00001182619| tRNA G00001182619	1.83	6.43E-04	0.17	9.20E-01
EBG00001182620| tRNA G00001182620	0.40	6.10E-01	0.54	4.18E-01

Figure A5.2 WT vs Δ*spoVG* and WT vs *spoVG*-ON sRNA Full table

		Start	Stop	Strand	WT v Δ log2	WT v Δ padj	WT vs ON log2	WT vs ON padj
SR0001	chr	3151	3343	-	-0.34	6.35E-01	1.36	2.24E-03
SR0002	chr	3324	3454	+	NA	NA	NA	NA
SR0003	chr	4262	4345	+	0.05	9.89E-01	0.21	9.59E-01
SR0004	chr	4303	4430	-	0.33	5.18E-01	0.92	1.15E-02
SR0005	chr	5053	5193	-	-0.12	9.15E-01	0.07	9.59E-01
SR0006	chr	7249	7383	+	-1.16	4.61E-03	0.28	6.62E-01
SR0007	chr	7600	7661	+	-1.27	3.92E-02	0.37	6.82E-01
SR0008	chr	8549	8625	-	-0.53	5.27E-01	0.83	2.08E-01
SR0009	chr	10915	11072	-	-0.23	6.62E-01	-0.60	1.09E-01
SR0010	chr	12319	12446	-	0.00	9.97E-01	-0.42	5.96E-01
SR0011	chr	15804	15873	+	-0.27	8.87E-01	0.21	9.42E-01
SR0012	chr	17717	17775	-	-0.08	9.89E-01	0.37	6.20E-01
SR0013	chr	20453	20602	-	-0.69	6.34E-02	0.80	1.73E-02
SR0014	chr	25903	25952	-	0.19	8.30E-01	1.03	1.98E-02
SR0015	chr	27083	27132	-	-0.02	9.89E-01	-0.48	5.36E-01
SR0016	chr	29143	29197	+	0.31	6.75E-01	-0.31	6.89E-01
SR0017	chr	30909	31000	+	0.72	7.01E-01	0.47	8.65E-01
SR0018	chr	32808	32854	+	-1.30	1.19E-01	-0.55	6.19E-01
SR0019	chr	34937	35008	-	0.05	9.89E-01	0.21	9.59E-01
SR0020	chr	39004	39085	-	0.05	9.89E-01	0.21	9.59E-01
SR0021	chr	39498	39674	-	-1.64	4.96E-02	0.09	9.59E-01
SR0022	chr	39746	39824	+	0.64	5.76E-01	-0.07	9.64E-01
SR0023	chr	39916	40070	+	-0.33	9.59E-01	0.03	9.92E-01
SR0024	chr	40608	40692	+	-0.48	7.34E-01	0.39	8.07E-01
SR0025	chr	41076	41147	+	-0.10	9.47E-01	0.86	3.88E-02
SR0026	chr	41649	41800	-	-0.67	9.55E-01	-0.56	9.59E-01
SR0027	chr	45022	45127	+	0.07	9.83E-01	-0.07	9.59E-01
SR0028	chr	45908	45970	-	0.37	6.58E-01	1.67	6.43E-04
SR0029	chr	46530	46597	+	0.16	9.89E-01	1.82	3.39E-01
SR0030	chr	47000	47049	-	0.52	6.26E-01	0.12	9.59E-01
SR0031	chr	47902	48000	+	-0.72	4.75E-01	0.10	9.59E-01
SR0032	chr	48088	48201	-	0.17	7.95E-01	-0.25	6.49E-01
SR0033	chr	49223	49324	-	-1.11	1.74E-01	0.53	6.09E-01
SR0034	chr	49815	49872	+	0.05	9.89E-01	0.21	9.59E-01
SR0035	chr	49847	49975	-	-0.58	1.73E-01	-0.16	8.25E-01
SR0036	chr	57840	57973	-	-0.30	5.82E-01	0.64	1.18E-01
SR0037	chr	58602	58757	+	0.13	8.71E-01	0.69	6.19E-02
SR0038	chr	60372	60439	-	0.05	9.89E-01	0.21	9.59E-01
SR0039	chr	61365	61528	+	0.10	9.52E-01	0.99	1.21E-02
SR0040	chr	61723	61807	-	-0.02	9.89E-01	0.75	1.25E-01
SR0041	chr	62800	63058	-	0.60	3.34E-01	0.99	5.26E-02
SR0042	chr	62874	62965	+	0.56	4.00E-01	1.11	3.69E-02
SR0043	chr	63122	63192	+	0.20	9.12E-01	-0.32	7.71E-01
SR0044	chr	64058	64128	+	0.05	9.89E-01	0.21	9.59E-01
SR0045	chr	67706	67810	-	0.77	9.17E-02	-0.85	7.05E-02
SR0046	chr	68117	68241	-	0.37	3.99E-01	-0.18	7.74E-01
SR0047	chr	69927	69997	-	0.33	5.39E-01	-0.71	9.44E-02
SR0048	chr	70112	70208	+	0.48	3.92E-01	0.28	6.82E-01
SR0049	chr	70662	70754	+	0.05	9.89E-01	0.80	7.53E-01
SR0050	chr	72696	72745	-	1.01	2.64E-01	-0.94	3.81E-01
SR0051	chr	73036	73111	+	0.05	9.89E-01	0.21	9.59E-01
SR0052	chr	75960	76009	+	0.05	9.89E-01	0.21	9.59E-01
SR0053	chr	80423	80539	-	-1.81	1.50E-02	-0.95	2.56E-01
SR0054	chr	82200	82258	+	0.05	9.89E-01	0.21	9.59E-01
SR0055	chr	86020	86069	+	-0.27	5.49E-01	-0.17	7.59E-01
SR0056	chr	86743	86853	-	0.46	9.64E-01	0.64	9.22E-01
SR0057	chr	88061	88228	-	-0.18	7.33E-01	0.15	8.17E-01
SR0058	chr	92262	92361	+	-0.13	9.52E-01	-0.32	7.00E-01
SR0059	chr	97554	97668	-	0.05	9.89E-01	0.21	9.59E-01
SR0060	chr	99576	99625	-	0.02	9.89E-01	0.21	7.27E-01
SR0061	chr	101607	101683	-	0.05	9.89E-01	0.21	9.59E-01

SR0062	chr	102785	102853	+	0.28	6.96E-01	0.29	7.00E-01
SR0063	chr	104400	104491	+	-0.49	2.39E-01	-0.80	1.84E-02
SR0064	chr	104727	104792	+	-0.62	2.77E-01	-0.67	2.10E-01
SR0065	chr	107081	107150	-	0.05	9.89E-01	0.21	9.59E-01
SR0066	chr	108374	108495	+	0.05	9.89E-01	0.21	9.59E-01
SR0067	chr	109635	109750	+	-0.23	8.38E-01	-1.27	2.13E-02
SR0068	chr	111621	111713	-	1.76	7.32E-01	0.20	9.76E-01
SR0069	chr	114070	114191	+	0.57	3.30E-01	0.14	9.34E-01
SR0070	chr	114758	114830	+	0.10	9.89E-01	-0.03	9.89E-01
SR0071	chr	114956	115046	+	0.05	9.89E-01	0.21	9.59E-01
SR0072	chr	115524	115593	+	-0.22	8.14E-01	-1.02	4.28E-02
SR0073	chr	115545	115617	-	0.05	9.89E-01	0.21	9.59E-01
SR0074	chr	117446	117496	+	-0.61	4.01E-01	-0.40	6.48E-01
SR0075	chr	117640	117725	-	-0.91	9.91E-02	0.12	9.55E-01
SR0076	chr	120029	120165	+	0.51	2.52E-01	0.70	6.84E-02
SR0077	chr	122496	122678	-	-0.22	9.35E-01	0.22	9.46E-01
SR0078	chr	124199	124250	+	1.09	3.49E-02	0.68	2.25E-01
SR0079	chr	124286	124448	-	11.04	NA	0.21	NA
SR0080	chr	125149	125221	-	0.05	9.89E-01	-0.18	9.63E-01
SR0081	chr	125198	125273	+	-0.29	6.08E-01	-0.98	1.21E-02
SR0082	chr	127478	127578	+	-0.32	5.66E-01	-0.52	2.52E-01
SR0083	chr	128171	128250	+	-0.48	5.76E-01	-0.62	4.41E-01
SR0084	chr	129662	129711	+	-0.40	4.70E-01	-0.24	7.20E-01
SR0085	chr	131268	131657	+	-0.27	9.33E-01	-0.76	6.19E-01
SR0086	chr	131278	131327	-	-0.19	9.89E-01	0.76	6.54E-01
SR0087	chr	133785	133890	-	0.33	5.55E-01	-0.04	9.61E-01
SR0088	chr	135801	135867	-	-0.12	9.60E-01	0.36	6.50E-01
SR0089	chr	138320	138376	+	0.13	8.86E-01	-1.30	2.24E-04
SR0090	chr	139474	139594	-	-0.66	3.04E-02	-0.08	9.37E-01
SR0091	chr	139700	139749	-	-0.99	1.83E-04	0.18	6.79E-01
SR0092	chr	141357	141457	+	-0.67	6.26E-02	0.25	6.13E-01
SR0093	chr	141905	141949	-	-0.59	3.23E-01	-0.42	5.37E-01
SR0094	chr	147733	147826	+	-0.03	9.89E-01	0.37	6.15E-01
SR0095	chr	150850	150898	+	-0.12	9.89E-01	0.20	9.59E-01
SR0096	chr	153045	153130	+	-0.11	9.51E-01	-0.84	6.66E-02
SR0097	chr	153203	153431	-	-0.60	1.63E-01	-0.38	4.36E-01
SR0098	chr	153604	153707	-	-0.38	5.89E-01	-0.99	4.84E-02
SR0099	chr	155117	155163	+	-0.84	1.05E-02	0.16	7.82E-01
SR0100	chr	155608	155772	-	0.36	9.74E-01	0.51	9.42E-01
SR0101	chr	156491	156609	+	0.05	9.89E-01	0.21	9.59E-01
SR0102	chr	156950	156999	-	0.58	4.49E-01	0.36	7.02E-01
SR0103	chr	157426	157486	+	-0.20	9.79E-01	-1.07	4.60E-01
SR0104	chr	157520	157585	-	0.81	1.61E-01	-0.67	2.44E-01
SR0105	chr	158500	158713	+	0.50	4.64E-01	0.96	7.71E-02
SR0106	chr	159827	159877	-	0.45	5.25E-01	-0.64	3.03E-01
SR0107	chr	161458	161509	+	-0.35	5.44E-01	-0.13	9.22E-01
SR0108	chr	162724	162773	+	-0.63	3.73E-01	0.39	6.42E-01
SR0109	chr	163509	163702	-	0.40	9.30E-01	0.71	7.68E-01
SR0110	chr	163976	164109	-	0.05	9.89E-01	0.21	9.59E-01
SR0111	chr	164373	164418	+	0.25	7.13E-01	1.34	4.16E-04
SR0112	chr	164713	164837	-	0.63	4.25E-01	1.30	3.43E-02
SR0113	chr	165045	165094	+	-0.37	5.81E-01	-0.18	8.72E-01
SR0114	chr	165969	166048	+	-0.44	5.96E-01	-0.32	7.41E-01
SR0115	chr	166396	166655	-	-0.33	9.58E-01	0.21	9.59E-01
SR0116	chr	166523	166587	+	-0.86	2.17E-01	-0.54	4.96E-01
SR0117	chr	169306	169359	-	0.05	9.89E-01	0.21	9.59E-01
SR0118	chr	170467	170544	+	0.05	9.89E-01	0.21	9.59E-01
SR0119	chr	172501	172571	+	-0.70	2.71E-01	-0.32	7.02E-01
SR0120	chr	172728	172781	+	-1.07	1.37E-01	0.09	9.59E-01
SR0121	chr	172735	172869	-	0.28	9.83E-01	0.43	9.42E-01
SR0122	chr	174087	174144	-	-5.90	3.01E-02	-0.57	9.59E-01
SR0123	chr	174394	174446	-	0.05	9.89E-01	0.21	9.59E-01
SR0124	chr	175079	175128	+	-0.14	9.65E-01	0.02	9.91E-01
SR0125	chr	175626	175675	-	-0.59	2.05E-01	-0.02	9.86E-01

SR0126	chr	176642	176691	+	-1.15	9.13E-02	-1.31	3.88E-02
SR0127	chr	177497	177688	+	-0.75	6.73E-02	-0.50	2.56E-01
SR0128	chr	178637	178735	-	0.05	9.89E-01	0.21	9.59E-01
SR0129	chr	180386	180435	+	-0.80	4.61E-03	-0.41	1.98E-01
SR0130	chr	180392	180485	-	0.05	9.89E-01	0.21	9.59E-01
SR0131	chr	181560	181679	-	-0.55	9.16E-01	-0.04	9.91E-01
SR0132	chr	181625	181673	+	-1.50	4.87E-03	-0.28	7.66E-01
SR0133	chr	182747	182807	-	-0.97	7.20E-01	0.02	9.97E-01
SR0134	chr	185485	185535	-	-0.09	9.73E-01	-0.78	1.29E-01
SR0135	chr	188410	188493	+	-0.04	9.89E-01	0.22	7.59E-01
SR0136	chr	188520	188701	-	-0.13	9.09E-01	0.40	4.47E-01
SR0137	chr	190061	190170	+	-0.53	3.12E-01	0.63	1.92E-01
SR0138	chr	190996	191046	+	0.05	9.89E-01	0.21	9.59E-01
SR0139	chr	191060	191137	-	-0.24	9.55E-01	-0.34	9.05E-01
SR0140	chr	191997	192046	+	-0.49	2.03E-01	0.29	5.23E-01
SR0141	chr	192094	192147	+	-0.64	3.12E-01	0.23	8.20E-01
SR0142	chr	193336	193454	-	-0.22	9.83E-01	0.21	9.59E-01
SR0143	chr	193545	193597	-	-0.45	6.94E-01	1.23	1.12E-01
SR0144	chr	193707	193829	+	0.15	8.93E-01	0.29	6.61E-01
SR0145	chr	196151	196257	+	0.54	9.14E-01	-0.51	9.47E-01
SR0146	chr	196508	196630	+	-0.39	9.79E-01	0.20	9.59E-01
SR0147	chr	198376	198426	+	-0.78	4.67E-01	0.00	9.98E-01
SR0148	chr	198383	198576	-	-0.41	7.30E-01	0.80	3.72E-01
SR0149	chr	198658	198723	+	-1.30	3.87E-01	0.20	9.59E-01
SR0150	chr	202693	202761	+	-0.09	9.89E-01	-0.20	9.42E-01
SR0151	chr	202719	202824	-	0.17	9.88E-01	0.76	6.03E-01
SR0152	chr	202958	203156	-	0.16	8.76E-01	0.78	9.30E-02
SR0153	chr	203288	203350	+	0.05	9.89E-01	0.21	9.59E-01
SR0154	chr	203424	203534	+	-0.06	9.89E-01	0.40	8.67E-01
SR0155	chr	204592	204663	-	-0.81	5.73E-02	-0.48	3.12E-01
SR0156	chr	204893	205094	-	-0.85	7.78E-02	-0.68	1.65E-01
SR0157	chr	205092	205165	+	0.52	5.66E-01	-0.40	7.00E-01
SR0158	chr	205346	205395	-	0.12	9.32E-01	-0.46	4.15E-01
SR0159	chr	206320	206382	+	0.25	9.44E-01	0.92	4.48E-01
SR0160	chr	206428	206477	+	0.09	9.89E-01	0.95	4.64E-01
SR0161	chr	207461	207628	+	-0.22	9.56E-01	-0.62	6.89E-01
SR0162	chr	208143	208283	-	0.03	9.89E-01	0.71	6.67E-01
SR0163	chr	210616	210744	-	0.33	7.84E-01	-0.52	6.19E-01
SR0164	chr	210844	210892	-	1.01	5.27E-01	-0.16	9.59E-01
SR0165	chr	211234	211296	+	0.84	2.40E-01	2.05	1.75E-04
SR0166	chr	215154	215257	-	0.29	6.99E-01	-0.84	1.03E-01
SR0167	chr	216448	216606	-	0.84	1.86E-02	-0.46	2.56E-01
SR0168	chr	218334	218546	+	-0.13	8.79E-01	1.31	7.14E-05
SR0169	chr	219103	219154	-	0.05	9.89E-01	0.21	9.59E-01
SR0170	chr	221344	221442	+	0.46	9.60E-01	1.21	6.89E-01
SR0171	chr	221936	222147	-	0.05	9.89E-01	-0.80	3.41E-02
SR0172	chr	222564	222703	+	-0.96	7.74E-01	-0.05	9.91E-01
SR0173	chr	223054	223124	-	-0.10	9.39E-01	-1.36	1.97E-04
SR0174	chr	223525	223661	+	0.05	9.89E-01	1.21	6.95E-01
SR0175	chr	223659	223775	-	-0.19	7.75E-01	-0.03	9.74E-01
SR0176	chr	226905	227203	-	-1.08	NA	-0.94	NA
SR0177	chr	229214	229308	+	-0.69	8.84E-01	0.21	9.59E-01
SR0178	chr	230033	230116	+	0.05	9.89E-01	0.21	9.59E-01
SR0179	chr	230783	230894	+	-0.70	2.79E-01	-0.63	3.23E-01
SR0180	chr	231582	231652	+	-0.59	5.82E-01	0.48	6.82E-01
SR0181	chr	231828	231887	-	-0.05	9.89E-01	0.62	2.92E-01
SR0182	chr	232846	232933	+	0.05	9.89E-01	0.21	9.59E-01
SR0183	chr	232863	232952	-	-0.14	9.44E-01	-0.31	7.31E-01
SR0184	chr	233547	233669	-	-0.15	9.50E-01	-0.54	4.97E-01
SR0185	chr	242397	242495	+	-0.92	1.64E-01	-0.28	7.80E-01
SR0186	chr	245945	246070	-	-2.50	2.16E-21	2.64	5.11E-24
SR0187	chr	246367	246464	-	-3.15	3.01E-33	2.35	5.02E-21
SR0188	chr	250167	250293	-	-0.84	4.99E-01	-0.50	7.45E-01
SR0189	chr	250385	250467	+	-1.16	4.61E-03	-0.01	9.92E-01

SR0190	chr	253091	253141	+	-0.09	9.89E-01	-0.44	6.58E-01
SR0191	chr	254196	254320	-	-0.44	2.85E-01	-0.77	2.27E-02
SR0192	chr	254551	254701	-	-0.55	4.07E-01	-0.83	1.47E-01
SR0193	chr	255970	256097	-	-0.01	9.93E-01	0.32	5.51E-01
SR0194	chr	256281	256345	+	0.56	4.32E-01	0.16	9.42E-01
SR0195	chr	257052	257123	+	0.05	9.89E-01	0.21	9.59E-01
SR0196	chr	260581	260796	-	0.06	9.89E-01	-1.22	7.17E-03
SR0197	chr	260769	260852	+	-0.17	8.71E-01	-0.16	8.90E-01
SR0198	chr	261078	261149	-	-0.26	7.81E-01	0.18	8.95E-01
SR0199	chr	263683	263729	-	-0.04	9.89E-01	0.87	6.10E-01
SR0200	chr	263804	263906	+	-0.79	4.02E-01	-0.88	3.24E-01
SR0201	chr	266747	266799	-	-1.06	5.68E-02	-0.42	5.73E-01
SR0202	chr	267703	267868	-	0.02	9.89E-01	-0.61	1.96E-01
SR0203	chr	269511	269626	+	-1.50	9.38E-03	-0.03	9.78E-01
SR0204	chr	270114	270175	+	-1.00	1.19E-01	-0.63	3.76E-01
SR0205	chr	273744	273890	+	0.08	9.89E-01	0.21	8.67E-01
SR0206	chr	274374	274472	-	0.31	6.51E-01	0.43	4.66E-01
SR0207	chr	276164	276260	+	-0.69	8.84E-01	0.21	9.59E-01
SR0208	chr	276500	276617	+	-0.59	2.45E-01	0.26	6.99E-01
SR0209	chr	278453	278546	-	0.05	9.89E-01	0.21	9.59E-01
SR0210	chr	280235	280355	-	0.33	9.80E-01	-0.51	9.48E-01
SR0211	chr	282150	282250	-	0.05	9.89E-01	0.21	9.59E-01
SR0212	chr	282439	282511	+	-0.44	2.57E-01	-0.45	2.28E-01
SR0213	chr	288401	288487	+	-0.97	1.15E-01	-0.84	1.70E-01
SR0214	chr	291828	291928	-	0.05	9.89E-01	0.21	9.59E-01
SR0215	chr	295449	295594	-	0.01	9.99E-01	12.38	1.22E-09
SR0216	chr	297224	297342	+	0.24	7.26E-01	-0.41	4.50E-01
SR0217	chr	299204	299253	+	0.14	9.17E-01	-0.14	9.20E-01
SR0218	chr	300174	300223	+	-0.52	2.88E-01	-0.66	1.36E-01
SR0219	chr	301612	301771	-	-0.17	9.89E-01	0.20	9.59E-01
SR0220	chr	308247	308372	-	-0.71	8.75E-01	0.46	9.48E-01
SR0221	chr	308446	308496	-	0.05	9.89E-01	0.21	9.59E-01
SR0222	chr	311513	311609	+	-0.67	9.45E-02	-0.32	5.19E-01
SR0223	chr	311567	311681	-	-0.64	4.57E-01	0.29	8.20E-01
SR0224	chr	312010	312115	-	0.49	9.57E-01	0.64	9.22E-01
SR0225	chr	317317	317439	-	-0.09	9.89E-01	0.55	7.80E-01
SR0226	chr	320204	320287	-	0.09	9.83E-01	0.68	2.19E-01
SR0227	chr	320801	320869	-	-0.30	7.30E-01	0.12	9.59E-01
SR0228	chr	322977	323052	+	-0.64	2.83E-01	-0.12	9.59E-01
SR0229	chr	323316	323394	-	0.44	9.68E-01	0.21	9.59E-01
SR0230	chr	324885	324951	+	-0.93	1.21E-01	-0.38	6.38E-01
SR0231	chr	327363	327412	-	0.05	9.89E-01	0.21	9.59E-01
SR0232	chr	327661	327819	-	0.17	9.33E-01	0.50	5.59E-01
SR0233	chr	327895	328102	+	-0.36	4.95E-01	1.10	3.15E-03
SR0234	chr	328956	329015	+	0.05	9.89E-01	0.21	9.59E-01
SR0235	chr	330430	330515	-	0.05	9.89E-01	0.21	9.59E-01
SR0236	chr	331681	331751	-	0.05	9.89E-01	0.21	9.59E-01
SR0237	chr	331733	331782	+	-0.96	1.63E-01	-1.01	1.18E-01
SR0238	chr	331922	332039	+	-0.85	9.45E-02	-0.77	1.19E-01
SR0239	chr	333152	333242	-	0.05	9.89E-01	0.21	9.59E-01
SR0240	chr	333808	333888	-	-0.29	9.89E-01	0.21	9.59E-01
SR0241	chr	334587	334654	-	-0.90	8.92E-02	0.53	3.76E-01
SR0242	chr	334785	334835	+	-0.68	8.85E-02	0.83	1.78E-02
SR0243	chr	335529	335578	-	-0.64	1.86E-01	0.58	2.20E-01
SR0244	chr	336511	336565	+	-1.02	4.74E-02	0.81	1.18E-01
SR0245	chr	338243	338293	+	-1.59	1.49E-03	0.80	1.18E-01
SR0246	chr	340302	340576	+	-1.02	2.09E-03	5.23	1.10E-92
SR0247	chr	340555	340650	-	-1.01	1.07E-02	0.39	4.42E-01
SR0248	chr	344861	344909	+	-0.29	6.56E-01	0.89	4.12E-02
SR0249	chr	344889	345010	-	-0.21	7.74E-01	0.61	1.83E-01
SR0250	chr	350380	350449	+	-0.29	7.21E-01	-0.15	9.16E-01
SR0251	chr	355027	355371	-	-0.03	9.89E-01	1.19	1.81E-01
SR0252	chr	356175	356224	-	-1.03	2.03E-01	0.35	7.46E-01
SR0253	chr	356987	357118	+	0.98	5.36E-02	-0.14	9.36E-01

SR0254	chr	358532	358589	-	1.36	1.12E-02	-0.78	2.15E-01
SR0255	chr	361001	361145	-	0.02	9.89E-01	-0.22	7.96E-01
SR0256	chr	361193	361301	+	2.43	2.70E-01	2.18	3.21E-01
SR0257	chr	362663	362714	-	0.05	9.89E-01	0.21	9.59E-01
SR0258	chr	365828	365879	-	-0.41	5.87E-01	0.45	5.47E-01
SR0259	chr	365936	365986	+	-0.61	6.03E-01	-0.11	9.59E-01
SR0260	chr	366768	366819	-	0.05	9.89E-01	0.21	9.59E-01
SR0261	chr	367895	368055	-	-0.98	6.99E-03	0.44	3.09E-01
SR0262	chr	368492	368541	-	-0.50	5.55E-01	-0.23	8.67E-01
SR0263	chr	369675	369724	-	-0.45	4.32E-01	-1.00	2.65E-02
SR0264	chr	373474	373545	+	-1.38	1.09E-01	-1.69	3.23E-02
SR0265	chr	373995	374099	-	0.05	9.89E-01	0.21	9.59E-01
SR0266	chr	376548	376623	-	-0.35	9.89E-01	-0.18	9.63E-01
SR0267	chr	376795	376859	-	0.05	9.89E-01	0.21	9.59E-01
SR0268	chr	380045	380094	+	-0.80	2.04E-01	-0.44	5.68E-01
SR0269	chr	380332	380478	-	0.05	9.89E-01	0.21	9.59E-01
SR0270	chr	384156	384208	-	-1.10	2.92E-01	1.55	6.87E-02
SR0271	chr	388256	388442	-	-0.38	4.43E-01	0.83	3.07E-02
SR0272	chr	389852	390012	+	-0.61	1.29E-01	0.63	9.50E-02
SR0273	chr	391800	391853	-	-1.19	1.50E-02	0.35	6.12E-01
SR0274	chr	392496	392605	-	0.05	9.89E-01	0.95	8.05E-01
SR0275	chr	394443	394499	-	0.05	9.89E-01	0.21	9.59E-01
SR0276	chr	394805	394853	+	0.44	1.49E-01	1.28	3.57E-08
SR0277	chr	395312	395387	-	-0.40	6.78E-01	1.76	2.89E-03
SR0278	chr	396334	396428	+	0.34	7.33E-01	1.56	8.54E-03
SR0279	chr	399917	400036	+	-0.40	5.99E-01	-1.12	3.69E-02
SR0280	chr	401309	401358	+	-0.42	5.27E-01	-0.76	1.44E-01
SR0281	chr	402480	402558	-	-0.42	5.27E-01	-0.69	2.11E-01
SR0282	chr	405124	405404	-	0.03	9.89E-01	-0.37	4.16E-01
SR0283	chr	408120	408192	-	-0.04	9.89E-01	0.87	2.80E-01
SR0284	chr	408412	408480	-	0.37	6.06E-01	1.61	4.76E-04
SR0285	chr	408662	408711	-	0.05	9.89E-01	0.21	9.59E-01
SR0286	chr	408989	409048	-	0.05	9.89E-01	0.21	9.59E-01
SR0287	chr	409131	409240	-	-0.35	9.89E-01	-0.18	9.63E-01
SR0288	chr	409907	409957	+	-0.28	6.06E-01	-0.27	6.31E-01
SR0289	chr	409907	409970	-	0.05	9.89E-01	0.21	9.59E-01
SR0290	chr	410343	410463	-	0.20	9.55E-01	0.27	9.13E-01
SR0291	chr	410714	410810	+	-0.57	7.34E-01	-0.46	8.18E-01
SR0292	chr	413076	413126	+	-0.62	3.53E-01	0.08	9.59E-01
SR0293	chr	413744	413790	-	-0.49	6.62E-01	-0.20	9.42E-01
SR0294	chr	413807	413899	+	0.05	9.89E-01	0.21	9.59E-01
SR0295	chr	414168	414264	-	-0.03	9.89E-01	-0.19	8.17E-01
SR0296	chr	416521	416589	-	-0.37	8.10E-01	0.35	8.27E-01
SR0297	chr	416920	416986	+	0.05	9.89E-01	0.21	9.59E-01
SR0298	chr	417750	417820	+	0.05	9.89E-01	0.21	9.59E-01
SR0299	chr	418364	418432	-	-1.29	3.43E-01	-0.95	5.30E-01
SR0300	chr	418627	418694	+	-0.52	5.57E-01	-0.18	9.35E-01
SR0301	chr	419241	419465	-	0.05	9.89E-01	0.21	9.59E-01
SR0302	chr	421545	421607	+	-0.14	9.89E-01	0.23	9.59E-01
SR0303	chr	421685	421769	-	-0.95	2.10E-01	-1.37	3.91E-02
SR0304	chr	423176	423275	+	0.05	9.89E-01	0.21	9.59E-01
SR0305	chr	423518	423638	-	-1.01	1.24E-01	-1.70	2.38E-03
SR0306	chr	423712	423769	+	0.05	9.89E-01	0.21	9.59E-01
SR0307	chr	424041	424108	-	0.05	9.89E-01	0.21	9.59E-01
SR0308	chr	425565	425704	+	0.22	8.63E-01	0.02	9.89E-01
SR0309	chr	428415	428516	-	-0.39	5.41E-01	-1.28	3.34E-03
SR0310	chr	428554	428603	+	0.64	8.79E-01	0.78	8.26E-01
SR0311	chr	428764	428818	+	0.05	9.89E-01	0.21	9.59E-01
SR0312	chr	428973	429036	+	0.05	9.89E-01	0.21	9.59E-01
SR0313	chr	429728	429863	-	0.05	9.89E-01	-0.04	9.91E-01
SR0314	chr	433843	433896	-	0.05	9.89E-01	0.21	9.59E-01
SR0315	chr	434558	434622	+	-0.24	8.73E-01	-0.44	6.62E-01
SR0316	chr	435208	435431	-	-0.36	8.02E-01	0.10	9.59E-01
SR0317	chr	435602	435653	+	0.05	9.89E-01	0.21	9.59E-01

SR0318	chr	438217	438308	-	0.81	7.39E-01	1.15	5.92E-01
SR0319	chr	438345	438393	-	0.46	8.27E-01	0.28	9.48E-01
SR0320	chr	438439	438555	-	-0.53	6.87E-01	0.09	9.59E-01
SR0321	chr	441461	441555	-	0.81	7.38E-01	1.14	5.95E-01
SR0322	chr	442772	442838	+	-0.62	2.03E-01	-0.18	8.20E-01
SR0323	chr	442926	443036	-	0.05	9.89E-01	0.21	9.59E-01
SR0324	chr	443571	443751	+	-1.58	9.88E-04	1.53	1.06E-03
SR0325	chr	444341	444409	-	-0.94	8.85E-02	0.71	2.08E-01
SR0326	chr	444712	444783	+	10.48	3.57E-12	0.21	9.59E-01
SR0327	chr	445010	445082	+	0.05	9.89E-01	0.21	9.59E-01
SR0328	chr	445300	445350	+	0.05	9.89E-01	0.21	9.59E-01
SR0329	chr	445765	445810	+	0.05	9.89E-01	0.21	9.59E-01
SR0330	chr	446158	446220	-	1.02	2.34E-01	1.43	5.32E-02
SR0331	chr	450390	450524	+	-0.73	2.39E-01	0.01	9.91E-01
SR0332	chr	451393	451459	+	1.47	1.66E-02	0.15	9.59E-01
SR0333	chr	453539	453684	-	0.05	9.89E-01	0.21	9.59E-01
SR0334	chr	454709	454759	-	0.05	9.89E-01	0.21	9.59E-01
SR0335	chr	455085	455211	-	0.05	9.89E-01	0.21	9.59E-01
SR0336	chr	456465	456514	-	0.33	9.60E-01	1.23	5.59E-01
SR0337	chr	456784	456906	+	0.05	9.89E-01	0.21	9.59E-01
SR0338	chr	457121	457196	-	-0.22	6.89E-01	-0.49	2.41E-01
SR0339	chr	457281	457455	+	0.05	9.89E-01	0.04	9.90E-01
SR0340	chr	461704	461802	+	-0.44	2.50E-01	-0.47	1.92E-01
SR0341	chr	465040	465110	-	0.18	8.07E-01	1.08	2.99E-03
SR0342	chr	466347	466447	+	0.30	5.27E-01	-0.82	1.83E-02
SR0343	chr	466545	466608	+	0.16	8.07E-01	-0.55	1.69E-01
SR0344	chr	466678	466756	+	-0.02	9.89E-01	-0.95	8.69E-03
SR0345	chr	467849	467895	+	-0.53	4.97E-01	-1.89	5.06E-04
SR0346	chr	469260	469381	-	0.04	9.89E-01	-0.12	9.76E-01
SR0347	chr	472002	472086	+	-0.47	6.89E-01	-1.82	1.40E-02
SR0348	chr	472138	472210	-	0.05	9.89E-01	0.21	9.59E-01
SR0349	chr	473672	473837	-	1.66	3.35E-01	-0.34	9.59E-01
SR0350	chr	474517	474567	-	0.70	5.08E-01	1.14	1.83E-01
SR0351	chr	475638	475711	+	0.05	9.89E-01	0.21	9.59E-01
SR0352	chr	476272	476353	+	-0.21	7.82E-01	-0.59	2.49E-01
SR0353	chr	477474	477631	-	-0.22	9.84E-01	0.20	9.59E-01
SR0354	chr	477997	478112	-	0.31	7.19E-01	0.70	2.51E-01
SR0355	chr	478971	479147	+	-0.02	9.89E-01	-0.27	7.00E-01
SR0356	chr	481083	481153	+	-0.06	9.89E-01	-0.10	9.59E-01
SR0357	chr	481228	481305	+	0.74	2.34E-01	0.51	4.66E-01
SR0358	chr	481249	481318	-	0.66	4.68E-01	0.57	5.71E-01
SR0359	chr	482082	482232	+	-1.08	9.41E-02	1.29	2.56E-02
SR0360	chr	482310	482392	+	-1.07	6.67E-02	-0.96	9.61E-02
SR0361	chr	483222	483283	-	-0.62	4.32E-01	-0.89	2.02E-01
SR0362	chr	484023	484080	+	0.05	9.89E-01	0.21	9.59E-01
SR0363	chr	485379	485426	-	-0.05	9.89E-01	0.41	7.20E-01
SR0364	chr	486427	486520	-	-0.35	5.48E-01	0.06	9.59E-01
SR0365	chr	486555	486748	+	0.05	9.89E-01	-0.05	9.74E-01
SR0366	chr	486834	486997	-	0.61	2.34E-01	0.43	4.48E-01
SR0367	chr	487719	487810	+	1.11	6.59E-01	-0.51	9.47E-01
SR0368	chr	487914	487967	+	0.05	9.89E-01	0.21	9.59E-01
SR0369	chr	489099	489172	-	-0.64	1.86E-01	-0.35	5.47E-01
SR0370	chr	489870	489959	+	0.05	9.89E-01	0.21	9.59E-01
SR0371	chr	489929	489976	-	-0.56	5.21E-01	-0.72	3.58E-01
SR0372	chr	490076	490126	-	-0.69	3.97E-01	-0.30	7.97E-01
SR0373	chr	490253	490308	-	-0.74	1.28E-01	-0.27	6.91E-01
SR0374	chr	490647	490735	+	-0.39	9.80E-01	-0.22	9.59E-01
SR0375	chr	493394	493458	+	0.05	9.89E-01	0.21	9.59E-01
SR0376	chr	493684	493730	+	0.05	9.89E-01	0.21	9.59E-01
SR0377	chr	494638	494724	-	-0.24	9.84E-01	0.99	5.99E-01
SR0378	chr	494853	494903	+	-0.32	5.69E-01	-0.02	9.79E-01
SR0379	chr	497126	497205	+	-0.39	9.73E-01	0.78	8.33E-01
SR0380	chr	498841	498951	+	0.05	9.89E-01	0.21	9.59E-01
SR0381	chr	503510	503626	-	0.15	8.63E-01	-0.08	9.59E-01

SR0382	chr	503545	503643	+	0.02	9.95E-01	0.78	8.31E-01
SR0383	chr	506700	506896	+	0.63	3.14E-01	0.44	5.45E-01
SR0384	chr	507041	507097	+	0.05	9.89E-01	0.21	9.59E-01
SR0385	chr	507280	507483	-	0.14	8.91E-01	0.27	6.62E-01
SR0386	chr	507662	507809	+	-0.58	1.38E-01	0.02	9.76E-01
SR0387	chr	511358	511498	+	0.26	9.89E-01	0.21	9.59E-01
SR0388	chr	513075	513177	-	-0.31	7.26E-01	0.16	9.16E-01
SR0389	chr	513193	513273	+	-1.23	8.95E-04	-0.62	1.37E-01
SR0390	chr	514927	514976	-	-1.08	3.38E-02	-0.67	2.20E-01
SR0391	chr	515495	515559	+	0.05	9.89E-01	0.21	9.59E-01
SR0392	chr	515629	515807	+	-0.83	1.21E-01	-2.18	2.70E-07
SR0393	chr	518453	518590	+	-0.24	9.89E-01	-0.37	9.59E-01
SR0394	chr	521556	521775	+	0.05	9.89E-01	0.21	9.59E-01
SR0395	chr	523418	523524	+	-0.39	4.55E-01	-1.01	9.39E-03
SR0396	chr	526293	526449	+	-0.50	3.79E-01	-1.82	5.61E-06
SR0397	chr	530238	530287	+	-0.37	7.72E-01	-1.26	1.09E-01
SR0398	chr	530686	530827	-	0.05	9.89E-01	0.21	9.59E-01
SR0399	chr	531636	531704	-	0.04	9.89E-01	1.68	2.15E-02
SR0400	chr	532157	532282	-	0.14	9.07E-01	0.69	1.29E-01
SR0401	chr	534455	534504	-	-0.41	6.33E-01	0.31	7.41E-01
SR0402	chr	534793	534926	+	-0.40	NA	4.05	NA
SR0403	chr	542236	542328	+	-0.34	6.58E-01	0.41	5.65E-01
SR0404	chr	545088	545138	+	0.05	9.89E-01	0.21	9.59E-01
SR0405	chr	547366	547581	+	0.15	9.57E-01	0.43	6.61E-01
SR0406	chr	547385	547688	-	0.46	4.57E-01	0.71	1.83E-01
SR0407	chr	547729	547797	-	0.34	8.79E-01	0.51	7.44E-01
SR0408	chr	550265	550328	+	-0.46	3.92E-01	-0.36	5.41E-01
SR0409	chr	551645	551708	+	-0.21	8.71E-01	0.15	9.50E-01
SR0410	chr	551650	551769	-	-0.46	6.30E-01	-0.17	9.48E-01
SR0411	chr	551853	551903	-	-0.41	8.09E-01	0.52	7.05E-01
SR0412	chr	551933	552192	+	0.06	9.89E-01	2.41	2.68E-04
SR0413	chr	552972	553062	-	-0.10	9.52E-01	0.19	7.96E-01
SR0414	chr	556204	556357	+	0.24	9.89E-01	-0.01	9.98E-01
SR0415	chr	556404	556549	-	0.27	6.89E-01	0.01	9.92E-01
SR0416	chr	559261	559321	+	0.47	4.54E-01	-1.30	6.82E-03
SR0417	chr	561897	561958	-	1.31	4.40E-04	0.59	1.83E-01
SR0418	chr	562185	562279	+	0.06	9.89E-01	-0.04	9.90E-01
SR0419	chr	565644	565716	-	0.07	9.89E-01	0.02	9.89E-01
SR0420	chr	565724	565773	+	0.75	5.27E-01	1.26	1.83E-01
SR0421	chr	567939	568009	+	0.05	9.89E-01	0.21	9.59E-01
SR0422	chr	568447	568633	+	-0.43	5.59E-01	-0.27	7.69E-01
SR0423	chr	568729	568781	+	0.05	9.89E-01	0.21	9.59E-01
SR0424	chr	569067	569162	-	-0.28	8.78E-01	0.69	5.03E-01
SR0425	chr	570669	570777	+	0.33	9.80E-01	-0.51	9.48E-01
SR0426	chr	571781	571854	+	-0.30	9.33E-01	1.14	3.41E-01
SR0427	chr	571797	571905	-	-0.06	9.60E-01	0.59	4.24E-02
SR0428	chr	572892	572943	+	-0.05	9.89E-01	-0.37	6.46E-01
SR0429	chr	577156	577205	+	-1.83	1.13E-02	0.14	9.59E-01
SR0430	chr	581323	581411	+	0.05	9.89E-01	0.21	9.59E-01
SR0431	chr	581843	581933	-	0.11	9.19E-01	-0.17	7.97E-01
SR0432	chr	584094	584193	-	0.08	9.89E-01	-0.13	9.59E-01
SR0433	chr	585174	585253	-	-0.20	7.36E-01	0.23	6.67E-01
SR0434	chr	586204	586314	+	-0.59	3.63E-01	-0.64	2.92E-01
SR0435	chr	587261	587358	-	-0.76	2.33E-01	0.43	5.61E-01
SR0436	chr	589486	589627	+	-0.18	9.89E-01	-0.01	9.98E-01
SR0437	chr	589788	589912	-	-1.78	NA	-0.92	NA
SR0438	chr	589932	589982	+	-1.04	5.83E-02	0.11	9.59E-01
SR0439	chr	590184	590242	-	-1.30	3.08E-01	0.08	9.62E-01
SR0440	chr	590903	590952	+	0.35	9.33E-01	0.59	8.01E-01
SR0441	chr	592484	592635	+	0.44	8.23E-01	0.21	9.59E-01
SR0442	chr	593038	593115	-	0.55	3.39E-01	-0.86	7.74E-02
SR0443	chr	594023	594072	-	0.63	1.13E-01	0.05	9.59E-01
SR0444	chr	596314	596485	+	0.29	9.26E-01	0.12	9.59E-01
SR0445	chr	596343	596440	-	0.17	7.85E-01	-0.22	7.11E-01

SR0446	chr	596709	596787	-	0.42	5.27E-01	0.25	7.65E-01
SR0447	chr	598507	598751	+	-0.95	6.90E-02	-0.08	9.59E-01
SR0448	chr	598753	598831	-	0.05	9.89E-01	0.21	9.59E-01
SR0449	chr	600136	600203	+	0.05	9.89E-01	0.21	9.59E-01
SR0450	chr	600593	600717	-	-0.67	8.66E-02	0.60	1.15E-01
SR0451	chr	600874	600966	+	-1.24	3.51E-02	0.18	9.11E-01
SR0452	chr	602840	602916	-	0.24	6.55E-01	0.38	4.01E-01
SR0453	chr	603273	603343	-	0.78	2.10E-01	-0.55	4.36E-01
SR0454	chr	604095	604190	+	-0.16	9.72E-01	-1.09	2.61E-01
SR0455	chr	604762	604807	-	-0.12	9.89E-01	-0.51	7.41E-01
SR0456	chr	604914	605000	-	0.05	9.89E-01	0.80	7.53E-01
SR0457	chr	605915	605979	+	-0.34	5.42E-01	-1.02	1.09E-02
SR0458	chr	606945	607277	+	0.73	1.69E-01	0.97	3.58E-02
SR0459	chr	607624	607706	-	1.05	2.94E-02	0.79	1.11E-01
SR0460	chr	609985	610065	+	0.36	4.57E-01	0.23	7.00E-01
SR0461	chr	610243	610352	+	0.04	9.89E-01	0.26	6.79E-01
SR0462	chr	611309	611375	+	0.05	9.89E-01	0.21	9.59E-01
SR0463	chr	613830	614008	+	-0.17	9.35E-01	0.03	9.84E-01
SR0464	chr	614003	614066	-	0.07	9.89E-01	-0.05	9.64E-01
SR0465	chr	614136	614219	+	0.12	8.65E-01	-0.04	9.59E-01
SR0466	chr	615492	615541	+	-0.17	8.11E-01	0.23	6.84E-01
SR0467	chr	618247	618551	-	0.26	9.57E-01	0.41	8.69E-01
SR0468	chr	620161	620224	-	-0.02	9.89E-01	0.32	9.22E-01
SR0469	chr	620762	620844	-	0.66	2.19E-01	0.39	5.40E-01
SR0470	chr	621047	621113	+	0.39	6.16E-01	0.28	7.68E-01
SR0471	chr	621537	621624	-	0.05	9.89E-01	0.21	9.59E-01
SR0472	chr	621854	621957	-	2.60	2.59E-02	-0.43	8.98E-01
SR0473	chr	621952	622120	+	-1.61	7.63E-02	0.47	7.27E-01
SR0474	chr	623117	623203	+	0.11	9.89E-01	0.01	9.98E-01
SR0475	chr	623333	623436	+	0.05	9.89E-01	0.21	9.59E-01
SR0476	chr	623903	623952	-	-0.98	1.84E-01	-0.50	5.89E-01
SR0477	chr	627097	627398	-	0.05	9.89E-01	0.33	9.39E-01
SR0478	chr	630426	630475	+	-0.15	9.37E-01	-0.95	1.03E-01
SR0479	chr	630577	630626	+	-0.14	9.57E-01	-0.38	7.00E-01
SR0480	chr	631726	631866	+	0.05	9.89E-01	0.21	9.59E-01
SR0481	chr	631929	631984	-	0.02	9.89E-01	1.07	3.56E-04
SR0482	chr	632527	632645	+	0.05	9.89E-01	0.21	9.59E-01
SR0483	chr	633099	633148	-	-0.82	4.08E-01	0.30	8.57E-01
SR0484	chr	633827	633895	-	-0.30	7.81E-01	-0.03	9.78E-01
SR0485	chr	634371	634506	-	-0.79	3.01E-01	-0.99	1.50E-01
SR0486	chr	636099	636222	+	-0.63	4.58E-01	0.75	3.09E-01
SR0487	chr	636248	636296	+	-0.23	9.67E-01	0.78	5.93E-01
SR0488	chr	636396	636446	+	0.19	8.14E-01	0.56	2.26E-01
SR0489	chr	636481	636548	+	0.20	8.72E-01	0.33	7.00E-01
SR0490	chr	638067	638272	+	0.05	9.89E-01	0.43	9.42E-01
SR0491	chr	638645	638847	-	0.36	3.28E-01	0.48	1.42E-01
SR0492	chr	639796	639887	-	-0.12	9.33E-01	-0.57	2.56E-01
SR0493	chr	640167	640372	-	-0.45	5.81E-01	-0.54	4.81E-01
SR0494	chr	643117	643283	-	0.63	1.86E-01	0.64	1.55E-01
SR0495	chr	645028	645102	+	0.05	9.89E-01	0.21	9.59E-01
SR0496	chr	645285	645347	+	-0.28	8.31E-01	-0.30	8.10E-01
SR0497	chr	645584	645633	-	-1.15	1.67E-01	0.92	2.65E-01
SR0498	chr	645671	645817	+	0.54	3.91E-01	0.97	5.43E-02
SR0499	chr	646212	646266	+	0.05	9.89E-01	0.21	9.59E-01
SR0500	chr	646576	646662	-	0.70	2.42E-01	-0.31	7.04E-01
SR0501	chr	647338	647424	+	0.23	8.38E-01	0.36	6.74E-01
SR0502	chr	647833	647946	+	0.52	2.74E-01	0.17	8.23E-01
SR0503	chr	648464	648534	+	-0.10	9.89E-01	0.30	8.95E-01
SR0504	chr	649059	649139	-	-0.24	8.75E-01	-0.69	4.08E-01
SR0505	chr	649984	650122	+	-1.12	1.91E-01	-0.63	5.38E-01
SR0506	chr	650666	650715	+	-0.39	5.78E-01	0.19	8.67E-01
SR0507	chr	651673	651718	-	0.05	9.89E-01	0.21	9.59E-01
SR0508	chr	652809	652858	+	-0.72	5.89E-01	-0.81	5.55E-01
SR0509	chr	653384	653520	+	-0.76	4.37E-01	-0.90	3.27E-01

SR0510	chr	656299	656348	+	0.05	9.89E-01	0.21	9.59E-01
SR0511	chr	656942	657012	+	-1.54	NA	-1.63	NA
SR0512	chr	656988	657108	-	0.86	5.32E-01	0.68	6.62E-01
SR0513	chr	657818	657937	-	1.36	2.18E-02	1.02	9.32E-02
SR0514	chr	658746	658855	-	1.45	4.57E-03	0.91	9.61E-02
SR0515	chr	658876	658925	+	0.13	9.89E-01	-0.07	9.64E-01
SR0516	chr	659033	659089	+	0.05	9.89E-01	0.21	9.59E-01
SR0517	chr	659351	659545	+	-0.02	9.89E-01	-0.54	7.97E-01
SR0518	chr	661247	661377	-	0.30	9.83E-01	-0.35	9.59E-01
SR0519	chr	661545	661641	+	-0.52	8.30E-01	0.47	8.40E-01
SR0520	chr	662542	662591	+	-2.93	6.62E-06	-1.59	2.63E-02
SR0521	chr	663063	663145	-	-3.65	1.16E-08	0.93	2.70E-01
SR0522	chr	664859	664908	+	-0.77	2.42E-01	0.99	7.95E-02
SR0523	chr	665387	665539	-	-0.18	9.89E-01	-0.01	9.98E-01
SR0524	chr	666067	666185	+	-0.06	9.89E-01	-2.30	1.22E-05
SR0525	chr	666439	666489	+	0.20	9.51E-01	-1.13	2.40E-01
SR0526	chr	667291	667438	+	0.33	5.69E-01	-0.22	7.68E-01
SR0527	chr	668891	668971	-	0.59	5.18E-01	-1.28	9.56E-02
SR0528	chr	669766	669895	-	-0.17	8.97E-01	-0.06	9.59E-01
SR0529	chr	670619	670734	+	-0.48	6.32E-01	-0.96	2.16E-01
SR0530	chr	670942	670991	+	-0.95	5.42E-01	-0.77	6.55E-01
SR0531	chr	671334	671395	-	0.51	8.20E-01	-0.82	6.63E-01
SR0532	chr	671661	671715	-	-0.16	9.89E-01	-0.41	8.95E-01
SR0533	chr	671922	672069	-	1.49	5.66E-01	0.63	9.13E-01
SR0534	chr	672027	672174	+	-0.48	4.39E-01	-0.20	8.42E-01
SR0535	chr	673237	673391	+	-0.68	7.00E-02	-0.43	2.85E-01
SR0536	chr	674248	674349	+	0.05	9.89E-01	0.21	9.59E-01
SR0537	chr	674835	674884	+	-1.95	1.86E-06	-0.50	3.46E-01
SR0538	chr	675672	675744	-	-1.34	1.52E-04	0.19	7.69E-01
SR0539	chr	676116	676165	-	-0.52	4.70E-01	0.19	8.95E-01
SR0540	chr	679320	679394	+	-0.77	2.01E-01	-1.68	5.94E-04
SR0541	chr	680433	680486	-	0.05	9.89E-01	0.21	9.59E-01
SR0542	chr	681883	681994	+	0.96	6.42E-02	-0.06	9.59E-01
SR0543	chr	681911	681991	-	0.05	9.89E-01	0.21	9.59E-01
SR0544	chr	682376	682524	-	0.05	9.89E-01	0.78	5.37E-01
SR0545	chr	684912	685001	+	-1.59	8.58E-02	-1.07	2.77E-01
SR0546	chr	686437	686562	-	-0.02	9.89E-01	0.35	5.15E-01
SR0547	chr	687870	687919	+	0.58	2.74E-01	-0.39	5.41E-01
SR0548	chr	688222	688271	+	-1.60	3.63E-01	0.17	9.59E-01
SR0549	chr	688778	688888	-	1.06	4.64E-02	0.92	7.95E-02
SR0550	chr	689567	689693	+	0.05	9.89E-01	0.21	9.59E-01
SR0551	chr	689900	690151	+	0.60	2.31E-01	0.84	5.32E-02
SR0552	chr	693165	693315	+	0.21	9.89E-01	0.37	9.46E-01
SR0553	chr	693535	693613	-	-0.58	2.30E-01	-0.13	9.11E-01
SR0554	chr	693652	693717	+	0.05	9.89E-01	0.21	9.59E-01
SR0555	chr	694649	694732	-	-0.61	6.21E-01	-0.78	5.15E-01
SR0556	chr	695610	695676	+	0.01	9.97E-01	1.06	7.45E-01
SR0557	chr	696669	696840	+	-1.46	5.26E-07	0.69	3.21E-02
SR0558	chr	697843	697973	+	-0.19	9.89E-01	0.56	8.61E-01
SR0559	chr	699758	699987	-	7.80	2.03E-06	-0.36	9.59E-01
SR0560	chr	700764	700817	+	0.22	7.12E-01	0.61	1.31E-01
SR0561	chr	700871	700960	-	0.05	9.89E-01	0.11	9.59E-01
SR0562	chr	702987	703052	+	-0.39	8.40E-01	0.75	5.74E-01
SR0563	chr	704005	704053	-	-0.69	3.05E-01	0.48	5.19E-01
SR0564	chr	706371	706618	+	-0.40	7.82E-01	-0.08	9.59E-01
SR0565	chr	708075	708215	-	-0.46	3.19E-01	-1.18	7.76E-04
SR0566	chr	708828	708901	+	0.05	9.89E-01	0.21	9.59E-01
SR0567	chr	710037	710087	+	0.05	9.89E-01	0.21	9.59E-01
SR0568	chr	711583	711679	-	0.23	7.79E-01	-1.15	1.17E-02
SR0569	chr	712781	712830	+	1.08	1.16E-01	-0.05	9.69E-01
SR0570	chr	713629	713680	+	-0.75	2.31E-01	-0.76	2.02E-01
SR0571	chr	713893	713942	-	0.05	9.89E-01	0.21	9.59E-01
SR0572	chr	714601	714780	-	0.33	9.73E-01	0.92	7.33E-01
SR0573	chr	714672	714720	+	-0.90	1.73E-01	1.13	3.42E-02

SR0574	chr	715920	716128	+	0.38	9.74E-01	-0.20	9.59E-01
SR0575	chr	719402	719450	-	-0.11	9.27E-01	-0.98	1.30E-02
SR0576	chr	719640	719782	+	0.05	9.89E-01	0.43	9.42E-01
SR0577	chr	719819	719903	-	-0.30	5.55E-01	-0.98	5.39E-03
SR0578	chr	720645	720755	+	0.05	9.89E-01	0.21	9.59E-01
SR0579	chr	722022	722071	-	-0.36	4.57E-01	-1.01	3.78E-03
SR0580	chr	722874	722936	+	0.05	9.89E-01	0.21	9.59E-01
SR0581	chr	722994	723136	+	-0.21	7.37E-01	-0.98	8.92E-03
SR0582	chr	723012	723154	-	-0.05	9.89E-01	-1.02	1.11E-03
SR0583	chr	723986	724144	-	0.46	9.60E-01	1.20	7.00E-01
SR0584	chr	724079	724129	+	-0.15	9.88E-01	0.80	4.58E-01
SR0585	chr	724200	724249	+	0.63	5.57E-01	-0.31	8.52E-01
SR0586	chr	724342	724419	+	0.05	9.89E-01	0.21	9.59E-01
SR0587	chr	727264	727353	-	-0.23	8.07E-01	-0.81	1.50E-01
SR0588	chr	729667	729792	-	-0.90	2.25E-02	-0.09	9.56E-01
SR0589	chr	730107	730159	+	0.05	9.89E-01	0.21	9.59E-01
SR0590	chr	730515	730591	-	0.09	9.55E-01	0.00	9.98E-01
SR0591	chr	731768	731852	+	-0.23	9.14E-01	2.23	1.06E-03
SR0592	chr	732148	732302	+	0.05	9.89E-01	-0.37	9.59E-01
SR0593	chr	732568	732628	+	0.05	9.89E-01	0.21	9.59E-01
SR0594	chr	732870	733019	+	0.04	9.89E-01	0.31	9.35E-01
SR0595	chr	735317	735452	+	0.55	6.29E-01	0.21	9.47E-01
SR0596	chr	735607	735720	+	-0.23	9.89E-01	-0.04	9.91E-01
SR0597	chr	737891	737969	-	0.23	6.69E-01	-0.36	4.29E-01
SR0598	chr	738038	738268	+	0.40	3.91E-01	0.85	1.77E-02
SR0599	chr	740426	740475	-	0.10	9.44E-01	-0.30	6.13E-01
SR0600	chr	742120	742170	+	0.34	5.27E-01	0.21	7.68E-01
SR0601	chr	742120	742223	-	0.01	9.97E-01	0.46	9.46E-01
SR0602	chr	742438	742623	-	-0.27	9.72E-01	0.22	9.59E-01
SR0603	chr	742476	742541	+	0.14	9.28E-01	1.59	2.33E-04
SR0604	chr	744349	744471	+	0.05	9.89E-01	0.21	9.59E-01
SR0605	chr	744877	745005	+	-1.14	6.14E-01	-0.25	9.59E-01
SR0606	chr	745039	745097	+	1.19	2.73E-01	-0.70	6.18E-01
SR0607	chr	745826	745919	-	-0.92	5.29E-02	-1.05	1.70E-02
SR0608	chr	747133	747384	+	0.16	8.23E-01	0.56	1.60E-01
SR0609	chr	747667	747729	+	-0.43	7.12E-01	0.00	9.98E-01
SR0610	chr	747919	748025	+	-0.03	9.89E-01	-0.69	5.26E-02
SR0611	chr	749585	749708	+	0.18	9.89E-01	0.22	9.59E-01
SR0612	chr	750582	750658	+	0.05	9.89E-01	0.21	9.59E-01
SR0613	chr	750817	750901	+	0.57	3.44E-01	0.74	1.72E-01
SR0614	chr	751120	751257	-	-0.92	2.52E-01	0.30	8.07E-01
SR0615	chr	751745	751794	-	-0.87	1.20E-01	-0.14	9.35E-01
SR0616	chr	754389	754503	-	-1.58	1.37E-02	-0.18	9.34E-01
SR0617	chr	756644	756712	-	-1.01	8.32E-02	-0.37	6.48E-01
SR0618	chr	757370	757432	-	-0.98	2.94E-02	-0.77	9.33E-02
SR0619	chr	760362	760423	-	-0.73	3.28E-01	-1.13	7.44E-02
SR0620	chr	760922	760971	-	-0.77	2.23E-01	-1.29	1.50E-02
SR0621	chr	761058	761177	-	-0.78	2.85E-01	-1.11	8.08E-02
SR0622	chr	761522	761598	+	0.05	9.89E-01	0.21	9.59E-01
SR0623	chr	761559	761716	-	0.07	9.89E-01	0.47	5.38E-01
SR0624	chr	763469	763518	+	0.42	2.32E-01	-0.12	8.53E-01
SR0625	chr	763777	763827	-	0.43	1.90E-01	0.12	8.31E-01
SR0626	chr	764001	764078	+	1.05	7.46E-01	0.64	9.14E-01
SR0627	chr	768400	768450	+	0.33	4.32E-01	-0.57	1.06E-01
SR0628	chr	768411	768575	-	0.19	9.89E-01	0.21	9.59E-01
SR0629	chr	769231	769280	+	0.40	6.82E-01	0.05	9.63E-01
SR0630	chr	769844	769938	+	0.36	5.35E-01	-1.14	5.39E-03
SR0631	chr	769854	770014	-	0.05	9.89E-01	-0.05	9.90E-01
SR0632	chr	770132	770181	+	0.01	9.90E-01	-1.05	6.07E-02
SR0633	chr	773079	773177	-	0.44	9.68E-01	0.21	9.59E-01
SR0634	chr	774200	774375	-	0.23	9.89E-01	-0.29	9.59E-01
SR0635	chr	774458	774512	+	0.08	9.89E-01	1.89	1.22E-02
SR0636	chr	776556	776696	-	0.05	9.89E-01	0.23	9.59E-01
SR0637	chr	787035	787090	-	0.32	3.38E-01	0.77	2.37E-03

SR0638	chr	788994	789090	+	-0.68	7.85E-01	0.60	8.07E-01
SR0639	chr	789050	789119	-	-0.47	6.51E-01	-0.01	9.92E-01
SR0640	chr	789136	789249	-	-0.86	4.59E-01	0.59	6.32E-01
SR0641	chr	789321	789371	+	0.05	9.89E-01	0.21	9.59E-01
SR0642	chr	789416	789475	-	0.28	8.24E-01	0.91	1.88E-01
SR0643	chr	790233	790281	+	-1.72	1.40E-03	-2.62	1.44E-07
SR0644	chr	791442	791497	+	-1.64	3.25E-02	-1.06	1.99E-01
SR0645	chr	792168	792255	-	-0.39	9.77E-01	0.52	9.45E-01
SR0646	chr	792294	792361	+	-0.73	8.73E-01	0.62	9.16E-01
SR0647	chr	793731	793785	-	1.27	3.53E-01	1.34	3.07E-01
SR0648	chr	796463	796547	+	0.21	6.76E-01	-1.02	7.25E-04
SR0649	chr	797921	797971	+	-0.05	9.89E-01	-1.16	1.92E-04
SR0650	chr	800315	800428	-	0.39	6.23E-01	0.83	1.66E-01
SR0651	chr	801846	801909	+	-0.63	2.71E-01	0.43	4.98E-01
SR0652	chr	803502	803604	-	-1.60	2.09E-03	-0.04	9.69E-01
SR0653	chr	804246	804295	+	-0.04	9.89E-01	1.02	4.31E-01
SR0654	chr	809919	810016	-	0.15	9.89E-01	0.13	9.59E-01
SR0655	chr	810040	810190	+	-0.68	2.21E-01	-1.78	3.41E-05
SR0656	chr	811230	811403	-	0.05	9.89E-01	0.21	9.59E-01
SR0657	chr	812265	812439	-	-2.32	6.31E-05	-1.75	2.76E-03
SR0658	chr	814185	814257	+	0.11	9.30E-01	0.01	9.90E-01
SR0659	chr	814592	814727	-	0.20	9.89E-01	0.70	7.23E-01
SR0660	chr	816639	816694	-	0.05	9.89E-01	0.21	9.59E-01
SR0661	chr	819328	819400	-	0.97	6.75E-02	0.12	9.57E-01
SR0662	chr	820365	820441	+	0.05	9.89E-01	0.21	9.59E-01
SR0663	chr	821254	821321	-	0.06	9.89E-01	-1.07	1.15E-01
SR0664	chr	821535	821667	+	0.34	9.39E-01	0.21	9.59E-01
SR0665	chr	822408	822454	-	-0.15	9.30E-01	-1.31	1.49E-02
SR0666	chr	822940	822989	-	-7.06	9.11E-76	4.59	4.62E-50
SR0667	chr	823166	823231	+	-1.18	1.18E-05	1.02	1.45E-04
SR0668	chr	826299	826381	+	0.05	9.89E-01	0.21	9.59E-01
SR0669	chr	827263	827335	+	0.07	9.89E-01	-0.09	9.82E-01
SR0670	chr	829053	829114	+	-1.45	4.07E-01	-1.14	5.59E-01
SR0671	chr	830827	830943	-	-0.37	9.85E-01	-0.20	9.59E-01
SR0672	chr	831633	831683	+	0.58	4.66E-01	1.26	3.57E-02
SR0673	chr	831982	832089	-	-0.31	8.79E-01	0.58	6.46E-01
SR0674	chr	832128	832190	+	-0.63	5.39E-01	-0.01	9.95E-01
SR0675	chr	834156	834226	-	-0.54	3.94E-01	0.26	7.61E-01
SR0676	chr	834779	834973	+	-0.44	3.43E-01	-0.12	9.04E-01
SR0677	chr	835511	835569	+	0.24	7.64E-01	0.06	9.59E-01
SR0678	chr	835714	835866	+	0.38	5.66E-01	0.94	4.99E-02
SR0679	chr	836154	836233	-	-0.82	2.63E-01	0.85	2.16E-01
SR0680	chr	839781	839903	+	-0.55	9.12E-01	0.21	9.59E-01
SR0681	chr	839800	839939	-	-0.60	2.83E-01	-0.55	3.11E-01
SR0682	chr	840916	841133	+	0.05	9.89E-01	0.21	9.59E-01
SR0683	chr	841215	841350	-	-0.64	1.94E-01	-0.93	2.64E-02
SR0684	chr	842145	842196	-	-1.07	1.17E-01	-0.78	2.74E-01
SR0685	chr	842471	842538	+	-0.05	9.89E-01	-0.03	9.88E-01
SR0686	chr	843316	843362	-	-0.30	7.13E-01	0.45	5.11E-01
SR0687	chr	848259	848343	-	0.39	6.63E-01	-0.41	6.46E-01
SR0688	chr	856162	856326	-	-0.25	6.29E-01	-0.86	1.16E-02
SR0689	chr	856710	856869	+	0.05	9.89E-01	0.63	8.42E-01
SR0690	chr	856824	856960	-	-0.44	4.32E-01	-0.97	2.74E-02
SR0691	chr	858409	858487	+	0.05	9.89E-01	0.21	9.59E-01
SR0692	chr	860131	860278	+	-1.73	7.18E-03	0.48	6.11E-01
SR0693	chr	860333	860544	-	-1.73	9.58E-04	0.46	5.45E-01
SR0694	chr	860872	860923	+	0.05	9.89E-01	0.21	9.59E-01
SR0695	chr	862452	862516	+	-0.95	3.23E-01	-0.81	4.15E-01
SR0696	chr	862625	862675	+	-0.68	2.27E-01	0.38	5.87E-01
SR0697	chr	863477	863549	-	-1.49	5.05E-03	-0.34	6.91E-01
SR0698	chr	867463	867533	+	0.05	9.89E-01	0.21	9.59E-01
SR0699	chr	868744	868895	-	-0.56	1.72E-01	0.39	3.70E-01
SR0700	chr	870007	870077	-	0.01	9.99E-01	0.18	9.60E-01
SR0701	chr	871538	871606	+	-0.23	7.52E-01	-1.24	2.60E-03

SR0702	chr	872610	872658	-	0.49	9.59E-01	0.21	9.59E-01
SR0703	chr	873630	873717	+	-0.18	8.79E-01	-0.66	2.63E-01
SR0704	chr	873674	873728	-	0.05	9.89E-01	0.21	9.59E-01
SR0705	chr	874159	874208	+	-0.26	7.57E-01	0.44	5.24E-01
SR0706	chr	875171	875261	+	0.23	9.39E-01	0.81	4.79E-01
SR0707	chr	881310	881422	-	0.05	9.89E-01	1.20	7.11E-01
SR0708	chr	881440	881553	+	0.01	9.89E-01	-1.70	5.82E-05
SR0709	chr	881987	882036	+	-0.18	9.27E-01	-1.62	6.44E-03
SR0710	chr	883224	883285	+	-0.38	5.48E-01	-1.09	1.46E-02
SR0711	chr	884032	884142	-	0.05	9.89E-01	0.21	9.59E-01
SR0712	chr	885800	885849	+	-0.17	8.63E-01	0.21	8.07E-01
SR0713	chr	886343	886497	-	0.25	9.23E-01	0.34	8.54E-01
SR0714	chr	888242	888377	+	-0.09	9.73E-01	-0.97	2.61E-02
SR0715	chr	889701	889829	+	0.03	9.89E-01	-1.11	4.39E-03
SR0716	chr	890350	890442	+	0.05	9.89E-01	0.21	9.59E-01
SR0717	chr	891803	891890	+	0.05	9.89E-01	0.21	9.59E-01
SR0718	chr	898930	898990	-	0.05	9.89E-01	0.21	9.59E-01
SR0719	chr	899690	899766	+	0.05	9.89E-01	0.21	9.59E-01
SR0720	chr	901558	901617	+	0.05	9.89E-01	0.21	9.59E-01
SR0721	chr	902869	903038	+	0.47	9.17E-01	0.21	9.59E-01
SR0722	chr	903124	903224	-	-0.20	7.74E-01	0.96	1.03E-02
SR0723	chr	905118	905186	+	0.39	8.38E-01	1.05	3.30E-01
SR0724	chr	908448	908578	+	-0.23	9.89E-01	0.21	9.59E-01
SR0725	lp17	2883	2933	-	1.08	4.04E-01	1.70	1.13E-01
SR0726	lp17	4269	4365	-	0.63	9.38E-01	1.53	6.56E-01
SR0727	lp17	6593	6703	+	0.78	4.77E-02	1.12	1.34E-03
SR0728	lp17	8155	8220	+	3.01	1.05E-13	1.24	1.11E-02
SR0729	lp17	8211	8257	-	2.66	4.83E-05	1.11	1.66E-01
SR0730	lp17	8407	8487	-	2.03	1.03E-09	1.54	1.04E-05
SR0731	lp17	9414	9567	+	0.59	2.32E-01	1.01	1.21E-02
SR0732	lp17	10026	10124	+	-0.10	9.89E-01	-0.54	8.20E-01
SR0733	lp17	10554	10615	-	1.57	2.99E-01	0.71	7.47E-01
SR0734	lp17	10785	10832	+	0.77	4.20E-01	1.88	6.27E-03
SR0735	lp17	10829	10901	-	0.25	9.30E-01	0.70	5.73E-01
SR0736	lp17	11749	11833	+	4.18	1.41E-01	3.63	2.07E-01
SR0737	lp17	12541	12594	-	0.23	9.65E-01	0.49	8.09E-01
SR0738	lp17	12902	12951	+	1.74	2.20E-02	-0.04	9.79E-01
SR0739	lp17	15175	15224	-	1.05	7.26E-01	-0.19	9.60E-01
SR0740	lp17	15321	15448	+	0.88	4.36E-01	0.39	8.30E-01
SR0741	lp17	16230	16279	+	1.34	5.65E-01	-0.50	9.48E-01
SR0742	lp21	1290	1340	-	1.57	4.98E-01	0.97	7.45E-01
SR0743	lp21	1488	1584	+	0.05	9.89E-01	0.21	9.59E-01
SR0744	lp25	4544	4593	-	-0.36	9.89E-01	-2.62	5.37E-01
SR0745	lp25	5310	5359	-	-0.89	4.01E-01	-4.78	7.40E-04
SR0746	lp25	7036	7267	-	-0.57	3.58E-01	-2.98	1.86E-11
SR0747	lp25	9409	9553	-	-0.62	2.17E-01	-2.73	6.04E-11
SR0748	lp25	10412	10464	-	0.05	9.89E-01	0.21	9.59E-01
SR0749	lp25	10817	10862	+	-0.95	4.09E-01	-3.10	3.78E-03
SR0750	lp25	11188	11252	-	0.34	9.73E-01	-1.80	5.41E-01
SR0751	lp25	12423	12473	+	-1.63	4.87E-03	-3.73	6.04E-12
SR0752	lp25	13269	13417	-	-2.30	5.23E-03	-4.70	3.23E-07
SR0753	lp25	14404	14512	-	-0.09	9.89E-01	-0.07	9.79E-01
SR0754	lp25	15673	15944	-	-0.78	1.73E-01	-4.54	2.92E-24
SR0755	lp25	15951	16076	+	-1.50	4.94E-03	-3.06	1.86E-09
SR0756	lp25	18781	18830	-	-0.12	9.89E-01	-3.12	8.26E-02
SR0757	lp25	19502	19589	+	-1.44	5.05E-01	-2.85	1.83E-01
SR0758	lp25	20437	20486	-	1.53	8.51E-01	-0.75	9.59E-01
SR0759	lp25	20980	21067	+	0.43	9.73E-01	-0.75	9.16E-01
SR0760	lp25	21790	21834	+	0.88	9.83E-01	-0.75	9.59E-01
SR0761	lp25	23037	23109	+	0.08	9.89E-01	-2.62	5.26E-01
SR0762	lp25	23581	23630	+	-1.58	3.69E-01	-2.13	2.05E-01
SR0763	lp25	23946	23995	+	-0.57	9.02E-01	-3.30	1.81E-01
SR0764	lp28-1	2136	2233	+	-0.74	5.27E-01	0.90	3.38E-01
SR0765	lp28-1	5855	5904	-	-0.81	9.22E-01	2.05	5.34E-01

SR0766	lp28-1	10442	10547	-	-1.77	9.56E-04	-0.21	8.48E-01
SR0767	lp28-1	12242	12293	-	-0.42	9.44E-01	1.02	6.54E-01
SR0768	lp28-1	13306	13355	+	-2.62	1.25E-04	0.76	2.69E-01
SR0769	lp28-1	16309	16358	-	-0.75	8.07E-01	1.23	5.30E-01
SR0770	lp28-2	2692	2761	-	2.02	7.70E-02	2.02	6.58E-02
SR0771	lp28-2	4254	4359	+	0.76	2.99E-01	0.73	3.07E-01
SR0772	lp28-2	7333	7420	-	0.53	8.07E-01	-1.30	4.45E-01
SR0773	lp28-2	11054	11172	+	0.98	1.95E-01	-0.46	6.51E-01
SR0774	lp28-2	18835	18885	+	1.27	1.45E-01	0.43	7.55E-01
SR0775	lp28-2	24347	24396	+	1.82	9.52E-02	0.84	5.75E-01
SR0776	lp28-2	24426	24490	-	1.76	5.81E-01	2.06	4.97E-01
SR0777	lp28-2	24514	24650	+	-1.62	5.56E-01	-1.45	6.19E-01
SR0778	lp28-2	25074	25148	+	0.05	9.89E-01	0.21	9.59E-01
SR0779	lp28-2	26424	26497	+	2.22	4.61E-03	0.13	9.59E-01
SR0780	lp28-2	28015	28127	+	-0.51	NA	0.29	NA
SR0781	lp28-2	28532	28781	+	-0.14	9.89E-01	-0.19	9.59E-01
SR0782	lp28-2	29410	29532	-	0.04	9.89E-01	0.58	8.51E-01
SR0783	lp28-2	29569	29618	-	0.05	9.89E-01	0.21	9.59E-01
SR0784	lp28-3	1594	1643	+	0.76	8.71E-01	1.61	5.59E-01
SR0785	lp28-3	2165	2244	-	-0.10	9.89E-01	-0.56	6.34E-01
SR0786	lp28-3	4412	4461	+	1.05	8.86E-01	-0.63	9.59E-01
SR0787	lp28-3	8351	8432	-	0.58	6.91E-01	-0.51	7.81E-01
SR0788	lp28-3	9510	9570	-	-2.02	5.60E-05	0.80	1.66E-01
SR0789	lp28-3	10436	10534	-	0.41	4.73E-01	0.61	2.08E-01
SR0790	lp28-3	11446	11507	-	0.30	9.62E-01	-0.23	9.59E-01
SR0791	lp28-3	16481	16565	+	0.44	7.45E-01	1.60	4.74E-02
SR0792	lp28-3	18496	18579	+	0.07	9.89E-01	-0.50	9.51E-01
SR0793	lp28-3	19459	19508	+	0.33	6.45E-01	1.02	2.95E-02
SR0794	lp28-3	23090	23141	+	-0.36	7.64E-01	-0.52	6.16E-01
SR0795	lp28-3	24448	24549	+	0.65	6.65E-01	1.78	7.10E-02
SR0796	lp28-3	25268	25327	-	-0.61	8.71E-01	-0.19	9.59E-01
SR0797	lp28-3	25656	25733	-	1.72	5.23E-01	0.21	9.59E-01
SR0798	lp28-4	1403	1452	-	-0.13	9.89E-01	-0.25	9.59E-01
SR0799	lp28-4	2779	2828	-	0.57	5.25E-01	0.64	4.53E-01
SR0800	lp28-4	4578	4627	+	1.06	3.19E-01	-0.02	9.92E-01
SR0801	lp28-4	4780	4877	-	1.01	1.68E-01	-0.13	9.59E-01
SR0802	lp28-4	4991	5056	+	0.31	7.64E-01	0.77	2.52E-01
SR0803	lp28-4	6472	6626	-	0.35	5.87E-01	-0.32	6.35E-01
SR0804	lp28-4	10785	10862	+	-0.09	9.83E-01	1.29	4.68E-03
SR0805	lp28-4	12723	12840	-	-1.38	1.66E-02	-1.19	3.71E-02
SR0806	lp28-4	13608	13734	+	0.05	9.89E-01	0.21	9.59E-01
SR0807	lp28-4	14110	14171	+	-0.97	5.12E-02	-0.38	5.68E-01
SR0808	lp28-4	14738	14811	+	1.08	8.10E-01	0.84	8.96E-01
SR0809	lp28-4	15656	15705	-	-0.29	9.73E-01	0.63	8.10E-01
SR0810	lp28-4	16622	16678	+	0.76	8.71E-01	0.21	9.59E-01
SR0811	lp28-4	18054	18137	+	1.09	1.86E-01	2.10	1.25E-03
SR0812	lp28-4	19115	19207	-	1.34	3.44E-02	0.50	5.68E-01
SR0813	lp28-4	24157	24211	-	-0.28	9.44E-01	0.04	9.88E-01
SR0814	lp28-4	24601	24764	-	0.25	9.89E-01	-0.57	9.06E-01
SR0815	lp28-4	26351	26421	+	2.70	4.87E-07	-1.02	1.42E-01
SR0816	lp36	747	807	+	0.05	9.89E-01	0.21	9.59E-01
SR0817	lp36	3097	3166	+	0.09	9.89E-01	1.12	7.73E-01
SR0818	lp36	5132	5181	+	-1.29	7.51E-01	-1.09	8.17E-01
SR0819	lp36	6782	6860	+	1.80	2.76E-01	1.06	6.21E-01
SR0820	lp36	8665	8903	-	0.03	9.89E-01	0.04	9.59E-01
SR0821	lp36	9167	9245	+	0.04	9.89E-01	-0.05	9.63E-01
SR0822	lp36	9642	9745	+	-0.29	9.89E-01	-0.53	9.48E-01
SR0823	lp36	11673	11748	+	0.44	9.68E-01	0.21	9.59E-01
SR0824	lp36	12209	12260	-	0.44	6.55E-01	-1.36	4.55E-02
SR0825	lp36	12718	12803	-	0.06	9.89E-01	0.48	5.59E-01
SR0826	lp36	12999	13107	+	7.69	NA	6.13	NA
SR0827	lp36	13278	13364	-	0.04	9.89E-01	0.47	9.56E-01
SR0828	lp36	14171	14220	+	0.82	4.68E-01	0.30	9.04E-01
SR0829	lp36	14207	14315	-	-0.42	9.14E-01	-0.27	9.59E-01

SR0830	lp36	15735	15794	-	1.31	1.75E-02	1.00	7.95E-02
SR0831	lp36	16054	16104	-	0.35	9.72E-01	1.07	6.85E-01
SR0832	lp36	16149	16291	+	0.26	8.07E-01	1.31	1.44E-02
SR0833	lp36	16937	16987	+	0.49	5.33E-01	0.93	1.20E-01
SR0834	lp36	18792	18871	-	0.53	7.20E-01	-0.43	8.26E-01
SR0835	lp36	21230	21314	+	-0.70	7.34E-01	0.73	6.85E-01
SR0836	lp36	22363	22451	+	-0.51	8.19E-01	-6.33	4.91E-06
SR0837	lp36	22421	22583	-	-1.53	4.44E-04	0.26	7.33E-01
SR0838	lp36	23166	23440	+	-0.74	5.58E-02	-0.57	1.50E-01
SR0839	lp36	25584	25675	-	0.25	8.09E-01	1.42	6.38E-03
SR0840	lp36	25705	25783	+	0.20	9.60E-01	1.84	3.00E-02
SR0841	lp36	26891	26940	-	1.27	1.35E-02	0.48	5.05E-01
SR0842	lp36	27908	27995	+	-0.64	1.32E-01	-0.34	4.98E-01
SR0843	lp36	27966	28060	-	0.05	9.89E-01	0.21	9.59E-01
SR0844	lp36	28345	28411	+	0.32	9.30E-01	0.69	7.00E-01
SR0845	lp36	28602	28663	-	0.44	6.22E-01	-0.51	5.67E-01
SR0846	lp36	30472	30528	-	-1.36	6.01E-01	-0.45	9.47E-01
SR0847	lp36	33046	33106	-	1.35	3.53E-01	-0.22	9.59E-01
SR0848	lp36	35057	35217	+	1.18	2.18E-03	1.62	3.34E-06
SR0849	lp36	36075	36145	+	0.05	9.89E-01	0.21	9.59E-01
SR0850	lp38	4505	4881	+	-1.16	1.96E-01	-1.21	1.50E-01
SR0851	lp38	4820	4889	-	-0.01	9.89E-01	-0.22	6.02E-01
SR0852	lp38	6872	6947	+	-1.35	4.51E-02	-0.63	4.47E-01
SR0853	lp38	10402	10463	-	0.24	8.24E-01	3.30	5.87E-15
SR0854	lp38	10511	10581	-	0.05	9.89E-01	0.21	9.59E-01
SR0855	lp38	11938	12047	+	0.72	2.21E-01	0.39	5.95E-01
SR0856	lp38	13386	13469	-	0.52	3.50E-01	2.07	7.63E-08
SR0857	lp38	14313	14362	+	0.93	6.85E-01	0.65	8.31E-01
SR0858	lp38	14513	14560	-	-0.33	9.71E-01	0.69	8.07E-01
SR0859	lp38	20309	20358	+	0.05	9.89E-01	0.21	9.59E-01
SR0860	lp38	23054	23103	+	1.00	1.36E-01	0.87	1.98E-01
SR0861	lp38	24109	24183	+	1.15	3.35E-01	0.22	9.59E-01
SR0862	lp38	24736	24810	+	0.90	4.09E-01	1.03	3.16E-01
SR0863	lp38	24777	24988	-	0.15	9.38E-01	0.66	2.92E-01
SR0864	lp38	26035	26126	+	-0.45	5.10E-01	-0.01	9.92E-01
SR0865	lp38	26484	26597	+	1.66	2.94E-02	1.33	8.29E-02
SR0866	lp38	26536	26600	-	1.64	4.05E-02	1.50	5.38E-02
SR0867	lp38	28965	29014	+	1.26	6.94E-01	-1.63	6.68E-01
SR0868	lp38	29116	29204	+	0.00	1.00E+00	-0.93	5.98E-01
SR0869	lp38	29541	29610	+	0.99	4.36E-01	0.57	7.38E-01
SR0870	lp38	29837	29893	-	0.01	9.92E-01	-0.23	9.06E-01
SR0871	lp38	30642	30724	-	0.05	9.89E-01	0.21	9.59E-01
SR0872	lp38	32186	32235	+	0.97	2.44E-01	0.68	4.75E-01
SR0873	lp38	33225	33332	+	1.28	3.47E-01	0.47	8.42E-01
SR0874	lp38	34706	34755	+	0.82	5.49E-01	0.83	5.56E-01
SR0875	lp38	35143	35223	-	0.05	9.89E-01	0.21	9.59E-01
SR0876	lp38	36354	36403	+	0.33	9.80E-01	-0.08	9.83E-01
SR0877	lp38	37024	37117	+	0.10	9.89E-01	-0.38	9.59E-01
SR0878	lp38	37312	37365	+	-0.92	9.85E-01	-0.75	9.59E-01
SR0879	lp38	38374	38508	-	3.41	2.67E-09	0.02	9.92E-01
SR0880	lp54	2261	2354	-	0.05	9.89E-01	0.21	9.59E-01
SR0881	lp54	3623	3672	-	0.05	9.89E-01	0.21	9.59E-01
SR0882	lp54	4604	4715	-	-0.66	5.55E-01	-0.05	9.78E-01
SR0883	lp54	8022	8074	-	0.77	1.28E-01	0.17	8.69E-01
SR0884	lp54	10502	10586	+	0.05	9.89E-01	0.21	9.59E-01
SR0885	lp54	11249	11304	+	-0.53	5.33E-01	-0.44	6.40E-01
SR0886	lp54	11313	11372	-	-0.97	1.77E-01	-0.82	2.50E-01
SR0887	lp54	11430	11587	-	-0.34	6.21E-01	0.22	7.97E-01
SR0888	lp54	11715	11849	+	0.97	4.15E-02	1.97	4.28E-07
SR0889	lp54	11974	12040	-	0.69	3.39E-01	1.19	4.38E-02
SR0890	lp54	12814	13093	+	0.31	5.82E-01	0.11	9.47E-01
SR0891	lp54	14845	15059	+	1.17	2.17E-01	1.15	2.08E-01
SR0892	lp54	15329	15379	+	0.85	2.34E-01	0.35	7.15E-01
SR0893	lp54	17585	17646	+	0.50	7.34E-01	-0.79	5.90E-01

SR0894	lp54	17624	17795	-	0.48	3.12E-01	-0.51	2.78E-01
SR0895	lp54	18718	18780	-	0.19	9.73E-01	-0.09	9.59E-01
SR0896	lp54	23118	23236	+	1.35	7.41E-04	0.16	8.73E-01
SR0897	lp54	23475	23538	-	1.55	8.29E-01	0.21	9.78E-01
SR0898	lp54	25104	25162	+	0.31	9.12E-01	1.37	2.03E-01
SR0899	lp54	25131	25289	-	-0.74	5.46E-01	1.30	1.81E-01
SR0900	lp54	29365	29422	-	0.24	8.45E-01	-1.26	4.38E-02
SR0901	lp54	29435	29515	+	0.05	9.89E-01	0.21	9.59E-01
SR0902	lp54	39336	39435	-	1.50	3.74E-01	0.24	9.59E-01
SR0903	lp54	39493	39539	-	1.37	3.92E-01	1.03	5.74E-01
SR0904	lp54	41163	41261	+	-0.19	9.32E-01	-0.07	9.59E-01
SR0905	lp54	41173	41266	-	1.13	1.15E-01	-0.04	9.79E-01
SR0906	lp54	41328	41380	-	-0.77	2.51E-01	-0.24	8.24E-01
SR0907	lp54	41530	41649	+	-0.68	1.92E-01	-1.06	1.55E-02
SR0908	lp54	42671	42743	-	0.05	9.89E-01	0.21	9.59E-01
SR0909	lp54	44646	44713	-	1.60	2.94E-02	0.77	3.95E-01
SR0910	lp54	44818	44870	-	0.05	9.89E-01	0.21	9.59E-01
SR0911	lp54	45194	45286	+	1.73	7.71E-03	0.22	8.99E-01
SR0912	lp54	46072	46181	-	0.52	7.09E-01	1.32	1.75E-01
SR0913	lp54	46406	46458	-	-0.61	7.70E-01	0.12	9.59E-01
SR0914	lp54	47340	47433	+	-0.93	6.29E-01	-0.38	9.25E-01
SR0915	lp54	48337	48441	+	1.25	4.95E-01	1.20	5.28E-01
SR0916	lp54	49370	49433	-	-0.39	9.52E-01	0.53	8.89E-01
SR0917	lp54	50265	50344	-	-1.57	8.48E-02	0.70	5.41E-01
SR0918	lp54	51191	51239	-	-0.71	4.72E-01	0.28	8.67E-01
SR0919	lp54	51485	51540	+	-1.16	6.15E-01	-2.25	2.43E-01
SR0920	lp56	1727	1773	-	-0.05	9.89E-01	0.05	9.59E-01
SR0921	lp56	4293	4342	-	-1.43	1.24E-01	0.63	6.02E-01
SR0922	lp56	19795	19847	-	0.25	7.01E-01	-2.13	8.22E-09
SR0923	lp56	22612	22685	-	0.78	7.96E-01	0.44	9.49E-01
SR0924	lp56	24875	24928	+	0.05	9.89E-01	0.21	9.59E-01
SR0925	lp56	31737	31810	-	-0.69	6.22E-01	-3.22	1.01E-02
SR0926	lp56	37477	37590	-	0.79	4.48E-01	0.62	5.99E-01
SR0927	lp56	41099	41203	-	-0.56	9.21E-01	-0.79	8.44E-01
SR0928	lp56	43488	43558	-	0.05	9.89E-01	0.21	9.59E-01
SR0929	lp56	49567	49649	+	1.02	2.88E-01	0.23	9.39E-01
SR0930	cp 9	133	283	+	0.00	1.00E+00	1.18	9.59E-01
SR0931	cp 9	2128	2308	+	2.48	2.83E-01	13.29	4.36E-25
SR0932	cp 9	2603	2653	+	NA	NA	NA	NA
SR0933	cp 9	2697	2774	-	NA	NA	NA	NA
SR0934	cp 9	2775	2915	+	NA	NA	NA	NA
SR0935	cp 9	4067	4159	+	NA	NA	NA	NA
SR0936	cp 9	5230	5289	+	NA	NA	NA	NA
SR0937	cp 9	5823	5890	+	NA	NA	NA	NA
SR0938	cp 9	5984	6034	-	NA	NA	NA	NA
SR0939	cp 9	6308	6404	+	NA	NA	NA	NA
SR0940	cp 9	6624	6722	-	NA	NA	NA	NA
SR0941	cp 9	7132	7181	-	NA	NA	NA	NA
SR0942	cp 9	7829	7897	+	NA	NA	NA	NA
SR0943	cp 9	8366	8437	-	NA	NA	NA	NA
SR0944	cp 9	9218	9267	+	NA	NA	NA	NA
SR0945	cp 26	870	955	+	-0.92	1.18E-02	1.78	3.07E-09
SR0946	cp 26	1973	2066	+	0.12	9.55E-01	-0.30	7.26E-01
SR0947	cp 26	2288	2338	+	0.28	9.60E-01	0.90	6.11E-01
SR0948	cp 26	2376	2476	+	-0.58	3.68E-01	1.93	1.48E-05
SR0949	cp 26	2406	2475	-	0.43	7.69E-01	1.36	1.23E-01
SR0950	cp 26	2604	2683	-	0.05	9.89E-01	0.21	9.59E-01
SR0951	cp 26	3191	3257	+	-0.22	7.54E-01	2.29	8.64E-11
SR0952	cp 26	6558	6607	+	-0.60	8.71E-01	0.24	9.59E-01
SR0953	cp 26	7013	7135	-	1.80	1.76E-05	0.92	5.56E-02
SR0954	cp 26	7267	7354	+	0.05	9.89E-01	0.21	9.59E-01
SR0955	cp 26	7671	7782	-	0.18	9.60E-01	0.40	7.71E-01
SR0956	cp 26	7673	7740	+	0.47	8.89E-01	0.05	9.87E-01
SR0957	cp 26	7794	7856	+	0.75	3.45E-01	2.09	3.48E-04

SR0958	cp 26	8033	8111	-	1.18	1.77E-02	1.03	3.58E-02
SR0959	cp 26	8638	8764	+	0.07	9.89E-01	-0.34	9.59E-01
SR0960	cp 26	10223	10292	-	0.52	6.55E-01	-0.05	9.77E-01
SR0961	cp 26	10732	10791	+	1.91	6.73E-02	1.80	7.91E-02
SR0962	cp 26	10804	10884	-	-1.05	6.69E-01	-1.25	6.05E-01
SR0963	cp 26	11217	11342	+	0.43	3.73E-01	-0.03	9.64E-01
SR0964	cp 26	11625	11690	-	0.13	9.89E-01	0.30	9.59E-01
SR0965	cp 26	11977	12247	+	0.97	7.51E-02	0.66	2.51E-01
SR0966	cp 26	12302	12351	-	0.27	7.49E-01	0.55	3.61E-01
SR0967	cp 26	13617	13679	+	1.30	4.24E-01	0.02	9.96E-01
SR0968	cp 26	13913	14140	+	-0.43	3.95E-01	-0.10	9.54E-01
SR0969	cp 26	16309	16407	-	0.80	8.62E-01	0.21	9.59E-01
SR0970	cp 26	17917	18032	-	0.38	6.94E-01	-0.35	7.53E-01
SR0971	cp 26	20105	20208	-	0.05	9.89E-01	0.21	9.59E-01
SR0972	cp 26	20473	20664	-	-1.65	NA	-2.33	NA
SR0973	cp 26	21021	21080	-	0.05	9.89E-01	0.21	9.59E-01
SR0974	cp 26	21879	21987	+	0.72	7.47E-01	0.37	9.44E-01
SR0975	cp 26	21903	21952	-	0.67	3.79E-01	0.83	2.27E-01
SR0976	cp 26	23233	23305	+	0.68	8.92E-01	-0.77	8.99E-01
SR0977	cp 32-1	16391	16498	+	-0.14	9.89E-01	-0.44	8.31E-01
SR0978	cp 32-1	17551	17705	+	0.66	5.67E-01	-0.03	9.86E-01
SR0979	cp 32-1	18870	18932	-	-0.21	9.84E-01	0.60	7.69E-01
SR0980	cp 32-1	22671	22740	-	-1.21	1.66E-02	-1.42	2.38E-03
SR0981	cp 32-3	16665	16711	-	0.22	9.89E-01	0.72	7.55E-01
SR0982	cp 32-3	19353	19421	-	-0.36	9.44E-01	1.53	3.01E-01
SR0983	cp 32-4	11486	11540	-	-0.02	9.89E-01	0.08	9.59E-01
SR0984	cp 32-4	18691	18778	-	0.90	6.48E-01	0.81	7.02E-01
SR0985	cp 32-4	22381	22447	+	-0.53	9.60E-01	0.96	8.17E-01
SR0986	cp 32-4	27534	27583	+	0.52	6.55E-01	-1.53	9.44E-02
SR0987	cp 32-4	28029	28167	-	-0.45	5.81E-01	0.36	6.85E-01
SR0988	cp 32-6	11520	11602	-	0.20	8.27E-01	0.14	9.34E-01
SR0989	cp 32-6	17657	17711	+	0.28	9.88E-01	-0.04	9.91E-01
SR0990	cp 32-6	18834	18884	-	-1.12	3.35E-01	1.27	2.18E-01
SR0991	cp 32-6	19451	19503	-	0.85	9.73E-02	0.72	1.69E-01
SR0992	cp 32-6	21424	21518	+	0.17	9.57E-01	-1.22	1.23E-01
SR0993	cp 32-6	27205	27254	-	0.43	9.12E-01	1.32	4.45E-01
SR0994	cp 32-6	27219	27266	+	0.63	2.90E-01	1.18	1.34E-02
SR0995	cp 32-7	12297	12411	+	0.44	9.68E-01	0.21	9.59E-01
SR0996	cp 32-7	18868	18934	-	-1.81	4.17E-02	1.31	1.07E-01
SR0997	cp 32-7	28487	28536	-	1.17	1.95E-01	0.82	4.08E-01
SR0998	cp 32-8	17578	17652	+	-0.67	9.01E-01	-0.50	9.56E-01
SR0999	cp 32-8	18849	18908	-	-1.32	5.38E-01	1.76	2.24E-01
SR1000	cp 32-8	20743	20904	+	0.42	9.24E-01	0.41	9.35E-01
SR1001	cp 32-8	22556	22605	-	-0.73	6.87E-02	-0.66	9.33E-02
SR1002	cp 32-8	23033	23091	+	0.40	9.81E-01	0.56	9.48E-01
SR1003	cp 32-9	17636	17737	+	0.65	8.81E-01	0.23	9.59E-01
SR1004	cp 32-9	18914	18980	-	0.05	9.95E-01	1.15	9.44E-01
SR1005	cp 32-9	27800	27896	+	0.40	8.64E-01	0.43	8.36E-01

REFERENCES

1. Innis, M. A., K. B. Myambo, D. H. Gelfand, and M. A. Brow. 1988. DNA sequencing with Thermus aquaticus DNA polymerase and direct sequencing of polymerase chain reaction-amplified DNA. Proceedings of the National Academy of Sciences 85:9436-9440.

2. Frigaard, N.-U., and C. Dahl. 2008. Sulfur Metabolism in Phototrophic Sulfur Bacteria. Advances in Microbial Physiology 54:103-200.

3. Lefèvre, C. T., and D. A. Bazylinski. 2013. Ecology, Diversity, and Evolution of Magnetotactic Bacteria. Microbiology and Molecular Biology Reviews 77:497-526.

4. Brito, E. M. S., Romero-Núñez, V.M., Caretta, C.A. et al. 2019. The bacterial diversity on steam vents from Paricutín and Sapichu volcanoes. Extremophiles 23:249-263.

5. Lladó, S., R. López-Mondéjar, and P. Baldrian. 2017. Forest Soil Bacteria: Diversity, Involvement in Ecosystem Processes, and Response to Global Change. Microbiology and Molecular Biology Reviews 81:e00063-16.

6. Cabral, J. P. S. 2010. Water Microbiology. Bacterial Pathogens and Water Int. J. Environ. Res. Public Health 7.

7. Bourdonnay, E., and T. Henry. 2016. Catch me if you can. eLife 5:e14721.

8. Bäumler, A., and F. C. Fang. 2013. Host Specificity of Bacterial Pathogens. Cold Spring Harbor Perspectives in Medicine 3.

9. Pavlov, M. Y., and M. Ehrenberg. 2013. Optimal control of gene expression for fast proteome adaptation to environmental change. Proceedings of the National Academy of Sciences 110:20527-20532.

10. Fisher, R. A., B. Gollan, and S. Helaine. 2017. Persistent bacterial infections and persister cells. Nature reviews. Microbiology 15:453-464.

11. Lytvynenko, I., H. Paternoga, A. Thrun, J. A. Maupin-furlow, C. M. T. Spahn, C. A. P. Joazeiro, I. Lytvynenko, H. Paternoga, A. Thrun, A. Balke, and T. A. Mu. 2019. Alanine Tails Signal Proteolysis in Bacterial Ribosome-Associated Quality Control Article Alanine Tails Signal Proteolysis in Bacterial Ribosome-Associated Quality Control. Cell:1-15.

12. Lobritz, M. A., P. Belenky, C. B. Porter, A. Gutierrez, J. H. Yang, E. G. Schwarz, D. J. Dwyer, A. S. Khalil, and J. J. Collins. 2015. Antibiotic efficacy is linked to bacterial cellular respiration. Proc. Natl. Acad. Sci. 112:8173-8180.

13. Pankey, G. A., and L. D. Sabath. 2004. Clinical Relevance of Bacteriostatic versus Bactericidal Mechanisms of Action in the Treatment of Gram-Positive Bacterial Infections. Clinical Infectious Diseases 38:864-870.

14. Ragheb, M., M. K. Thomason, C. Hsu, P. Nugent, J. Gage, N. Ariana, A. Kariisa, C. N. Merrikh, S. I. Miller, and H. Merrikh. 2019. Inhibiting the evolution of antibiotic resistance. Molecular Cell 73:206-221.

15. Steere ACC, M. S., Snydman DR & Andiman WA. 1976. A cluster of arthritis in children and adults in Lyme, Connecticut. Arthritis and Rheumatism 19:824-824.

16. Steere, A. C., S. E. Malawista, D. R. Snydman, R. E. Shope, W. A. Andiman, M. R. Ross, and F. M. Steele. 1977. Lyme arthritis: an epidemic of oligoarticular arthritis in children and adults in three Connecticut communities. Arthritis Rheum. 20:7-17.

17. Steere, A. C., R. T. Schoen, and E. Taylor. 1987. The clinical evolution of Lyme arthritis. Ann. Intern. Med. 107:725-731.

18. Burgdorfer, W., A. G. Barbour, S. F. Hayes, J. L. Benach, E. Grunwaldt, and J. P. Davis. 1982. Lyme disease - a tick-borne spirochetosis? Science 216:1317-1319.

19. Steere, A. C., R. L. Grodzicki, J. E. Craft, M. Shrestha, A. N. Kornblatt, and S. E. Malawista. 1984. Recovery of Lyme disease spirochetes from patients. Yale J. Biol. Med. 57:557-560.

20. Steere, A. C., R. L. Grodzicki, A. N. Kornblatt, J. E. Craft, A. G. Barbour, W. Burgdorfer, G. P. Schmid, E. Johnson, and S. E. Malawista. 1983. The spirochetal etiology of Lyme disease. N. Engl. J. Med. 308:733-740.

21. Walter, K. S., G. Carpi, A. Caccone, and M. A. Diuk-Wasser. 2017. Genomic insights into the ancient spread of Lyme disease across North America. Nature Ecology & Evolution 1:1569-1576.

22. Takayama, K., R. J. Rothenberg, and A. G. Barbour. 1987. Absence of lipopolysaccharide in the Lyme disease spirochete, *Borrelia burgdorferi*. Infect. Immun. 55:2311-2313.

23. Fraser, C. M., S. Casjens, W. M. Huang, G. G. Sutton, R. Clayton, R. Lathigra, O. White, K. A. Ketchum, R. Dodson, E. K. Hickey, M. Gwinn, B. Dougherty, J.-F. Tomb, R. D. Fleischmann, D. Richardson, J. Peterson, A. R. Kerlavage, J. Quackenbush, S. Salzberg, M. Hanson, R. van Vugt, N. Palmer, M. D. Adams, J. Gocayne, J. Weidmann, T. Utterback, L. Watthey, L. McDonald, P. Artiach, C. Bowman, S. Garland, C. Fujii, M. D. Cotton, K. Horst, K. Roberts, B. Hatch, H. O. Smith, and J. C. Venter. 1997. Genomic sequence of a Lyme disease spirochaete, *Borrelia burgdorferi*. Nature 390:580-586.

24. Berger, B. W., R. C. Johnson, C. Kodner, and L. Coleman. 1992. Cultivation of *Borrelia burgdorferi* from erythema migrans lesions and perilesional skin. J. Clin. Microbiol. 30:359-361.

25. Hansen, K., and E. Asbrink. 1989. Serodiagnosis of erythema migrans and acrodermatitis chronica atrophicans by the *Borrelia burgdorferi* flagellum enzyme-linked immunosorbent assay. J. Clin. Microbiol. 27:545-551.

26. Steere, A. C., S. E. Malawista, J. A. Hardin, S. Ruddy, P. W. Askenase, and W. A. Andiman. 1977. Erythema chronicum migrans and Lyme arthritis. The enlarging clinical spectrum. Ann. Intern. Med. 86:685-698.

27. Hu, L. T. 2016. Lyme Disease. Annals of Internal Medicine 164:ITC65-ITC80.

28. Steere, A. C., S. E. Malawista, J. H. Newman, P. N. Spieler, and N. H. Bartenhagen. 1980. Antibiotic therapy in Lyme disease. Ann. Intern. Med. 93:1-8.

29. Steere, A. C. 1997. Diagnosis and treatment of Lyme arthritis. Med. Clin. N. Am. 81:179-194.

30. Steere, A. C., W. P. Batsford, M. Weinberg, J. Alexander, H. J. Berger, S. Wolfson, and S. E. Malawista. 1980. Lyme carditis: cardiac abnormalities of Lyme disease. Ann. Intern. Med. 93:8-16.

31. Steere, a. C., J. a. Hardin, and S. E. Malawista. 1977. Erythema chronicum migrans and Lyme arthritis: cryoimmunoglobulins and clinical activity of skin and joints. Science (New York, N.Y.) 196:1121-1122.

32. Lochhead, R. B., D. Ordoñez, S. L. Arvikar, J. M. Aversa, L. S. Oh, B. Heyworth, R. Sadreyev, A. C. Steere, and K. Strle. 2019. Interferon-gamma production in Lyme arthritis synovial tissue promotes differentiation of fibroblast-like synoviocytes into immune effector cells. Cellular Microbiology 21:e12992.

33. Lochhead, R. B., S. L. Arvikar, J. M. Aversa, R. I. Sadreyev, K. Strle, and A. C. Steere. 2019. Robust interferon signature and suppressed tissue repair gene expression in synovial tissue from patients with postinfectious, Borrelia burgdorferi-induced Lyme arthritis. Cellular Microbiology 21:e12954.

34. Sulka, K. B., K. Strle, J. T. Crowley, R. B. Lochhead, R. Anthony, and A. C. Steere. 2018. Correlation of Lyme Disease–Associated IgG4 Autoantibodies With Synovial Pathology in Antibiotic-Refractory Lyme Arthritis. Arthritis & Rheumatology 70:1835-1846.

35. Stefan, N., S. Elsner, M. Schnaidt, D. Wernet, and M. Stumvoll. 1999. Autoimmune thrombocytopenia associated with *Borrelia burgdorferi*. Clin. Infect. Dis. 28:927.

36. Wormser, G. P., S. O'Connell, A. R. Pachner, I. Schwartz, E. D. Shapiro, G. Stanek, and F. Strle. 2018. Critical analysis of a doxycycline treatment trial of rhesus

macaques infected with Borrelia burgdorferi. Diagnostic Microbiology and Infectious Disease 92:183-188.

37. Li X, M. G., Damle N, Sikand VK, Glickstein L, Steere AC. 2011. Burden and viability of Borrelia burgdorferi in skin and joints of patients with erythema migrans or Lyme arthritis. Arthritis Rheum 63:2238-47.

38. Jutras, B. L., R. B. Lochhead, Z. A. Kloos, J. Biboy, K. Strle, C. J. Booth, S. K. Govers, J. Gray, P. Schumann, W. Vollmer, L. K. Bockenstedt, A. C. Steere, and C. Jacobs-Wagner. 2019. Borrelia burgdorferi peptidoglycan is a persistent antigen in patients with Lyme arthritis. Proceedings of the National Academy of Sciences:201904170.

39. Beck, G., J. L. Benach, and G. S. Habicht. 1990. Isolation, preliminary chemical characterization, and biological activity of Borrelia burgdorferi peptidoglycan. Biochemical and Biophysical Research Communications 167:89-95.

40. Steere, A. C., F. Strle, G. P. Wormser, L. T. Hu, J. A. Branda, J. W. R. Hovius, X. Li, and P. S. Mead. 2016. Lyme borreliosis. Nature Reviews Disease Primers 2.

41. Brown, R. N., and R. S. Lane. 1992. Lyme disease in California: a novel enzootic transmission cycle of *Borrelia burgdorferi*. Science 256:1439-1442.

42. Jacquet, M., D. Genne, A. Belli, E. Maluenda, A. Sarr, and M. Voordouw. 2017. The abundance of the Lyme diseaase pathogen *Borrelia afzelii* declines over time in the tick vector *Ixodes ricinus*. Parasites & Vectors.

43. Sarr, A., A. Gomez-chamorro, J. Durand, C. Cayol, O. Rais, and M. J. Voordouw. 2018. Competition between strains of Borrelia afzelii inside the rodent host and the tick vector. Proc of the Royal Academy B 285:17-20.

44. Piesman, J., N. S. Zeidner, and B. S. Schneider. 2003. Dynamic changes in *Borrelia burgdorferi* populations in *Ixodes scapularis* (Acari: Ixodidae) during transmission: studies at the mRNA level. Vector Borne Zoonotic Dis. 3:125-132.

45. Schoeler, G. B., and R. S. Lane. 1993. Efficiency of transovarial transmission of the Lyme disease spirochete, *Borrelia burgdorferi*, in the western blacklegged tick, *Ixodes pacificus* (Acari: Ixodidae). J. Med. Entomol. 30:80-86.

46. Stanek, G., and F. Strle. 2018. Lyme borreliosis–from tick bite to diagnosis and treatment. FEMS Microbiology Reviews:1-26.

47. Piesman, J., G. O. Maupin, E. G. Campos, and C. M. Happ. 1991. Duration of adult female *Ixodes dammini* attachment and transmission of *Borrelia burgdorferi*, with description of a needle aspiration isolation method. J. Infect. Dis. 163:895-897.

48. Piesman, J., J. R. Oliver, and R. J. Sinsky. 1990. Growth kinetics of the Lyme disease spirochete (*Borrelia burgdorferi*) in vector ticks (*Ixodes dammini*). Am. J. Trop. Med. Hyg. 42:352-357.

49. Spielman, A., M. L. Wilson, J. F. Levine, and J. Piesman. 1985. Ecology of *Ixodes dammini*-borne babesiosis and Lyme disease. Ann. Rev. Entomol. 30:439-460.

50. Vandyk, J. K., D. M. Bartholomew, W. a. Rowley, and K. B. Platt. 1996. Survival of Ixodes scapularis (Acari: Ixodidae) exposed to cold. Journal of medical entomology 33:6-10.

51. Sonenshine, D. E. 1991. Biology of Ticks, vol. 1. Oxford University Press, New York.

52. Coons, L. B., R. Rosell-Davis, and B. I. Tarnowski. 1986. Bloodmeal digestion in ticks, p. 248-279. *In* J. R. Sauer and J. A. Hair (ed.), Morphology, physiology, and behavioral biology of ticks. Ellis Horwood Limited, New York.

53. Horn, M., M. Nussbaumerová, M. Šanda, Z. Kovářová, J. Srba, Z. Franta, D. Sojka, M. Bogyo, C. R. Caffrey, P. Kopáček, and M. Mareš. 2009. Hemoglobin Digestion in Blood-Feeding Ticks: Mapping a Multipeptidase Pathway by Functional Proteomics. Chemistry and Biology 16:1053-1063.

54. Dautel, H., and W. Knülle. 1996. The supercooling ability of ticks (Acari, Ixodoidea). Journal of Comparative Physiology - B Biochemical, Systemic, and Environmental Physiology 166:517-524.

55. Davis, G. E. 1942. Tick vectors and life cycles of ticks. Am. Assn. Adv. Sci. 18:67-76.

56. Gylfe, Å., S. Bergström, J. Lundström, and B. Olsen. 2000. Reactivation of *Borrelia* infection in birds. Nature 403:724-725.

57. Nieto, N. C., W. T. Porter, J. C. Wachara, T. J. Lowrey, L. Martin, P. J. Motyka, and D. J. Salkeld. 2018. Using citizen science to describe the prevalence and distribution of tick bite and exposure to tick-borne diseases in the United States. PLOS One 13:1-14.

58. Mendoza-Roldan, J. A., V. Colella, R. P. Lia, V. L. Nguyen, D. M. Barros-Battesti, R. Iatta, F. Dantas-Torres, and D. Otranto. 2019. Borrelia burgdorferi (sensu lato) in ectoparasites and reptiles in southern Italy. Parasites & Vectors 12:35.

59. Swanson, K. I., and D. E. Norris. 2007. Detection of Borrelia burgdorferi DNA in Lizards from Southern Maryland. Vector-Borne and Zoonotic Diseases 7:42-49.

60. Arsnoe, I. M., G. J. Hickling, H. S. Ginsberg, R. McElreath, and J. I. Tsao. 2015. Different populations of blacklegged tick nymphs exhibit differences in questing

behavior that have implications for human Lyme disease risk. PLoS ONE 10:e0127450.

61. Han, S., C. Lubelczyk, G. J. Hickling, A. A. Belperron, L. K. Bockenstedt, and J. I. Tsao. 2019. Ticks and Tick-borne Diseases Vertical transmission rates of Borrelia miyamotoi in Ixodes scapularis collected from white-tailed deer. Ticks and Tick-borne Diseases:0-1.

62. Bissett, M. L., and W. Hill. 1987. Characterization of *Borrelia burgdorferi* strains isolated from *Ixodes pacificus* ticks in California. J. Clin. Microbiol. 25:2296-2301.

63. Burgdorfer, W., R. S. Lane, A. G. Barbour, R. A. Gresbrink, and J. R. Anderson. 1985. The western black-legged tick, *Ixodes pacificus*, a vector of *Borrellia burgdorferi*. Am. J. Trop. Med. Hyg. 34:925-930.

64. Peavey, C. A., and R. S. Lane. 1995. Transmission of *Borrelia burgdorferi* by *Ixodes pacificus* nymphs and reservoir competence of deer mice (*Peromyscus maniculatus*) infected by tick-bite. J. Parasitol. 81:175-178.

65. Piesman, J., K. L. Clark, M. C. Dolan, C. M. Happ, and T. R. Burkot. 1999. Geographic survey of vector ticks (*Ixodes scapularis* and *Ixodes pacificus*) for infection with the Lyme disease spirochete, *Borrelia burgdorferi*. J. Vector Ecol. 24:91-98.

66. Rose I, Y. M., Bonilla DL, Fedorova N, Lane RS, et al. 2019. Phylogeography of Borrelia spirochetes in Ixodes pacificus and Ixodes spinipalpis ticks highlights differential acarological risk of tick-borne disease transmission in northern versus southern California PLOS ONE 14:e0214726.

67. Centers for Disease Control and Prevention. 2013. CDC provides estimate of Americans diagnosed with Lyme disease each year. http://www.cdc.gov/media/releases/2013/p0819-lyme-disease.html.

68. Centers for Disease Control and Prevention. 2014. Lyme disease. www.cdc.gov/lyme.

69. Sonenshine, D. E. 2018. Range Expansion of Tick Disease Vectors in North America: Implications for Spread of Tick-Borne Disease International Journal of Environmental Research and Public Health 15.

70. Magnarelli, L. A., J. F. Anderson, and D. Fish. 1987. Transovarial transmission of *Borrelia burgdorferi* in *Ixodes dammini* (Acari:Ixodidae). J. Infect. Dis. 156:234-236.

71. Anderson, J. F. 1989. Epizootiology of *Borrelia* in *Ixodes* tick vectors and reservoir hosts. Rev. Infect. Dis. 11:S1451-S1459.

72. Persing, D. H., S. R. Telford, A. Spielman, and S. W. Barthold. 1990. Detection of *Borrelia burgdorferi* infection in *Ixodes dammini* ticks with the polymerase chain reaction. J. Clin. Microbiol. 28:566-572.

73. Ewing, C., A. Scorpio, D. R. Nelson, and T. N. Mather. 1994. Isolation of *Borrelia burgdorferi* from saliva of the tick vector, *Ixodes scapularis*. J. Clin. Microbiol. 32:755-758.

74. Pinger, R. R., L. Timmons, and K. Karris. 1996. Spread of *Ixodes scapularis* (Acari:Ixodidae) in Indiana: collections of adults in 1991-1994 and description of a *Borrelia burgdorferi*-infected population. J. Med. Entomol. 33:852-855.

75. Canale-Parola, E. 1997. Physiology and evolution of spirochetes. Bacteriol. Rev. 41:181-204.

76. Casjens, S. R., E. F. Mongodin, W. G. Qiu, B. J. Luft, S. E. Schutzer, E. B. Gilcrease, W. M. Huang, M. Vujadinovic, J. K. Aron, L. C. Vargas, S. Freeman, D. Radune, J. F. Weidman, G. I. Dimitrov, H. M. Khouri, J. E. Sosa, R. A. Halpin, J. J. Dunn, and C. M. Fraser. 2012. Genome stability of Lyme disease spirochetes: comparative genomics of *Borrelia burgdorferi* plasmids. PLoS One 7:e33280.

77. Charon, N. W., A. Cockburn, C. Li, J. Liu, K. A. Miller, M. R. Miller, M. A. Motaleb, and C. W. Wolgemuth. 2012. The unique paradigm of spirochete motility and chemotaxis. Annual review of microbiology 66:349-70.

78. Goldstein, S. F., N. W. Charon, and J. A. Kreiling. 1994. *Borrelia burgdorferi* swims with a planar waveform similar to that of eukaryotic flagella. Proc. Natl. Acad. Sci. USA 91:3433-3437.

79. Motaleb, M. A., L. Corum, J. L. Bono, A. F. Elias, P. Rosa, D. S. Samuels, and N. W. Charon. 2000. *Borrelia burgdorferi* periplasmic flagella have both skeletal and motility functions. Proceedings of the National Academy of Sciences 97:10899-904.

80. Li, C., R. G. Bakker, M. A. Motaleb, M. L. Sartakova, F. C. Cabello, and N. W. Charon. 2002. Asymmetrical flagellar rotation in Borrelia burgdorferi nonchemotactic mutants. Proceedings of the National Academy of Sciences of the United States of America 99:6169-6174.

81. Kumar, B., K. Miller, N. W. Charon, and J. Legleiter. 2017. Periplasmic flagella in Borrelia burgdoferi function to maintain cellular integrity upon external stress. Plos One 12:11-13.

82. Barbour, A. G., and C. F. Garon. 1987. Linear plasmids of the bacterium *Borrelia burgdorferi* have covalently closed ends. Science 237:409-411.

83. Simpson, W. J., C. F. Garon, and T. G. Schwan. 1990. Analysis of supercoiled circular plasmids in infectious and non-infectious *Borrelia burgdorferi*. Microb. Pathog. 8:109-118.

84. Casjens, S., N. Palmer, R. Van Vugt, W. M. Huang, B. Stevenson, P. Rosa, R. Lathigra, G. Sutton, J. Peterson, R. J. Dodson, D. Haft, E. Hickey, M. Gwinn, O. White, and C. M. Fraser. 2000. A bacterial genome in flux: the twelve linear and nine circular extrachromosomal DNAs of an infectious isolate of the Lyme disease spirochete Borrelia burgdorferi. Molecular Microbiology 35:490-516.

85. Tilly, K., C. Checroun, and P. A. Rosa. 2012. Plasmid Requirements for Borrelia burgdorferi plasmid maintenance. Plasmid 68:1-12.

86. Casjens, S. R., L. Di, S. Akther, E. F. Mongodin, B. J. Luft, S. E. Schutzer, C. M. Fraser, and W.-g. Qiu. 2018. Primordial origin and diversification of plasmids in Lyme disease agent bacteria. BMC Genomics:1-24.

87. Saint Girons, I., and B. E. Davidson. 1992. Genome organization of *Borrelia burgdorferi*, p. 111-118. *In* J. Ingilis and J. W. Sitkowski (ed.), Lyme Disease: Molecular and Immunologic Approaches. Cold Spring Harbor Laboratory Press, Cold Spring Harbor, N.Y.

88. Casjens, S., and W. M. Huang. 1996. The linear chromosomes of *Borrelia burgdorferi* and the other Lyme disease spirochetes, p. in press. *In* F. de Bruijn, G. Weinstock, and J. Lupski (ed.), Bacterial Genomes: Physical Structure and Analysis. Chapman and Hall, New York.

89. Busch, U., G. Will, C. Hizo-Teufel, B. Wilske, and V. Preac-Mursic. 1997. Long term *in vitro* cultivation of *Borrelia burgdorferi* sensu lato strains: influence on plasmid patterns, genome stability and expression of proteins. Res. Microbiol. 148:109-118.

90. Stewart, P. E., G. Chaconas, and P. Rosa. 2003. Conservation of plasmid maintenance functions between linear and circular plasmids in *Borrelia burgdorferi*. J. Bacteriol. 185:3202-3209.

91. Iyer, R., O. Kalu, J. Purser, S. Norris, B. Stevenson, and I. Schwartz. 2003. Linear and circular plasmid content in *Borrelia burgdorferi* clinical isolates. Infect. Immun. 71:3699-3706.

92. Casjens, S. R., E. B. Gilcrease, M. Vujadinovic, E. F. Mongodin, B. J. Luft, S. E. Schutzer, C. M. Fraser, and W. G. Qiu. 2017. Plasmid diversity and phylogenetic consistency in the Lyme disease agent *Borrelia burgdorferi*. BMC Genomics 18:165.

93. Grimm, D., K. Tilly, D. M. Bueschel, M. A. Fisher, P. F. Policastro, F. C. Gherardini, T. G. Schwan, and P. A. Rosa. 2005. Defining plasmids required by

Borrelia burgdorferi for colonization of tick vector *Ixodes scapularis* (Acari: Ixodidae). J. Med. Entomol. 42:676-684.

94. Stevenson, B., N. El-hage, M. A. Hines, C. Miller, K. Babb, and J. C. Miller. 2002. Differential Binding of Host Complement Inhibitor Factor H by Borrelia burgdorferi Erp Surface Proteins : a Possible Mechanism Underlying the Expansive Host Range of Lyme Disease Spirochetes Differential Binding of Host Complement Inhibitor Factor H. Infect. Immun. 70:491-497.

95. Xu, Y., C. Kodner, L. Coleman, and R. C. Johnson. 1996. Correlation of plasmids with infectivity of *Borrelia burgdorferi* sensu stricto type strain B31. Infect. Immun. 64:3870-3876.

96. Iyer, R., O. Kalu, I. Schwartz, and B. Stevenson. 1999. Clinical isolates of *Borrelia burgdorferi* from Lyme disease patients contain multiple 32kb circular plasmids, abstr. D/B-260, p. 259, Abstracts of the 99th General Meeting of the American Society for Microbiology. American Society for Microbiology, Washington, D.C.

97. Stewart, P. E., R. Byram, D. Grimm, K. Tilly, and P. A. Rosa. 2005. The plasmids of *Borrelia burgdorferi*: essential genetic elements of a pathogen. Plasmid 53:1-13.

98. Strother, K. O., A. Broadwater, and D. A. D. Silva. 2005. Plasmid Requirements for Infection of Ticks by Borrelia burgdorferi. Vector-Borne and Zoonotic Diseases 5:237-245.

99. Charon, N. W., E. P. Greenberg, M. B. H. Koopman, and R. J. Limberger. 1992. Spirochete chemotaxis, motility, and the structure of the spirochetal periplasmic flagella. Res. Microbiol. 143:597-603.

100. Li, C., M. A. Motaleb, M. Sal, S. F. Goldstein, and N. W. Charon. 2000. Spirochete periplasmic flagella and motility. J. Mol. Microbiol. Biotechnol. 2:345-354.

101. Sultan, S. Z., P. Sekar, X. Zhao, A. Manne, J. Liu, R. M. Wooten, and M. A. Motaleb. 2015. Motor rotation is essential for the formation of the periplasmic flagellar ribbon, cellular morphology, and Borrelia burgdorferi persistence within Ixodes scapularis tick and murine hosts. Infection and Immunity 83:1765-1777.

102. Motaleb, M. A., M. R. Miller, R. G. Bakker, C. Li, and N. W. Charon. 2007. Isolation and Characterization of Chemotaxis Mutants of the Lyme Disease Spirochete Borrelia burgdorferi Using Allelic Exchange Mutagenesis, Flow Cytometry, and Cell Tracking. Methods in Enzymology 422.

103. Sal, M. S., C. Li, M. A. Motalab, S. Shibata, S. I. Aizawa, and N. W. Charon. 2008. Borrelia burgdorferi uniquely regulates its motility genes and has an intricate flagellar hook-basal body structure. Journal of Bacteriology 190:1912-1921.

104. Dombrowski, C., W. Kan, M. A. Motaleb, N. W. Charon, R. E. Goldstein, and C. W. Wolgemuth. 2009. The elastic basis for the shape of Borrelia burgdorferi. Biophysical Journal 96:4409-4417.

105. Dunham-Ems, S. M., M. J. Caimano, U. Pal, C. W. Wolgemuth, C. H. Eggers, A. Balic, and J. D. Radolf. 2009. Live imaging reveals a biphasic mode of dissemination of *Borrelia burgdorferi* within ticks. The Journal of Clinical Investigation 119:3652-3665.

106. Golde, W. T., K. J. Kappel, G. Dequesne, C. Feron, D. Plainchamp, C. Capiau, and Y. Lobet. 1994. Tick transmission of *Borrelia burgdorferi* to inbred strains of mice induces an antibody response to P39 but not to outer surface protein A. Infect. Immun. 62:2625-2627.

107. Crippa, M., O. Rais, and L. Gern. 2002. Investigations on the mode and dynamics of transmission and infectivity of *Borrelia burgdorferi* sensu stricto and *Borrelia afzelii* in *Ixodes ricinus* ticks. Vector Borne Zoon. Dis. 2:3-9.

108. Boyle, W. K., H. K. Wilder, A. M. Lawrence, and J. E. Lopez. 2014. Transmission dynamics of *Borrelia turicatae* from the arthropod vector. PLoS Neglected Trop. Dis. 8:e2767.

109. Sze, C. W., K. Zhang, T. Kariu, U. Pal, and C. Li. 2012. Borrelia burgdorferiNeeds Chemotaxis To Establish Infection in Mammals and To Accomplish Its Enzootic Cycle. Infection and Immunity 80:2485-2492.

110. Adams, P. P., C. F. Avile, N. Popitsch, I. Bilusic, R. Schroeder, M. Lybecker, and M. W. Jewett. 2017. In vivo expression technology and 5′ end mapping of the Borrelia burgdorferi transcriptome identify novel RNAs expressed during mammalian infection. Nucleic Acids Research 45:775-792.

111. Narasimhan, S., F. Santiago, R. A. Koski, B. Brei, J. F. Anderson, D. Fish, and E. Fikrig. 2002. Examination of the *Borrelia burgdorferi* transcriptome in *Ixodes scapularis* during feeding. J. Bacteriol. 184:3122-3125.

112. Bouquet, J., M. J. Soloski, A. Swei, C. Cheadle, S. Federman, J.-n. Billaud, and A. W. Rebman. 2016. Longitudinal Transcriptome Analysis Reveals a Sustained Differential Gene Expression Signature in Patients Treated for Acute Lyme Disease. mBio 7:1-11.

113. Iyer, R., and I. Schwartz. 2016. Microarray-based comparative genomic and transcriptome analysis of *Borrelia burgdorferi*. Microarrays 5:pii: E9.

114. Angel, T. E., B. J. Luft, X. Yang, C. D. Nicora, D. G. Camp, J. M. Jacobs, and R. D. Smith. 2010. Proteome analysis of Borrelia burgdorferi response to environmental change. PLoS ONE 5:e13800.

115. Dowdell, A. S., M. D. Murphy, C. Azodi, S. K. Swanson, L. Florens, S. Chen, and W. R. Zückert. 2017. Comprehensive spatial analysis of the *Borrelia burgdorferi* lipoproteome reveals a compartmentalization bias toward the bacterial surface. J. Bacteriol. 199:e00658-16.

116. Toledo, A., Z. Huang, J. L. Coleman, E. London, and J. L. Benach. 2018. Lipid rafts can form in the inner and outer membranes of Borrelia burgdorferi and have different properties and associated proteins. Molecular Microbiology 108:63-76.

117. Pal, U., X. Li, T. Wang, R. R. Montgomery, N. Ramamoorthi, A. M. deSilva, F. Bao, X. Yang, M. Pypaert, D. Pradhan, F. S. Kantor, S. Telford, J. F. Anderson, and E. Fikrig. 2004. TROSPA, an *Ixodes scapularis* receptor for *Borrelia burgdorferi*. Cell 119:457-468.

118. de Silva, A. M., S. R. Telford, L. R. Brunet, S. W. Barthold, and E. Fikrig. 1996. *Borrelia burgdorferi* OspA is an arthropod-specific transmission-blocking Lyme disease vaccine. J. Exp. Med. 183:271-275.

119. Philipp, M. T. 1998. Studies on OspA: a source of new paradigms in Lyme disease research. Trends Microbiol. 6:44-47.

120. Alverson, J., S. F. Bundle, C. D. Sohasky, M. C. Lybecker, and D. S. Samuels. 2003. Transcriptional regulation of the *ospAB* and *ospC* promoters of *Borrelia burgdorferi*. Mol. Microbiol. 48:1665-1677.

121. Yang, X. F., U. Pal, S. M. Alani, E. Fikrig, and M. V. Norgard. 2004. Essential role for OspA/B in the life cycle of the Lyme disease spirochete. J. Exp. Med. 199:641-648.

122. He, M., T. Oman, H. Xu, J. Blevins, M. V. Norgard, and X. F. Yang. 2008. Abrogation of ospAB constitutively activates the Rrp2-RpoN-RpoS pathway (sigmaN-sigmaS cascade) in *Borrelia burgdorferi*. Mol. Microbiol. 70:1453-1464.

123. Brissette, C. A., A. Verma, A. Bowman, A. E. Cooley, and B. Stevenson. 2009. The *Borrelia burgdorferi* outer-surface protein ErpX binds mammalian laminin. Microbiology 155:863-872.

124. Verma, A., C. A. Brissette, A. Bowman, and B. Stevenson. 2009. *Borrelia burgdorferi* BmpA is a laminin-binding protein. Infect. Immun. 77:4940-4946.

125. Grab, D. J., C. Givens, and R. Kennedy. 1998. Fibronectin-binding activity in *Borrelia burgdorferi*. Biochim. Biophys. Acta. 1407:135-145.

126. Kim, J. H., J. Singvall, U. Schwartz-Linek, B. J. B. Johnson, J. R. Potts, and M. Höök. 2004. BBK32, a fibronectin binding MSCRAMM from *Borrelia burgdorferi*, contains a disordered region that undergoes a conformational change on ligand binding. J. Biol. Chem. 279:41706-41714.

127. Raibaud, S., U. Schwarz-Linek, J. H. Kim, H. T. Jenkins, E. R. Baines, S. Gurusiddappa, M. Höök, and J. R. Potts. 2005. *Borrelia burgdorferi* binds fibronectin through a tandem β-zipper, a common mechanisms of fibronectin binding in staphylococci, streptococci, and spirochetes. J. Biol. Chem. 280:18803-18809.

128. Brissette, C. A., T. Bykowski, A. E. Cooley, A. Bowman, and B. Stevenson. 2009. *Borrelia burgdorferi* RevA antigen binds host fibronectin. Infect. Immun. 77:2802-2812.

129. Gaultney, R. A., T. Gonzalez, A. M. Floden, and C. A. Brissette. 2013. BB0347, from the Lyme disease spirochete *Borrelia burgdorferi*, is surface exposed and interacts with the CS1 heparin-binding domain of human fibronectin. PLoS ONE 8:e75643.

130. Hellwage, J., T. Meri, T. Heikkilä, A. Alitalo, J. Panelius, P. Lahdenne, I. J. T. Seppälä, and S. Meri. 2001. The complement regulatory factor H binds to the surface protein OspE of *Borrelia burgdorferi*. J. Biol. Chem. 276:8427-8435.

131. Kraiczy, P., J. Hellwage, C. Skerka, M. Kirschfink, V. Brade, P. F. Zipfel, and R. Wallich. 2003. Immune evasion of *Borrelia burgdorferi*: mapping of a complement inhibitor factor H-binding site of BbCRASP-3, a novel member of the Erp protein family. Eur. J. Immunol. 33:697-707.

132. Kraiczy, P., J. Hellwage, C. Skerka, H. Becker, M. Kirschfink, M. M. Simon, V. Brade, P. F. Zipfel, and R. Wallich. 2004. Complement resistance of *Borrelia burgdorferi* correlates with the expression of BbCRASP-1, a novel linear plasmid-encoded surface protein that interacts with human factor H and FHL-1 and is unrelated to Erp proteins. J. Biol. Chem. 279:2421-2429.

133. Miller, J. C., and B. Stevenson. 2004. Increased expression of *Borrelia burgdorferi* factor H-binding surface proteins during transmission from ticks to mice. Int. J. Med. Microbiol. 293 S37:120-125.

134. Kennedy, M. R., S. R. Vuppala, C. Siegel, P. Kraiczy, and D. R. Akins. 2009. CspA-mediated binding of human factor H inhibits complement deposition and confers serum resistance in *Borrelia burgdorferi*. Infect. Immun. 77:2773-2782.

135. Rogers, E. A., S. V. Abdunmur, J. V. McDowell, and R. T. Marconi. 2009. Comparative analysis of the properties and ligand binding characteristics of CspZ, a factor H binding protein, derived from *Borrelia burgdorfer* isolates of human origin. Infect. Immun. 77:4396-4405.

136. Marcnkiewicz, A. L., I. Lieknina, S. Kotelovica, X. Yang, P. Kraiczy, U. Pal, Y. P. Lin, and K. Tars. 2018. Eliminating factor H-Binding activity of Borrelia burgdorferi CspZ combined with virus-like particle conjugation enhances its efficacy as a Lyme disease vaccine. Frontiers in Immunology 9:1-11.

137. Zhi, H., J. Xie, and J. T. Skare. 2018. The classical complement Pathway is required to control Borrelia burgdorferi levels During experimental infection. Frontiers in Immunology 9:1-12.

138. Bankhead, T., and G. Chaconas. 2007. The role of VlsE antigenic variation in the Lyme disease spirochete: persistence through a mechanism that differs from other pathogens. Mol. Microbiol. 65:1547-1558.

139. Rogovskyy, A. S., and T. Bankhead. 2013. Variable VlsE is critical for host reinfection by the Lyme disease spirochete. PLoS One 8:e61226.

140. Rogovskyy, A. S., T. Casselli, Y. Tourand, C. R. Jones, J. P. Owen, K. L. Mason, G. A. Scoles, and T. Bankhead. 2015. Evaluation of the importance of VlsE antigenic variation for the enzootic cycle of Borrelia burgdorferi. PLoS ONE 10:1-21.

141. Embers, M. E., F. T. Liang, J. K. Howell, M. B. Jacobs, J. E. Purcell, S. J. Norris, B. J. B. Johnson, and M. T. Philipp. 2018. Antigenicity and recombination of VlsE, the antigenic variation protein of *Borrelia burgdorferi*, in rabbits, a host putatively resistant to long-term infection with this spirochete. FEMS immunology and medical microbiology:421-429.

142. Caimano, M. J., M. R. Kenedy, T. Kairu, D. C. Desrosiers, M. Harman, S. Dunham-Ems, D. R. Akins, U. Pal, and J. D. Radolf. 2011. The hybrid histidine kinase Hk1 is part of a two-component system that is essential for survival of *Borrelia burgdorferi* in feeding *Ixodes scapularis* ticks. Infect. Immun. 79:3117-3130.

143. He, M., Z. Ouyang, B. Troxell, H. Xu, A. Moh, J. Piesman, M. V. Norgard, M. Gomelsky, and X. F. Yang. 2011. Cyclic di-GMP is essential for the survival of the Lyme disease spirochete in ticks. PLoS Pathog. 7:e1002133.

144. Novak, E. a., S. Z. Sultan, and M. a. Motaleb. 2014. The cyclic-di-GMP signaling pathway in the Lyme disease spirochete, Borrelia burgdorferi. Frontiers in cellular and infection microbiology 4:56-56.

145. Zhang, J.-J., T. Chen, Y. Yang, J. Du, H. Li, B. Troxell, M. He, S. E. Carrasco, M. Gomelsky, and X. F. Yang. 2018. Positive and Negative Regulation of Glycerol Utilization by the c-di-GMP Binding Protein PlzA in *Borrelia burgdorferi*. Journal of Bacteriology 200:e00243-18.

146. Caimano, M. J., S. Dunham-Ems, A. M. Allard, M. B. Cassera, M. Kenedy, and J. D. Radolf. 2015. Cyclic di-GMP modulates gene expression in Lyme disease spirochetes at the tick-mammal interface to promote spirochete survival during the blood meal and tick-to-mammal transmission. Infect. Immun. 83:3043-3060.

147. He, M., J. J. Zhang, M. Ye, Y. Lou, and X. F. Yang. 2014. Cyclic Di-GMP receptor PlzA controls virulence gene expression through RpoS in Borrelia burgdorferi. Infection and Immunity 82:445-452.

148. Pitzer, J. E., S. Z. Sultan, Y. Hayakawa, G. Hobbs, M. R. Miller, and M. A. Motaleb. 2011. Analysis of the *Borrelia burgdorferi* cyclic-di-GMP-binding protein PlzA reveals a role in motility and virulence. Infect. Immun. 79:1815-1825.

149. Groshong, A. M., N. E. Gibbons, X. F. Yang, and J. S. Blevins. 2012. Rrp2, a prokaryotic enhancer-like binding protein, is essential for viability of *Borrelia burgdorferi*. J. Bacteriol. 194:3336-3342.

150. Yin, Y., Y. Youyun, X. Xiang, Q. Wang, Z.-N. Yang, J. Blevins, Y. Lou, and X. F. Yang. 2016. Insight into the dual functions of bacterial enhancer-binding protein Rrp2 of *Borrelia burgdorferi*. Journal of Bacteriology 198:1543-52.

151. Blevins, J. S., H. Xu, M. He, M. V. Norgard, L. Reitzer, and X. F. Yang. 2009. Rrp2, a sigma54-dependent transcriptional activator of *Borrelia burgdorferi*, activates *rpoS* in an enhancer-independent manner. J. Bacteriol. 191:2902-2905.

152. Smith, A. H., J. S. Blevins, G. N. Bachlani, X. F. Yang, and M. V. Norgard. 2007. Evidence that RpoS (σ^S) in *Borrelia burgdorferi* is controlled directly by RpoN (σ^{54}/σ^N). J. Bacteriol. 189:2139-2144.

153. Dunham-Ems, S. M., M. J. Caimano, C. H. Eggers, and J. D. Radolf. 2012. *Borrelia burgdorferi* requires the alternative sigma factor RpoS for dissemination within the vector during tick-to-mammal transmission. PLoS Pathog. 8:e1002532.

154. Grove, A. P., D. Liveris, R. Iyer, M. Petzke, J. Rudman, M. J. Caimano, J. D. Radolf, and I. Schwartz. 2017. Two Distinct Mechanisms Govern RpoS-Mediated Repression of Tick-Phase Genes during Mammalian Host Adaptation by Borrelia burgdorferi , the Lyme Disease Spirochete. mBio 8:e01204-17.

155. Jutras, B. L., A. M. Chenail, D. W. Carroll, M. C. Miller, H. Zhu, A. Bowman, and B. Stevenson. 2013. Bpur, the Lyme disease spirochete's PUR-domain protein: identification as a transcriptional modulator and characterization of nucleic acid interactions. J. Biol. Chem. 288:26220-26234.

156. Jutras, B. L., G. Jones, A. Verma, N. A. Brown, A. D. Antonicello, A. M. Chenail, and B. Stevenson. 2013. Post-transcriptional autoregulation of the Lyme disease bacterium's BpuR DNA/RNA-binding protein. J. Bacteriol. 195:4915-4923.

157. Babb, K., T. Bykowski, S. P. Riley, M. C. Miller, E. DeMoll, and B. Stevenson. 2006. *Borrelia burgdorferi* EbfC, a novel, chromosomally-encoded protein, binds specific DNA sequences adjacent to *erp* loci on the spirochete's resident cp32 prophages. J. Bacteriol. 188:4331-4339.

158. Riley, S. P., T. Bykowski, A. E. Cooley, L. H. Burns, K. Babb, C. a. Brissette, A. Bowman, M. Rotondi, M. C. Miller, E. DeMoll, K. Lim, M. G. Fried, and B. Stevenson. 2009. Borrelia burgdorferi EbfC defines a newly-identified, widespread family of bacterial DNA-binding proteins. Nucleic acids research 37:1973-83.

159. Jutras, B. L., A. Bowman, C. A. Brissette, C. A. Adams, A. Verma, A. M. Chenail, and B. Stevenson. 2012. EbfC (YbaB) is a new type of bacterial nucleoid-associated protein, and a global regulator of gene expression in the Lyme disease spirochete. J. Bacteriol. 194:3395-3406.

160. Burns, L. H., C. A. Adams, S. P. Riley, B. L. Jutras, A. Bowman, A. M. Chenail, A. E. Cooley, L. A. Haselhorst, A. M. Moore, K. Babb, M. G. Fried, and B. Stevenson. 2010. BpaB, a novel protein encoded by the Lyme disease spirochete's cp32 prophages, binds to *erp* Operator 2 DNA. Nucleic Acids Res. 38:5443-5455.

161. Chenail, A. M., B. L. Jutras, C. A. Adams, L. H. Burns, A. Bowman, A. Verma, and B. Stevenson. 2012. *Borrelia burgdorferi* cp32 BpaB modulates expression of the prophage NucP nuclease and SsbP single-stranded DNA-binding protein. J. Bacteriol. 194:4570-4578.

162. Jutras, B. L., A. Verma, C. A. Adams, C. A. Brissette, L. H. Burns, C. R. Whetstine, A. Bowman, A. M. Chenail, W. R. Zückert, and B. Stevenson. 2012. BpaB and EbfC DNA-binding proteins regulate production of the Lyme disease spirochete's infection-associated Erp surface proteins. J. Bacteriol. 194:778-786.

163. Jutras, B. L., C. R. Savage, W. K. Arnold, K. G. Lethbridge, D. W. Carroll, K. Tilly, A. Bestor, H. Zhu, J. Seshu, W. R. Zückert, P. E. Stewart, P. A. Rosa, C. A. Brissette, and B. Stevenson. 2019. The Lyme disease spirochete's BpuR DNA/RNA-binding protein is differentially expressed during the mammal–tick infectious cycle, which affects translation of the SodA superoxide dismutase. Molecular Microbiology 0.

164. Jutras, B. L., A. M. Chenail, C. L. Rowland, D. Carroll, M. C. Miller, T. Bykowski, and B. Stevenson. 2013. Eubacterial SpoVG homologs constitute a new family of site-specific DNA-binding proteins. PLoS One 8:e66683.

165. Banner, C. D. B., C. P. M. Jr, and R. Losick. 1983. Deletion Analysis of a Complex Promoter for a Developmentally Regulated Gene from Bacillus subtilis. J Mol Bio. 168:351-365.

166. Rosenbluh, A. M. Y., C. D. B. Banner, R. Losick, and P. C. Fitz-james. 1981. Identification of a New Developmental Locus in Bacillus subtilis by Construction of a Deletion Mutation in a Cloned Gene Under Sporulation Control. J. Bacteriol. 148:341-351.

167. Fürbass, R., M. Gocht, P. Zuber, and M. A. Marahiel. 1991. Interaction of AbrB, a transcriptional regulator from *Bacillus subtilis* with the promoters of the transition state-activated genes *tycA* and *spoVG*. Mol. Gen. Genet. 225:347-354.

168. Zuber, P., J. M. Healy, and R. Losick. 1987. Effects of Plasmid Propagation of a Sporulation Promoter on Promoter Utilization and Sporulation in Bacillus subtilis. J Bacteriol 169:461-469.

169. Matsuno, K., and A. L. Sonenshein. 1999. Role of SpoVG in asymmetric septation in *Bacillus subtilis*. J. Bacteriol. 181:3392-3401.

170. Meier, S., C. Goerke, C. Wolz, K. Seidl, D. Homerova, B. Schulethess, J. Kormanec, B. Berger-Bachi, and M. Bischoff. 2007. σB and the σB-dependent *arlRS* and *yabJspoVG* loci affect capsule formation in *Staphylococcus aureus*. Infect. Immun. 75:4562-4571.

171. Schulthess, B., S. Meier, D. Homerova, C. Goerke, C. Wolz, J. Kormanec, B. Berger-Bachi, and M. Bischoff. 2009. Functional characterization of the σB-dependent *yabJ-spoVG* operon in *Staphylococcus aureus*: role in methicillin and glycopeptide resistance. Antimicrob. Agents Chemother. 53:1832-1839.

172. Kim, H.-h., B.-j. Lee, and A.-r. Kwon. 2010. Expression , Crystallization , and Preliminary X-ray Crystallographic Analysis of Putative SpoVG from Staphylococcus aureus. Archives of Parm. Research 33:1285-1288.

173. Schulthess, B., D. A. Bloes, P. François, M. Girard, J. Schrenzel, M. Bischoff, and B. Berger-Bächi. 2011. The σB -dependent *yabJ-spoVG* operon is involved in the regulation of extracellular nuclease, lipase, and protease expression in *Staphylococcus aureus*. J. Bacteriol. 193:4954-4962.

174. Bischoff, M., S. Brelle, S. Minatelli, and V. Molle. 2016. Stk1-mediated phosphorylation stimulates the DNA-binding properties of the Staphylococcus aureus SpoVG transcriptional factor. Biochemical and Biophysical Research Communications 473:1223-1228.

175. Burke, T. P., and D. A. Portnoy. 2016. SpoVG is a conserved RNA-binding protein that regulates *Listeria monocytogenes* lysozyme resistance, virulence, and swarming motility. mBio 7:e00240.

176. Simon, M. M., U. E. Schaible, R. Wallich, and M. D. Kramer. 1991. A mouse model for *Borrelia burgdorferi* infection: approach to a vaccine against Lyme disease. Immunol. Today 12:11-16.

177. Sertour, N., V. Cotté, M. Garnier, L. Malandrin, E. Ferquel, and V. Choumet. 2018. Infection Kinetics and Tropism of Borrelia burgdorferi sensu lato in Mouse After Natural (via Ticks) or Artificial (Needle) Infection Depends on the Bacterial Strain. Frontiers in Microbiology 9.

178. Honarvar, N. 1994. Borrelia Burgdorferi Infection in Mice: Aspects of Inflammation and Immune Responses. Axford J.S., Rees D.H.E. (eds) Lyme Borreliosis. NATO ASI Series (Series A: Life Sciences) 260.

179. Bunikis, J., J. Tsao, C. J. Luke, M. G. Luna, D. Fish, and A. G. Barbour. 2004. *Borrelia burgdorferi* infection in a natural population of *Peromyscus leucopus* mice: a longitudinal study in an area where Lyme borreliosis is highly endemic. J. Inf. Dis. 189:1515-1523.

180. Zimmer, G., U. E. Schaible, M. D. Kramer, G. Mall, C. Museteanu, and M. M. Simon. 1990. Lyme carditis in immunodeficient mice during experimental infection of *Borrelia burgdorferi*. Virchows Arch. Path. Ana. Histopathol. 417:129-135.

181. Barthold, S. W., and L. K. Bockenstedt. 1993. Passive immunizing activity of sera from mice infected with *Borrelia burgdorferi*. Infect. Immun. 61:4696-4702.

182. de Souza, M. S., A. L. Smith, D. S. Beck, L. J. Kim, G. M. Hansen, and S. W. Barthold. 1993. Variant responses of mice to *Borrelia burgdorferi* depending on the site of intradermal inoculation. Infect. Immun. 61:4493-4497.

183. Gern, L., U. E. Schaible, and M. M. Simon. 1993. Mode of inoculation of the Lyme disease agent *Borrelia burgdorferi* influences infection and immune responses in inbred strains of mice. J. Infect. Dis. 167:971-975.

184. Sengupta, M., and S. Austin. 2011. Prevalence and Significance of Plasmid Maintenance Functions in the Virulence Plasmids of Pathogenic Bacteria. Infection and Immunity 79:2502-2509.

185. Thomas C.M., J.-B. G., Kostelidou K., Thorsted P., Zatyka M. 1998. Replication and Maintenance of Bacterial Plasmids. Molecular Microbiology NATO ASI Series 103:99-120.

186. Purser, J. E., and S. J. Norris. 2000. Correlation between plasmid content and infectivity in *Borrelia burgdorferi*. Proc. Natl. Acad. Sci. USA 97:13865-13870.

187. Freedman, J. C., E. A. Rogers, J. L. Kostick, H. Zhang, R. Iyer, I. Schwartz, and R. T. Marconi. 2010. Identification and molecular characterization of a cyclic-di-GMP effector protein, PlzA (BB0733): additional evidence for the existence of a functional cyclic-di-GMP regulatory network in the Lyme disease spirochete, *Borrelia burgdorferi*. FEMS Immunol. Med. Microbiol. 58:285-294.

188. Rogers, E. A., D. Terekhova, H. M. Zhang, K. M. Hovis, I. Schwartz, and R. T. Marconi. 2009. Rrp1, a cyclic-di-GMP-producing response regulator, is an important regulator of *Borrelia burgdorferi* core cellular functions. Mol. Microbiol. 71:1551-1573.

189. Byram, R., R. A. Gaultney, A. M. Floden, C. Hellekson, B. L. Stone, A. Bowman, B. Stevenson, B. J. B. Johnson, and C. A. Brissette. 2015. *Borrelia burgdorferi* RevA significantly affects pathogenicity and host response in the mouse model of Lyme disease. Infect. Immun. 83:3675-3683.

190. Grimm, D., A. F. Elias, K. Tilly, and P. A. Rosa. 2003. Plasmid stability during in vitro propagation of *Borrelia burgdorferi* assessed at a clonal level. Infect. Immun. 71:3138-3145.

191. Savage, C. R., B. L. Jutras, A. Bestor, K. Tilly, P. A. Rosa, Y. Tourand, P. E. Stewart, C. A. Brissette, and B. Stevensona. 2018. Borrelia burgdorferi SpoVG DNA- and RNA-binding protein modulates the physiology of the Lyme disease spirochete. Journal of Bacteriology 200.

192. Iyer, R., M. J. Caimano, A. Luthra, D. Axline, A. Corona, D. A. Iacobas, J. D. Radolf, and I. Schwartz. 2015. Stage-specific global alterations in the transcriptomes of Lyme disease spirochetes during tick feeding and following mammalian host-adaptation. Mol. Microbiol. 95:509-538.

193. Schwan, T. G., W. Burgdorfer, M. E. Schrumpf, and R. H. Karstens. 1988. The urinary bladder, a consistent source of *Borrelia burgdorferi* in experimentally infected white-footed mice (*Peromyscus leucopus*). J. Clin. Microbiol. 26:893-895.

194. Love, M. I., Huber, W., Anders, S. 2014. Moderated estimation of fold change and dispersion for RNA-seq data with DESeq2. Genome Biology 15.

195. Lybecker, M. C., and D. S. Samuels. 2017. Small RNAs of *Borrelia burgdorferi*: characterizing functional regulators in a sea of sRNAs. Yale J. Biol. Med. 90:317-323.

196. Hinnebusch, J., and A. G. Barbour. 1992. Linear- and circular-plasmid copy numbers in *Borrelia burgdorferi*. J. Bacteriol. 174:5251-5257.

197. Bignell, C., and C. M. Thomas. 2001. The bacterial ParA-ParB partitioning proteins. J Biotech 91:1-34.

198. Hu, L., A. G. Vecchiarelli, K. Mizuuchi, K. C. Neuman, and J. Liu. 2015. Directed and persistent movement arises from mechanochemistry of the ParA/ParB system. Proceedings of the National Academy of Sciences 112:E7055-E7064.

199. Zhang, H., and M. A. Schumacher. 2017. Structures of partition protein ParA with nonspecific DNA and ParB effector reveal molecular insights into principles governing Walker-box DNA segregation. Genes & Development 31:481-492.

200. Jutras, B. L., A. M. Chenail, and B. Stevenson. 2013. Changes in bacterial growth rate govern expression of the *Borrelia burgdorferi* OspC and Erp infection-associated surface proteins. J. Bacteriol. 195:757-764.

201. Arnold, W. K., C. R. Savage, C. A. Brissette, J. Seshu, J. Livny, and B. Stevenson. 2016. RNA-Seq of *Borrelia burgdorferi* in multiple phases of growth reveals insights into the dynamics of gene expression, transcriptome architecture, and noncoding RNAs. PLoS One 11:e0164165.

202. Dowdell, A. S., M. D. Murphy, C. Azodi, S. K. Swanson, L. Florens, S. Chen, and W. R. Zückert. 2017. Comprehensive Spatial Analysis of the *Borrelia burgdorferi* Lipoproteome Reveals a Compartmentalization Bias Toward the Bacterial Surface. Journal of Bacteriology:JB.00658-16.

203. Valentin Amrhein, S. G., Blake McShane. 2019. Scientists rise up against statistical significance. Nature 305-307.

204. Nikolic, N. 2019. Autoregulation of bacterial gene expression: lessons from the MazEF toxin–antitoxin system. Current Genetics 65:133-138.

205. Camarero, J. A., A. Shekhtman, E. A. Campbell, M. Chlenov, T. M. Gruber, D. A. Bryant, S. A. Darst, D. Cowburn, and T. W. Muir. 2002. Autoregulation of a bacterial σ factor explored by using segmental isotopic labeling and NMR. Proceedings of the National Academy of Sciences 99:8536-8541.

206. Narula J, T. A., Igoshin OA. 2016. Role of Autoregulation and Relative Synthesis of Operon Partners in Alternative Sigma Factor Networks. . PLOS Computational Biology.

207. Gallia, G. L., E. M. Johnson, and K. Khalili. 2000. Pur α: a multifunctional single-stranded DNA and RNA binding protein. Nucleic Acids Res. 28:3197-3205.

208. Holmqvist, E., and J. Vogel. 2018. RNA-binding proteins in bacteria. Nature Reviews Microbiology:601-615.

209. Bunikis, I., S. Kutschan-Bunikis, M. Bonde, and S. Bergström. 2011. Multiplex PCR as a tool for validating plasmid content of *Borrelia burgdorferi*. J. Microbiol. Methods 86:243-247.

210. Pappas, C. J., R. Iyer, M. M. Petzke, M. J. Caimano, J. D. Radolf, and I. Schwartz. 2011. *Borrelia burgdorferi* requires glycerol for maximum fitness during the tick phase of the enzootic cycle. PLoS Pathog. 7:e1002102.

211. Eiglmeier, K., W. Boos, and S. T. Cole. 1987. Nucleotide sequence and transcriptional startpoint of the *glpT* gene of *Escherichia coli*: extensive sequence homology of the glycerol-3-phosphate transport protein with components of the hexose-6-phosphate transport system. Mol. Microbiol. 1:251-258.

212. Schwan, T. G., J. M. Battisti, S. F. Porcella, S. J. Raffel, M. E. Schrumpf, E. R. Fischer, J. a. Carroll, P. E. Stewart, P. Rosa, and G. a. Somerville. 2003. Glycerol-3-phosphate acquisition in spirochetes: Distribution and biological activity of glycerophosphodiester phosphodiesterase (GlpQ) among Borrelia species. Journal of Bacteriology 185:1346-1356.

213. Schwan, T. G., M. E. Schrumpf, B. J. Hinnebusch, D. E. Anderson, and M. E. Konkel. 1996. GlpQ: an antigen for serological discrimination between relapsing fever and Lyme borreliosis. J. Clin. Microbiol. 34:2483-2492.

214. Tommassen, J., K. Eiglmeier, S. T. Cole, P. Overduin, T. J. Larson, and W. Boos. 1991. Characterization of two genes, *glpQ* and *ugpQ*, encoding glycerophosphyl diester phosphodiesterases of *Escherichia coli*. Mol. Gen. Genet. 226:321-327.

215. Glatz, E., M. Persson, and B. Rutberg. 1998. Antiterminator protein GlpP of Bacillus subtilis binds to glpD leader mRNA. Microbiology 144:449-456.

216. Iuchi, S., and S. T. Cole. 1990. Multiple Regulatory Elements for the glpA Operon Encoding Anaerobic Glycerol-3-Phosphate Dehydrogenase and the glpD Operon Encoding Aerobic Glycerol-3-Phosphate Dehydrogenase in Escherichia coli : Further Characterization of Respiratory Control. J Bacteriol 172:179-184.

217. Yang, B., and T. J. Larson. 1998. Multiple promoters are responsible for transcription of the glpEGR operon of Escherichia coli K-12. Biochimica et Biophysica Acta (BBA) - Gene Structure and Expression 1396:114-126.

218. Zhao, N., W. O. N. Oh, D. Trybul, K. S. Thrasher, T. J. Kingsbury, and T. J. Larson. 1994. Characterization of the Interaction of the glp Repressor of Escherichia coli K-12 with Single and Tandem glp Operator Variants. J Bacteriol 176:2393-2397.

219. Pettigrews, D. W., D.-p. Ma, C. a. Conrad, and J. R. Johnsonn. 1988. Escherichia coli Glycerol Kinase. Biochemistry 263:135-139.

220. Yeh, J. I., U. Chinte, and S. Du. 2008. Structure of glycerol-3-phosphate dehydrogenase, an essential monotopic membrane enzyme involved in respiration and metabolism. Proceedings of the National Academy of Sciences 105:3280-3285.

221. Drecktrah, D., L. S. Hall, P. Rescheneder, M. Lybecker, and D. S. Samuels. 2018. The Stringent Response-Regulated sRNA Transcriptome of Borrelia burgdorferi. Frontiers in Cellular and Infection Microbiology 8:1-12.

222. Mallory, K. L., D. P. Miller, L. D. Oliver, J. C. Freedman, J. L. Kostick-Dunn, J. A. Carlyon, J. D. Marion, J. K. Bell, and R. T. Marconi. 2016. Cyclic-di-GMP binding induces structural rearrangements in the PlzA and PlzC proteins of the Lyme disease and relapsing fever spirochetes: a possible switch mechanism for c-di-GMP-mediated effector functions. Pathogens and Disease 74.

223. Liang, F. T., E. Aberer, M. Cinco, L. Gern, C. M. Hu, Y. N. Lobet, M. Ruscio, P. E. Voet, V. E. Weynants, and M. T. Philipp. 2000. Antigenic conservation of an immunodominant invariable region of the VlsE lipoprotein among European pathogenic genospecies of *Borrelia burgdorferi* SL. J. Inf. Dis. 182:1455-1462.

224. Ohnishi, J., B. Schneider, W. B. Messer, J. Piesman, and A. M. deSilva. 2003. Genetic variation at the *vlsE* locus of *Borrelia burgdorferi* within ticks and mice over the course of a single transmission cycle. J. Bacteriol. 185:4432-4441.

225. Sung, S. Y., J. V. McDowell, and R. T. Marconi. 2001. Evidence for the contribution of point mutations to *vlsE* variation and for the apparent constraints on the net accumulation of sequence changes in *vlsE* during infection with Lyme disease spirochetes. J. Bacteriol. 183:5855-5861.

226. Verhey, T. B., M. Castellanos, and G. Chaconas. 2018. Antigenic Variation in the Lyme Spirochete: Insights into Recombinational Switching with a Suggested Role for Error-Prone Repair. Cell Reports 23:2595-2605.

227. Zhang, J.-R., and S. J. Norris. 1998. Genetic variation of the *Borrelia burgdorferi* gene *vlsE* involves cassette-specific, segmental gene conversion. Infect. Immun. 66:3698-3704.

228. Liang, F. T., L. C. Bowers, and M. T. Philipp. 2001. C-terminal invariable domain of VlsE is immunodominant but its antigenicity is scacely conserved among strains of Lyme disease spirochetes. Infect. Immun. 69:3224-3231.

229. Liang, F. T., R. H. Jacobson, R. K. Straubinger, A. Grooters, and M. T. Philipp. 2000. Characterization of a *Borrelia burgdorferi* VlsE invariable region useful in canine Lyme disease serodiagnosis by enzyme-linked immunosorbent assay. J. Clin, Microbiol. 38:4160-4166.

230. Liang, F. T., J. M. Nowling, and M. T. Philipp. 2000. Cryptic and exposed invariable regions of VlsE, the variable surface antigen of *Borrelia burgdorferi* sl. J. Bacteriol. 182:3597-3601.

231. Lin, T., L. Gao, D. G. Edmondson, M. B. Jacobs, M. T. Philipp, and N. S.J. 2009. Central role of the Holliday junction helicase RuvAB in *vlsE* recombination and infectivity of *Borrelia burgdorferi*. PLoS Pathog. 5:e1000679.

232. Liveris, D., V. Mulay, S. Sandigursky, and I. Schwartz. 2008. *Borrelia burgdorferi vlsE* antigenic variation is not mediated by RecA. Infect. Immun. 76:4009-4018.

233. Zhang, J.-R., and S. J. Norris. 1998. Kinetics and in vivo induction of genetic variation of *vlsE* in *Borrelia burgdorferi*. Infect. Immun. 66:3689-3697.

234. Zhou, W., and D. Brisson. 2017. Correlation between antigenicity and variability in the vls antigenic variation system of Borrelia burgdorferi. Microbes and Infection 19:267-276.

235. Bontemps-Gallo, S., C. Gaviard, C. L. Richards, T. Kentache, S. J. Raffel, K. A. Lawrence, J. C. Schindler, J. Lovelace, D. P. Dulebohn, R. G. Cluss, J. Hardouin, and F. C. Gherardini. 2018. Global Profiling of Lysine Acetylation in Borrelia burgdorferi B31 Reveals Its Role in Central Metabolism. Frontiers in Microbiology 9:1-15.

236. van Heijenoort, J. 2007. Lipid Intermediates in the Biosynthesis of Bacterial Peptidoglycan. Microbiology and Molecular Biology Reviews 71:620-635.

237. Emiola A, G. J., Andrews SS 2015. A Complete Pathway Model for Lipid A Biosynthesis in Escherichia coli. PLOS ONE 10.

238. Stazic, D., D. Lindell, and C. Steglich. 2011. Antisense RNA protects mRNA from RNase E degradation by RNA–RNA duplex formation during phage infection. Nucleic Acids Research 39:4890-4899.

239. Fabien Darfeuille, Cecilia Unoson, Jorg Vogel, and E. G. H. Wagner. 2007. An Antisense RNA Inhibits Translation by Competing with Standby Ribosomes. Molecular Cell 26:381-392.

240. Grove, A. P., D. Liveris, R. Iyer, M. Petzke, J. Rudman, M. J. Caimano, J. D. Radolf, and I. Schwartz. 2017. Two distinct mechanisms govern RpoS-Mediated repression of tick-phase genes during mammalian host adaptation by *Borrelia burgdorferi*, the Lyme disease spirochete. MBio 8.

241. Bugrysheva, J. V., C. J. Pappas, D. A. Terekhova, R. Iyer, H. P. Godfrey, I. Schwartz, and F. C. Cabello. 2015. Characterization of the RelBbu regulon in *Borrelia burgdorferi* reveals modulation of glycerol metabolism by (p)ppGpp. PLoS ONE 10:e0118063.

242. Hoxmeier, J. C., A. C. Fleshman, C. D. Broeckling, J. E. Prenni, M. C. Dolan, K. L. Gage, and L. Eisen. 2017. Metabolomics of the tick-Borrelia interaction during the nymphal tick blood meal. Scientific Reports 7:44394-44394.

243. Katayama, T., S. Ozaki, K. Keyamura, and K. Fujimitsu. 2010. Regulation of the replication cycle: conserved and diverse regulatory systems for DnaA and *oriC*. Nat. Rev. Microbiol. 8:163-170.

244. Bork, J. M., M. M. Cox, and R. B. Inman. 2001. The RecOR proteins modulate RecA protein function at 5' ends of single-stranded DNA. EMBO J. 20:7313-7322.

245. von Lackum, K., and B. Stevenson. 2005. Carbohydrate utilization by the Lyme borreliosis spirochete, *Borrelia burgdorferi*. FEMS Microbiol. Lett. 243:173-179.

246. Bykowski, T., K. Babb, K. von Lackum, S. P. Riley, S. J. Norris, and B. Stevenson. 2006. Transcriptional regulation of the *Borrelia burgdorferi* antigenically variable VlsE surface protein. J. Bacteriol. 188:4879-4889.

247. Casjens, S., N. Palmer, R. van Vugt, W. M. Huang, B. Stevenson, P. Rosa, R. Lathigra, G. Sutton, J. Peterson, R. J. Dodson, D. Haft, E. Hickey, M. Gwinn, O. White, and C. Fraser. 2000. A bacterial genome in flux: the twelve linear and nine circular extrachromosomal DNAs of an infectious isolate of the Lyme disease spirochete *Borrelia burgdorferi*. Mol. Microbiol. 35:490-516.

248. Phelan JP, K. A., Ramsey ME, Lundt ME, Sharma B, et al. 2019. Genome-wide screen identifies novel genes required for Borrelia burgdorferi survival in its Ixodes tick vector. PLOS Pathogens 15.

249. McCown, P. J., K. A. Corbino, S. Stav, M. E. Sherlock, and R. R. Breaker. 2017. Riboswitch diversity and distribution. RNA 23:995-1011.

250. Serganov, A., and D. J. Patel. 2007. Ribozymes, riboswitches and beyond: regulation of gene expression without proteins. Nature reviews. Genetics 8:776-790.

251. Kraemer, J. A., A. G. Sanderlin, and M. T. Laub. 2019. The Stringent Response Inhibits DNA Replication Initiation in E. coli by Modulating Supercoiling of oriC. mBio 10:e01330-19.

252. Jenal, U., A. Reinders, and C. Lori. 2017. Cyclic di-GMP: second messenger extraordinaire. Nature Reviews Microbiology 15:271.

253. Id, R. T. 2019. Cyclic diguanylate riboswitches control bacterial pathogenesis mechanisms. PLOS Pathogens:1-7.

254. Gupta, K. R., P. Baloni, S. S. Indi, and D. Chatterji. 2016. Regulation of growth, cell shape, cell division and gene expression by second messengers (p)ppGpp and c-di-GMP in Mycobacterium smegmatis. Journal of Bacteriology 198:JB.00126-16.

255. Russell, M. H., A. N. Bible, X. Fang, J. R. Gooding, S. R. Campagna, M. Gomelsky, and G. Alexandrea. 2013. Integration of the second messenger c-di-GMP into the chemotactic signaling pathway. mBio 4:1-11.

256. Schirmer, T., and U. Jenal. 2009. Structural and mechanistic determinants of c-di-GMP signalling. Nature reviews. Microbiology 7:724-735.

257. Kalia, D., G. Merey, S. Nakayama, Y. Zheng, J. Zhou, Y. Luo, M. Guo, B. T. Roembke, and H. O. Sintim. 2013. Nucleotide, c-di-GMP, c-di-AMP, cGMP, cAMP, (p)ppGpp signaling in bacteria and implications in pathogenesis. Chem. Soc. Rev. 42:305-341.

258. Whiteley, A. T., J. B. Eaglesham, C. C. D. O. Mann, B. R. Morehouse, B. Lowey, E. A. Nieminen, O. Danilchanka, D. S. King, A. S. Y. Lee, J. J. Mekalanos, and P. J. Kranzusch. 2019. Bacterial cGAS-like enzymes synthesize diverse nucleotide signals. Nature 567:194-199.

259. He, P., C. Deng, B. Liu, L. Zeng, W. Zhao, Y. Zhang, X. Jiang, X. Guo, and J. Qin. 2013. Characterization of a bifunctional enzyme with (p)ppGpp-hydrolase/synthase activity in I. FEMS Microbiol. Lett. 348:133-142.

260. Gomelsky, M. 2011. cAMP, c-di-GMP, c-di-AMP and now cGMP: bacteria use them all! Mol. Microbiol. 79:562-565.

261. Römling, U. 2008. Great times for small molecules: c-di-AMP, a second messenger candidate in Bacteria and Archaea. Science signaling 1:pe39-pe39.

262. Abdul-Sater, A. A., I. Tattoli, L. Jin, A. Grajkowski, A. Levi, B. H. Koller, I. C. Allen, S. L. Beaucage, K. A. Fitzgerald, J. P. Ting, J. C. Cambier, S. E. Girardin,

and C. Schindler. 2013. Cyclic-di-GMP and cyclic-di-AMP activate the NLRP3 inflammasome. EMBO Rep. 14:900-906.

263. Choi, P. H., K. Sureka, J. J. Woodward, and L. Tong. 2015. Molecular basis for the recognition of cyclic-di-AMP by PstA, a PII -like signal transduction protein. MicrobiologyOpen:doi: 10.1002/mbo3.243.

264. Jin, L., K. K. Hill, H. Filak, J. Mogan, H. Knowles, B. Zhang, A. L. Perraud, J. C. Cambier, and L. L. Lenz. 2011. MPYS is required for IFN response factor 3 activation and type I IFN production in the response of cultured phagocytes to bacterial second messengers cyclic-di-AMP and cyclic-di-GMP. J. Immunol. 187:2595-2601.

265. Woodward, J. J., A. T. Iavarone, and D. A. Portnoy. 2010. c-di-AMP secreted by intracellular *Listeria monocytogenes* activates a host type I interferon response. Science 328:1703-1705.

266. Corrigan, R. M., J. C. Abbott, H. Burhenne, V. Kaever, and A. Gründling. 2011. c-di-AMP is a new second messenger in *Staphylococcus aureus* with a role in controlling cell size and envelope stress. PLoS Pathog. 7:e1002217.

267. Gándara, C., and J. C. Alonso. 2015. DisA and c-di-AMP act at the intersection between DNA-damage response and stress homeostasis in exponentially growing *Bacillus subtilis* cells. DNA Repair 27:1-8.

268. Gundlach, J., L. Krüger, C. Herzberg, A. Turdiev, A. Poehlein, I. Tascón, M. Weiß, D. Hertel, R. Daniel, I. Hänelt, V. T. Lee, and J. Stülke. 2019. Sustained sensing in potassium homeostasis : Cyclic di-AMP controls potassium uptake by KimA at the levels of expression and activity. Journal of Bio. Chem. 294:1-20.

269. Oppenheimer-Shaanan, Y., E. Wexselblatt, J. Katzhendler, E. Yavin, and S. Ben-Yehuda. 2011. c-di-AMP reports DNA integrity during sporulation in *Bacillus subtilis*. EMBO Rep. 12:594-601.

270. Grimm, D., K. Tilly, R. Byram, P. E. Stewart, J. G. Krum, D. M. Bueschel, T. G. Schwan, P. F. Policastro, A. F. Elias, and P. A. Rosa. 2004. Outer-surface protein C of the Lyme disease spirochete: a protein induced in ticks for infection of mammals. Proc. Natl. Acad. Sci. USA 101:3142-3147.

271. Schwan, T. G., J. Piesman, W. T. Golde, M. C. Dolan, and P. A. Rosa. 1995. Induction of an outer surface protein on *Borrelia burgdorferi* during tick feeding. Proc. Natl. Acad. Sci. USA 92:2909-2913.

272. Tilly, K., J. G. Krum, A. Bestor, M. W. Jewett, D. Grimm, D. Bueschel, R. Byram, D. Dorward, M. J. Vanraden, P. Stewart, and P. Rosa. 2006. *Borrelia burgdorferi* OspC protein is required exclusively in a crucial early stage of mammalian infection. Infect. Immun. 74:3554-3564.

273. Carrasco, S. E., B. Troxell, Y. Yang, S. L. Brandt, H. Li, G. E. Sandusky, K. W. Condon, C. H. Serezani, and X. F. Yang. 2015. Outer Surface Protein OspC Is an Antiphagocytic Factor That Protects *Borrelia burgdorferi* from Phagocytosis by Macrophages. Infection and Immunity 83:4848-4860.

274. Alverson, J., S. F. Bundle, C. D. Sohaskey, M. C. Lybecker, and D. S. Samuels. 2003. Transcriptional regulation of the *ospAB* and *ospC* promoters of *Borrelia burgdorferi*. Mol. Microbiol. 48:1665-1677.

275. Schwan, T. G., and J. Piesman. 2000. Temporal changes in outer surface proteins A and C of the Lyme disease-associated spirochete, *Borrelia burgdorferi*, during the chain of infection in ticks and mice. J. Clin. Microbiol. 38:382-388.

276. Marconi, R. T., D. S. Samuels, and C. F. Garon. 1993. Transcriptional analyses and mapping of the *ospC* gene in Lyme disease spirochetes. J. Bacteriol. 175:926-932.

277. Pal, U., X. Yang, M. Chen, L. K. Bockenstedt, J. F. Anderson, R. A. Flavell, M. V. Norgard, and E. Fikrig. 2004. OspC facilitates *Borrelia burgdorferi* invasion of *Ixodes scapularis* salivary glands. J. Clin. Invest. 113:220-230.

278. Sadziene, A., B. Wilske, M. S. Ferdows, and A. G. Barbour. 1993. The cryptic *ospC* gene of *Borrelia burgdorferi* B31 is located on a circular plasmid. Infect. Immun. 61:2192-2195.

279. Sarkar, A., B. M. Hayes, D. P. Dulebohn, and P. A. Rosa. 2011. Regulation of the virulence determinant OspC by bbd18 on linear plasmid lp17 of *Borrelia burgdorferi*. J. Bacteriol. 193:5365-5373.

280. Skare, J. T., D. K. Shaw, J. P. Trzeciakowski, and J. A. Hyde. 2016. In vivo imaging demonstrates that *Borrelia burgdorferi ospC* is uniquely expressed temporally and spatially throughout experimental infection. PLoS ONE 11:e0162501.

281. Babb, K., N. El-Hage, J. C. Miller, J. A. Carroll, and B. Stevenson. 2001. Distinct regulatory pathways control the synthesis of *Borrelia burgdorferi* infection-associated OspC and Erp surface proteins. Infect. Immun. 69:4146-4153.

282. Drecktrah, D., L. S. Hall, L. L. Hoon-Hanks, and D. S. Samuels. 2013. An inverted repeat in the ospC operator is required for induction in *Borrelia burgdorferi*. PLoS One 8:e68799.

283. Xu, Q., K. McShan, and F. T. Liang. 2007. Identification of an *ospC* operator critical for immune evasion of *Borrelia burgdorferi*. Mol. Microbiol. 64:220-231.

284. Arnold, W. K., C. R. Savage, K. G. Lethbridge, T. C. Smith, C. A. Brissette, J. Seshu, and B. Stevenson. 2018. Transcriptomic insights on the virulence-controlling CsrA, BadR, RpoN, and RpoS regulatory networks in the Lyme disease spirochete. Plos One 13:1-39.

285. Ouyang, Z., S. Narasimhan, G. Neelakanta, M. Kumar, U. Pal, E. Fikrig, and M. V. Norgard. 2012. Activation of the RpoN-RpoS regulatory pathway during the enzootic life cycle of *Borrelia burgdorferi*. BMC Microbiol. 12:44. doi: 10.1186/1471-2180-12-44.

286. Corrigan, R. M., and A. Gründling. 2013. Cyclic di-AMP: another second messenger enters the fray. Nat. Rev. Microbiol. 11:513-524.

287. Rosenberg, J., A. Dickmanns, P. Neumann, K. Gunka, J. Arens, V. Kaever, J. Stulke, R. Ficner, and F. M. Commichau. 2015. Structural and biochemical analysis of the essential diadenylate cyclase CdaA from *Listeria monocytogenes*. J. Biol. Chem.

288. Mehne, F. M., K. Gunka, H. Eilers, C. Herzberg, V. Kaever, and J. Stülke. 2013. Cyclic di-AMP homeostasis in *Bacillus subtilis*: both lack and high level accumulation of the nucleotide are detrimental for cell growth. J. Biol. Chem. 288:2004-2017.

289. Witte, C. E., A. T. Whiteley, T. P. Burke, J. D. Sauer, D. A. Portnoy, and J. J. Woodward. 2013. Cyclic di-AMP is critical for *Listeria monocytogenes* growth, cell wall homeostasis, and establishment of infection. mBio 4:e00282-13.

290. Whetstine, C. R., J. G. Slusser, and W. R. Zückert. 2009. Development of a single-plasmid-based regulatable gene expression system for *Borrelia burgdorferi*. Appl. Environ. Microbiol. 75:6553-6558.

291. Stevenson, B., T. G. Schwan, and P. A. Rosa. 1995. Temperature-related differential expression of antigens in the Lyme disease spirochete, *Borrelia burgdorferi*. Infect. Immun. 63:4535-4539.

292. Stevenson, B., L. K. Bockenstedt, and S. W. Barthold. 1994. Expression and gene sequence of outer surface protein C of Borrelia burgdorferi reisolated from chronically infected mice . . Infect. Immun. 62:3568-3571.

293. Meyer, M. M. 2017. The role of mRNA structure in bacterial translational regulation. Wiley Interdisciplinary Reviews: RNA 8:e1370.

294. Xu, Q., K. McShan, and F. T. Liang. 2008. Verification and dissection of the *ospC* operator by using *flaB* promoter as a reporter in *Borrelia burgdorferi*. Microb. Pathog. 45:70-78.

295. Breaker, R. R. 2011. Review Prospects for Riboswitch Discovery and Analysis. Molecular Cell 43:867-879.

296. Nelson, J. W., N. Sudarsan, K. Furukawa, Z. Weinberg, J. X. Wang, and R. R. Breaker. 2013. Riboswitches in eubacteria sense the second messenger c-di-AMP. Nat. Chem. Biol. 9:834-839.

297. Rosinski-Chupin, I., O. Soutourina, and I. Martin-Verstraete. 2014. Riboswitch Discovery by Combining RNA-Seq and Genome-Wide Identification of Transcriptional Start Sites, 1 ed, vol. 549. Elsevier Inc.

298. Theisen, M., M. Borre, M. J. Mathiesen, B. Mikkelsen, A.-M. Lebech, and K. Hansen. 1995. Evolution of the *Borrelia burgdorferi* outer surface protein OspC. J. Bacteriol. 177:3036-3044.

299. Wang, I.-N., D. E. Dykhuizen, W. Qiu, J. J. Dunn, E. M. Bosler, and B. J. Luft. 1999. Genetic diversity of *ospC* in a local population of *Borrelia burgdorferi sensu stricto*. Genetics 151:15-30.

300. Livey, I., C. P. Gibbs, R. Schuster, and F. Dorner. 1995. Evidence for lateral transfer and recombination in OspC variation in Lyme disease *Borrelia*. Mol. Microbiol. 18:257-269.

301. Lybecker, M. C., C. A. Abel, A. L. Feig, and D. S. Samuels. 2010. Identification and function of the RNA chaperone Hfq in the Lyme disease spirochete *Borrelia burgdorferi*. Mol. Microbiol. 78:622-635.

302. Lybecker, M. C., and D. S. Samuels. 2007. Temperature-induced regulation of RpoS by a small RNA in *Borrelia burgdorferi*. Mol. Microbiol. 64:1075-1089.

303. Qiu, W. G., S. E. Schutzer, J. F. Bruno, O. Attie, Y. Xu, J. J. Dunn, S. R. Casjens, and B. J. Luft. 2004. Genetic exchange and plasmid transfers in *Borrelia burgdorferi sensu stricto* revealed by three-way genome comparisons and multilocus sequence typing. Proc. Natl. Acad. Sci. USA 101:14150-14155.

304. Azam, T. A., and A. Ishihama. 1999. Twelve species of the nucleoid-associated protein from *Escherichia coli.* Sequence recognition specificity and DNA binding affinity. J. Biol. Chem. 274:33105-33113.

305. Dillon, S. C., and C. J. Dorman. 2010. Bacterial nucleoid-associated proteins, nucleoid structure and gene expression. Nat. Rev. Microbiol. 8:185-195.

306. Gray, W. T., S. K. Govers, Y. Xiang, B. R. Parry, M. Campos, S. Kim, C. Jacobs-wagner, W. T. Gray, S. K. Govers, Y. Xiang, B. R. Parry, M. Campos, and S. Kim. 2019. Nucleoid Size Scaling and Intracellular Organization of Translation across Bacteria Article Nucleoid Size Scaling and Intracellular Organization of Translation across Bacteria. Cell 177:1632-1648.e20.

307. Hinnebusch, B. J., and A. J. Bendich. 1997. The bacterial nucleoid visualized by fluorescence microscopy of cells lysed within agarose: comparison of *Escherichia coli* and spirochetes of the genus *Borrelia*. J. Bacteriol. 179:2228-2237.

308. Luijsterburg, M. S., M. C. Noom, G. J. L. Wuite, and R. T. Dame. 2006. The architectural role of nucleoid-associated proteins in the organization of bacterial chromatin: a molecular perspective. J. Struct. Biol. 156:262-272.

309. Thanbichler, M., S. C. Wang, and L. Shapiro. 2005. The bacterial nucleoid: a highly organized and dynamic structure. J. Cell. Biol. 96:506-521.

310. Wang, W., G. W. Li, C. Chen, X. S. Xie, and X. Zhuang. 2011. Chromosome organization by a nucleoid-associated protein in live bacteria. Science 333:1445-1449.

311. Jutras, B. L., M. Scott, B. Parry, J. Biboy, J. Gray, W. Vollmer, and C. Jacobs-Wagner. 2016. Lyme disease and relapsing fever *Borrelia* elongate through zones of peptidoglycan synthesis that mark division sites of daughter cells. Proc. Natl. Acad. Sci. 113:9162-9170.

312. Ray-Soni, A., M. Bellecourt, and R. Landick. 2016. Mechanisms of Bacterial Transcription Termination: All Good Things Must End. Annu Rev Biochem 85:319-47.

313. Archambault, L., J. S. Borchert, J. Bergeron, S. Snow, and P. J. Schlax. 2013. Measurements of mRNA degradation in *Borrelia burgdorferi*. J. Bacteriol. 195:4879-4887.

314. Drecktrah, D., M. Lybecker, N. Popitsch, P. Rescheneder, L. S. Hall, and D. S. Samuels. 2015. The *Borrelia burgdorferi* RelA/SpoT homolog and stringent response regulate survival in the tick vector and global gene expression during starvation. PLoS Pathog. 11:e1005160.

315. Xu, Q., Y. Shi, P. Dadhwal, and F. T. Liang. 2012. RpoS regulates essential virulence factors remaining to be identified in *Borrelia burgdorferi*. PLoS ONE 7:e53212.

316. Sonenshein, A. L. 1999. Role of SpoVG in Asymmetric Septation in Bacillus subtilis. J Bacteriol 181:3392-3401.

317. Wadhams, G. H., and J. P. Armitage. 2004. Making Sense of it All: Bacterial Chemotaxis. Nature reviews. Molecular cell biology 5:1024-1037.

318. Szurmant, H., and G. W. Ordal. 2004. Diversity in chemotaxis mechanisms among the bacteria and archaea. Microbiology and molecular biology reviews : MMBR 68:301-319.

319. Porter, S. L., G. H. Wadhams, and J. P. Armitage. 2011. Signal processing in complex chemotaxis pathways. Nature reviews Microbiology 9:153-165.

320. Ringgaard, S., M. Zepeda-Rivera, X. Wu, K. Schirner, B. M. Davis, and M. K. Waldor. 2014. ParP prevents dissociation of CheA from chemotactic signaling arrays and tethers them to a polar anchor. Proceedings of the National Academy of Sciences of the United States of America 111:E255-64.

321. Xie, Z., L. E. Ulrich, I. B. Zhulin, and G. Alexandre. 2010. PAS domain containing chemoreceptor couples dynamic changes in metabolism with chemotaxis. Proceedings of the National Academy of Sciences of the United States of America 107:2235-2240.

322. Zusman, D. R., A. E. Scott, Z. Yang, and J. R. Kirby. 2007. Chemosensory pathways, motility and development in Myxococcus xanthus. Nature reviews. Microbiology 5:862-872.

323. Charon, N. W., A. Cockburn, C. Li, J. Liu, K. A. Miller, M. R. Miller, M. Motaleb, and C. W. Wolgemuth. 2012. The unique paradigm of spirochete motility and chemotaxis. Annu. Rev. Microbiol. 66:349-370.

324. Charon, N. W., and S. F. Goldstein. 2002. Genetics of motility and chemotaxis of a fascinating group of bacteria: the spirochetes. Annu. Rev. Genet. 36:47-73.

325. Motaleb, M. a., S. Z. Sultan, M. R. Miller, C. Li, and N. W. Charon. 2011. CheY3 of Borrelia burgdorferi is the key response regulator essential for chemotaxis and forms a long-lived phosphorylated intermediate. Journal of bacteriology 193:3332-41.

326. Hammerschmidt, C., A. Koenigs, C. Siegel, T. Hallström, C. Skerka, R. Wallich, P. F. Zipfel, and P. Kraiczy. 2014. Versatile roles of CspA orthologs in complement inactivation of serum-resistant Lyme disease spirochetes. Infect. Immun. 82:380-392.

327. Kellenberger, C. a., J. Sales-Lee, Y. Pan, M. M. Gassaway, A. E. Herr, and M. C. Hammond. 2015. A minimalist biosensor: Quantitation of cyclic Di-GMP using the conformational change of a riboswitch aptamer. RNA biology 6286:00-00.

328. Cordelia A. Weiss, J. A. H., Kuanqing Liu, Benjamin P. Tu, Wade C. Winkler. 2019. Single cell microscopy reveals that levels of cyclic di-GMP vary among Bacillus subtilis subpopulations. Journal of Bacteriology 201:e00247-19.

329. Hammond, X. C. W. S. C. W. M. C. 2016. Next-generation RNA-based fluorescent biosensors enable anaerobic detection of cyclic di-GMP. Nucleic Acids Research 44:1-10.

330. Christen, M., H. D. Kulasekara, B. Christen, B. R. Kulasekara, L. R. Hoffman, and S. I. Miller. 2010. Asymmetrical distribution of the second messenger c-di-GMP upon bacterial cell division. Science 328:1295-1297.

331. Xu, Q., K. McShan, and F. T. Liang. 2019. Two regulatory elements required for enhancing ospA expression in Borrelia burgdorferi grown in vitro but repressing its expression during mammalian infection Generation of constructs. Microbiology Society:2194-2204.

332. Ma, Y., and J. J. Weis. 1993. *Borrelia burgdorferi* outer surface lipoproteins OspA and OspB possess B-cell mitogenic and cytokine-stimulatory properties. Infect. Immun. 61:3843-3853.

333. He, M., J. Zhang, M. Ye, Y. Lou, and X. F. Yang. 2013. The cyclic dimeric-GMP receptor PlzA controls virulence gene expression through RpoS in *Borrelia burgdorferi*. Infect. Immun. 82:445-452.

334. Yang, Y., A. Wolfe, and X. F. Yang. 2018. Identification of Acetylated proteins in *Borrelia burgdorferi*. Methods in Molecular Microbiology 1690:177-182.

335. Christensen, D. G., J. T. Baumgartner, X. Xie, K. M. Jew, N. Basisty, and B. Schilling. 2019. Mechanisms , Detection , and Relevance of Protein Acetylation in Prokaryotes. mBio 10:1-20.

336. Blow, M. J., T. A. Clark, C. G. Daum, A. M. Deutschbauer, A. Fomenkov, R. Fries, J. Froula, D. D. Kang, R. R. Malmstrom, R. D. Morgan, J. Posfai, K. Singh, A. Visel, K. Wetmore, Z. Zhao, E. M. Rubin, J. Korlach, L. A. Pennacchio, and R. J. Roberts. 2016. The Epigenomic Landscape of Prokaryotes. PLOS Genetics 12:e1005854-e1005854.

VITA

CHRISTINA R. SAVAGE, B.SC.

Department of Microbiology, Immunology and Molecular Genetics • University of Kentucky College of Medicine
643 Light Hall
2215 Garland Ave
Nashville TN 37232
(859) 492-6427 • christina.savage@vanderbilt.edu

EDUCATION

2013-present Graduate Student, University of Kentucky, Lexington, KY. Anticipated graduation: Summer 2019

2011 B.Sc. *cum laude*, Biology, North Park University, Chicago, IL

RESEARCH EXPERIENCE

2013-present Graduate Research Assistant, University of Kentucky
Advisor: Brian Stevenson, Ph.D.
Functional analyses of the DNA- and RNA-binding protein SpoVG in *Borrelia burgdorferi.*

2017 Tick dissection and physiology workshop with Jeff Grabowski, Ph.D. Biology of Vector-Borne Viruses Section, Laboratory of Virology, NIAID, National Institutes of Health Rocky Mountain Laboratories and University of North Dakota. Grand Forks, ND

2010-2011 Undergraduate Research Assistant, North Park University, Chicago IL
Advisors: Justin Topp, Ph.D., Matthew Schau, Ph.D.
Surveillance of *Ixodes scapularis* ticks in the Chicago-land area for the presence of *Anaplasma phagocytophilum.*

2010 Summer Research Internship, Infectious Diseases Research Laboratory, Ann and Robert H. Lurie Children's Hospital of Chicago, Chicago IL
Evaluation of isolates from multiple MRSA outbreaks in the hospital to determine whether there was a single origin, or multiple origins.

PUBLICATIONS

Jutras BL*, **Savage CR*,** Arnold WK*, Lethbridge KL, Carroll D, Tilly K, Bestor A, Zhu H, Stewart P, Rosa PA, Seshu J, Brissette CA, Stevenson B. The Lyme disease spirochete's BpuR DNA- / RNA-binding protein is differentially expressed during the mammal-tick infectious cycle and affects translation of the SodA superoxide dismutase. *Molecular Microbiology.* *Co-first author

Arnold WK*, **Savage CR***, Lethbridge KG, Smith TC, Brissette CA, Seshu, J, Stevenson B. Transcriptomic insights on the virulence-controlling CsrA, BadR, RpoN, and RpoS regulatory networks in the Lyme disease spirochete. *PLoS ONE.* 2018 13: e0203286. *Co-first author

Savage CR, Jutras BL, Bestor A, Tilly K, Rosa PA, Tourand Y, Stewart PE, Brissette CA, Stevenson B. *Borrelia burgdorferi* SpoVG DNA- and RNA-binding protein modulates physiology of the Lyme disease spirochete. *Journal of Bacteriology*. 2018 200:e00033-18.

Arnold WK, **Savage CR**, Brissette CA, Seshu J, Livny J, Stevenson B. RNA-Seq of *Borrelia burgdorferi* in multiple phases of growth reveals insights into the dynamics of gene expression, transcriptome architecture, and noncoding RNAs. *PLoS ONE*. 2016 11: e0164165. doi:10.1371/journal.pone.0164165.

Woodman ME, **Savage CR**, Arnold WK, Stevenson B. Direct PCR of intact bacteria (Colony PCR). *Current Protocols in Microbiology.* 2016 DOI: 10.1002/cpmc.14.

Savage CR, Arnold WK, Gjevre-Nail A, Koestler BJ, Bruger EL, Barker JR, Waters, CM, Stevenson B. Intracellular concentrations of *Borrelia burgdorferi* cyclic di-AMP are not changed by altered expression of the CdaA synthase. *PLoS ONE*. 2015 10: e0125440. doi: 10.1371/journal.pone.0125440.

Arnold WK, **Savage CR**, Antonicello AD, Stevenson B. Apparent role for *Borrelia burgdorferi* LuxS during mammalian infection. *Infection and Immunity* 2015 83:1347–1353. doi: 10.1128/IAI.00032-15.

HONORS & AWARDS

2018 College of Medicine Fellowship for Excellence in Graduate Research, University of Kentucky
2016 Dissertation Enhancement Award, University of Kentucky
2011 Larry H. Knipp award for excellent Teaching Assistant, North Park University
2010 Tri-Beta Research Grant *Bios* Vol. 82, No. 1 (March 2011), pp. 35
2010 A.B. Modine Scholarship in Biology, North Park University

INVITED TALKS AND LECTURES

2015 DNA binding protein SpoVG influences regulation of glycerol metabolism in *Borrelia burgdorferi.* International Conference on Lyme Borreliosis. Vienna, Austria. Sep. 30, 2015
2016 DNA binding protein SpoVG influences regulation of glycerol metabolism in *Borrelia burgdorferi* Gordon Research Seminar on Microbial Stress. South Hadley, MA. July 16, 2016
2017 A tale of two proteins: their interactions, and role in adaptation to stressful environments. Department of Biomedical sciences, University of North Dakota. April 13, 2017
2018 DNA-and RNA-binding protein SpoVG modulates multiple aspects of cell physiology in *Borrelia* burgdorferi, the Lyme disease spirochete. Gordon Research Conference on Microbial Stress. South Hadley, MA. July 17, 2018
2018 Tales of survival: navigating challenging environments from the perspectives of the Lyme disease bacterium and a graduate student. Dep. of Biology, North Park University, Chicago IL. Nov. 9, 2018
2018 *Borrelia burgdorferi* changes its coat to survive, and traverse the enzootic cycle. Guest lecturer for the General Microbiology course at North Park University: Biol 2910. November 9, 2018

CONFERENCE SESSION CHAIR

2018 Gordon Research Seminar on Signal Transduction in Microorganisms, Ventura California.

2018 Gordon Research Seminar on The Biology of Spirochetes, Ventura California.

POSTER PRESENTATIONS

2018 How did I get here, and where am I going? The tale of a bacterium trying to survive. Gordon Research Conference on Microbial Stress, South Hadley, MA.

2018 Nucleic acid-binding SpoVG, and c-di-GMP-binding PlzA modulate response to environmental cues in the Lyme Disease Spirochete *Borrelia burgdorferi.* Gordon Research Conference on Biology of Spirochetes, Ventura CA.

2018 Nucleic acid-binding SpoVG, and c-di-GMP-binding PlzA modulate response to environmental cues in the Lyme Disease Spirochete *Borrelia burgdorferi.* Gordon Research Conference on Signal Transduction in Microorganisms, Ventura CA.

2017 Nucleic acid-binding proteins SpoVG and c-di-GMP-binding PlzA modulate response to environmental cues in *Borrelia burgdorferi.* International Symposium on Tick-Borne Pathogens. Vienna, Austria.

2017 Nucleic acid-binding proteins SpoVG and c-di-GMP-binding PlzA modulate response to environmental cues in *Borrelia burgdorferi.* Midwest Microbial Pathogenesis. Notre Dame, IN

2017 Nucleic acid-binding proteins SpoVG and c-di-GMP-binding PlzA modulate response to environmental cues in *Borrelia burgdorferi*. Molecular Genetics of Bacteria and Phages. Madison, WI.

2017 *B. burgdoreferi* CheA1 influences growth rate and adaptation to glycerol, but does not contribute to chemotaxis. Third annual Postdoctoral Research symposium, Lexington KY.

2017 *Borrelia* b*urgdorferi* CheA1 influences growth rate and modulates transcriptional adaptation to glycerol. BLAST (Bacterial locomotion and signal transduction). New Orleans, LA

2016 DNA-binding protein SpoVG influences regulation of glycerol metabolism and growth rate in *Borrelia burgdorferi*. Midwest Microbial Pathogenesis Conference. Urbana-Champagne, IL

2016 DNA-binding protein SpoVG influences regulation of glycerol metabolism and growth rate in *Borrelia burgdorferi*. Molecular Genetics of Bacteria and Phages. Madison, WI.

2016 DNA-binding protein SpoVG influences regulation of glycerol metabolism and growth rate in *Borrelia burgdorferi.* Gordon Research Conference on Microbial Stress. South Hadley, MA.

2016 DNA-binding protein SpoVG influences regulation of glycerol metabolism in *Borrelia burgdorferi.* Gordon Research Conference on Spirochetes. Ventura, California.

2016 DNA-binding protein SpoVG influences regulation of glycerol metabolism and growth rate in *Borrelia burgdorferi*. Second Annual Postdoctoral Research Symposium. Lexington, KY.

2015 DNA-binding protein SpoVG influences regulation of glycerol metabolism in *Borrelia burgdorferi.* 2015. 1st Annual Infectious Diseases Day, University of Kentucky.

DEPARTMENT SEMINARS

2018 SpoVG appears to be an essential global regulator of transcription and translation throughout the enzootic cycle of *Borrelia burgdorferi.*

2017 A tale of two proteins: their interactions, and role in adaptation to stressful environments.

2016 DNA-binding protein SpoVG influences regulation of glycerol metabolism in *Borrelia burgdorferi.*

2014 Chromatin Isolation by RNA Purification (ChIRP): A novel technique provides functional and structural insights into non-coding RNAs.

MENTORING EXPERIENCE

2018 October-December: Rotation student Zaria Elery
2018 August-October: Rotation student Mackenzie Ryan
2018 May-July: High school student Thomas Noll
2018 January-March: Rotation student Tanner DuCote
2017 October-December: Rotation student Lucy Yanckello
2017 August-October: Rotation student Rachel Thompson
2017-2019 Undergraduate Liza Khenner
2017 March-May: Rotation student Gabby Keb
2016 August-September: Rotation student Beth Oates

TEACHING EXPERIENCE

2017-2018 Chemotaxis lecture in the graduate Structure and Function of Microorganisms course MI 710.
Invited to design and teach the chemotaxis lectures in an upper level graduate course. Wrote and graded exam questions. Fall 2017 and Fall 2018

2009-2011 Teaching Assistant for Microbiology lab Biol-2910, North Park University.

PROFESSIONAL & SERVICE ACTIVITIES, MEMBERSHIPS

2018 Invited to serve as a mentor in the inaugural Graduate Student Mentorship program, in which each first year student is paired with a senior graduate student.

2018 Judge, Fayette County District Science Fair, Lexington, KY

2017 Judge, Fayette County District Science Fair, Lexington, KY

2017 Science Fair Judge, Morton Middle School, Lexington, KY

2016-present Founding member of BGSO (Biomedical Graduate Student Organization), and member of the Outreach Committee
Planned and participated in events in the Lexington area aimed at facilitating science and non-science outreach in the community. Events included judging local science fairs, various festivals (both open-house, and at specific schools) with hands-on demonstrations and experiments, GEMS (girls in engineering and science) conference for elementary and middle

	school girls, food drives for the local food pantry, cooking meals at the Ronald McDonald House, and bingo nights at Hope Lodge for cancer-affected families.
2016-present	Member. American Association for the Advancement of Science
2015	Poster Judge, Annual Postdoctoral Poster session, University of Kentucky
2015	Science Fair Judge, Morton Middle School, Lexington, KY
2014-present	*Ad Hoc* Reviewer, PLoS ONE